Vegetation and Discharge Effects on the Hydraulic Residence Time Distribution within a Natural Pond

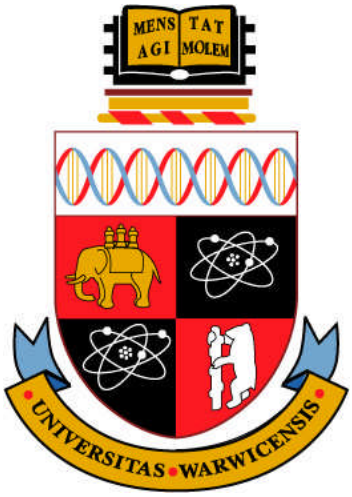

Visoth Tiev

This thesis is submitted in partial fulfilment of the requirements for the degree of Doctor of Philosophy in Civil Engineering

University of Warwick
Department of Civil and Mechanical Engineering

February 2011

ABSTRACT

Results are presented from sets of field and laboratory experiments conducted to measure and quantify the Hydraulic Residence Time Distribution in treatment ponds containing vegetation. The field measurements were taken in the Lyby field pond (Sweden) with complementary experiments on a distorted, laboratory scale model pond designed and built in the University of Warwick's engineering laboratory. Rhodamine WT Dye tracer experiments were used in both the Lyby field pond and the distorted physical scale model to investigate vegetation and discharge affects on HRTD characteristics and the technique of PIV (Particle Image Velocimetry) was used in the distorted physical scale model to investigate how surface flow profiles were affected by different vegetation and discharge configurations.

The results show that the distorted physical scale pond did not reflect the HRTD characteristics of the field site, with the actual residence time, (t_m), for the distorted physical scale pond ranging from 85 % to 125% of its nominal residence time. For the distorted scale model, pond vegetation and discharge did not affect the relative HRTD centroid, e_m, or the actual residence time, t_m. This finding is attributed to the unique pond geography and associated aspect ratios However, flow rates did have a significant effect on the HRTD e_0 (time of first dye arrival at the outlet) and e_p (time of peak dye concentration). Changes in vegetation were found to have little effect on e_0 and e_p. For the laboratory pond, vegetation had a significant control on the surface flow field whereas, flow rates did not – the latter suggests that surface flow fields are not representative of the internal flow field in different layers of the pond.

The experiments demonstrate that the specific shape of the distorted physical scale pond in this study enables optimal actual resident times to be achieved over a wide range of vegetation and flow rate configurations. If full scale field ponds based upon this design give the same stable centroid results, then this would be a substantial breakthrough in pond design, which would aid the design and management of pond treatment and allow more robust optimisation of treatment efficiency.

TABLE OF CONTENTS

DECLARATION

I declare that the work in this thesis has been composed by me and no portion of the work has been submitted in support of an application for another degree or qualification of this or any other university or other institute of learning. The work is my own except where this has been indicated and all quotations have been distinguished by quotation marks and the sources of information have been acknowledged.

ACKNOWLEDGEMENTS

More than three years that I have worked on this thesis I have received help, assistance and guidance from many people and organisations.

I acknowledge with thanks financial assistance from Warwick University, School of Engineering, in the form of a 3 year PhD studentship. Part of this work was subsequently presented at the EU Asia-Link CALIBRE 5th Workshop on "Environmental Priorities and Training Priorities" in Vientiane in December 2010 – the European Commission is thanked for their financial assistance (Contract No. KH/Asia-Link/04 142966) that enabled this opportunity as well as the completion of the writing up of this thesis. This document can under no circumstances be regarded as reflecting the position of the European Union or any of the other funders.

I am grateful and delighted to all involved in the production of this thesis, especially my supervisor Prof. Ian Guymer (The University of Warwick, United Kingdom), my second supervisors Dr. Jean O. Lacoursière, Dr. Lena Vought (KTH, Kristianstad, Sweden), Dr. Kkaus M. Richter, Dr. Jonathan Pearson (The University of Warwick), Dany Va (Royal University of Phnom Penh, Cambodia), Prof. David Polya (The University of Manchester, United Kingdom) my wife and daughter (Dalyan Pov and Sonyta Tiev) and also my sister and parents (Sophi Em, Uy Sin Tiev and Kim Hang Em).

LIST OF FIGURES

LIST OF TABLES

CHAPTER: I

1 Introduction

1.1 Background

Constructed wetlands (artificial pond systems) and natural wetlands (natural pond systems) have been widely used as tools to manage water resources. They have been used as recipients of stormwater runoff, including that which drains agricultural lands and urban developments. In the past decades, wetlands have been considered as areas which have lower economic value and therefore have been drained and converted to other uses. However, in recent years wetlands have been viewed as fulfilling a number of critical ecological functions, including providing wildlife habitat and food chain support and improving surface water quality runoff through physical, chemical and biological mechanisms (Stockdale, 1991).

Pond hydraulics are very important for understanding the influence of a wide range of physical, chemical and biological mechanisms throughout a pond system. Finney and Middlebrooks (1980), stated that “the hydraulic retention time is used in many of the design methods; it is recommended that future research on pond performance consider the effect of physical and climatic conditions on hydraulic residence time. Once residence time can accurately be predicted, perhaps present design methods can be modified to predict pond performance satisfactorily”. To determine expected water quality improvements, it is essential to understand quantitatively various options to optimise flow paths and maximise the Hydraulic Residence Time Distribution (HRTD). HRTD is one of the important parameters and acts as an efficiency indicator of natural ponds.

There are many detailed studies (Mangelson and Watters (1972); Racault *et al.* (1984); Chapple (1985); Macdonald and Ernst (1986); Marecos do Monte and Mara (1987); Moreno (1990); Uluatam and Kurum (1992); Pedahzur *et al.* (1993); Fredrick and Lloyd (1996); Wood (1997); Brissaud *et al.* (2000); Shilton *et al.* (2000); Vorkas and Lloyd (2000), Schmid (2004); and Shilton (2005)) which have focused on wastewater stabilisation ponds (constructed pond systems, mainly rectangular in shape, in which the physical, chemical and biological functions are the same as a part of a natural wetland), which are used extensively to serve the wastewater treatment needs of urban areas (cities and towns), agriculture and industry. However, there are few studies (Duncan, 1997; Salter, 1999; Wörman, 2006, 2007) which look in detail at the physical, chemical and biological mechanisms of natural ponds or natural wetlands.

Furthermore, in contrast to wastewater wetlands, where a high degree of engineering is possible in creating an efficient shape for a treatment pond, the stormwater pond must often fit into existing water courses and this may lead to pond layouts that are less than ideal from a hydraulic point of view (see the review by Duncan (1997) of stormwater treatment sites in 51 locations in 4 countries). However, there is a dearth of data on controls on Hydraulic Residence Time Distributions (HRTD) of naturally-shaped ponds used for stormwater storage and treatment.

Therefore, this research aims to model accurately the solute Hydraulic Residence Time Distribution (HRTD) of a naturally-shaped wetland pond using a physical scale model and investigate how this varies with different vegetation conditions over a range of discharges.

1.2 Research Needs and Aim of Thesis

The general aim of this study is to contribute to understanding the influence of discharge and vegetation on the Hydraulic Residence Time Distribution (HRTD) of a naturally-shaped pond. To achieve this aim, the variability of discharge and vegetation over a whole year cycle was firstly investigated in a naturally-shaped field pond and, secondly, detailed studies on a physical scale laboratory model were carried out using a range of vegetation and discharge rates informed by the field studies. This provided a data set quantifying the influence of discharge and vegetation on the HRTD for both lab scale and full scale field application. The research aims to demonstrate a method for determining a meaningful concept of

residence time of a naturally-shaped pond, which is suitable for an engineer to assess the design of treatment processes.

1.3 Specific Objectives and Approach

The specific objectives of this study were to:

(i) quantify hydraulics, rendered as a HRTD, of a naturally-shaped field pond, at different times of the year and, consequently, over a range of different discharge rates and vegetation conditions (type and extent of cover)

(ii) use the observed discharge rates and vegetation conditions at the field pond to inform the range of conditions for testing of a laboratory physical scale model

(iii) quantify the hydraulics, of a laboratory physical scale model over the selected range of discharge rates and vegetation conditions

The experiments are particularly to be designed to determine:

- The effect of discharge and vegetation on HRTD
- The effect of discharge and vegetation on pond mixing, focussing on short circuiting as well as dispersion

An ideal field site to study a naturally-shaped pond was found to be the Lyby field-pond, designed by Jean Lacoursiere (pers. comm.) and located in Sweden.

A physical scale laboratory model of this pond was designed and constructed at the University of Warwick.

CHAPTER: II

2 Literature Review

2.1 Overview of Chapter

This literature review starts with an introduction to the different types of treatment systems such as stormwater ponds, wet-ponds, constructed and natural wetland, and waste stabilization pond systems. The review then moves on to pond-scale design, focussing on factors affecting pond design, discharge scale calculation, synthesized vegetation conditions and methods for determining Hydraulic Residence Time Distribution (HRTD). To understand more on the details of HRTD, there follow reviews on relevant aspects of hydrology and pollutant transport, covering: hydraulic properties of subsurface flow in wetlands, flow through saturated media, open channel flow, laminar and turbulent flow, advective transport, advective dispersive transport in saturated media and in open channel flow, solutions for the mixing equations and non-Fickian dispersion models, the reaction rate constant (degradation kinetics; self purification rate of the system),

tracer study techniques, physical and mathematical modelling of solute transport (including outlining parameters such as Froude number, Reynolds numbers, the conflict between satisfying Froude and Reynolds number similarity simultaneously, inlet and outlet location of the tracer, computational fluid dynamics, sensitivity analysis with uncertainty of parameters), visualising surface flow fields by using MatPIV and, finally, details of the existing Swedish constructed pond systems (runoff treatment design concept ; vegetation) relevant to the field pond studied.

There has been a considerable amount of research conducted over the years on design and operation of retention ponds, waste stabilization pond systems and natural and constructed wetlands. There is continuing research in all areas relating to ponds and understanding both past and current research will enable the project objectives to be achieved.

Wet ponds and wetlands cover large areas of the world's surface. They can be found on every continent, except Antarctica, and subsequently in all climatic zones (Vymazal, 1998). Comprehensive summaries of the basic functions and purposes of wet pond or retention ponds, covering all aspects of pond design and maintenance for the major types of pond, are given by David (1998), Shilton (2005) and Johan *et al*. (2007). Johan *et al*., (2007) review the results of computer simulations and independent measurements of friction losses (as well as wetland geometry) and state that variations in bottom topography associated with the formation of several deep zones decrease the variance in water residence times, but to a minor extent. Shilton (2007) defines wet ponds as treatment technology systems in his opening paragraph: 'Pond treatment technology serves the

wastewater treatment needs of agriculture, industry, cities and towns around the world and is one of the most common treatment technologies in use today. Indeed, for thousands of communities with many millions of people, from developing countries to modern industrialised nations, the only thing standing between raw wastewater and a local waterway is often a pond treatment system.

2.2 Treatment Types

2.2.1 Stomwater pond , wetponds

The type of wastewater and stormwater treatment usually dictates the complexity of the pond system. A typical wet pond system consisting of one pond is detailed in Figure 2-1.

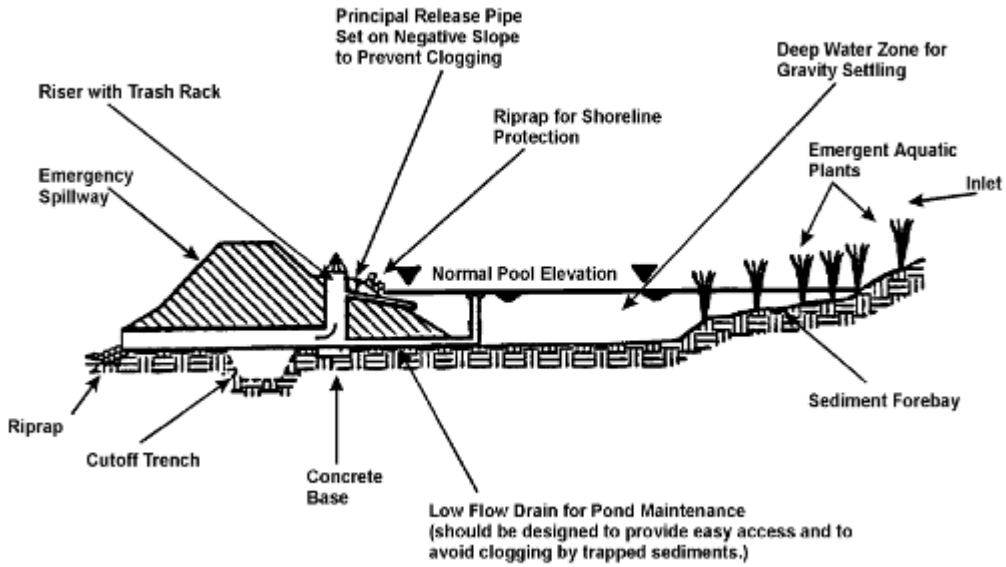

Figure 2-1. Typical Layout of a Wet Detention Pond (from Maryland Department of the Environment, 1986).

2.2.2 Constructed and natural wetlands

The term wetland is used to collectively describe areas of water-saturated land that cover a diverse spectrum of ecological systems (IWA (2000). Spatially they are defined as transitional environments between dry land and deeply flooded land

(Kadlec and Knight, 1996). According to Vymazal (1998), the three major components that characterize wetlands are the vegetation, the hydrology and the soil.

Vegetation: "Hydrophytic plants species with the ability to grow, reproduce and persist in anaerobic soil conditions. Plants, with roots systems, that emerge above the water surface."

Hydrology: "Standing water, which provides a habitat for aquatic organisms as living algae and populations of microbes, submerged and floating plant species and fish or other vertebrate animals."

Hydric soils: "Wetlands have unique soils, classified as water saturated hydric soil, which may develop anaerobic conditions and support chemical reducing processes."

Wetlands have been utilised widely for wastewater treatment purposes for centuries. Whilst, in many cases, the reasoning behind this was disposal rather than treatment, uncontrolled discharges of wastewater has led to eutrophication and irreversible degradation of many wetland areas. Due to increased environmental awareness by the public, constucted wetlands and managed, natural wetlands are now being used extensively and accepted for the treatment of water, wastewater, stormwater and sewage. Relying on natural ecological processes, wetlands are going further than traditional wastewater treatment methods in supporting ideas of environmental and sustainable engineering.

Constructed wetlands are engineered systems designed to simulate the processes occuring in natural wetlands but they have the advantage of being a controlled environment. Constructed wetlands have been considered in two main groups,

(Figure 2-2, 2-3 and 2-4), namely Subsurface Flow treatment wetlands (SSF) and Free Water Surface treatment wetlands (FWS).

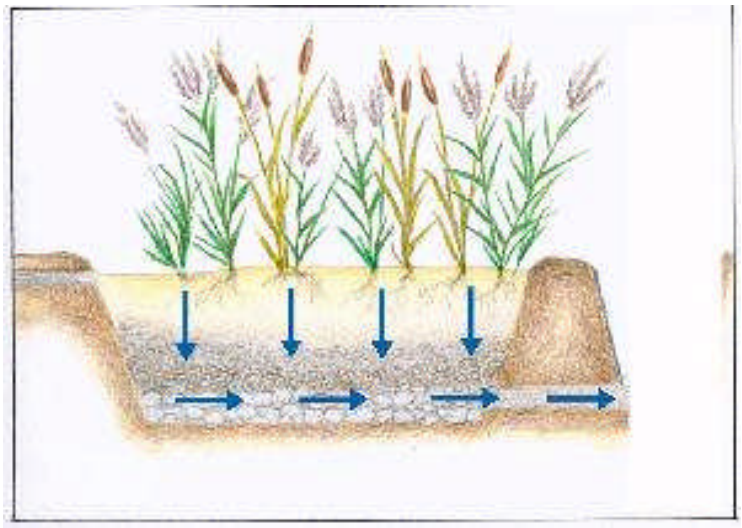

Figure 2-2. Subsurface flow wetland with vertical flow (http://www.iridra.it/index_eng htm)

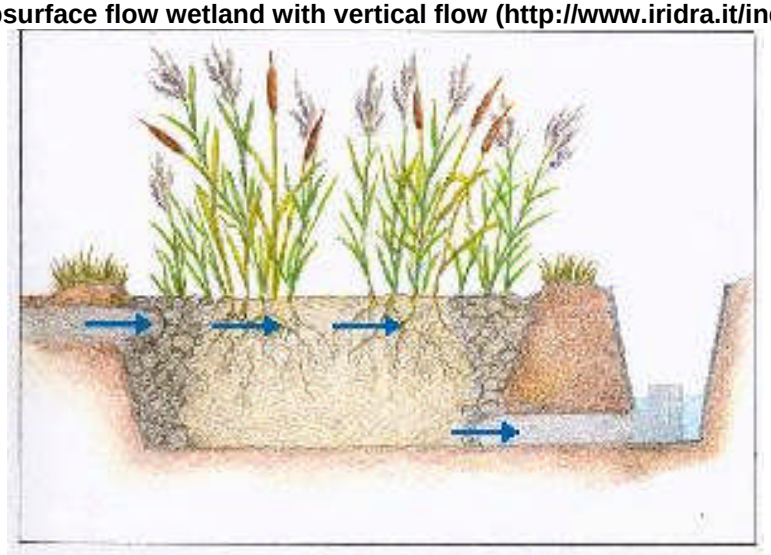

Figure 2-3. Subsurface flow wetland with horizontal flow (http://www.iridra.it/index_eng.htm)

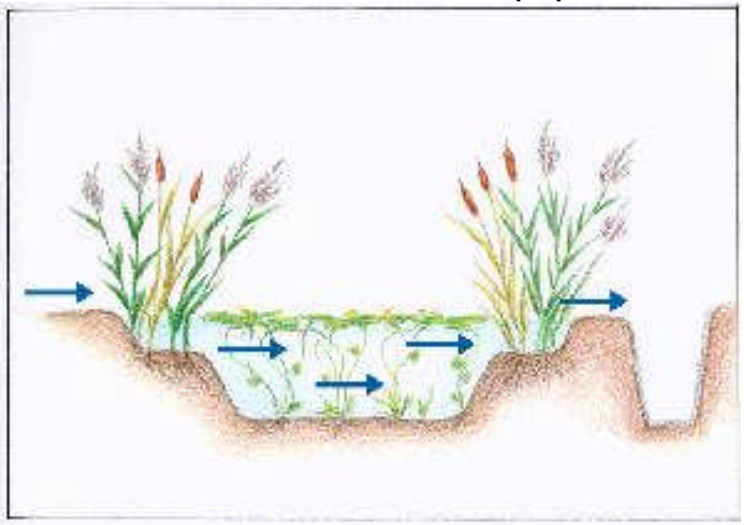

Figure 2-4. Water surface wetland with different vegetation (http://www.iridra.it/index_eng.htm)

There are two kinds of subsurface flow (SSF) wetlands, namely subsurface flow wetlands with vertical flow (Figure 2-2) and subsurface flow wetland with horizontal flow (Figure 2-3). In both cases, the supporting medium used is usually sand or gravel, sometimes a less porous soil with clay particles, IWA (2000). The subsurface flow with vertical flow wetland uses basins filled with a porous medium for the support of vegetation (Figure 2-2); wastewater or stormwater is fed intermittently in batches on top of the wetland, flooding its surface and then drains vertically by gravity through the porous medium. The drainage network at the base of the bed collects the effluent water. The bed is drained completely before the next batch of water is applied, causing the pore space to be filled with air. The rapidly-applied, next dose of water traps the air in the pore space. This process results in a good oxygen transfer. Vertical subsurface flow wetlands are very similar to rustic biological filters (Cooper *et al*., 1996). The advantage of the subsurface vertical flow wetlands is that they hold back suspended solids and settleable substances.

The subsurface flow with horizontal flow wetland (Figure 2-3) uses support media similar to the vertical flow wetland but the wastewater or stormwater usually enters the system continuously in the inlet zone, where it is distributed evenly over the cross-section. The liquid substances then flow slowly through the porous medium on a horizontal flow path. The water is collected at the end of the porous medium at the outlet zone and finally discharged.

The free water surface treatment wetland (FWS) (Figure 2-4) mimics directly the hydrological regime of natural wetlands. FWS are shallow ponds, containing 20 to 30 cm of rooting soil (Kadlec and Knight, 1996) and water flows over the soil surface from an inlet point to an outlet point. Anaerobic microbial processes dominate in the water column in deeper zones of FWS in the absence of light, similar to the processes occurring in facultative ponds. There are five different combinations or classifications of FWS wetlands, *viz*. FWS wetlands with emergent Macrophytes, FWS with free-floating macrophytes, FWS with floating leaved, bottom-rooted Macrophytes, FWS with submersed macrophytes and FWS with floating mats, rafted reed beds. FWS wetlands with emergent macrophytes consist of shallow basins, where the base is a soil matrix to support the roots of the vegetation. Water control structures maintain a shallow depth (with typical water depths ranging from a few centimetres up to few metres) and water flows above the soil with sediments and litter. The live and dead plants extend above the wetland water. Plants that are used are macrophytes such as cattails (*Typha spp.),* common reed (*Phragmites australis*), bulrushes (*Scripus spp.*) or sedges (*Cyperus spp*.). The large cross sectional areas result in low flow velocities, allowing settling of incoming suspended solids (SS) (Hey, 1994). Pollutants may cycle within the water body or at the surface of the soil base. Microbial growth, vegetation and the soil sorbs parts of the dissolved fractions of these pollutants. The re-aeration at the water surface is the oxygen source for this reaction. While the deeper sections and the sediments are usually anaerobic, the near-surface areas are aerobic. Free water surface wetlands are generally less costly to build and operate than other systems and are also relatively easy to construct; however, they require larger areas of land on which to be built, IWA (2000).

FWS with free floating macrophytes are different from FWS with emerged Macrophytes Since this system does not need soil as a support medium for the plants. This Floating Aquatic Plant (FAP) system utilizes species of floating vascular plants, typically water hyacinth (*Eichhornia crassipes*), duckweed (*Lemna spp.*) or water lettuce (*Pistia stratiotes*). These plants use photosynthesis at or above the water surface to convert atmospheric carbon dioxide into oxygen (Brix, 1993).

FWS with floating-leaved, bottom-rooted macrophytes is a mix of both FWS wetlands with emergent macrophytes and FWS with free-floating Macrophytes. The plants themselves have roots, they utilise soil at the system's base as a support medium. However, their leaves float on top of the water surface. The plants used with this system are lotus (*Nelumbo spp*.), cowlily (*Nuphar spp*.) and water lilies (*Nymphaea spp*.), IWA (2000).

FWS with submersed Macrophytes have their photosynthetic plant tissue below the water surface. The plant might or might not be rooted, being buoyant and suspended in the water column. The submersed macrophytes used in FWS are water milfoil (*Myriophyllum spp*.), naiads (*Najas spp*.) and waterweed (*Elodea spp*.).

FWS with flow mats, rafted reed beds, emergent macrophytes can form floating mats, being buoyant through air trapped in roots and stems and becoming stable when roots and rhizomes of a large group of plants are woven together.

Macrophytes are capable of forming these mats. Plants used for this type of wetland are cattail (*Typha spp*.), pennywort (*Hydrocoltyle umbellate*), giant sweetgrass (*Glyceria maxima*) and common reed (*Phragmites australis*). Rafts with some penetrable mat (Macrophytes) are planted and often give initial stability and buoyant support. The pollutants removal is similar to FWS with free-floating Macrophytes, where the root systems take up nutrients and support microbial communities, IWA (2000).

2.2.3 Waste stabilization pond systems

There are a number of variations of wastewater stabilization pond systems. The way ponds are designed and applied depends upon the loading and their characteristics. Variants include: Anaerobic Ponds, Anoxic Ponds, Facultative Ponds, Aerated Ponds/Lagoon Ponds, Maturation Ponds and High-Rate Algal Ponds (Shilton, 2007).

Anaerobic Ponds, designed to receive high organic loading, are typically found at the front end of a series of ponds. Their treatment function is to undertake bulk removal of the organic load within a short period (Shilton, 2007).

Anoxic Ponds (Almasi and Pescod, 1996) operate in the area of organic loading that exists between typical values used for design of anaerobic and facultative ponds (see paragraph below). Almasi and Pescod (1996) consider that ponds designed to operate in the anoxic range have the potential to avoid the odour risk that has been associated with anaerobic ponds, while reducing the high land area and time requirements that are associated with facultative ponds.

Facultative Ponds are ponds that operate with aerobic and anaerobic zones, as shown in Figure 2-5 below. They may be either primary or secondary, in the sense that the former receives raw wastewater, whilst the latter receives effluent that has undergone pre-treatment in anaerobic pond.

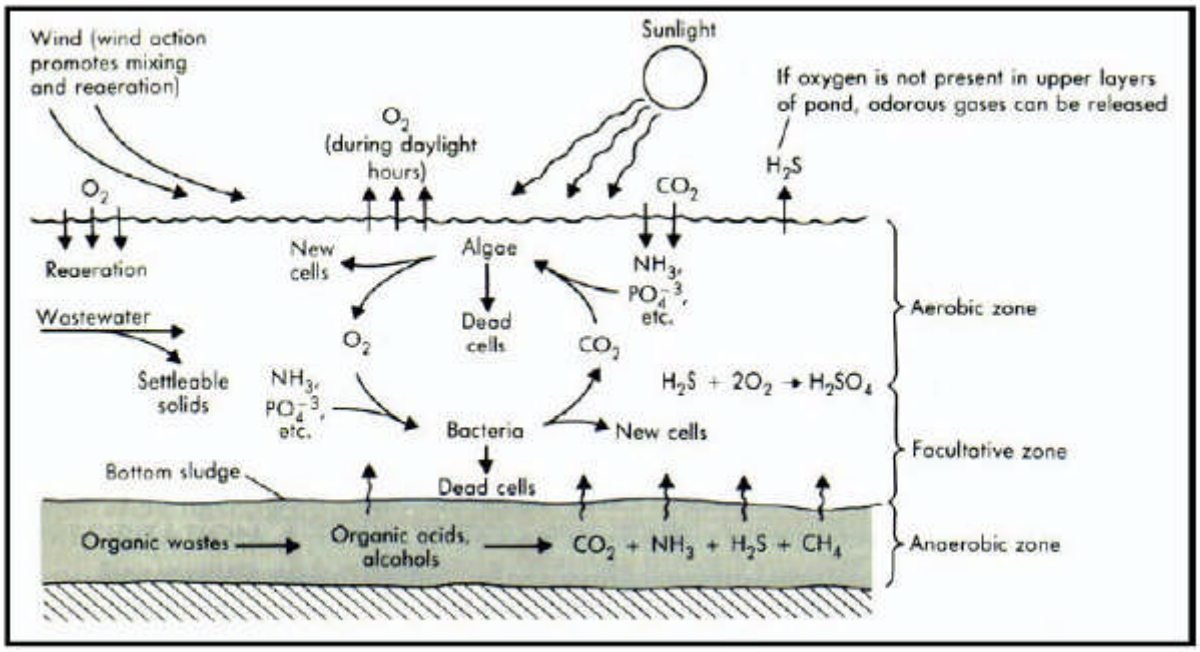

Figure 2-5. Facultative pond (from Tchobanoglous and Schroeder, 1985, pg. 635)

Aerated Ponds or Lagoon Ponds are retrofitted facultative ponds with surface aerators to boost dissolved oxygen (DO) levels and/or to improve mixing. These ponds require a high power input for aeration and, in some cases, incorporate biomass return (for example, sludge recirculation). The advantage of these systems is that they require shorter hydraulic residence times (HRT) and water depth can be increased without increasing algal populations.

Maturation Ponds or Polishing Ponds, have a primary function to remove pathogens but they can also achieve significant nutrient removal due to long HRT (Mara *et al*.,1992). Mara (*ibid)* notes that, if anaerobic and secondary facultative

pond systems are used, an effluent suitable for restricted irrigation will be produced. Therefore, additional maturation ponds will only be needed if a higher quality effluent is required.

High-Rate Algal Ponds have continued to be developed and implemented (particularly in the United States and Israel) since the early 1960s (Shelef and Azov, 1987). These systems are shallower than facultative ponds and operate with shorter HRTs.

2.3 Pond Design

2.3.1 Factors affecting pond design

The two main driving factors of a design are the rate of discharge into the pond and the required quality of the effluent leaving the pond (or system). These factors dictate the number and type of ponds required for the specific location. Having clearly established these requirements, it is then possible to think about the shape, size and aesthetics of the pond (Persson, 2000). Once the HRT is obtained from the HRTD, the dimensions and shape of the pond can be calculated. Different types of pond require different depths; some such as facultative ponds must be shallow (typically 1.5 m) because they are driven by the sun (Shilton, 2005). The shape of the pond has a large impact on the hydraulic performance of a pond. Angular ponds suffer from dead zones (that can stagnate), re-circulating and short-cutting (Jansons *et al*., 2005; Persson, 2000). There are a number of other properties that a designer must take into account and/or design to get the required performance:.

- Length to Width ratio – studies such as those of Jansons *et al* (2005) and Persson (2000) have shown that elongated ponds with a high aspect ratio, say 5:1, have better hydraulic efficiency, higher removal rates and zones of diminished mixing.
- Depth – Depends on the treatment process used (aerobic or anaerobic).
- Vegetation – The location, characteristics and density can have a large effect on the hydraulic performance of a pond due to biological uptake.
- Profile – The shape of the bed and banks. This is affected by considerations such as maintenance and safety around the pond.

2.3.2 Methods for determining hydraulic retention[1] times

Theoretical HRT, t_n, is calculated assuming plug flow conditions using equation 2.1 (Levenspiel, 1966). Theoretical HRT is a simple ratio of the pond volume to the rate of inflow.

$$t_n = \frac{V}{Q} \qquad (2.1)$$

where: t_n = Theoretical (nominal) Hydraulic Retention Time, V = Pond Volume and Q = Average (or design) Flow rate.

This equation does not take into account any other parameters that may affect the HRT (Persson, 2003). In field ponds the primary reasons for ponds not attaining their theoretical HRT is sludge accumulation (reducing the volume) and varying flow rates (Shilton, 2005). Varying flow rates mean that the pond may not be

[1] The terms *residence* and *retention* are interchangeable in this context

working at the designed loading rate, altering the HRT. As sludge accumulates and the volume reduces, HRT decreases.

For constructed and Natural Wetlands, Stormwater Pond or Wet-pond, Waste stabilization pond systems, the residence (retention) time will be influenced primarily by two factors; hydrology (the temporal distribution of the inflows) and hydraulics (the flow fields that develop in the pond/basin during an event). Wind interactions, groundwater, evaporate-transpiration, precipitation and environmental conditions also have an effect but consideration of these is beyond the scope and purpose of this study For detailed modelling taking account of these variables, see Konyha *et al* (1992).

With regard to the inflows, US EPA (1986) recommend that the performance of any control device that treats urban runoff should be characterised in such a way that the variability and intermittent nature of storm runoff is recognised and accounted for. The importance of the flow patterns and the movement of inflows through the basin have been noted previously by a number of researchers. Kadlect (1994), estimated flow patterns to assist in the derivation of a compartmental model of a wetland using a series of continuous stirred tank reactors. Hey *et al* (1994) noted that in stormwater wetlands the outlet concentrations represent displaced water which would not have been affected by reactions taking place during the storm. Wu *et al* (1996), in a study of several stormwater wetlands, found that a removal efficiency of 100% was obtained for several small storms due to the total retention of runoff volume.

When calculating HRT, the type of flow experienced within the pond must be considered. There are three main types of mixing in the flow regime, namely plug, completely-mixed and non-ideal flow. Plug flow assumes that there is no mixing or diffusion as the water moves through the pond (Shilton, 2005; Levenspiel, 1966), as shown in Figure 2-6. Completely-mixed flow, shown in Figure 2.7, assumes that the water is instantaneously and completely mixed upon entering the pond (Shilton, 2005).

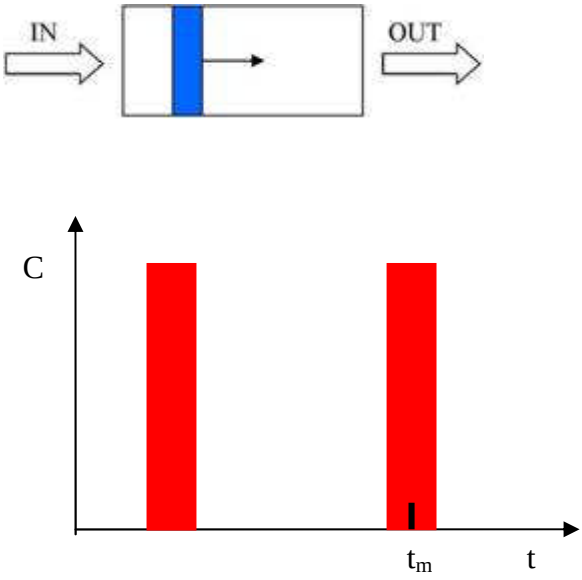

Figure 2-6. Plug flow.

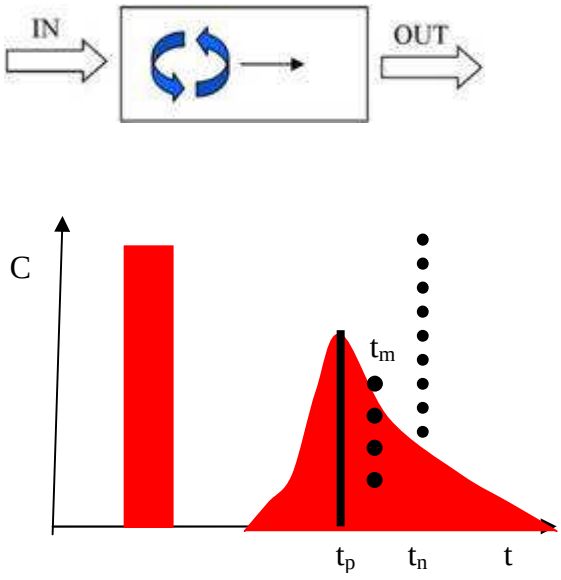

Figure 2-7. Partly mixed flow, t_p is time to peak, t_m is actual residence time and t_n is theoretical residence time.

Figure 2-6 and 2.7 shows the nature of plug flow and completely mixed flow.

The first vertical red bar on Figure 2.6 represents the slug of pollutant or tracer (*e.g*. a dye) entering the pond, and the second bar represents the distribution of dye concentration at some subsequent time, assuming that the flow conforms to plug flow in which there is no mixing. In plug flow conditions the dye passes

through to the outlet point in one block, clearly indicating the actual retention time, t_m. In figure 2.7, the curve represents the distribution of dye concentrations with time for completely mixed conditions. This curve is called the hydraulic residence time distribution (HRTD). Two quantities are shown for this distribution, namely the time to peak concentration, t_p, and the actual HRT, t_m (Bojcevska, 2005). The HRTD function, *f(t)*, for an impulse tracer introduced into steady flow conditions (the conditions modeled in this project) is given in equation 2.2..

$$f(t) = \frac{QC(t)}{\int_0^\infty QC(t)dt} = \frac{C(t)}{\int_0^\infty C(t)dt} \tag{2.2}$$

where *C* = Concentration of a given tracer.

The actual HRT is defined as the centroid of the HRTD (Bojcevska, 2005).

$$t_m = \int_0^\infty tf(t)dt \tag{2.3}$$

Another fundamental parameter is the variance, σ^2, which is a measure of the spread of the HRTD and is given by equation 2.4. In plug flow, where there is no dispersion other than advection, the HRTD has a variance equalling 0.

$$\sigma^2 = \frac{\int_0^\infty (t - t_m)^2 f(t)dt}{\int_0^\infty f(t)dt} \tag{2.4}$$

A common measure of the extent of plug flow is the number of stirred tanks (N) used in a tank-in-series model (Kadlec & Knight, 1996. Fogler, 1992). The higher the value of N, the more plug flow-like is the flow. Here, N is defined as

$$N = \frac{t_n^2}{\sigma^2} \tag{2.5}$$

The relationship between the theoretical and actual retention times can be defined in terms of an effective volume ratio, e_m, derived by Thackston *et al* (1987) as:

$$e_m = \frac{t_m}{t_n} = \frac{V_{effective}}{V_{total}} \tag{2.6}$$

Where: $V_{effective}$ is the effective volume of a pond and V_{total} is its total volume, The effective volume is the total volume minus the dead volume, which is the volume of water that does not interact with the water flowing through the system (Bojcevska, 2005). The effective volume is strongly influenced by the length-to-width ratio (Bojcevska,2005; Persson and Wittgren, 2004), though this conclusion was based upon considerations of rectangular ponds rather than more natural shapes. The ratio *e* is an indicator of hydraulic performance (Kadlec & Knight, 1996). A low effective volume will result in a low HRT, which, in turn, reduces its treatment efficiency.

Persson (2000) used the quotient e_{16} to measure short-circuiting, here defined as t_{16} divided by the nominal retention time, t_n, where t_{16} is the time of passage of the 16th percentile through the outlet. Here,

$$e_{16} = \frac{t_{16}}{t_n} \tag{2.7}$$

The first dye arrival time, t_0 , is a measure of short-circuiting and is a useful quantity with which to compare the sensitivity of short-circuiting from one tracer to another. The quotient e_0 is also used, defined here in terms of t_0 and the nominal retention time, t_n, where t_0 is the time for the first passage of dye mass through the outlet, see equation 2.8:

$$e_0 = \frac{t_0}{t_n} \qquad (2.8)$$

Kadlec (1994) and Holland *et al* (2004) used peak travel time as a surrogate to tracer retention time, since there is no need to measure volumes or flows, nor to measure a complete response curve. Unfortunately, all data and all models lead to the same conclusion: peak times are much shorter than tracer retention times, often by a factor of two. So, in this study, peak travel time was used as a comparative parameter, to illustrate the effect of vegetation and discharge on hydraulic performance and efficiency. Peak travel time, e_p ,is defined as:

$$e_p = \frac{t_p}{t_n} \qquad (2.9)$$

Less than perfect mixing and the occurrence of dead zones will always contribute to actual retention times in natural ponds being shorter than theoretical retention times. In this study, the vegetation conditions and discharge rates minimising this difference are therefore investigated.

2.4 Hydrology and Pollutant Transport

2.4.1 Hydrology

Wastewater effluent flow-rates are in a constant state of change. Domestic wastewater discharge varies through a daily cycle, as well as in response to climatic conditions in the sewerage catchments. Ponds, however, provide equalisation of these hydraulic peak-flows (Shelef and Kanarek, 1995). This effect results from the large surface area of the system. The rate of discharge from the pond, if controlled by a weir structure, is proportional to the water height. Although a 'flood' flow might enter the pond in a short period, the resultant increase in the height (and, thus, the discharge rate) is small due to the large area of the pond in which the 'flood' flow is stored. Thus flow attenuation occurs.

The interaction of the large surface area and evaporation should be considered. In dry areas evaporative losses can be very high and may be classified as a method of "ultimate disposal" (Shelef and Kanarek, 1995). Seepage through the base and sides of ponds can also represent significant losses if a pond is unlined and located in an area of permeable soils. Evaporation and/or seepage can account for the loss of significant quantities of water from a pond. In design manuals, such as that by Mara and Pearson (1998), accounting for these effects becomes an integral part of the design process.

Stratification refers to density-induced separation of the pond into layers, with each layer being characterised by different oxygen, redox and temperature characteristics. Generally, in the pond or wetland systems, the upper layer is

aerobic while the lower layer is anoxic, which means that the different layers can also have quite different chemical and biological characteristics.

Stratification may also be detrimental to the hydraulic behaviour of a pond system. It is possible that an inflow may 'short cut' across the top of a stratified pond instead of mixing into its full volume. This effect may be magnified, or occur in its own right, if the influent flow has a significantly different temperature from that of the main body of the pond and is not well mixed upon entry.

Flow patterns, regardless of whether they occur in open channels, pipes, ponds or wetlands, may be laminar, turbulent or in transition, depending upon the Reynolds number *Re* of the flow. The value of the Froude number *Fr* of the flow determines whether the flow is may also be critical, subcritical or supercritical, in the sense that *Fr* is respectively unity, less than unity or greater than unity. Here, *Re* is defined as $Re = UL/v$, where *U* and *L* are typical velocity and horizontal length scales respectively of the flow and *v* is the kinematic viscosity of the fluid. *Fr* is defined as $Fr^2 = U^2/gH$, where *H* is a typical vertical length scale of the flow and *g* is the acceleration due to gravity

2.4.2 Advective transport

The movement of a solute which is carried along with the bulk motion of the fluid is called advective transport (Charbeneau, 2000). For steady flow without sources and sinks, uni-directional (*x*) advective transport may be described by

$$\frac{\partial c}{\partial t} + v * \frac{\partial c}{\partial x} = 0 \qquad (2.5)$$

where

$\frac{\partial c}{\partial t}$ rate of change of concentration with time

v_x fluid velocity in the *x* direction

$\frac{\partial c}{\partial x}$ concentration gradient

2.4.3 Advective dispersive transport in open channel flow

Tracer flow may be modelled with equation 2.5 assuming a fully saturated homogenous and isotropic medium, a steady-state flow and validity of Darcy's law. The modelled flow is idealised plug flow, though this is not observed in reality, where the solute spreads due to mixing processes, collectively named hydrodynamic dispersion (see Figure 2.7). The term hydrodynamic dispersion incorporates the effect of mechanical mixing during fluid advection and the effect of molecular diffusion. Since molecular diffusion is only of importance at low velocities, the hydrodynamic dispersion in most applications is caused entirely by the turbulent motion of the fluid. For uniform flow, the process is known as mechanical (or turbulent) diffusion, while, where velocity gradients are present in the advecting flow, the mixing process is termed turbulent dispersion. The spreading of solute in the direction of the bulk flow is named longitudinal diffusion (dispersion); the spreading in the directions perpendicular to the flow is named transverse diffusion (dispersion).

The solute flux through a small control volume is again considered. The flux of water has the velocity v with its components (v_x, v_y, v_z) in the *x*, *y* and *z* directions.

Using Fick's first law, it can be stated that the mass of solute transported in the x direction is

$$J = e_x \frac{\partial C}{\partial x} dA \qquad (2.6)$$

where e_x is the turbulent diffusion coefficient in the x direction

Now the advection dispersion equation can be derived in a manner similar to the equation for the transport of solutes in a medium as:

$$\left[e_x \frac{\partial^2 C}{\partial x^2} + e_y \frac{\partial^2 C}{\partial y^2} + e_z \frac{\partial^2 C}{\partial z^2} \right] - \left[v_x \frac{\partial C}{\partial x} + v_y \frac{\partial C}{\partial y} + v_z \frac{\partial C}{\partial z} \right] = \frac{\partial C}{\partial t} \qquad (2.7)$$

We assume that e_x, e_y, e_z and v_x, v_y, v_z do not vary with *x*, *y*, *z*, *t*.

2.4.4 The Dispersion Number

Fick's Law describes the process of molecular diffusion. If general dispersion in, say, the x-direction is considered to have equivalent behaviour, then the dispersion of a tracer, C, can be described by:

$$\frac{\partial C}{\partial t} = D \frac{\partial^2 C}{\partial x^2} \qquad (2.8)$$

where D is coefficient of axial dispersion. If u and L are the velocity component and the length scale respectively in the *x*-direction, then the dimensionless form of the equation can be derived as:

$$\frac{\partial C}{\partial \theta} = d\frac{\partial^2 C}{\partial z^2} - \frac{\partial C}{\partial z} \qquad (2.9)$$

where:

θ $t/t_{mean} = tu/L$;

z $(ut + x)/L$;

d (D/uL).

The dimensionless constant d is known as the dispersion number and can be derived experimentally from the results of, say, a tracer study. In reality, the dispersion number is a function of the numerous physical influences that can affect fluid movement in a pond. These influences include:

- The flow rate and its variation over time;
- The inlet size, position and orientation;
- The outlet position and design;
- Wind shear and its variation over time;
- Pond geometry (including influences of baffles);
- Temperature/density effects.

For the design of new ponds, an accurate method of predicting the dispersion number has been sought in a number of research studies. Arceivala (1981), using data from the literature, proposed four simple empirical equations for the prediction of the coefficient of axial dispersion, D, from which the dispersion number can be determined:

- Wider than thirty metres with baffles, $D = 33W$;

- Wider than thirty metres without baffles, $D = 16.7W$;
- Narrower than ten metres with baffles, $D = 11W^2$;
- Narrower than ten metres without baffles, $D = 2W^2$;

where W is the pond width.

Alternatively, Ferrara and Harleman (1981) used an equation derived by Fischer (1967) for flow in channels of large width to depth ratio to determine the coefficient of axial dispersion, D:

$$D = 0.225\frac{u^* L^2}{k^2 R_h} \tag{2.10}$$

where

u^* shear velocity,

L pond length,

k von Karman's constant, and

R_h hydraulic radius.

Polprasert and Bhattarai (1985) also considered Fischer's work, but developed it further by drawing on work into the prediction of dispersion in streams and rivers to propose the following predictive equation for the dispersion number:

$$d = \frac{0.184\left[\theta v\left(W + 2z\right)\right]^{0.489} W^{1.551}}{\left(LZ\right)^{1.489}} \tag{2.11}$$

where

θ hydraulic retention time,

ν kinematic viscosity,

W pond width,

Z pond depth,

L length of fluid travel from inlet to outlet .

Marecos do Monte (1985) undertook tracer studies on two Portuguese facultative waste stabilisation ponds and compared the dispersion numbers obtained against those predicted by the Polprasert and Bhattarai equation. There was little agreement between the predicted and the measured results, leading her to state that the predictive equation cannot be considered to be valid for all ponds. She concluded that, for design, the completely-mixed reactor equation should be applied as it yields the more conservative pond sizing.

Agunwamba (1991) published a review of dispersion number prediction equations. He wrote that the existing equations had yet to prove useful due to the disparity between experimental and predicted results. To explain this problem he suggested that the omission of factors such as “wind speed, dead zones, secondary currents and seasonal effects, sampling time after tracer release, pond breadth to depth ratio and Reynolds number disparity (p 241) could be to blame.

Agunwamba *et al.,* (1992) presented an alternative predictive equation for the dispersion number (*d*):

$$d = 0.10201\left(\frac{u*}{u}\right)^{-0.81963}\left(\frac{H}{L}\right)\left(\frac{H}{W}\right)^{-\left(0.98074+1.38485\frac{H}{W}\right)} \qquad (2.12)$$

where

u flow velocity, (measured in m/day);

$u*$ shear velocity, (m/day);

H pond depth (m);

L pond length (m);

W pond width (m).

In the same year, Agunwamba (1992) also published a new method of dispersion number determination requiring only data on the bacteria variation along the pond as input. This method was claimed to be “simple, accurate and economical” (p 361) in comparison to the use of tracer studies but if we look carefully at the equation 2.12, the formula still does not explicitly take into account the numerous variables that may control dispersion number. To date there have been no known publications that have used this new technique”.

In conclusion, it can be argued that the dispersion number itself is effectively a ‘fudge factor’ that attempts to account for the wide range of influences that affect fluid flow through a pond system. As presented above, it can be seen that a significant amount of research has gone into attempts to develop predictive equations for the dispersion number. A number of these equations have been independently reviewed and have had problems when tested against different data sets. None of these equations have gained widespread use as a recognised design method.

2.4.5 The Froude number *Fr*

The Froude number (see earlier) represents the ratio of inertial to gravity forces in the equation of motion governing fluid flow:

$$Fr = \frac{v}{\sqrt{gy}} \tag{2.13}$$

Where:

Fr = Froude number;

v = depth-averaged horizontal fluid velocity,

g = acceleration due to gravity,

y = depth of the fluid.

As discussed earlier, at values of *Fr* greater than unity a high velocity, shooting flow exists which is termed *supercritical*. At values less than unity, *sub-critical* flow exists, which is characterised by a comparatively deeper, much slower moving flow. The Froude number is always of importance when the influence of gravity is significant (Kobus, 1980), as, for instance, in all flows with a free surface.

In a Froude number based model design, Shilton (2007) used scale relationships for determining the model flow rate and residence (retention) time as follows, where the subscripts ‘m’ and ‘p’ refer to model and prototype (full-scale), respectively:

Based on equation 2.13 where:

For Froude number similarity:

$$Fr_m = Fr_p \tag{2.14}$$

$$\frac{v_m}{\sqrt{y_m}} = \frac{v_p}{\sqrt{y_p}} \tag{2.15}$$

$$\frac{\sqrt{y_m}}{\sqrt{y_p}} = \frac{v_m}{v_p} \tag{2.16}$$

$$\frac{y_m}{y_p} = \frac{v_m^2}{v_p^2} \tag{2.17}$$

Considering that $\frac{y_m}{y_p}$ is a scale factor for length, S_y, and $\frac{v_m}{v_p}$ is the scale factor for velocity, S_v, then:

$$S_y = S_v^2 \tag{2.18}$$

The scale factor for flow rate (S_Q) can be derived from the continuity equation:

$$Q = Av \tag{2.19}$$

Where:

$$A = YxL$$

It follows that (where S_L is a scale factor of pond depth):

$$S_Q = S_L S_y S_v \tag{2.20}$$

and since:

$$S_v = S_y^{0.5} \tag{2.21}$$

$$S_Q = S_y^{3/2} S_L \tag{2.22}$$

Time (*t*) is also scaled, with S_T being the scale factor for time and its relationship to S_L can be found simply by considering velocity with its units of Length/Time:

$$S_v = \frac{S_L}{S_T} \tag{2.23}$$

So, rearranging for S_T gives:

$$S_T = \frac{S_L}{S_v} = \frac{S_L}{S_y^{1/2}} \tag{2.24}$$

2.4.6 Reynolds number

A second dimensionless number requiring consideration in the design of a model pond is the Reynolds number, which represents the ratio of inertial forces to viscous forces in the equation of motion. Here,

$$\mathrm{Re} = \frac{vy}{\upsilon} \qquad (2.25)$$

where, as discussed earlier,:

Re = Reynolds number;

v = fluid velocity,

y = characteristic length,

υ = kinematic viscosity,

For a high Reynolds number, viscous forces are small compared with inertial forces, whilst low Reynolds numbers characterise conditions in which viscous forces dominate. The transition from laminar to turbulent flow is determined primarily by the value of the Reynolds number *Re* of the flow, though the transition value of *Re* depends upon which type of flow (pipe, channel etc) is being considered. In the pond systems, the characteristic length is taken as the hydraulic mean depth, although, typically, the actual pond depth is simply used instead since the hydraulic mean depth tends to this value for wide and shallow flows .

2.4.7 Froude and Reynolds number similarity

The problem that will always arise when considering the application of these two dimensionless numbers is that dynamic similarity cannot be satisfied simultaneously for both *Fr* and *Re* when scaling down to a laboratory sized system. For example, for a length scale of 1:30 (model : prototype) and using the same fluid (water) in the model and prototype, the flow velocity in the model must reduced by $\sqrt{30}$ if Froude number similarity is to be satisfied, but must increase by factor of 30 if the Reynolds number is to be kept constant.

The only way, in principle, to satisfy both of the similarity conditions on *Fr* and *Re* is to alter the kinematic viscosity of the fluid used in the model. In fact, there is no fluid having the kinematic viscosity required to satisfy any scale other than full scale, for water as the prototype fluid. Thus, it is necessary to relax similarity constraints on either *Re* or *Fr* when carrying out scale model experiments. Because the properties of most turbulent flows do not change significantly with changes in *Re,* the similarity constraint on *Re* is often relaxed in hydraulic model studies of flows with free surfaces; in such circumstances the model is designed solely in terms of Froude number matching,

2.5 The reaction rate constant

One property all of the models presented in the preceding sections have in common is their dependence on the first order rate coefficient, *k*. Indeed, Thirumurthi (1974), stated that evaluation of *k* was the key to the whole design process.

As mentioned previously, the rate of pathogen and organic degradation/removal is typically assumed to follow first order kinetics. There has been little discussion in the literature of the validity of using the first order assumption, however; given its significance, it would seem to warrant more interest. Thirumurthi (1991), discussed a laboratory scale experiment that showed this rate could be proportional to the substrate concentration to the power of 1.1. Wood (1987), has also questioned the validity of this assumption as it implies the rates of processes such as oxygen mass transfer and algal growth are such that they are not rate limiting. In practice, the majority of researchers and designers have accepted the assumption of first order kinetics and have gone on to implement its use.

There are a large number of predictive equations for estimating the first order rate constant, *k*, for the removal of organic substrate and faecal coliforms. One of the better documented studies is that of Thirumurthi (1974), who published a relatively involved method of determining *k*:

$$k = k_s C_o C_{Te} C_{Toc} \qquad (2.26)$$

k_s a 'standard' value of *k*,

C_{Te} correction factor for temperature;

C_o correction factor for organic load;

C_{Tox} correction factor for industrial toxic chemicals.

Using data from the literature combined with results from a pond in Canada, Thirumurthi (*ibid*.) used the plug flow equation to back-calculate 'field *k*' values using the average influent and effluent BOD and the ponds theoretical retention

time. These 'field *k*' values were then adjusted for temperature and organic load to produce k_s values.

Thirumurthi (*ibid*.) reported that the average k_s value for all the ponds studied was 0.056/day and that the range was from 0.042 to 0.071/day. But these numbers were themselves based on averages of k_s values calculated for ponds at different times, and averages of multiple ponds at different sites. An example of this is a pond that had k_s values ranging from 0.0026 to 0.0968/day over the nineteen dates that data were collected. Overall the raw field values actually had a range of 0.0017 to 0.128/day!

This method of using field data to back-calculate *k* via one of the ideal flow equations is the usual method for determining *k* values. But, as illustrated in the example given above, this method has shortcomings. For example, Thirumurthi noted that fluctuations in the k_s values were partly due to the variation of the BOD over time. Additionally, the actual hydraulic characteristics of the different ponds were ignored by using the theoretical retention time.

There are many alternative approaches to Thirumurthi's work. For example, for BOD removal, Marais (1966), found that the best fit for experimental data was given by:

$$k_T = 1.2(1.085)^{T-35} \qquad (2.27)$$

Alternatively, Mara (1975) proposed:

$$k_T = 0.3(1.05)^{T-20} \quad (2.28)$$

where:

k_T first order reaction rate constant, (1/day);

T temperature, (^oC).

In addition to the removal of BOD, equations are also available for pathogen decay. However, the general approach in all these studies has involved back-calculation from field data via an ideal flow equation. In order to avoid the problems of the variation that result from using field data, a number of researchers have considered the use of laboratory-based studies for the determination and study of the first order rate constant.

In a more comprehensive study, Uhlmann (1979) examined the treatment performance of small model ponds as a function of organic loading, retention time and temperature. These ponds were fed on with synthetic wastewater and held under controlled artificial lighting. The reaction rate constants were then back-calculated via the plug flow equation. In a subsequent paper, Uhlmann *et al.* (1983) undertook a regression analysis of the data to produce an equation for prediction of the reaction rate constant based on organic loading, mean retention time and mean temperature.

Wood, (1987) reviewed the research of Thirumurthi and Nashashibi (1967), and Uhlmann (1979, 1983). He was particularly critical of the way these studies used the ideal flow models to back-calculate the reaction rate constants while, in

practice, the model ponds were fed in discrete daily additions. Using a semi-continuous flow model he re-calculated the reaction rate constants and showed that this procedure yielded significantly different results. Wood also went on to conclude that there was a need to determine the rate limiting steps and their kinetic parameters.

Most recently Brissaud *et al.* (2000) noted that rate constants given in the literature vary widely as a function of the water depth, temperature, solar radiation, organic load and the hydraulic model used. Because of this variation, they used pilot-scale experimental ponds to determine the reaction rate constant for faecal coliform removal in a maturation pond. Two pilot scale ponds were used, each of 1 m depth, filled with lagoon water and left exposed to the climatic conditions. The derived kinetic rate constant of 0.6 day^{-1} was then combined with tracer data information from a full-scale pond to predict theoretically the treatment efficiency of the full-scale ponds under study. These results compared very favourably with the actual treatment efficiencies measured for these ponds.

2.5.1 Degradation rate kinetics

The pattern of the depletion of pollutant with time is called degradation rate kinetics. The kinetics or the rate of degradation processes can be expressed quantitatively by the law of mass action, where the rate is proportional to the concentration of the reactants (Chapra, 1997; Hammer, 1896). Degradation rate kinetics can be estimated from measurements in laboratory tests, either in a closed system in the form of a batch test or in an open system with steady state conditions of flow rates, pollutant loads and pollutants leaving the system.

For open systems, the continuously stirred tank reactor (CSTR) can be used to develop degradation kinetics for continuously loaded reactors. As a completely mixed tank with a fixed volume *V*, an inlet flow rate Q_{in}, an outlet flow rate Q_{out} and influent and effluent concentrations C_{in} and C_{out} the change of concentration in the reactor can be described as follow:

$$V\frac{dC}{dt} = Q_{in}C_{in} - Q_{out}C_{out} - kVC_{out} \tag{2.29}$$

In the completed reaction or the steady state condition $dC/dt = 0$ and $Q_{in} = Q_{out} = Q$, so we obtain:

$$C_{in} - C_{out} - k\frac{V}{Q}C_{out} = 0 \Rightarrow C_{out} = \frac{C_{in}}{1 + k\frac{V}{Q}} \tag{2.30}$$

where $V/Q = HRT$, the hydraulic residence time of the reactor. So, the plot of the ratio C_{in}/C_{out} versus the residence time will therefore give a line whose slope is *k*.

For Batch Tests, with a constant volume of a medium that contains a pollutant of an initial concentration $C_P = C_0$ assumed, the change in concentration C_p of a substance with time *t* in this volume can be expressed as:

$$\frac{dC_p}{dt} = -kf(Cp, Cw, ...) \tag{2.31}$$

This relationship specifies that the rate of reaction is dependent on the product of a temperature dependent constant *k* and a function of the concentrations (C_p, C_w…) of the reactants. The functional relationship can be determined experimentally. So, the above equation can be rewritten as:

$$\frac{dC_p}{dt} = -kC_p^{\alpha}C_w^{\beta} \tag{2.32}$$

$$\frac{dC}{dt} = -kC_{aw}^{n} \tag{2.33}$$

where

C concentration of each reactant

k the reaction rate

n the reaction order

In water research, values of n = 0 or n = 1 are mostly used and the following calculations follow:

With n = 0 and the initial conditions of $C = C_0$ at t = 0:

$$C(t) = C_0 - kt \tag{2.34}$$

When n = 1:

$$\ln C - \ln C_0 = -kt \Rightarrow C(t) = C_0 \exp^{-kt} \tag{2.35}$$

This model describes an exponential degradation and the plot of concentration versus time shows a decrease to an asymptotic value of zero (Figure 2-8). The case of non-zero background concentrations necessitates the introduction of a further parameter, C^*, in addition to the first order rate constant k to model field observations as below:

$$C(t) - C^* = (C_0 - C^*)\exp^{-kt} \tag{2.36}$$

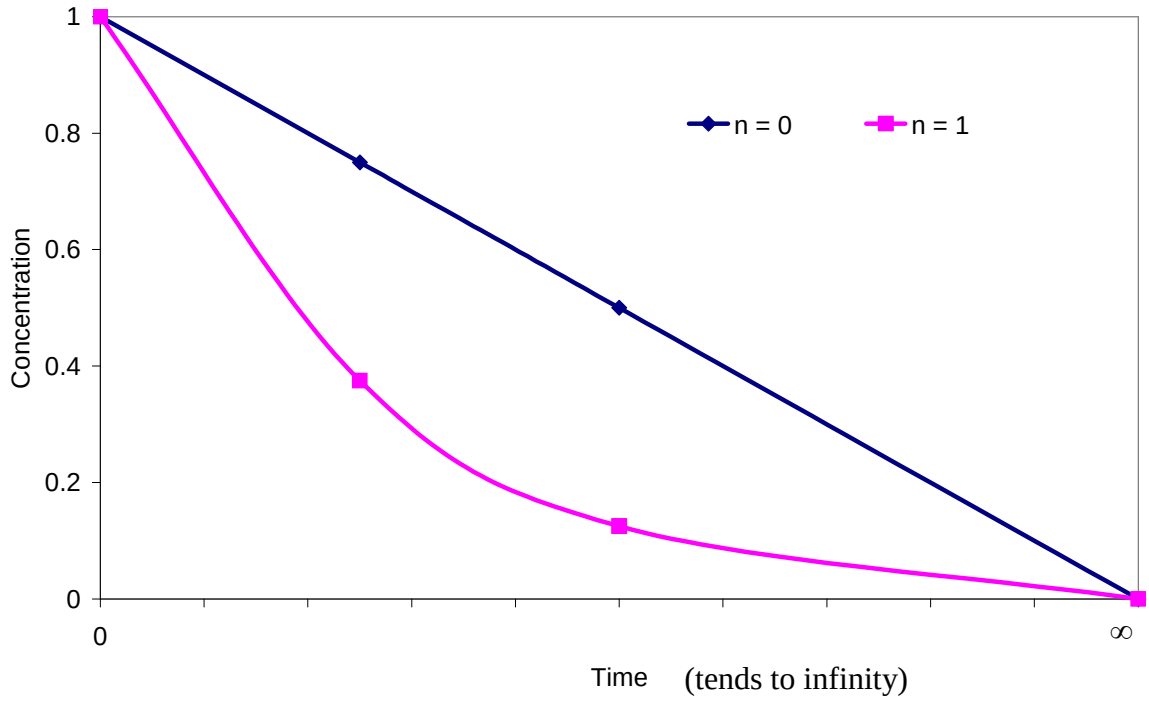

Figure 2-8. Pollutant degradation with time for zeroth-order (n = 0) and 1st-order (n = 1).

2.6 Tracer Studies and Particle Image Velocimetry

To date, the large majority of all research investigations into pond, wet-pond, and wetland hydraulics has been based upon the use of fluorescent tracing techniques (*e.g* Stimulus response technique).

2.6.1 The Stimulus response technique

This method involves disturbing a system and measuring how it responds. The response data are then analysed to determine the system characteristics. In fluorescent tracer studies, the initial input to the system may be random, cyclic, step-like or pulsed as illustrated in Figure 2-9. The simplest and most commonly used technique is the pulse input where a slug of tracer is added at the inlet and the subsequent tracer concentration at the discharge from the pond is measured at the outlet or anywhere between the inlet and the outlet.

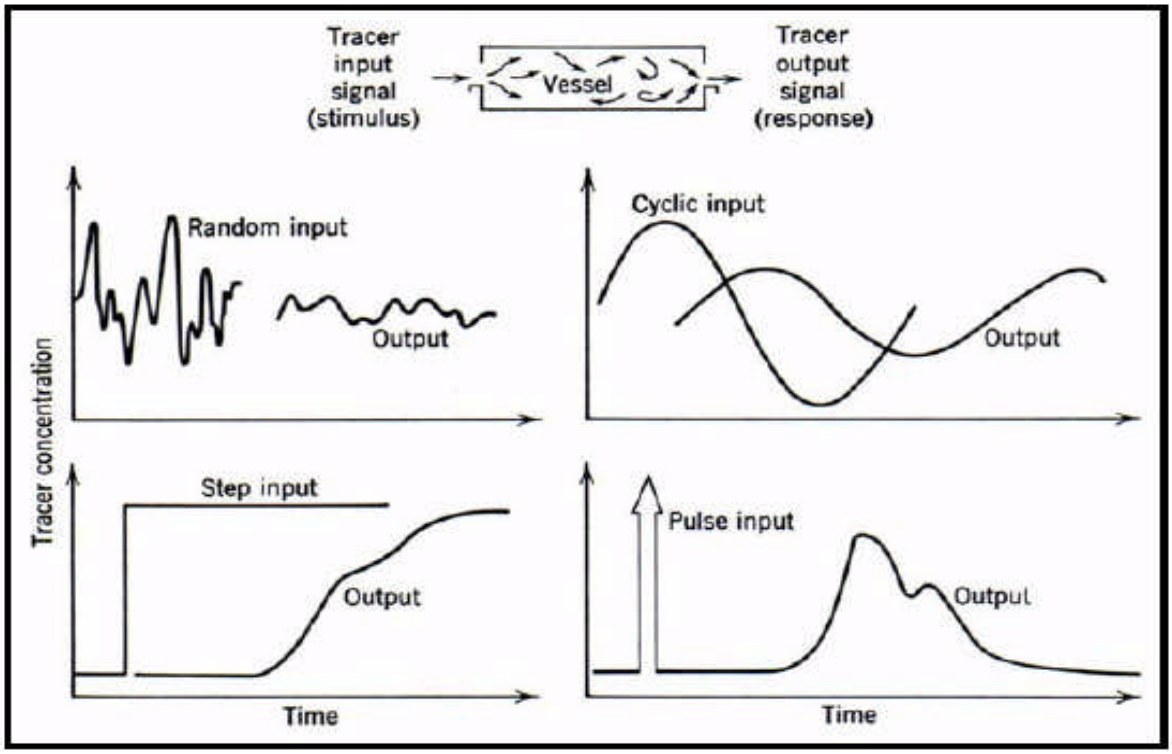

Figure 2-9. Levenspiel Tracer Technique (Levenspiel, 1972, pg.256).

The hydraulic retention time distribution curve covers the time from the addition of the tracer (at the starting time t = 0), until the first tracer is measured leaving the outlet and then continues until the average gradient between a few measurement points is equal to zero. The other key factors that can be determined from the response data are the mean travel time and the dispersion number. The dispersion number has been discussed in section 2.3 and 2.4, where (in 2.3) another fundamental expression of dispersion number is introduced, namely the variance, σ^2, which is a measure of the spread of the HRTD.

2.6.2 Previous tracer studies

There are many sources of information on wastewater treatment systems. This literature review has reviewed the information most relevant to this project. The

large majority of the research undertaken on pond hydraulics has used the stimulus response tracer technique. Previous studies, amongst others, include Shilton (2005), Wörman et al (2007); Wörman and Kronnäs (2005); Schmid (2004); Mangelson and Watters (1972); Racault *et al.* (1984); Chapple (1985); Macdonald and Ernst (1986); Marecos do Monte and Mara (1987); Moreno (1990); Uluatam and Kurum (1992); Pedahzur *et al.* (1993); Fredrick and Lloyd (1996); Wood (1997); Salter (1999); Brissaud *et al.* (2000); Shilton *et al.* (2000); and Vorkas and Lloyd (2000).

Two works (Wörman and Kronnäs 2005; Wörman *et al*., 2007) provide information on the effects of heterogeneous vegetation in treatment wetlands. Both use tracer studies in the field, along with numerical simulations to research the HRT. By comparing the simulations with observations, it is possible to change factors to see if they can reproduce the observed results and hence explain what may have caused them.

Shilton, 2005) provides a useful introduction to wastewater treatment, with very relevant and essential background information on pond treatment technology. A problem with performing tracer studies in the field is that it is hard to vary conditions to see how they influence the HRT. The HRT can only be investigated under the vegetation conditions present in the pond at the time of the study. This makes it hard to see what effect vegetation has, as it cannot be easily varied. Wörman *et al* (2007), in their paper on the Ekeby Wetland treatment in Sweden, highlight some of the uncertainties in the methods used to calculate HRT. The

nominal residence time is made uncertain by the variation of inflow over time and the inability to accurately estimate the volume of water in ponds in the field.

The tracer study results from the field however mean that the results from the simulation can be compared to observed results in both these papers. Having two sources of data will mean that any conclusions drawn are more reliable because data from the two sources can be compared. Although the data in both these studies were collected in a different way from that adopted in this project, the general effects that vegetation was found to have will still apply.

Two sources of research which provide information on the use of scale model ponds in a laboratory are drogue tracking by image processing for the study of laboratory scale pond hydraulics (Wörman and Kronnäs 2005), and salt tracer experiments in constructed wetland ponds with emergent vegetation (Schmid, 2004). In a paper on drogue tracking by image processing (Wörman and Kronnäs 2005) provides very relevant information on the use of scale models to investigate pond retention times. The paper is very useful as it highlights the flaws with stimulus response tracer studies research. The main problem highlighted is that stimulus response tracer studies do not directly quantify the flow velocity and mixing patterns that exist in the pond. The paper describes an alternative technique to improve the study of a flow regime in a pond by image processing. The paper also highlights the advantages of using a scale model pond for researching pond hydraulics.

In a paper on salt tracer experiments in constructed wetland ponds with emergent vegetation, Schmid (2004), researches the formation of density stratification due to

salt tracer injections. The injection of salt (which has a higher density than the freshwater into which it is injected as a tracer) can have strong density effects that will influence the usefulness of breakthrough curves. The retention times found in this article will suffer from these effects, meaning that any retention times gained may not be useful. However, information regarding the modelling of vegetation can be used. The vegetation simulated was uniformly distributed unlike other research which had heterogeneous vegetation.

Other less relevant papers include Persson (2000), which focuses on 13 ponds with hypothetically-different layouts and analyses how the hydraulic performance differs and Kadlec (1990), which reports a detailed investigation into vegetation and the water flow around vegetation.

Mangelson and Watters's (1972) study is one of the earliest and most extensive. This work involved a series of studies on both field ponds and a physical model. The study using the physical model is reviewed in section 2.7.5 below. Their field studies were undertaken on three ponds of a seven-pond system located in Logan, Utah, using rhodamine WT as the tracer. Two tracer studies were undertaken on one pond while a single study was performed on each of the other two. The authors make little comment on these field studies apart from comparing their dimensionless hydraulic characteristics with those obtained from their scale model ponds so as to validate the physical modelling technique that was then used in more extensive studies

More recently Frederick and Lloyd (1996), undertook an evaluation of the retention time and short-circuiting in a waste stabilisation pond in the Cayman Islands using

Serratia marcescens bacteriophage as a tracer. They determined that while the theoretical retention time for the facultative pond under study was 11.5 days, the experimental mean retention time was less than 2 days with the first elements of tracer short-circuiting through the system in only 3-6 hours. They noted that thermal stratification was not present in the pond and mainly attributed the short-circuiting to the prevailing wind that was believed to drive the influent quickly down the length of the pond to the outlet. Vorkas and Lloyd (2000) presented another of the most recent papers in this area. They reported on a tracer study undertaken on a pond system in Colombia. Again severe short-circuiting was evident. After only 6 hours, 1% of the tracer had already left the pond, where the theoretical retention time, t_n, was 11.5 days.

Wood (1997), reported that tracer studies using Rhodamine WT were undertaken on ten ponds in Tasmania, Australia, as part of a study undertaken by the Department of Environment and Planning. Five of these were undertaken on non-aerated ponds, but of these two were noted as having “inaccuracy in flow and geometric data”. The remaining three ponds were all at one site operating in parallel and had similar sizes and flow-rates. Wood (1997) reported that they had a theoretical retention time of 46 days each. The ponds were configured to test the effect of a baffle and different inlet/outlet arrangements. Unfortunately, the tracer studies were only conducted for 17 days. It might also be noted that in presenting these results, two of the curves start with a high concentration at zero time, which is erroneous. After presenting this information, Wood reported that the similarity of the tracer results made them unsuitable for modelling and suggested that wind effects were probably to blame for this. Wood (1997) then reports on a

second experimental programme undertaken on sugar mill ponds near Mackay in Queensland, Australia, as part of a Sugar Research and Development Corporation project. Tracer studies were conducted on the third and fourth pond of a five-pond system each of which had a theoretical retention time of 9.5 days but the measured value was 4 days only.

Salter (1999) reported on tracer studies carried out using sodium fluoride, at the Holm Wood and Chesham wastewater treatment plants in England. The Holm Wood study is interesting in that it was operated at an extremely short retention time. The mean retention time was found to be 26 hours, which was in close agreement to the calculated theoretical retention time. Salter (*ibid*) reported that the peak in tracer concentration occurred after 12 hours, showing significant short-circuiting. However, in comparison to other studies, the fact that the peak is not reached until halfway to the mean retention time would, conversely, be considered as demonstrating excellent hydraulic performance.

Salter (1999), reported that the short-circuiting was greatest when the flow was high (Test 1), but that the best hydraulic regime also occurred under high flow conditions (Test 2). This study is relatively unique in that it has presented three replicate tracer experiments on a single field pond. The results clearly indicate that some significant degrees of variation can occur between different studies in the same pond. Salter suggested that this may have been due to climatic conditions such as thermal stratification or wind.

Shilton *et al.* (2000) presented replicate tracer studies obtained from work undertaken on a pond at the Linton Army Camp in the Manawatu region of New Zealand. The tracer response curves in this study show a very rapid rise to a high peak, followed by a slow, steady decline with a long tail. The authors described the curves as similar to what would be expected from a mixed reactor suffering from short-circuiting. Using the tracer information collected, a method described by Levenspiel (1972) for analysis of nonlinear reactions in reactors having non-ideal flow, was used to calculate treatment efficiencies. The authors used this calculation to illustrate that the initial period of the tracer data, corresponding to very short retention periods, accounts for the majority of the pollutant that escapes treatment in the pond system. This highlights the potentially severe impact that short-circuiting can have on attempts to achieve high treatment efficiencies. In the context of pond hydraulics research it also highlights the importance of acquiring adequate data in the initial stages of a tracer study.

Practically every researcher who has undertaken a tracer study has noted the existence of hydraulic short-circuiting. However, these comments have only ever been made in the context of the particular studied system. Given this consistent pattern, it is now perhaps appropriate to conclude that this behaviour is, indeed, a fundamental characteristic of all pond systems.

The limitation of stimulus response tracer studies is that they provide only 'black-box' results rely very much on the effects of vegetation condition and pond shapes (mainly focus on the rectangular tanks only). Few traces have been conducted on the physical scales and prototypes and the data they produce is a function of the

fluid flow pattern within the pond, but this technique gives no direct insight as to what is the effect of vegetation and discharges on the flow patterns are.

2.6.3 Particle Image Velocimetry (PIV), MatPIV

Shilton (2007) using a drogue tracking technique to determine flow fields in the ponds. The use of surface drogues for the measurement of water currents is not new, but they are more typically found in studies of larger water bodies with nearly uniform depth. Martin *et al* (1990) used drogues for their studies of advective transport in small aquaculture ponds; Shilton (2007) used the technique to study the speed and direction of the fluid movement in the model pond as many instruments were ruled out because of the very low velocities found in the ponds or the other instruments were expensive or not available for the project. The flow measurement software MatPIV, is similar but more flexible than drogue technique which can measure speed and direction of fluid movement in the diversity depth of model pond. MatPIV is a program written by Sveen (see Sveen and Cowen, 2004) and is based on 3 different sets of demo-images which are taken from the papers by Grue *et al* (1999) and Jensen *et al* (2001). It is one of at least three available, free toolboxes and is by far the largest presently available, both when functionality and number of users are considered.

Particle Image Velocimetry is a relatively old technique but it has only become a ‘digital’ tracking process within the last 15 years; it is an effective tool for the investigation of pond retention times and is considered to be a simple yet effective method of illustrating flow effects. Its use enables us to calculate the length of time for which water has been held in a pond. With this information gathered, one can start to gain an idea of the water quality in a pond and furthermore set about

making changes to the pond to achieve an optimum holding time. This review is intended to discuss the technical concepts on which PIV is based, the retention times for ponds and previous literature on and surrounding the subject such as:

a) Specifying the coordinate system

b) Masking out regions of the flow

c) Calculating velocities

d) Filtering the result

e) Visualizing the results

Gurlek and Besir (2010) studied by means of PIV the flow structure around a rectangular body located close to a ground board in a free-surface water channel. The rectangular body was set with $\alpha = 0^o$ and $\alpha = 10^o$ yaw angles referenced to the flow direction and measurements were performed on the vertical and horizontal planes. The PIV technique provides instantaneous and time-averaged flow fields. For $\alpha = 0^o$, the results indicated that the flow structure in the wake region varied significantly with the elevation level from the ground surface. An asymmetric large circulating flow region was identified in the wake region for $\alpha = 10^o$. The instantaneous flow fields revealed the presence of small-scale-vortices in the main flow over the separation line. The vortices emerging from the leading edge of the model rotated in the flow direction, giving rise to entrainment between the incoming and wake flow regions.

In Rostami *et al* (2007), the study focussed on a comparison of both white light PIV measurements and empirical data and CFD simulation. The objective of the work was to assess the white light sheet PIV as a cost-effective and safe alternative for laser systems whilst keeping the accuracy limits required for

hydraulic model tests. The accuracy requirements for experimental work in hydrodynamics are usually less stringent than in aeronautical and mechanical engineering. Models in hydraulic engineering are larger, so that measurement volumes and light sheets can also be larger and wider. In addition, many hydraulic engineering laboratories consist of open spaces, so that the safety precautions required for laser work can be very difficult to implement. A white light (WL) source of PIV applications results in significantly easier experimental conditions as well as substantially reduced costs. It should be noted that the price of this system is very low when compared with using laser PIV model (almost 1:300). The development of a white light source for PIV applications means that experiments can be conducted with a standard PIV system in virtually any locations. The study shows that, based on WL PIV measurements, the mean velocity profile of each experiment had an excellent agreement with the empirical results. The comparison of WL PIV with CFD simulation velocities indicated that in a range of velocity between 0.095 to 0.194 m/s, the general error of the PIV measurement was an average of about 0.5 to 1.5%. This finding provides further evidence that WL PIV can be applied successfully in open channel flow analysis and open space experimental runs.

Hoyt and Sellin (2000) studied a comparison of PIV results with those obtained using a newly developed turbulent-flow tracer, for flow around a shallow-immersion cylinder and showed that the tracer and PIV displays give almost identical indications of the flow patterns. Since the tracer results are obtained on video, time-dependent streamline information becomes available, thus allowing detailed analysis of fluctuating flows.

Ismail and Ulrich, (2007) focussed on large scale PIV-measurement on the water surface for turbulent open-channel flows, in order to investigate the effects of processes in the water column on the dynamics of free surface flow. Three different sets of PIV measurements revealed a clear surface pattern of secondary currents of a second kind. The long-term temporal average of large stream-wise vortices in the water column results in relatively stable secondary currents of alternating sense of rotation scaling with water depth. Stable large stream-wise vortices always occur close to the sidewall and their successive superposition generates secondary currents in the long term. Vortex structures are detected from the instantaneous velocity map of water surface obtained by using a reference frame technique and from moving camera PIV measurements. Vortex visualization experiments show vertical motions with a vertical axis, mainly associated with up-welling regions of the secondary currents. The vortex size was found to be roughly equal to the water depth.

2.7 The Knowledge Gaps Prior to the Study

To summarise, the knowledge gaps prior to this study have shown that there was insufficient experimental evidence, either at full or model scale on the effect of different vegetation distributions and discharge on the hydraulic residence time distribution. Moreover, there was no previous natural pond study on the effect of different vegetation distribution and discharge, on surface flow fields of the whole pond. For example , Kjellin *et al* (2007) and Worman and Kronnas (2005) looked at the controlling factors for water residence time and the flow patterns in Ekeby treatment wetland in Sweden and the effect of pond shape and vegetation heterogeneity on flow and treatment performance of constructed wetlands. Kjellin et al (2007), used only one tracer experiment to describe the impact of different

factors on water flow patterns and then used computer simulations, (2D flow, transport model) to evaluate the relative importance of bottom topography, vegetation distribution, water exchange with stagnant zones and dispersion. The results concluded that the bottom topography of the pond decreased the variance in water residence times to a minor extent (only 10%), whereas, heterogeneity in vegetation significantly contributed (60-80%) to the spread in hydraulic residence times. Kjellin *et al* (2007) have indicated that there were uncertainties in the method used to calculate HRT, by the variation of inflow over time and in the ability to accurately estimate the volume of the ponds. Most other published tracer studies concluded that in the field it is hard to vary conditions to see how they influence the HRT, as the HRT can only be investigated under the vegetation present in the pond at the time of the study.

Secondly, there were inconsistencies in the findings of different researchers comparing the actual residence time with the theoretical residence time. For example, Kjellin *et al* (2007), indicated the actual residence time greater than the theoretical residence time (t_m = 4.2 days > t_n = 3.1 days), whereas this result is inconsistent with many other research. In general with different wetland and pond treatment systems the theoretical residence time is far longer than the actual residence time.

Next, most of previous research has shown a lack of repeat measurements in the field and there is no previous study looking on the physical model of the wetland pond except the physical scale model of the waste stabilization pond. This indicates there is a need for the experiment on the physical scale model and more accurate or different measurement of quantities such as a contiguous measurement tracer, as well as particle image velocity, looking on the whole flow profiles of the system.

Finally, previous field work was limited due to discrete sampling $\Delta t \approx 1$ hr due to limitations of man power or it was too expensive to achieve $\Delta t \approx 1$ min. New equipment allows continuous measurement. Laboratory and field work has been limited as no measurements of the very low velocities or the flow profiles was

possible without disturbing the flow. digital cameras; the availability of computers and digital cameras etc now allow the use of PIV.

CHAPTER: III

3 Methodology

3.1 Preliminary set up on Physical Models

A physical model, tested under controlled conditions in a laboratory, appeared to offer a useful tool for gaining improved insights into the hydraulic characteristics of treatment ponds. The work undertaken by Shilton (2007) focussed on refining this experimental technique and identifying potential sources of error and external influence. His work considered thermal convection, air shear, the inlet energy, molecular diffusion, the gravitational spread of tracer, vibration and the Coriolis force. To avoid these effects, new experiments were set up and run with the following condition:- The potential influences of molecular diffusion, the Coriolis force and vibration were ruled out from having significance in these experiments due to, respectively, the high velocity at the pond inlet, the small horizontal scale and the stability control in the laboratory environment . The effect of air shear could also be eliminated by locating the model pond within the confines of an

enclosed room and by covering the model with plastic. The effect of thermal convection and the gravitational spread of tracer were minimised by installing two water tanks to control the temperature of the inlet water to the pond system.

3.2 Design of Laboratory Model

As discussed in Chapter 2, the experimental design of scale models requires application of the principles of similarity and dimensional analysis if they are to yield meaningful results that are representative of full-scale systems.

3.2.1 Adoption of Froude Number Similarity

For reasons outlined previously (Section 2.4.5), it was decided to design the laboratory pond model according to Froude number similarity. It was understood from the outset of this study that Reynolds number effects may be important to consider for flow velocities, so that a minimum Reynolds number criterion was proposed. For such a given Reynolds number, if the water depth in the model is known then a corresponding minimum flow velocity in the model pond can be calculated.

As discussed later in this chapter, the depth of the laboratory pond was selected to be 250 mm. This meant that for a Reynolds number of 500 (the threshold assumed for laminar flow in an open channel) the minimum velocity criterion was $U < 2$ mm/s, see section 2.4.6. As the flow velocity varies throughout the pond there is a wide variation of Reynolds numbers within the system. However, particular attention should be given to the main flow path for this carries the tracer from the inlet to the outlet and disperses it into the main body of the pond. The difficulty in assessing the potential effect of the in-pond Reynolds number is that it

is not until the experiment is set up and data are actually obtained, that the local Reynolds numbers can be determined.

3.2.2 Model Pond Roughness

Once the dimensions of the model pond have been determined by scaling with S_L and S_y and the model's flow rate and residence time have been calculated by scaling with S_Q and S_T, the design should ensure that the surface of the model has the correct roughness.

Manning's equation for wide, open channel flow is defined as:

$$v = \frac{y^{2/3} s^{1/2}}{n} \tag{3.1}$$

where:

v = velocity, (m/s);

n = Manning's roughness coefficient (s/m$^{1/3}$);

y = depth of fluid, (m);

s = hydraulic gradient = head loss, h (m) over a horizontal length, l (m).

Rearranging for n gives:

$$n = \frac{y^{2/3} s^{1/2}}{v} = \frac{y^{2/3}}{v}\left(\frac{h}{l}\right)^{1/2} \tag{3.2}$$

To determine an appropriate scale factor for model roughness, S_n, consider the above equation in terms of its scale factors:

$$S_n = \frac{S_y^{2/3} S_y^{1/2}}{S_v S_L^{1/2}} \tag{3.3}$$

Substitute equation (2.18) into equation (3.3) then:

$$S_n = \frac{S_y^{2/3} S_y^{1/2}}{S_y^{1/2} S_L^{1/2}} = \frac{S_y^{2/3}}{S_L^{1/2}} \tag{3.4}$$

In undistorted modelling applications, the hydraulic gradient is unchanged between model and prototypes. For a 'dredged earth canal' Douglas *et al* (1995) and Chow (1959) cite values of Manning's roughness coefficient of 0.025 to 0.033. For this example, a value of 0.03 was assumed. Therefore, for a 1:15 scale model:

$$n_m = 0.03 \frac{S_y^{2/3}}{S_L^{1/2}} = 0.03 \frac{\left(\frac{1}{15}\right)^{2/3}}{\left(\frac{1}{30}\right)^{1/2}} = 0.027 \tag{3.5}$$

To translate this into a particle size for construction of the model pond the Strickler equation (Raudkivi,1998) can be used:

$$n = \frac{\frac{1}{0.5^{1/2}} D_{50}^{1/6}}{20} \tag{3.6}$$

where D_{50} is the 50-percentile particle diameter of a particle size distribution, (m). Substitute equation (3.5) in (3.6) then this can be calculated as:

$$D_{50} = ((0.5)^{1/2} 20 n_m)^6 = 3.11mm$$

3.2.3 Froude Number-based design of model and prototype pond specification

The details of the prototype which exists in Sweden and upon which the present model studies are based are:

Length $_{Prototype}$	=	60 m	(external scale only)
Width $_{Prototype}$	=	60 m	(external scale only)
Depth $_{Prototype}$	=	2.5m	(maximum water depth)

The model pond was designed to be the largest size that could be practicably accommodated into the constant temperature laboratory used for this study. The resulting external dimensions of the model used are:

Length $_{model}$ = 2 m (1/30 of Length $_{Prototype}$, external scale only)

Width $_{model}$ = 2 m (1/30 of Width $_{Prototype}$, external scale only)

Depth $_{model}$ = 0.175 m (1/15 of Depth $_{Prototype}$, maximum water depth)

Reducing the depth of the model pond result in increased problems with small irregularities in the pond level and excessively low Reynolds numbers. With regards to the effects of surface tension on the model pond, Shilton (2007) suggested this could influence the results at depths of less than 30 – 40 mm and, therefore, the model depth should be kept above 60 – 70 mm.

Increasing the depth means that the pond represents a smaller full-scale prototype. After consideration of these factors the model was scaled to 1:15 of the real model, with maximum water depth of 170 mm. However, due to inaccurate information on the original scale, the design was changed from 1:15 to 1:30 for horizontal scale (length and width) and still 1:15 for vertical scale (water depth), Figure 3-1 and Appendix A. This then sets the pond volume as:

V_{model} = 0.179 m^3

From this basis, the scaling factors for the flow and time can be calculated using the relationships derived in equation (2.22).

$$S_Q = S_y^{3/2} S_L = \left(\frac{1}{15}\right)^{3/2}\left(\frac{1}{30}\right) = 1742.84 \tag{3.7}$$

$$S_T = \frac{S_L}{S_y^{1/2}} = \frac{30}{15^{1/2}} = 7.746 \tag{3.8}$$

With regard to wall roughness, the calculations undertaken in previous sections indicated the 50-percentile particle diameter required was 3.1 mm. To create this roughness, appropriate sand was applied using a marine paint to the bottom and sides of the model pond.

The inlet was fabricated using two small V-notch weir tanks connected in series, in order to stabilize the pulse discharge from the peristaltic pump, connected to the model pond by pvc tubing, Figure 3-1. The outlet from the pond consisted of a weir plate through the end wall of the pond at a depth of 0 mm to control pond water level. On the outside, a weir plate, connected to the pond's overspill riffle, was fixed to the pond's frame with the flow discharging into a funnel and then pumped through a fluorometer sampling system, see Appendix A, Figure 3-2 and Figure 3-3.

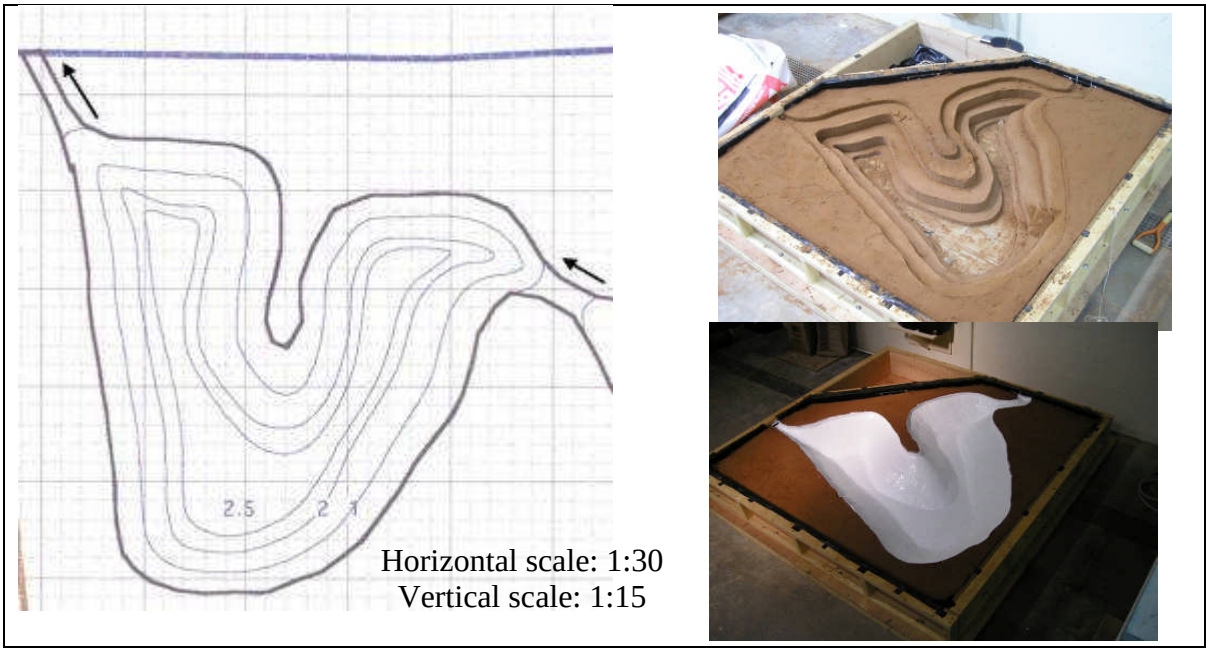

Figure 3-1. Construction of physical scale model, pictures taken by Ian C. 2007.

3.2.4 Data Collection

To quantify the hydraulics within the model pond, tracer analysis was employed. This technique is described in the following sections.

3.3 Tracer Studies in Model Pond

The use of a tracer is a common method for studying the hydraulics of reactors and was used in this work. This technique and its associated theory are well documented by Levenspiel (1972) and has been summarised in the literature review, Section 0.

By plotting the tracer concentration leaving the system over a period of time after an instantaneous or slug input, the retention of fluid elements within the pond is characterised. This plot is generally known as the hydraulic retention distribution time (HRTD). The HRTD is a function of the fluid flow pattern that exists within the pond itself, as discussed in the previous section 2.3. Measurement of the HRTD is very useful as it defines the overall response of the system and allows the 'cause'

(flow pattern) and the ‘effect’ (distribution of fluid elements over a period of time) to be compared. Additionally, the HRT distribution provides experimental data against which a mathematical model can be evaluated. The centroid of HRTD is the Actual Hydraulic Residence Time (HRT or t_m), so it is an essential quantity as it defines the centroid of mass of the trace which can used to compare with the theoretical residence time ($t_n = V/Q$).

The tracer used in this work was Rhodamine WT. This is a fluorescent tracer capable of being accurately measured at very low concentrations, thereby allowing very small quantities to be used as the slug injection. After the addition of a slug of tracer at the inlet, the concentration leaving the outlet was determined using a fluorimeter (AU-10 Turner Designed). The experimental set-up of this technique is shown in Figure 3-2 and Appendix A below:

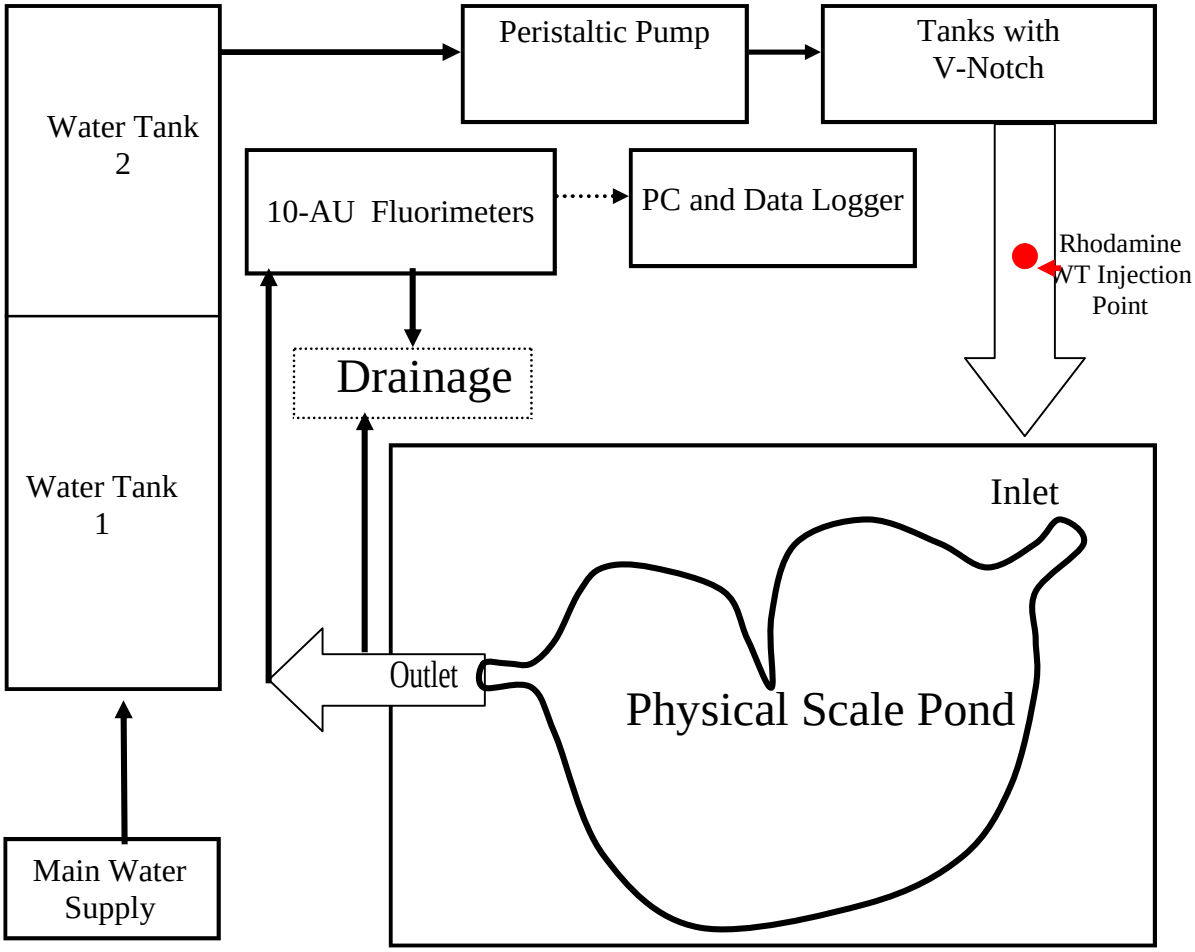

Figure 3-2. Experimental set-up for tracer study on physical scale pond.

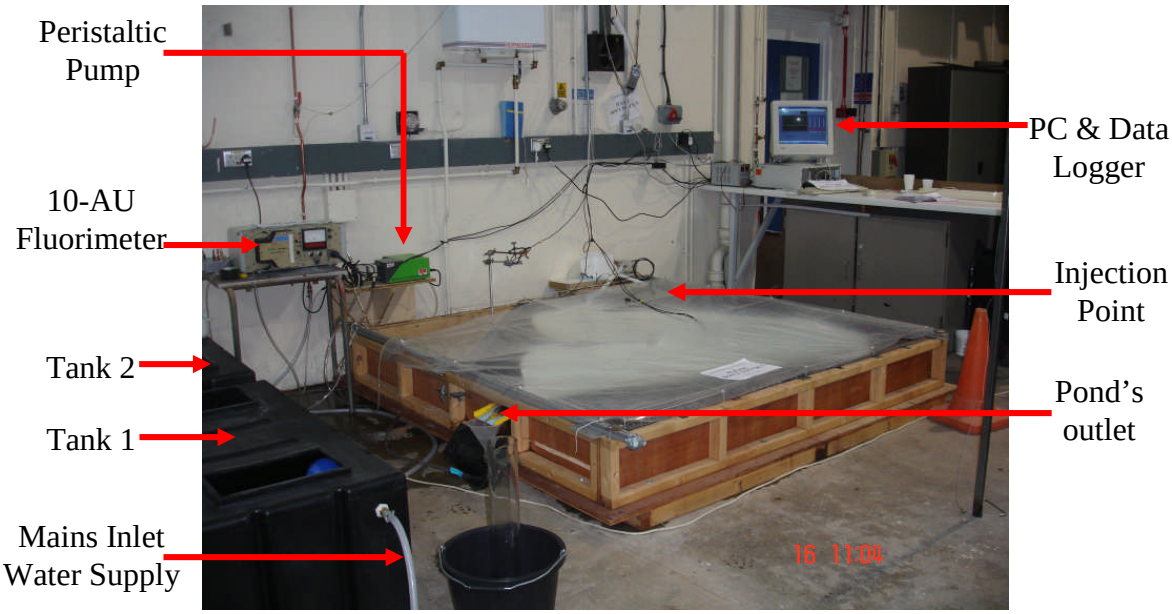

Figure 3-3. Picture of experimental set-up of tracer study on physical scale pond.

In the majority of the experiments, a 1:100 dilution by volume of the tracer concentration was used. The main reason for diluting the stock solution came from the observations in the preliminary research which showed that in high concentration, the tracer was more inclined to settle due to greater density, rather than be freely carried along with the inflow as required.

The 10-AU Fluorometer was calibrated at X1 with manual step so that the voltage produced could be related to outlet concentration based on different standard calibration curves as shown in Figure 3-4, Figure 3-5, Figure 3-6 and Appendix A.

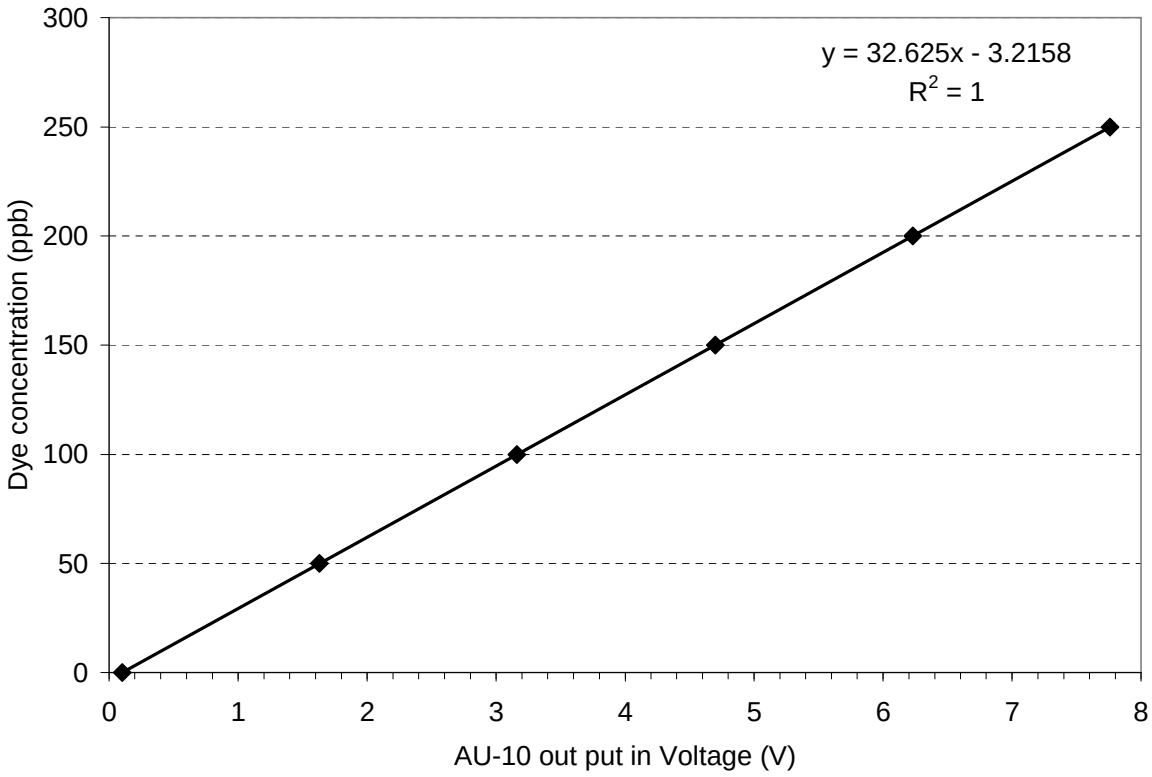

Figure 3-4. Au-10 Fluorometer calibration chart (Phase I on 04 March 2008).

The 10-AU calibration equation of Y= 32.625*X -3.2158 has been used to convert the output results from 10-AU as voltage to parts per billion (ppb). 100 experiments have been used to establish this calibration equation, where all those experiments which have been run in between 16 February to 30 September 2008, see Appendix A, and the example in Figure 3-6.

Due to the long period of experimental runs, the gradually-changing background condition of the pond's water led to changes in reading sensitivity of 10-AU Fluorometer. Different 10-AU calibration equations have been obtained such as Y= 253.16*X - 5.0633, Y= 288.21*X + 1.0809, Y= 521.55*X – 9.5809 and Y= 638.33*X -1.689, Figure 3-5, in order to convert the output results from 10-AU as voltage to ppb for different conditions.

(As shown in Appendix A, the calibration equation, Y= 253.16*X - 5.0633 has been used for 14 experiments starting from 12 February to 30 March 2009; the calibration equation, Y= 288.21*X + 1.0809 has been used for 19 experiments from 1st April to 2nd June 2009; the calibration equation, Y= 521.55*X – 9.5809, has been used for 6 experiments run starting between 4th to 24th June 2009 and the calibration equation, Y= 638.33*X -1.689, has been used for 6 experiments from 30th June to 8th July 2009).

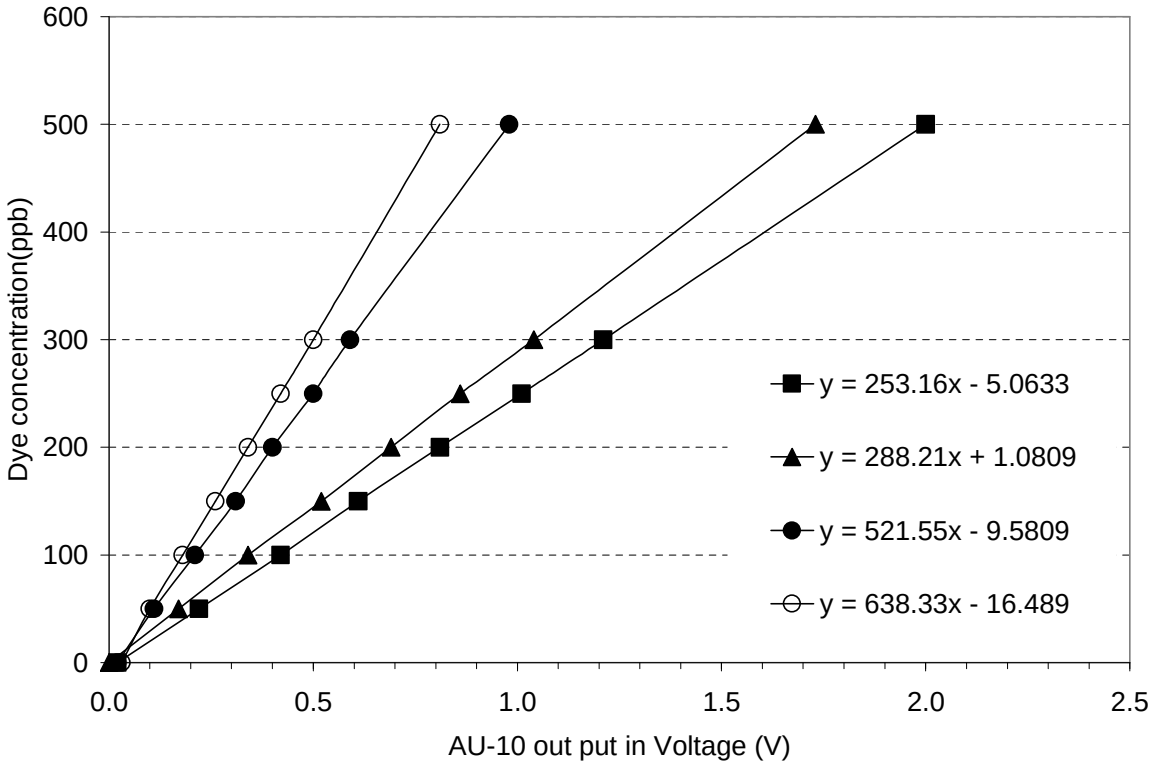

Figure 3-5. Au-10 Fluorometer calibration chart (Phase II and III).

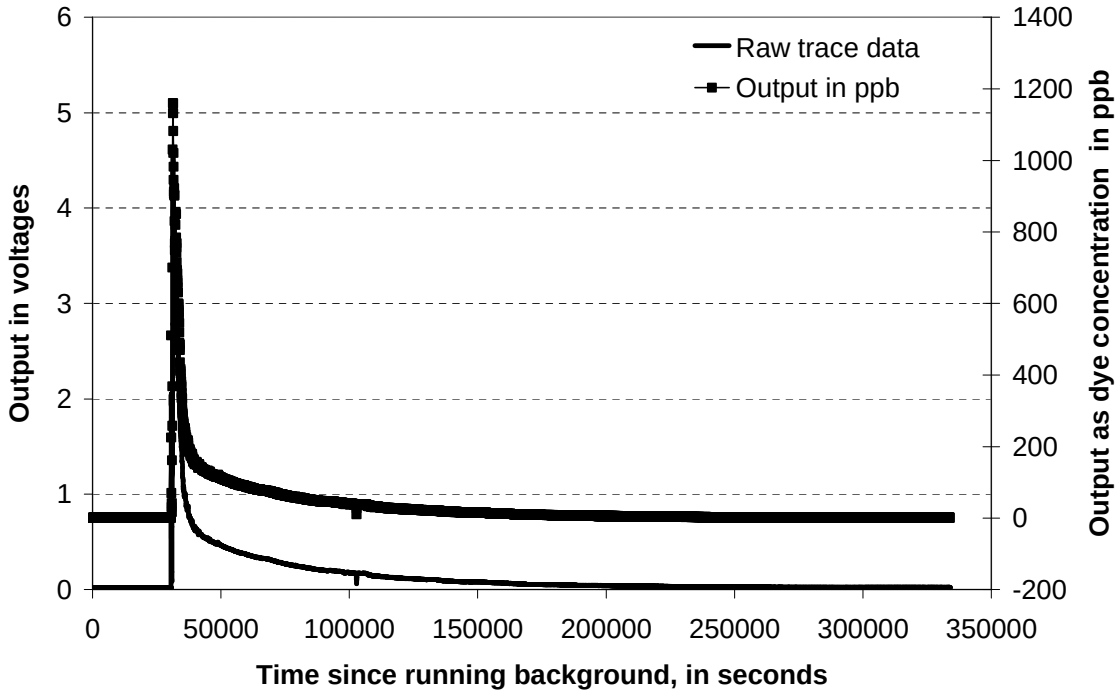

Figure 3-6. Example of the conversion of raw trace data to trace data with dye concentration using calibration equation curve Y= 253.16*X -5.0633.

The early and late 200 points background of each trace have been used to remove the background levels from the raw data of HRTD of each trace, see Appendix A and example in Figure 3-15.

For runs, with different discharge and vegetation, different quantities of tracer were added with the aim of maximizing the response from the fluorometer (for improved resolution and, therefore, accuracy) without exceeding the maximum value (1000 - 1500 ppb) below which the fluorometer could be used. For the purpose of comparison between these different experimental runs and against mathematical modelling simulations, it was necessary to standardise the output data. The typical approach (Kadlec & Knight,1996) is to make the results dimensionless so that the area under the HRTD plot is relative to the peak concentration of the trace (where it assumed that the all peak concentration of each trace is equal 1) and the relative time of the trace where the dimensionless of the time is equal to t_m/t_n whilst t_n is assumed to be 1. An example of dimensionless chart for a discharge 4.4 ml/s at 0E vegetation condition, showing both relative peak and relative time, is illustrated below.

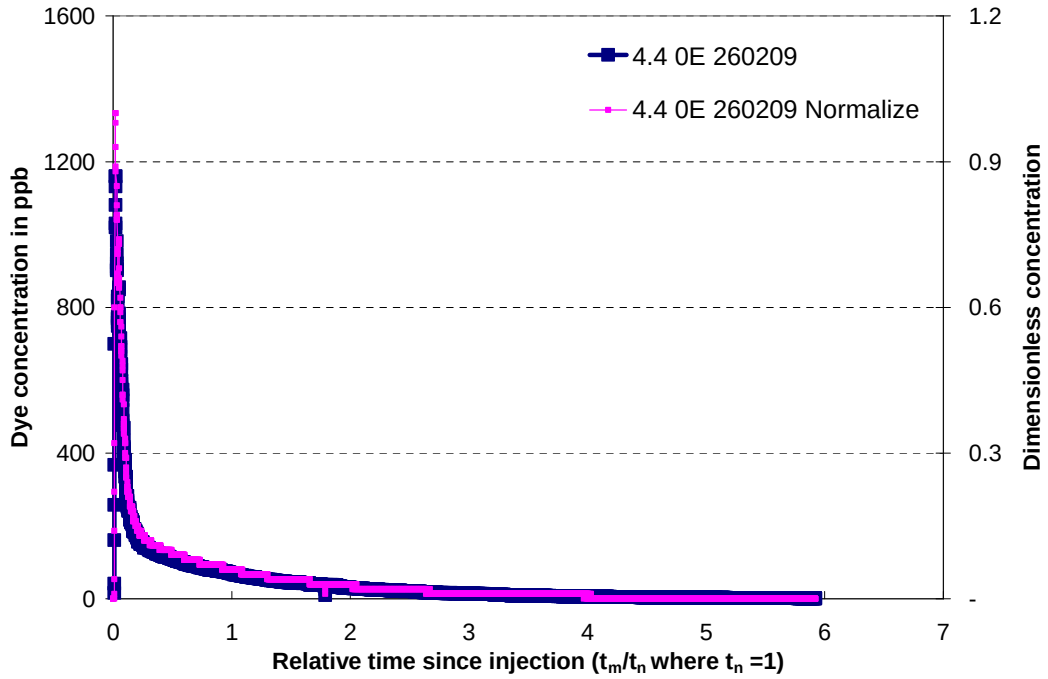

Figure 3-7. Chart of HRTD of trace with discharge 4.4 ml/s at non vegetation (0E) with dimensionless of peak concentration (peak = 1) and relative time (t_m/t_n where t_n =1).

3.4 Experimental Configuration in Model Pond

The field pond system was designed by Dr. Jean Lacoursière and Dr. Lena Vough and consisted of three ponds in series, linked to a local watercourse. The outline of the pond can be described as 'U' shaped with a central tongue of land jutting into the body of the pond. The shape of the pond was designed to try to maximise the retention time of the water compared to the capacity of the pond. The benefit of this is that the bigger magnitude of retention would ease pressure on the stream's capacity during storm periods and could also promote conditioning. However, the pond is operated under natural conditions where discharge and vegetation exhibits local seasonal variations.

Wetlands in general, have a huge number of variables: flows, shape, inlet and outlet configurations that could have been investigated in these studies. It was not

the objective of this work to test all such variations. Rather, a representative range of the key variables has been selected for testing, as detailed below.

3.4.1 Experimental Variables

a) Discharge

It is important to note that, throughout this thesis, the Hydraulic Retention Time (HRT, the centroid of HRTD) to which reference is made is that of the full size 'prototype' pond that the scale model represents. Runs were undertaken on the 9 different discharges to define the HRT. Based on range of design discharges of the field pond in Sweden, discharges Q_p of 7.5,10, 20, 30, 40, 50, 60, 70 and 80 l/s were considered. Based on equation (3.8) the following model discharges (Q_m) 4.4, 5.74, 11.48, 17.21, 22.95, 28.69, 34.43, 40.15 and 45.90 ml/s for the physical scale pond were set up, Table 3-1.

The selected experimental discharges has been tested and the corresponding hydraulic retention distribution time to prototype pond (HRT_p) were predicted in terms of the parameter of hydraulic retention distribution time of model pond (HRT_m), based on equation (3.8), derived as:

$$HRT_p = 7.7459\ HRT_m \qquad (3.9)$$

b) Vegetation Condition Set Up

Vegetation conditions were designed by using cotton pipe as emergent plant and sisal grass as submerged plants (see Figure 3-8). An emergent plant survey from the field pond in Sweden has shown that the stem of emergent plants covered less than 1% of emergent plant coverage area (as surface area) and the maximum

distance of 7.2 m of pond cross section which emergent plants can spread from the pond's edge. The cotton pipes (diameter 9 mm) were used to set up the simulated lab-emergent vegetation in the laboratory and have been deployed on 6 contour lines (where 0 lines meant no vegetation which represented by 0E, 2 lines meant 11% of emergent plants based on pond cross-section which represented by 11E, 4 lines meant 22% of emergent plants based on pond cross-section which represented by 22E , 6 lines meant 27% of emergent plants based on pond cross-section which represented by 27E and 6 lines double meant double density of 27E which represented by 27ED), see Figure 3-8, Figure 3-9 and Table 3-1. The gap starting from the pond's edge and between each line is 40 mm (represented for 1.2 m for full scale) and the gap between each cotton pipe is 50 mm (representing less than 1% of stem surface covered). The experiment also was tested with higher density (about 2%) of emergent plant by using double cotton pipes on the same surface covering the area of the total 6 lines known as 27ED.

In the field pond, submerged plants grow on a yearly cycle (with the density reflecting seasonal variation) and mainly grow below the open surface area of the pond (*i.e* not in the emergent plant coverage area). Sisal grass, fine string with about 0.1mm, was used to simulate submerged plant at laboratory scale; three sub-categories have been considered, namely Low (L), Medium (M) and High (H). The sub-category L is 52.5 g dry mass of sisal grass (represented as about 30% of maximum submerged plant growth in the pond) added to below the pond's open surface (its depth distributed across bottom of the pond to represent the growth of submerged

plant from the bottom of the pond). Categories M and H had the same distribution condition as category L, the only difference is based on the addition of dry mass of sisal grass, 105g (represented as about 60% of maximum submerged plant grown in the pond) and 157.5 g (represented as about 100% of maximum submerged plant grown in the pond) respectively.

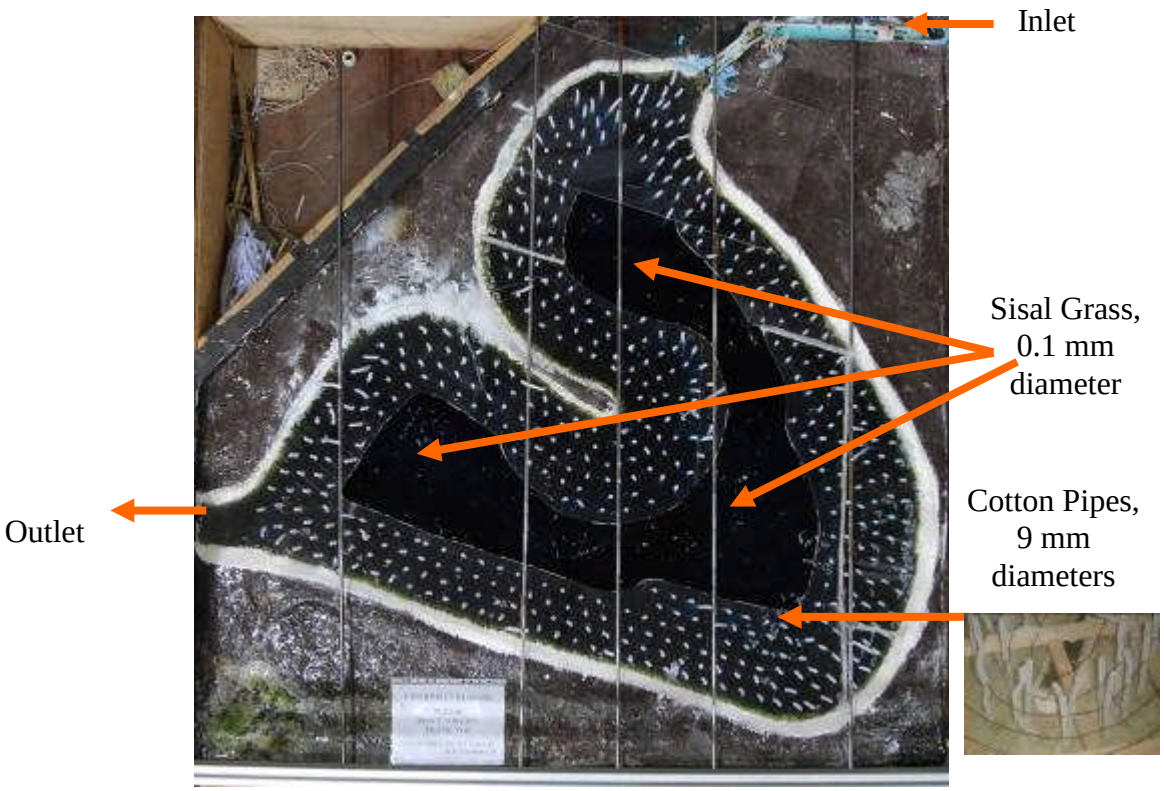

Figure 3-8. Experimental set up in laboratory scale pond.

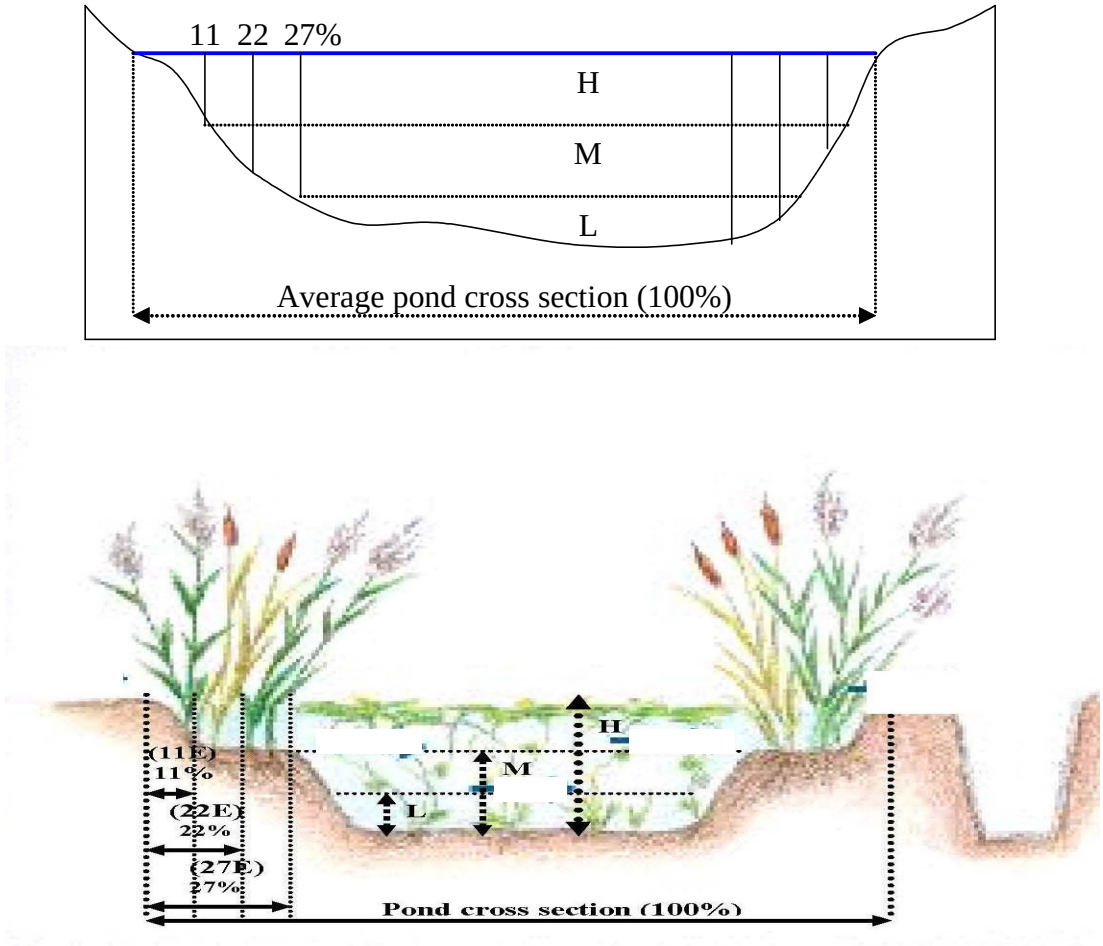

Figure 3-9. Experimental set up of vegetation in laboratory scale pond.

3.4.2 Experimental Runs

Nine flow rates were considered, based on values of 5 to 80 l/s from the real pond in Sweden, one inlet and outlet riffle with similar size and three vegetation conditions. Phase I, Phase II and Phase III, represent no plant, only emergent plants and submerged and emergent plant conditions respectively (see Figure 3-8). The experiments were tested for several configurations. The planning of the runs was undertaken during the course of the experimentation as it was necessary to review the design of new runs and number of runs based on the results of work completed. Table 3-1 shows the different run configurations undertaken.

Discharge, Qin (ml/s)	Phase I (No vegetation)	Phase II (Only emergent vegetation)				Phase III (emergent and submerged vegetation)		
	0 E	11E	22E	27E	27ED	27EL	27EM	27EH
	Number of experimental run							
4.4	5(3)	1(1)	1(1)	2(1)	0	1(1)	1(1)	1(1)
5.74	4(1)	4(1)	4(1)	4(1)	3	1(1)	1(1)	1(1)
11.48	6(2)	1(1)	1(1)	1(1)	0	1(1)	1(1)	2(1)
17.21	5(1)	3(1)	4(1)	4(1)	3	1(1)	1(1)	1(1)
22.96	8(2)	1(1)	2(2)	1(1)	0	1(1)	1(1)	3(1)
28.69	4	3	3	3	0	0	0	0
34.43	4	3	3	3	3	0	0	0
40.15	4	3	3	3	0	0	0	0
45.90	4	4	3	3	3	0	0	0

Table 3-1. Summary of physical scale experimental running conditions.

*Note***: (..)** *Number in the bracket is the number of trace which has PIV results*

3.5 Practical Image Analysis and MatPIV

As mentioned in the previous section of the literature review, MatPIV is a program which tracks the movement of particles (speed and direction of the fluid movement) in the model pond. Drogue tracking by image analysis was used in a full scale waste stabilization pond (Shilton, 2001). Different instruments used for hydraulic research were ruled out due to very low velocities and small scales found in ponds (Wood, 1997). A Doppler-based system would has been ideal and has been used in similar applications such as the study of flow in clarifiers (Rasmussen, 1997) but such systems are not suited well to measurements on a full scale (or even big model scale); no such apparatus was available for this project. Particle image analysis was available and this technique was developed to track the movement of very small particles that were floating on the fluid surface. This technique for studying hydraulic behaviour in physical scale natural shape wetland or natural

shape pond treatment system was never previously used by any other researchers.

The particles used were distributed uniformly over the surface water of the model pond (particles still move freely with the flow for the water in the pond) whilst the constant discharge was retained. 200 still images were taken with an interval between each image of 12 seconds, the selection of number of image and the time interval being based on consideration of accuracy and time required to transfer image from camera to PC. The particle image velocimetry (PIV) analysis system consisted of a still camera positioned facing down about 3 m above scale pond. This camera transferred images to a computer equipped with recorder card (National Instrument), as illustrated in Figure 3-10.

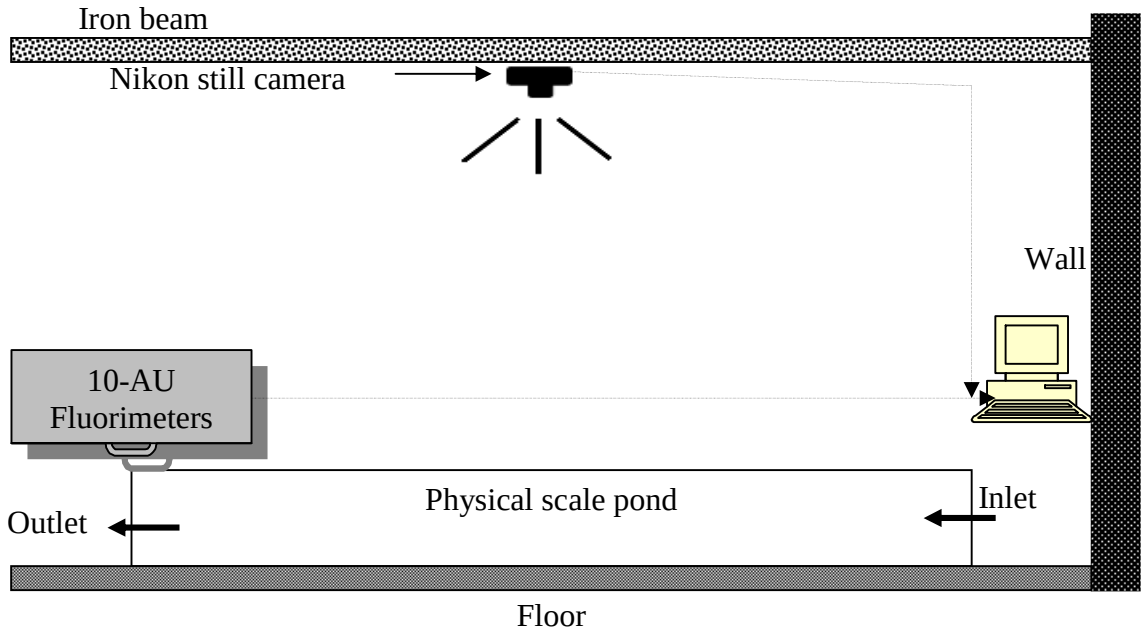

Figure 3-10. Experimental set-up for image analysis on model pond.

All images were manually selected to make sure there was 12 s from each frame and the selected images were adjusted to the size based on 2 m x 2 m of pond's

frame. They were then analysed by Davis, and MathPIV software to compare the results from Davis (which were written to produce contour velocity fields and coloured path lines of the surface flow velocity). The processing of images was split into four distinct steps, namely image calibration, background determination, particle determination and particle tracking, Figure 3-11.

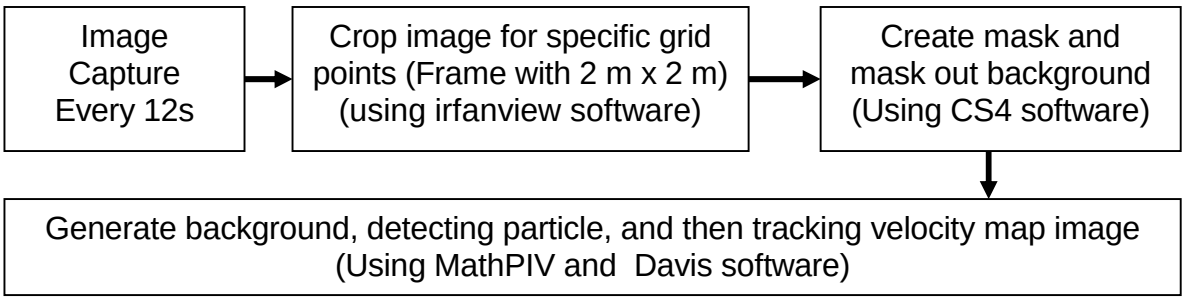

Figure 3-11. Flow chart of image processing with different software.

3.6 Typical data collection and processes

3.6.1 Dye trace processes with different discharges and vegetation conditions

To understand the effect of vegetation on hydraulic retention time in a small scale pond, an experiment was set up, using solute tracer techniques, with three main conditions. The first condition was without vegetation (run with eight different discharges), the second condition was with different emergent vegetation configurations and the third was with different emergent and submerged vegetation configurations. All the experimental runs were conducted on the constructed distorted physical scale pond based on 1:30, X:Y (length and width) and 1:15 vertical scale model of the real pond in Sweden. Polyester-cotton pipe with 9 mm diameter were used as the synthetic vegetation and was deployed vertically up to the bottom of the pond with 50 mm interval, in X and Y directions.

Dilution techniques (Dye traces) were conducted for the assessment of the hydraulic performance of the different free surface flow conditions within the scaled model pond in the University of Warwick, School of Engineering. The dye used in all tests was diluted Rhodamine WT, a fluorescent liquid. The instrument used for the observation of the dye leaving the free surface pond was a model 10 Analogue "10–AU" Fluorometer, manufactured by "TURNER DESIGNS", Sunnyvale California. The 0 – 5 V (output) from the fluorometer was connected to a National Instrument data logger and then all data were stored in PC. A half to one millilitres of diluted Rhodamine WT (10^{-2} l/l or 10^{-1} l/l) was slug injected into the inlet UPCV pipe (which was used to stabilize in inlet discharge from the two small storage tanks that had been used to reduce pulses flow from peristaltic pump), see Figure 3-12**.** Temporal concentration distributions of the dye were observed at the outlet structure, which was used to collect partial or whole outlet discharges of the pond, Figure 3-13. The outflow was pumped through the reading chamber of the fluorometer, with a temporal resolution of one sample per second over time periods need for completion of each trace. With different discharges this ranged from 8 hrs to 14 days.

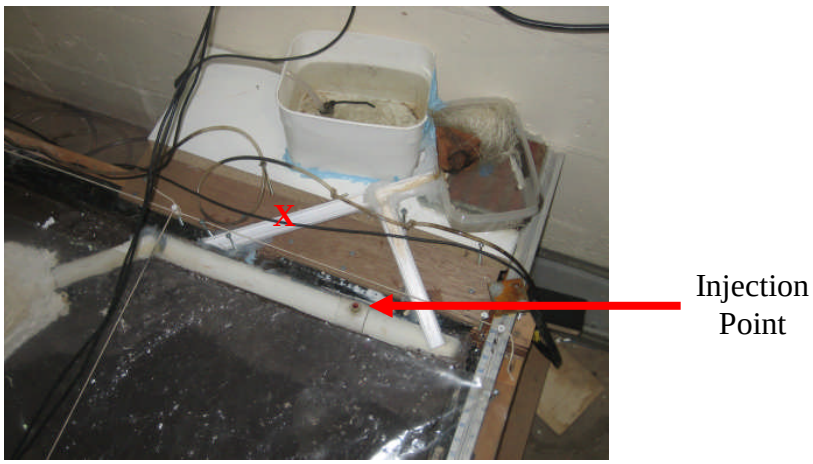

Figure 3-12. Inlet of scale model pond.

Figure 3-13. Outlet of scale model pond.

3.6.2 Trace data processing and analysis

The effect of vegetation and discharge on HRTD, HRT were observed and studied and the cumulative mass distribution (C%) was determined by plotting the raw data output versus time, leaving the system over a period of time after an instantaneous on slug input. With this technique, we can define whether the trace is complete, see Figure 3-14. The fluorometer outputs were converted to dye concentration values (ppb) using the 10 – AU's calibration curve as stated in section 3.2.4, see Figure 3-14.

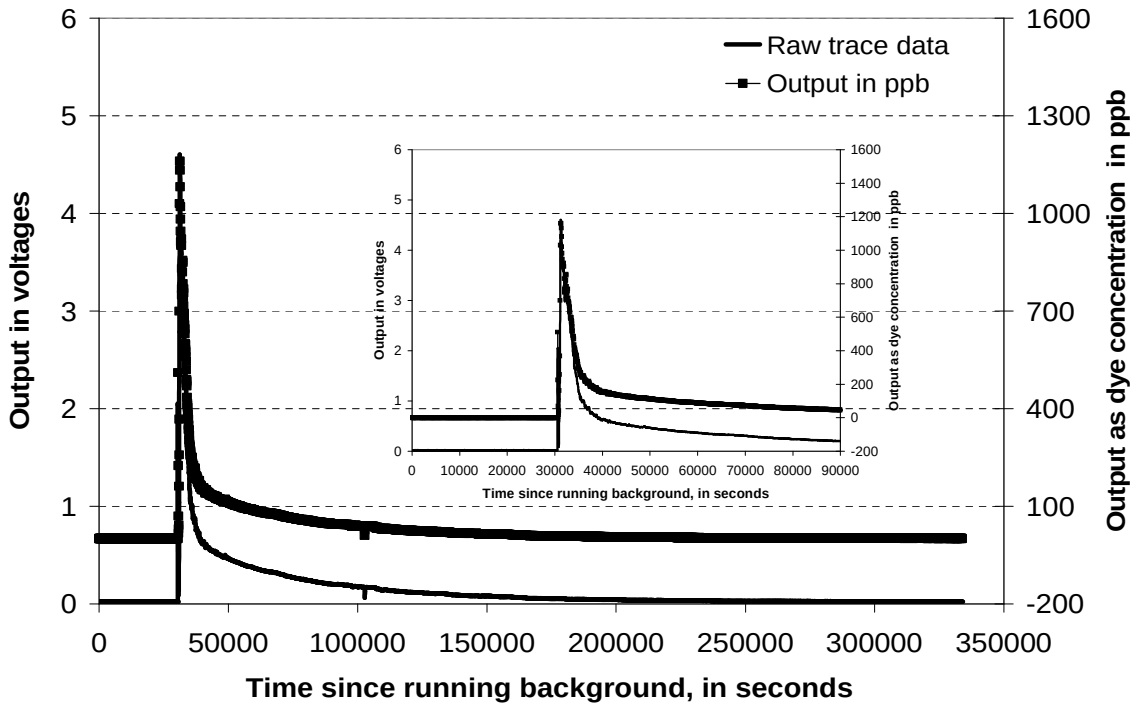

Figure 3-14. Raw data plot and dye concentration plot.

The time to complete each trace ranged from 8 hrs to 14 days, because the results from the first and the last background were different for each trace. So defining when each trace was completed and where is the real trace data, and determining the times of first and last observed dye concentration arrival at the outlet were estimated by linear reduction from the original distribution curve, Figure 3-15. The linear reduction equation was generated by two averaged background points (before dye arrival at the outlet and at the end of trace) or which each point was generated by the average of 200 points of the background data points directly from 10 – AU raw data, Figure 3-15.

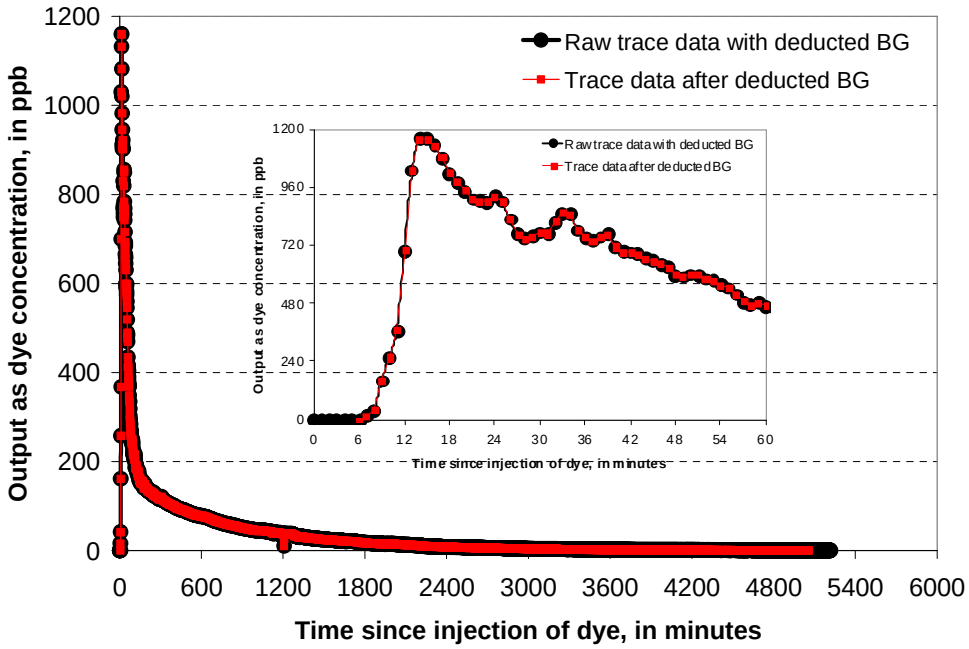

Figure 3-15. HRTD with and without background removal.

The same problem as with the background concentration resulted in the mass recovery also varying +/- 20% of the mass Rhodamine WT slug injected. So in order to compare the mass dye distribution from one to another, the mass was assumed to be 100% recovered for each trace, see example Figure 3-16. From the mass recovery (C%) distribution or curve, it is possible to define the exact time(t_0) when the first dye arrival was detected at the outlet and when 5%, Peak, 25%, 55%, 95%.etc. of mass dye passed through the outlet of the system, see Table 3-2.

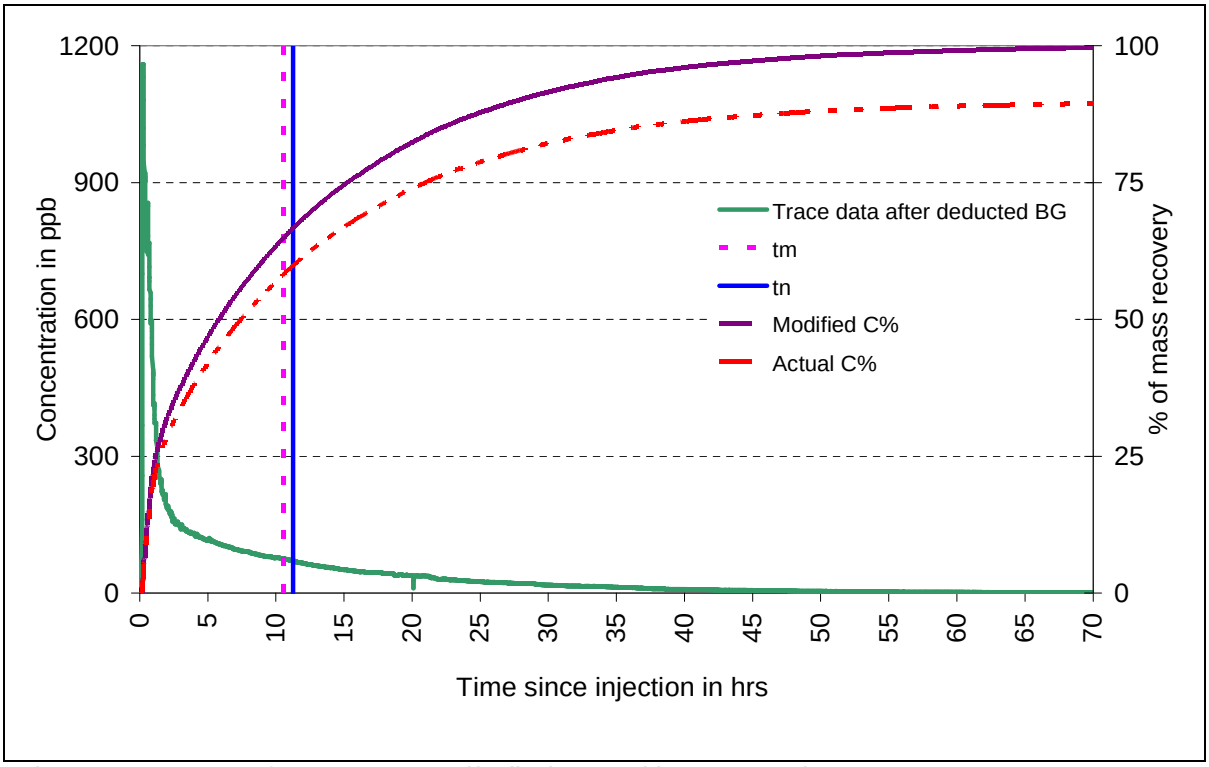

Figure 3-16. HRTD of a trace at 4.4 ml/s discharge without vegetation.

As stated by Kadlec & Knight (1996), see section 3.2.4, it is necessary to express the results in dimensionless form, not only for the purpose of comparison between these different experimental runs and against mathematical modelling simulations, but also to compare between different experimental runs with different discharges and vegetation configurations and also compare between the laboratory results to the field results. It was necessary to standardise the output data, see Figure 3-17. Moreover, the equation 2.1, 2.2, 2.3, 2.4 and 2.6 in section 2 have been used to produce the result of t_n, HRTD, t_m, e_o, e_p and e_m of each experimental run. An example of detail results for a trace run with 4.4 ml/s discharge without vegetation is given in Table 3-2.

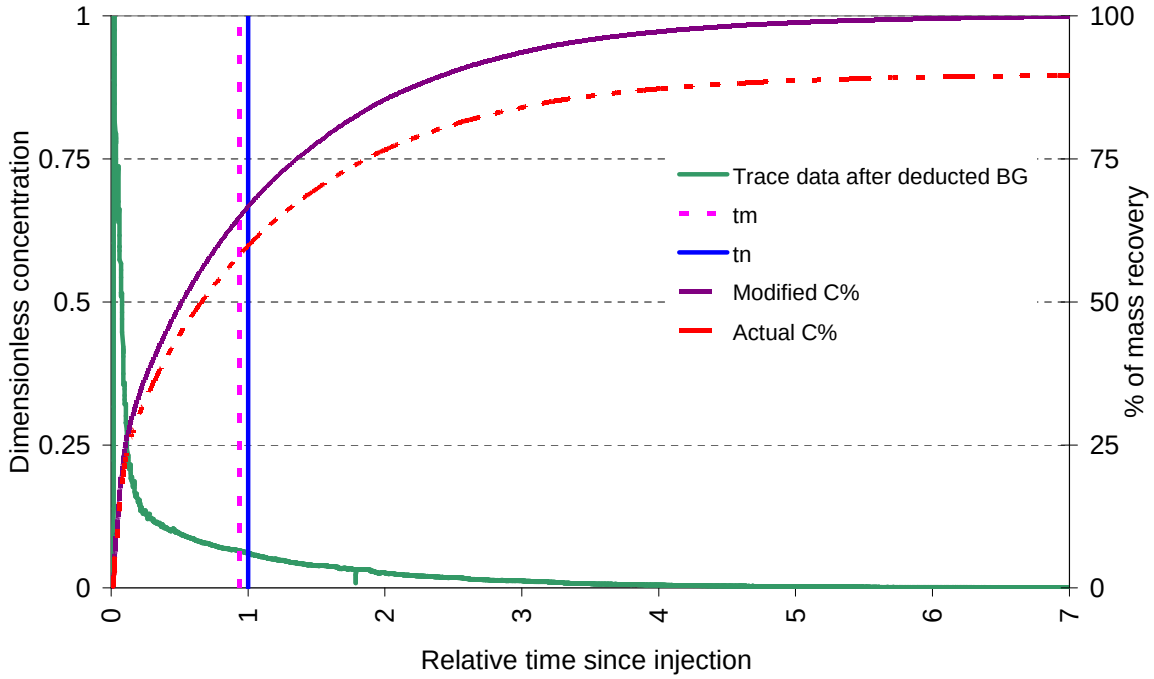

Figure 3-17. Example of normalized HRTD of a trace at 4.4 ml/s discharge without vegetation.

Discharge, Qin (ml/s)	Vegetation Conditions	Run No.	Calculated from data value						Theory	Normalize or relative time			
			t_0	t_{25}	t_p	t_{55}	t_m	t_{95}	t_n (=1)	e_0	e_p	e_m	σ^2
			(mins)							t_0/t_n	t_p/t_n	t_m/t_n	as relative time
4.4	0E	1	7	52	10	432	507	2209	675	0.01	0.01	0.75	0.85

Table 3-2. Summary of mean retention time "t_m" and percentage of cumulative mass passed through.

3.6.3 Visualisation of surface flow profile using PIV techniques

In this study, the dye tracer data are only shown in terms of the distribution of dye mass passing through the pond's outlet. PIV techniques have been used to visualize the surface flow profiles, enabling us to understand how the surface flow profile responds when the discharge and/or vegetation conditions have been changed.

Preliminary tests were carried out with a Nikon camera but with different models (*e.g* D40, D100 and D300 digital SLR) to ensure the captured image quality was of an acceptable level and, furthermore, that the seeding could be clearly distinguished from the 2.4 m height above the pond at which the camera was to be situated. The camera was connected to the desktop computer via a USB cable and controlled using the Nikon Camera Control Pro software. It was established that the computer was only able to capture and save an image every 6 s, thus determining the minimum time between images for the investigation. This relatively long time between the image capture was deemed to be acceptable due to the relatively slow flow of the pond and subsequent slow movement of the particles on the surface. The shutter speed was set to a value of 1/12 second, with an exposure of +11/3EV and an aperture value of f/3.8 to account for the deficient lighting surrounding the laboratory area. Approximately 200 to 400 pictures were taken for each trace to gain an accurate representation of the surface flow profile, see Figure 3-18. Before analysing in Davis and/or MatPIV software, all the original images were processed, according to the 2 m x 2 m of pond design layout frame, by using IrfanView software to automate multi-crop pictures; see Figure 3-19 and CS4 software to mask the internal boundary of pond and the background image, see Figure 3-20 and Figure 3-21.

A number of different tracer particles were tested for the PIV technique during the preliminary experiments, to gain an idea of which particles produced the results with the highest accuracy. In a number of particle tracking experiments, polystyrene seeding is utilized (Ruffel, 1998), it was however observed that such seeding clung to the edges of the pond as a result of the high surface tension.

Glitter was also tested because of its high reflectivity; this, however, formed large coagulations that remained throughout the flow and thus did not give an accurate representation of the surface flow. A droplet of hand wash liquid was mixed into the feeder tank in an attempt to break the surface tension and subsequently prevent the coagulation of particles on the surface. It was observed, however, that this completely changed the surface flow of the pond, causing all particles to take a single track flow from inflow to the outlet without the dispersion of particles at all, again not truly representing the surface flow profile.

It was decided that polymer plastic granules, Talisman 407, a relatively cheap seeding, performed to the higher accuracy for the experiment, as they could be added into the primary feeder tank and dispersed within the liquid before deposition into the pond. Although clumping of the particles was observed to some extent, this seemed an unavoidable occurrence within the investigation. The clumping however was seen to reduce as the particles had time to disperse more evenly and, moreover, the Davis and MatPIV software were capable of tracking the larger clump of particles. (Talisman 407 particles have been used previously as flow trackers in laboratory experiments; hollow glass particles could have been used instead of Talisman 407 at the expense of less clump and slightly more accuracy in term of detecting surface flow profiles, but they were significantly and prohibitively more expensive).

In 40 traces, covering 5 different discharges and 7 vegetation conditions, out of overall 145 traces with 9 different discharges and 8 vegetation conditions, the surface flow profiles have been measured using the PIV technique, see Table 3-1.

Food colouring has also been used to dye the water, as it helped to reduce surface water reflection while taking pictures from top of the physical scale pond. It was added in the 2 stabilization tanks and given at least 2 to 4 hours to evenly disperse throughout the pond (note all the procedure have to follow the step by step of Rhodamine WT trace shown in section 3.6.1). With the camera is in place and connected to the computer, seeding was added into the primary feeder tank, at least 20 minutes after Rhodamine WT injection, at the rate that allowed for adequate pond cover while preventing the creation of large particle clumping. The seeding was then being given about 15 to 30 minutes to split up and settle to produce an accurate surface flow representation, Figure 3-18. The camera then continued to capture about 200 to 400 images of the full representation surface flow image.

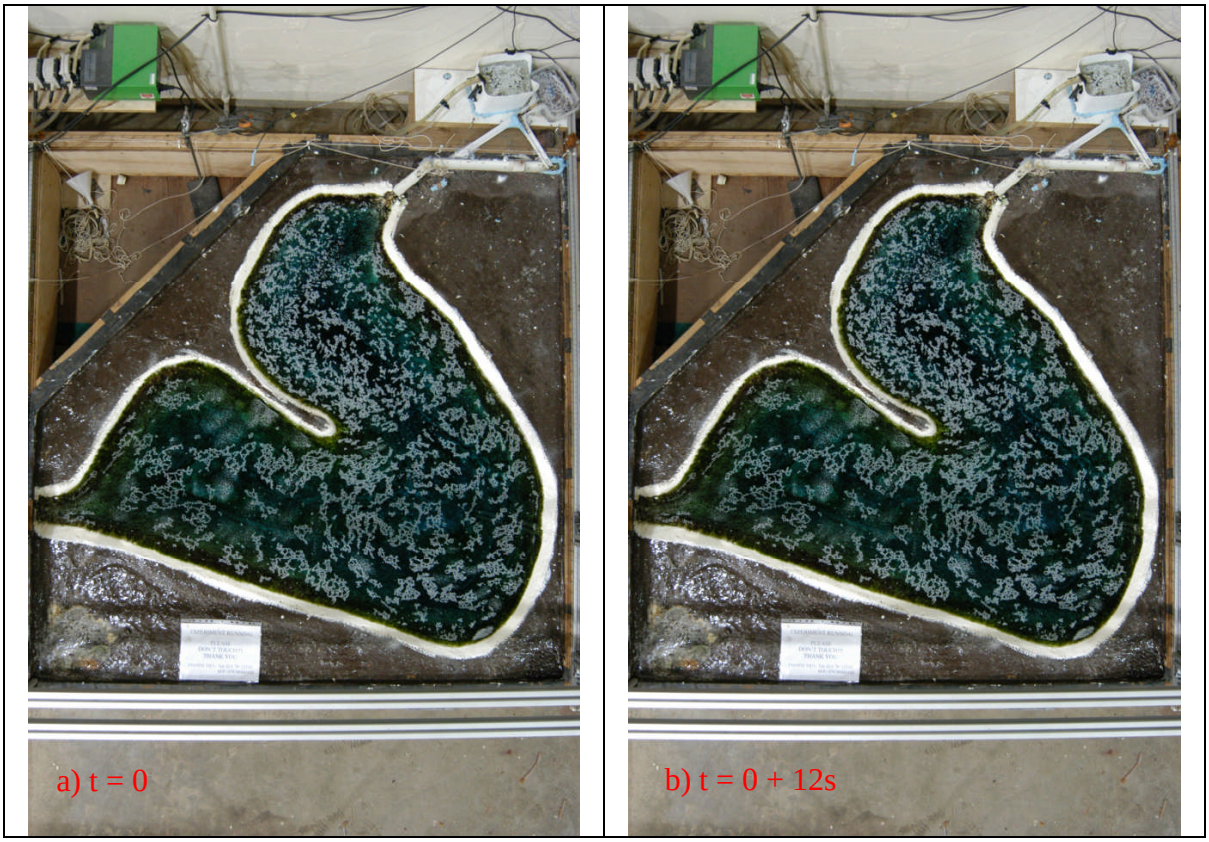

Figure 3-18. Original images captured by still camera with speed of 12"/ frame, Q_{in} 4.4 ml/s with 0E.

Once images have been captured, the IrfanView software was used to pre-correct images, by auto-cropping the pictures, as explained in detail of its overall processes in section 3, according to the pond frame marked as 2 m x 2 m of pond design layout, Figure 3-19.

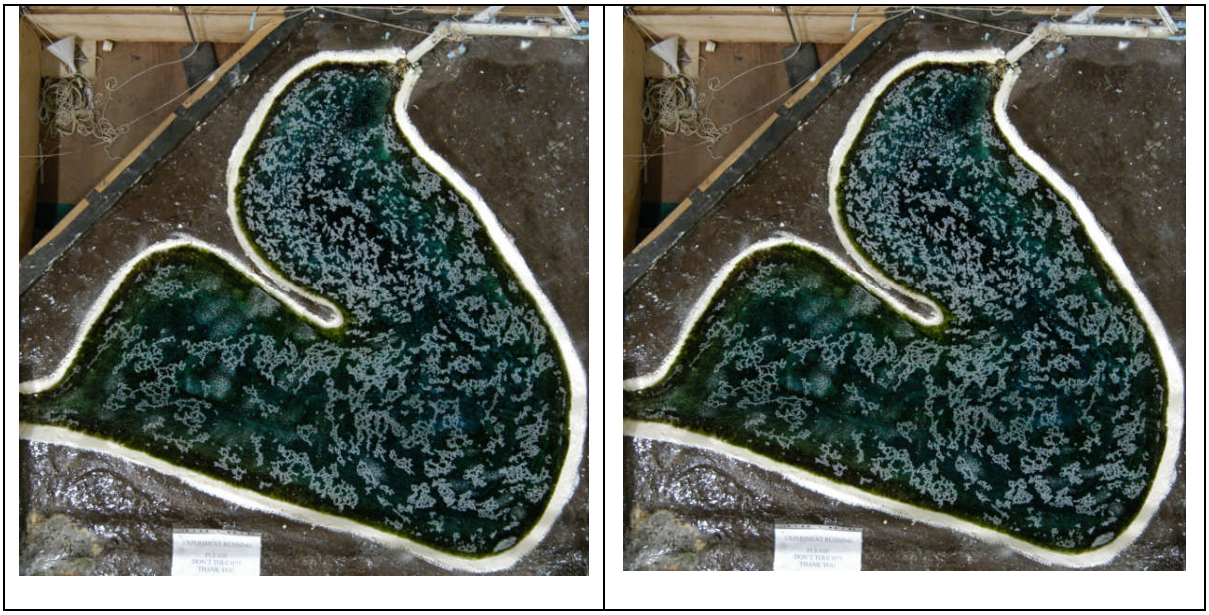

Figure 3-19. Cropped image based pond frame by using IrfanView Software.

Whilst all images were cropped, the Photoshop CS4 software was used to mask out the pond boundary and create a background reference image, according to the actual internal pond design geometry (see Figure 3-20 and Figure 3-21),then running in Davis software and/or MatPIV.

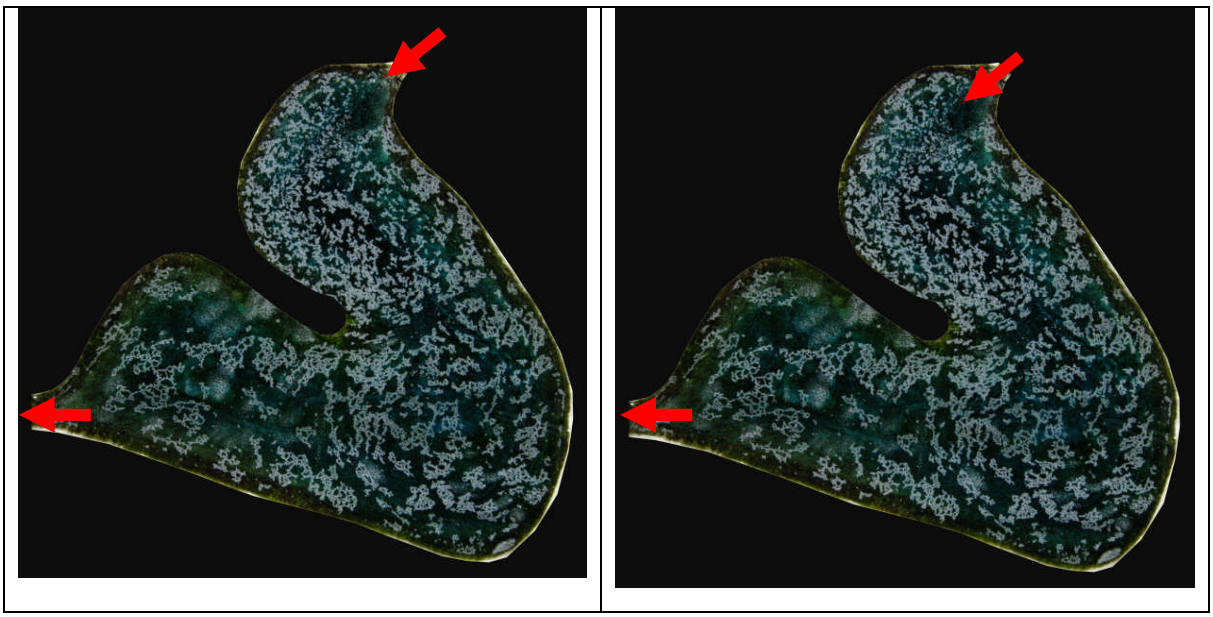

Figure 3-20. Masked images by using Photoshope CS4 Software.

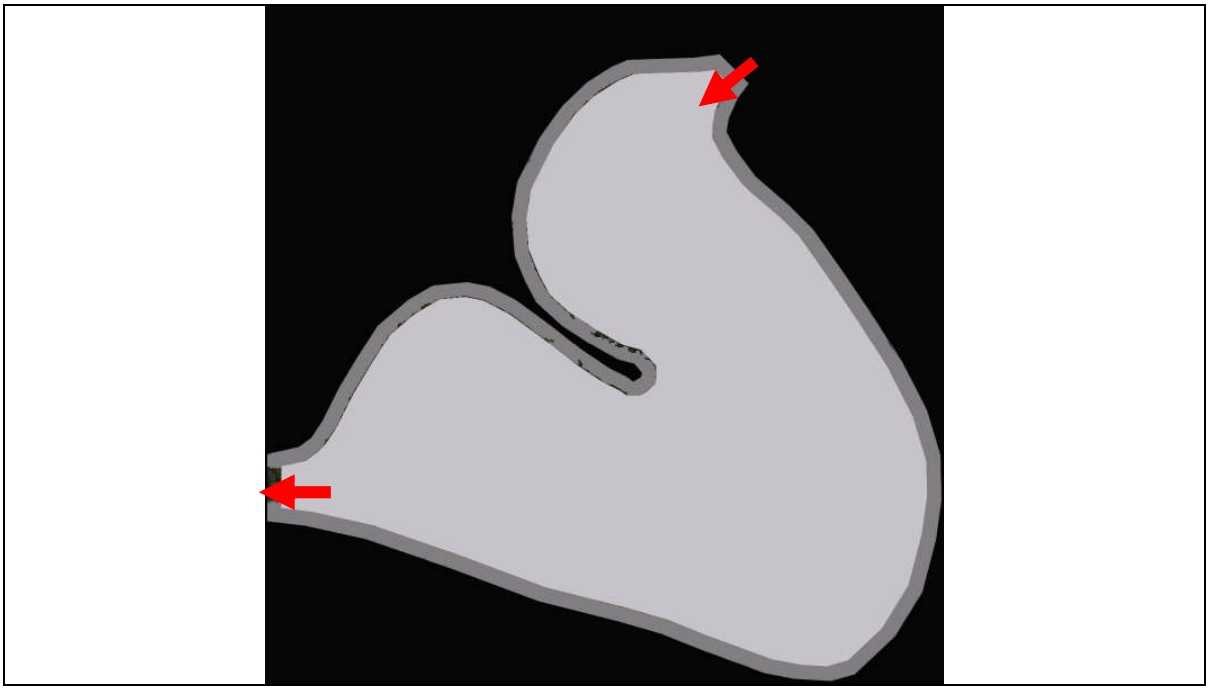

Figure 3-21. Masked image as background for processing in MatPIV and Davis Software.

Once all images of each trace were captured, cropped and masked, by using Still Frame Camera, the IrfanView Software and the Photoshop CS4 Software, respectively. The surface flow field results have been developed by using the Davis and MatPIV Software with marked internal boundary images from each trace and its background reference image, see Figure 3-22 and Figure 3-23.

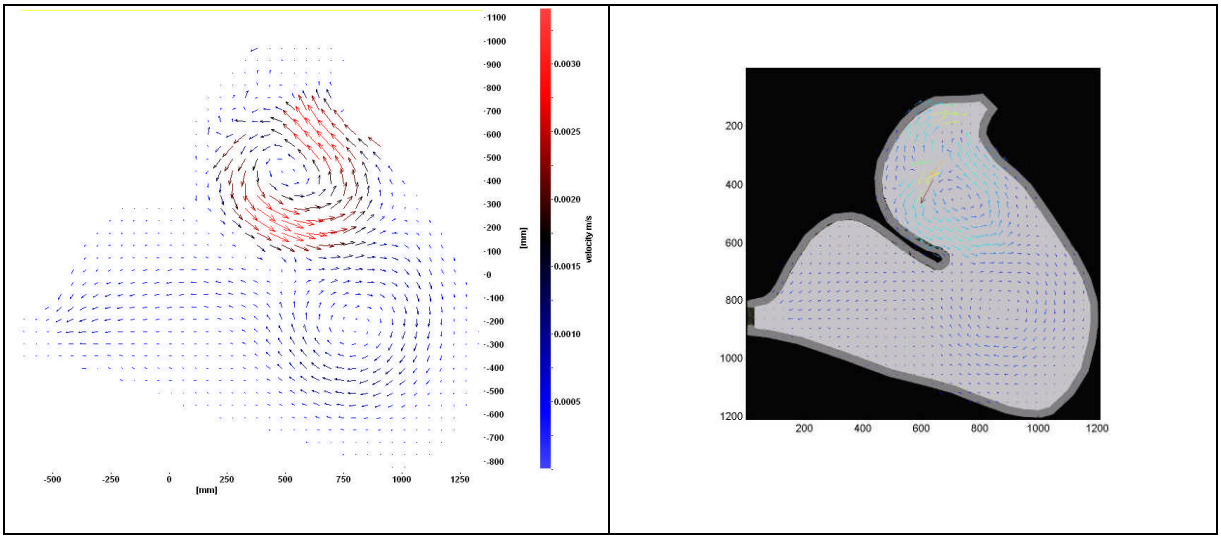

Figure 3-22. Surface flow field results from Davis and MatPIV Software.

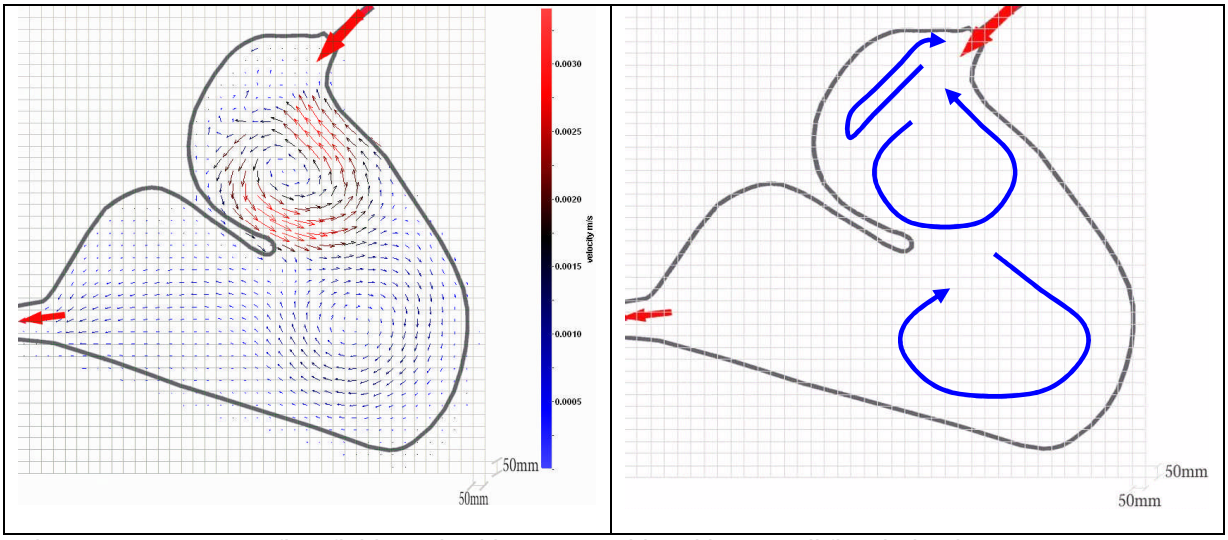

Figure 3-23. Average flow field result with 50 mm grid and its overall flow behaviour.

3.7 Design and Hydraulic Studies on Prototype Pond

The research conducted on constructed wetlands hydraulics, waste stabilisation pond hydraulics have involved tracer experiments on full-scale field system or ponds. What is, however, lacking in the literature in any direct measurement of the internal fluid flow pattern within the treatment pond. Another shortcoming of these previous studies is that 'field' systems are never in steady-state. They have transient inflow-rates and large surface areas that are exposed to constantly changing wind and temperature conditions.

Although the scale models were carefully designed to represent full-scale systems, there will always be a question of how successfully this modelling is achieved. Ideally, some experimentation on full-scale field ponds is also required. In this project, 3 tracer studies were conducted at the field pond across different seasonal variations, see Figure 3-24 and Appendix B.

The constructed pond, or field pond, system was designed by Dr. Jean Lacoursière and financed by the Swedish Water Board (see Figure 3-24). The objective of the scheme is to promote water-retaining structures throughout Sweden for the treatment of nutrients in farmland runoff. The pond system consists of 3 ponds in series, all linked to a local watercourse. The focus of this report is on the lower of the 3 ponds (on the left of the diagram as shown in Figure 3-24). This schematic is derived from the 'as originally-built' plan layout for the pond. The shape of the pond was designed to maximise the retention time of the water through a control on the capacity of the pond; the benefit of this is that the retention is designed to ease pressure on the stream's capacity during storm periods and also promote conditioning, see Appendix B.

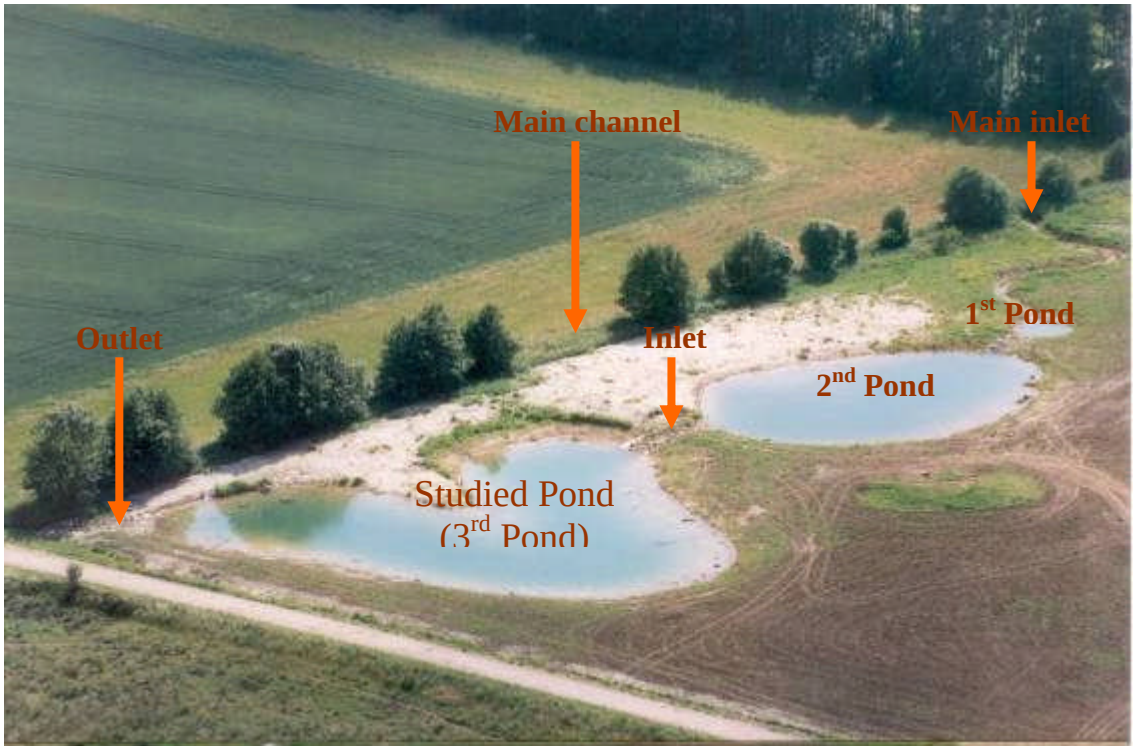

Figure 3-24. As original build' Pond Structure (Constructed in July 2001).

The runoff treatment design concept was focussed on the main flow into the pond system, a flow that is primarily from the stream and accumulated from surrounding

agricultural runoff. The redirection of flow from the stream to the pond system is facilitated by an earthen weir, which allows the flow to be divided once a certain height of water flow into the stream is exceeded. The maximum flow is approximately 45 l/s during a time of storm and the typical flow value entering the pond lies between 10 l/s and 20 l/s for the summer season (Dr. Jean Lacoursière – personal communication).

3.7.1 Field Tracer Studies

This work on the prototype pond used the same stimulus response technique as described for the laboratory tracer studies. The only exception was that the outputs were measured by an SCUFA fluorometer and/or Cyclops 7 at the outlet of the designed flume.

3.7.2 Ponds Studies

One Sweden Field Pond was studied, from the three ponds in series, as part of this project. The ponds service the community of Horby of Southern Sweden. In this case, the advantages of using a third pond include:

- Lower suspended sediment concentrations compared with primary and secondary ponds;
- Improved water quality;
- Reduced flow fluctuation due to buffering effect in primary and secondary ponds.

Lyby is a small rural community located 50 km east of the city of Malmö, with a population of approximately 100 capita. The water source from agricultural run off

of the surrounding area enters a channel and the water volume is then transferred to the primary pond (sedimentation trap pond) via a small channel of similar size to the main channel. The effluent from the primary pond is discharged to the second pond and then the third pond, through a control v-notch flume designed, and installed in July 2007. The v-notch device was based on the BS V-notch weir standard, as a control structure for the first flume (upper flume) and as riffle for the second flume (middle flume), which was the subject of this study, see Figure 3-24.

Rhodamine WT tracing studies were conducted for the assessment of the effect vegetation and discharge on the hydraulic performance of the Lyby pond. Cyclops, SCUFA and Handheld fluorometers were used to measure dye leaving at the pond's outlet as well as inside the pond. The fluorometers were equipped with probes for fluorescence and turbidity measurements (excepted Cyclops) with temperature correction (only for SCUFA) and internal data logger.

3.8 Experiment set up and data processing

3.8.1 The Lyby pond treatment wetlands

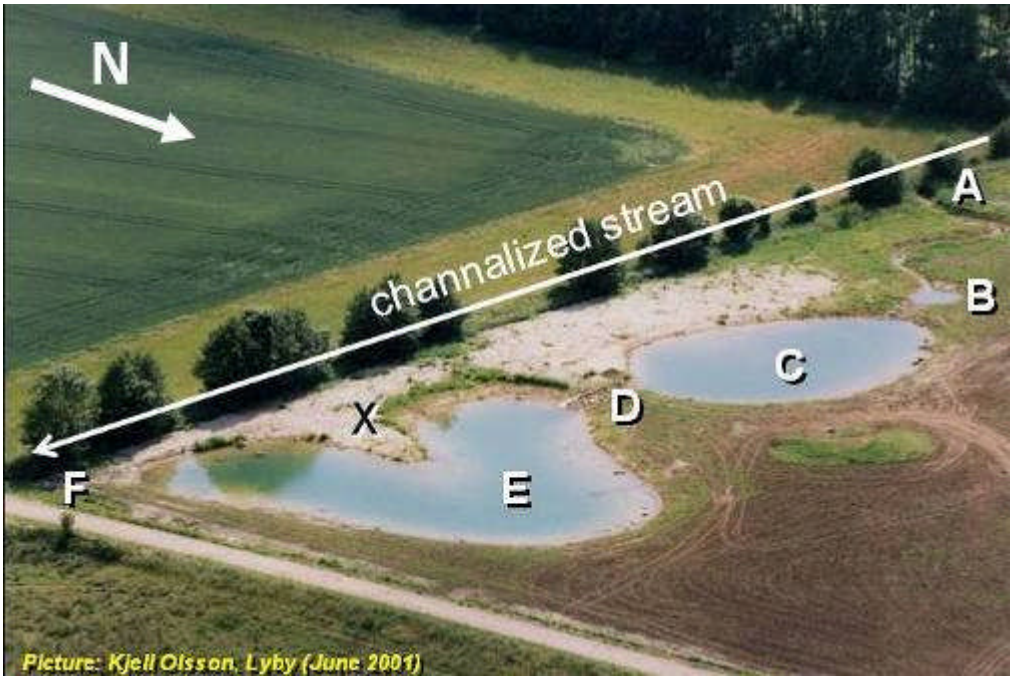

Figure 3-25. Overall layout of Lyby pond treatment wetlands after constructed in 2001.

Note: (A) Inflow stream; (B) Sediment trap; (C) First wetland; (D) Connecting riffle; (E) Second wetland; (F) System outflow; (X) Observation tower.

3.8.2 Inlet and outlet pond set up and V-Notch Weir calibration

To understand the hydrographs or discharges of inlet and outlet from the bottom pond, two flumes, with 90^{o} V-notch weir, were constructed based on BS 3680-4A:1981, see Figure 3-25, Figure 3-26, Figure 3-27 and Appendix B.

Figure 3-26. Volumetric (bucket) measurement.

Figure 3-27. Dye trace and constructed flume at outlet of study pond.

Two techniques were used to calibrate the two constructed flumes and the results from the combined bucket and solute discharge formula, were used to determine

the value of the coefficient, C_e, shown in Figure 3-28 and the general Sweden V-notch flume plotting head (m) and Q (l/s) shown in Figure 3-29.

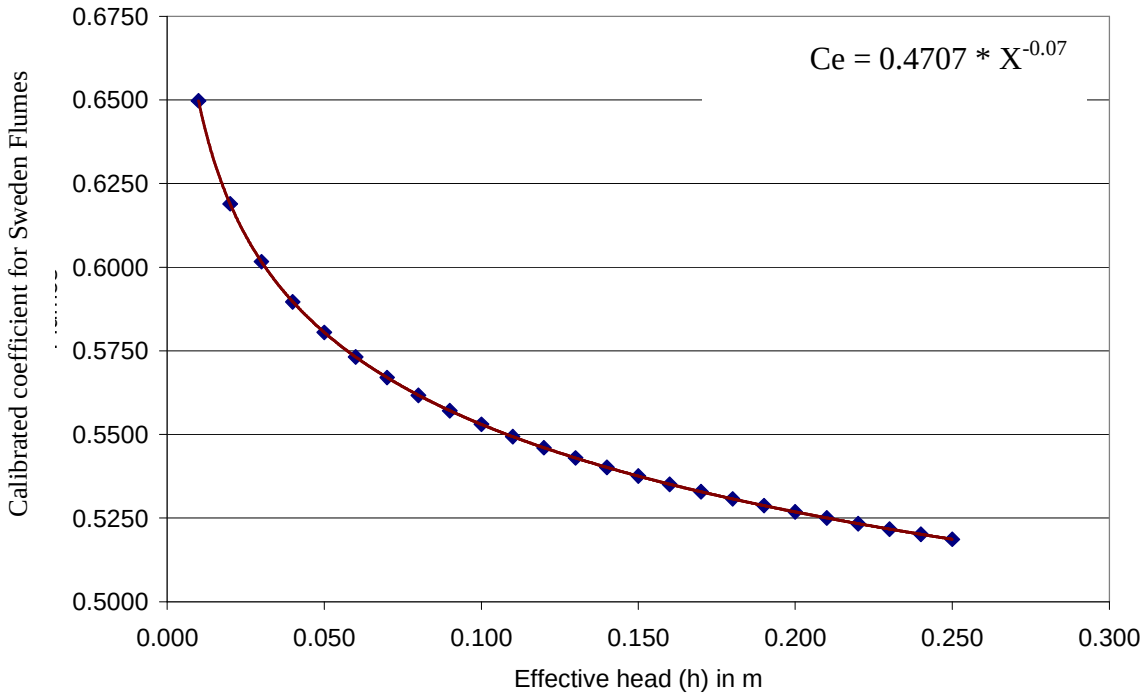

Figure 3-28. Coefficient for Sweden Constructed Flume.

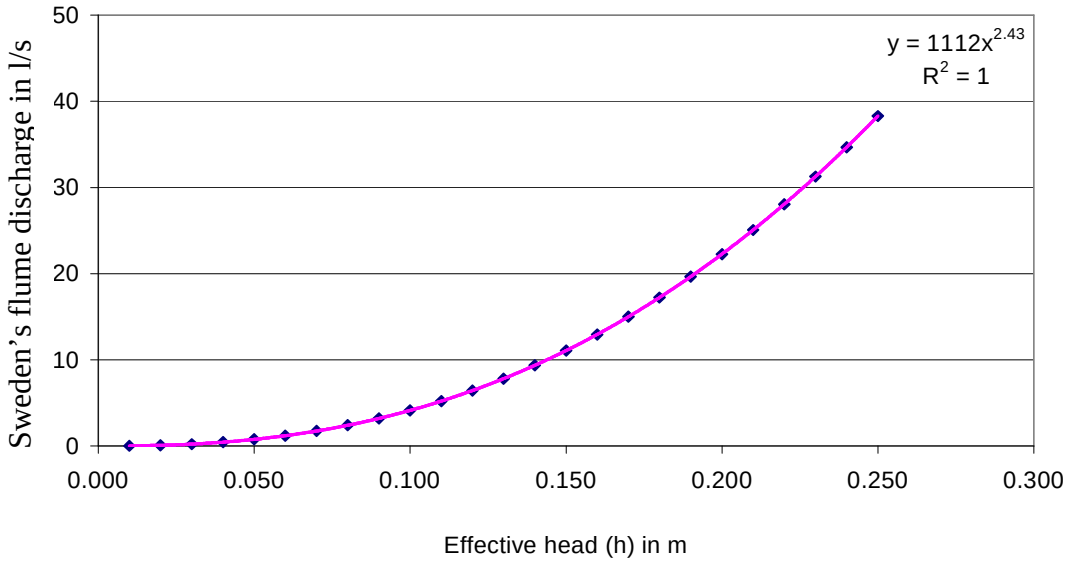

Figure 3-29. Sweden V-notch Flume Calibration.

The results from the combined bucket and solute discharge formula clearly show that there were differences between the resuts using BS 3680-4A: 1981 standard V-notch Weir and our Sweden V-notch Weir see Figure 3-30. This difference may be caused by the accuracy of flume levelling or some other unanticipated conditions. Further studies will use Sweden V-notch Weir as a tool to measure inlet and outlet discharges from the lower pond.

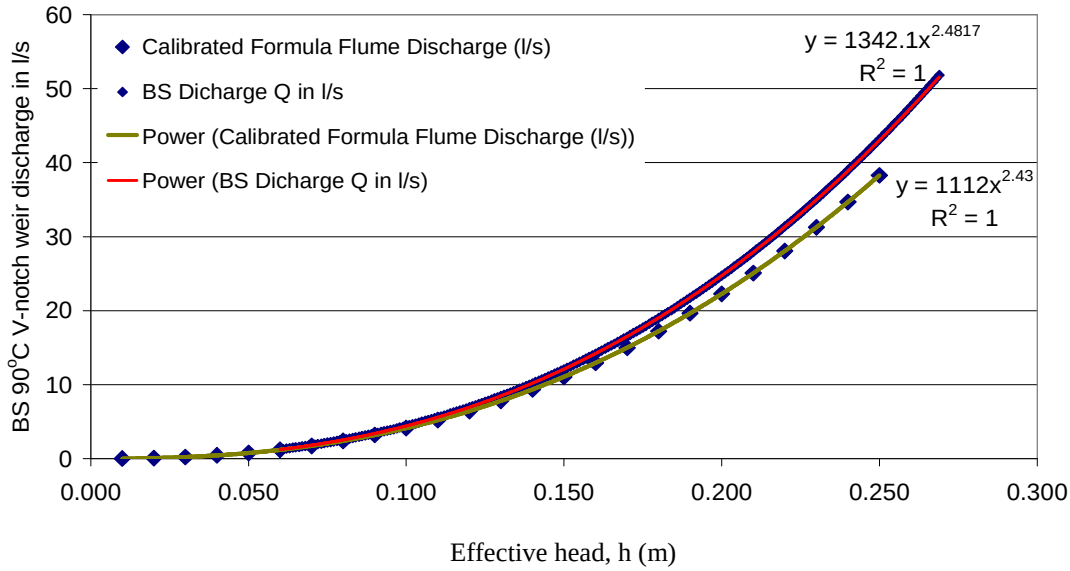

Figure 3-30. Sweden V-notch Flume Calibration and BS standard.

3.8.3 **Vegetation Survey and its effect on Hydraulic Flow Profiles**

A detailed survey on pond depth and vegetation was conducted across the lower pond in March 2009 but a previous estimation of vegetation was conducted in July 2007 and July 2008. These primary results have been used to design and set up the vegetation condition in model scale pond. Wooden poles were deployed as references surrounding the pond and some points used the existing fence poles.

A theodolite was placed in two different positions; each position measured the angle to all of the reference points. String or rope attached with measuring tape was been lined from one wooden pole reference point to another and the pond depth was measured every 2 m on both side of string lining crossing the pond, and for all the cross section areas, Figure 3-31. The boundary of vegetation in the pond had been noted while conducting the depth survey, as a result of which a detailed survey of vegetation was conducted which focussed on different kinds and distribution density of vegetation, Figure 3-32.

Figure 3-31 . The boundary of vegetation and pond geometery survey in April 2009.

Figure 3-32. Vegetation boundary and density survey in April 2009.

3.8.4 **Pond and vegetation survey**

a. Pond survey

The field pond surveys were carried out at Lyby ponds during spring (March 2009). Lyby Pond surveys were undertaken at a time of year when most vegetation population had died out. The total station Geodimeter® System 600 was used to measure the detail of vegetation covered, as well as the depth of the pond.

The concreted water pipe laid across the road was used as the main reference point (PR), with its level being 1.01 m higher than the pond water level. The Church lamp post was used as the second reference point. After setting up these two main reference points, the instrument measured (i) the spot height of the pond (SPT) to calculate the pond volume (2,072 m^3, see Figure 3-34), (ii) the fence post (used as a reference to measure the change of vegetation through out the year),

(iii) the vegetation boundary (VB, to distinguish between the water surface and the submerged and emergent plant cover), (iv) the V-notch weir and (v) the inlet and outlet weir flume (VN, IW & OW), see Figure 3-33.

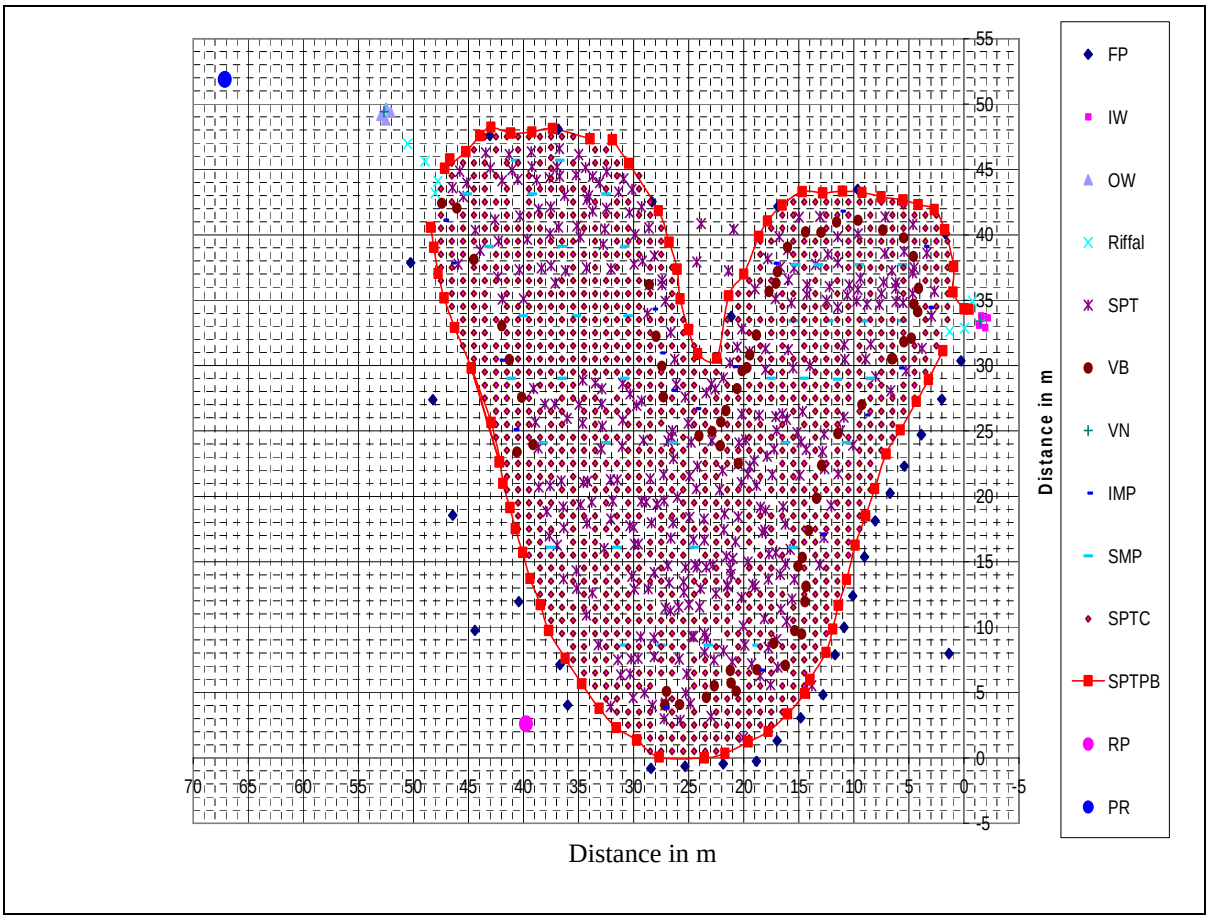

Figure 3-33. Lyby pond surveying set up July 2008.

Key:

SPT:	Spot Height	FP:	Fence Post
V:	Vegetation	VB:	Vegetation Boundary
VN:	V-Notch Weir	IW:	Inlet Weir Flume
OW:	Outlet Weir Flume	IMP:	Emergent plant
SMP:	Submerge Plant	SPTC:	Spot Height Created

SPTPB: Spot Height Pond Boundary
RP: Reference Point
PR: Concreted Pipe reference (1.01 meters above pond water surface)

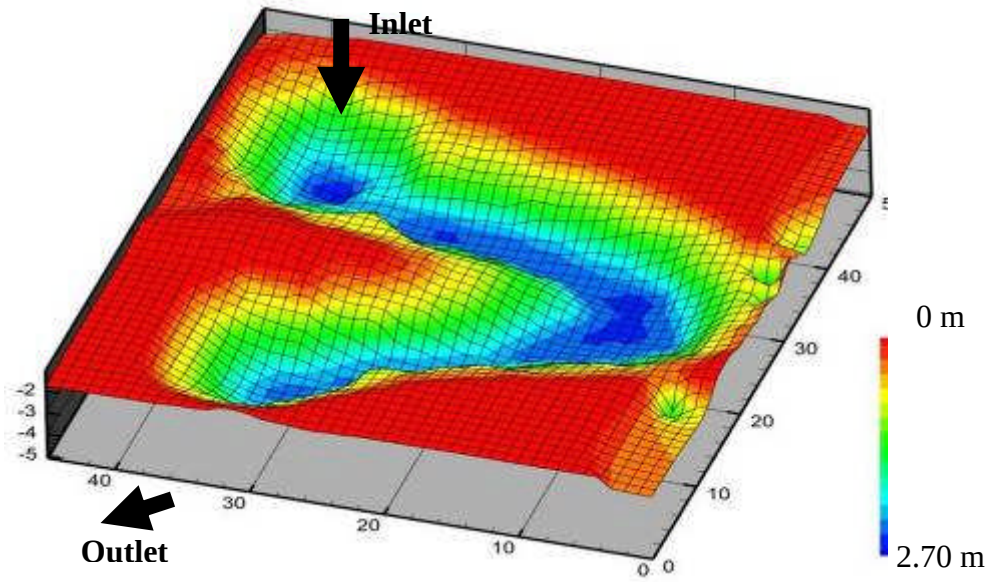

Figure 3-34. Lyby pond detail survey on July 2008.

b. Vegetation survey

There are five groups or categories (free-floating, marginal, algae, submerged and emergent) of aquatic plants in the pond but the vegetation arises mostly from four different kinds of plants such as *Cattail* (Typha Spp. Marginal Plant), *Watercress* (Emergent plant), *Ribbon leaf pondweed* (Emergent) and *Myriophyllum heterophyllum coontail* ***(***Ceratophyllum demersum***).*** Based on pond water surface, the estimated coverage of those plant is about 20%, 2%, 2% and 70% (with the calculation based on photos taken and the original pond layout Figure 3-35 & Figure 3-36).

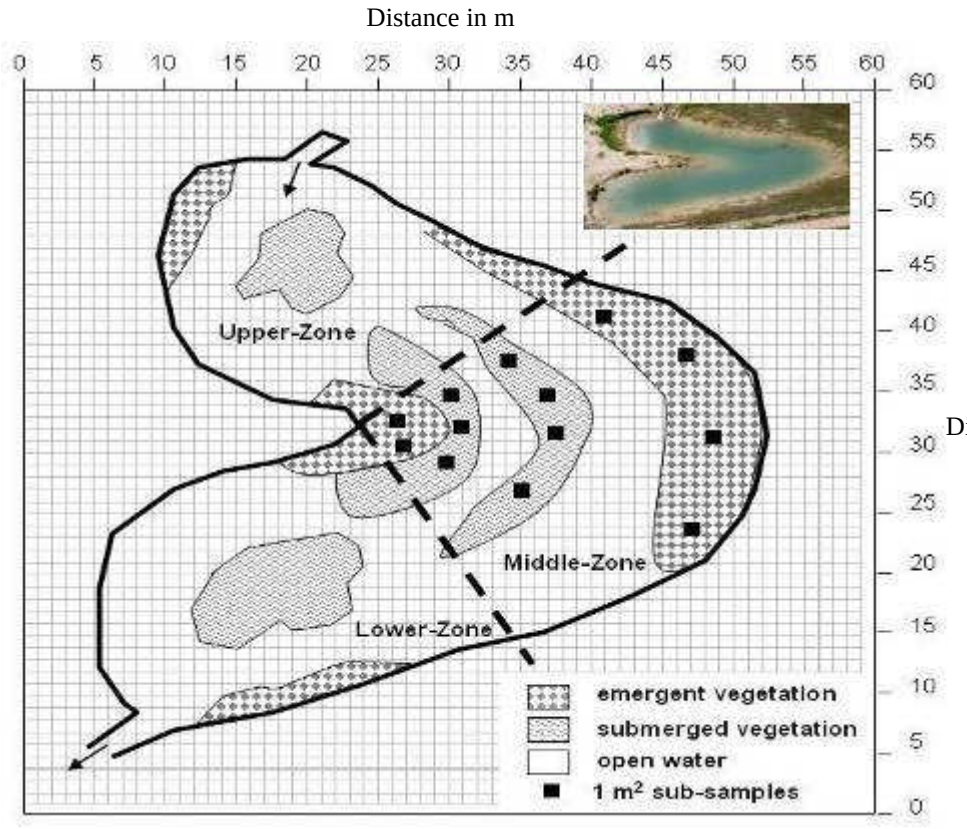

Figure 3-35. Vegetation covered in Lyby pond.

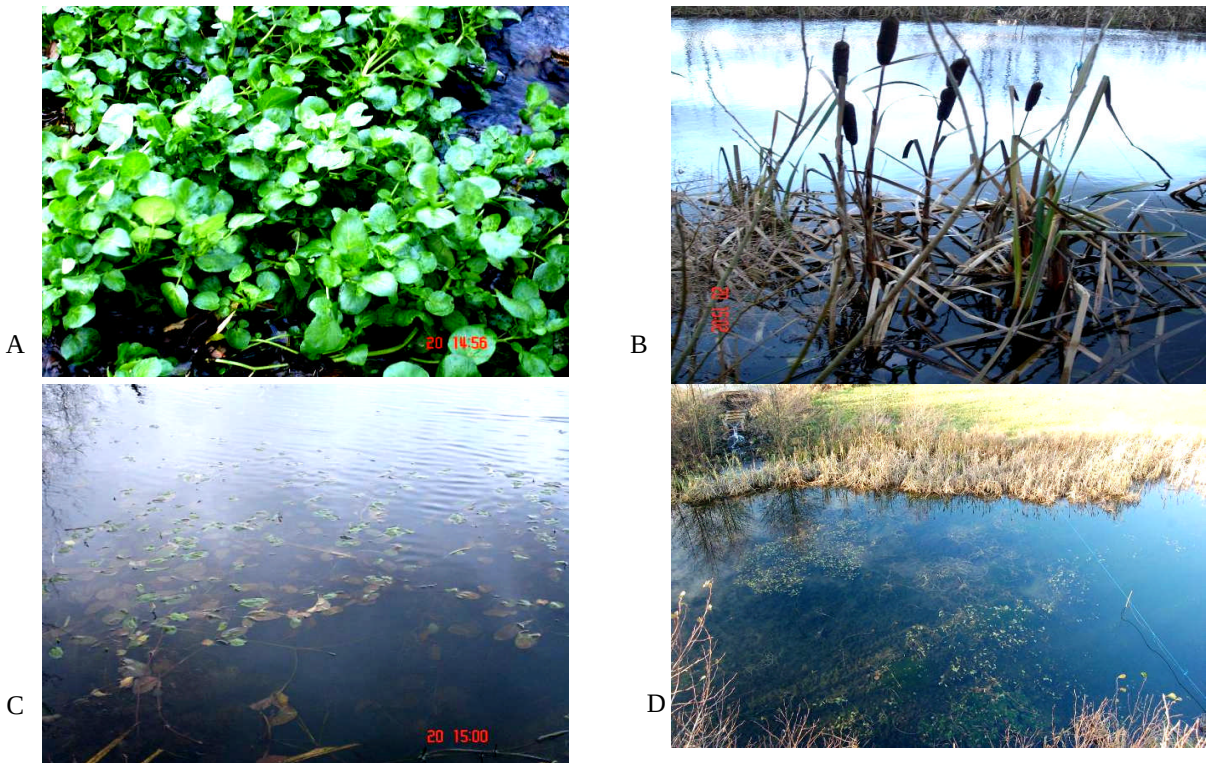

Figure 3-36. Four main kind of aquatic plants existed in Lyby pond; A: Watercress, B: Cattail (Typha spp.), C: Ribbon leaf pondweed and D: Myriophyllum heterophyllum coontail (Ceratophyllum demersum).

3.8.5 Instruments calibration and stability tests

The last two full traces (July 2007 and March 2008) showed unacceptable results (Appendix C). There were three reasons suspected for these problems, namely instrumental malfunctions which yielded unusable results: one was the instrument set up or calibration and the other was the pond ecosystem. Few tests were conducted on calibration of instruments (Scufas, Cyclops and handheld, see Figure 3-37, Figure 3-38 & Figure 3-39); three sets of laboratory calibrations on SCUFAs were also conducted. A series of calibrations and stability tests was conducted on the instruments, namely stream and background outlet flume water tests, calibrated in a glass beaker and read in the black buckets. The results show that all instruments responded very well and confirmed that the previous problem on different traces was due to a faulty instrument cable. The other one was due to destruction of the instrument's sensor by leeches, see Appendix C.

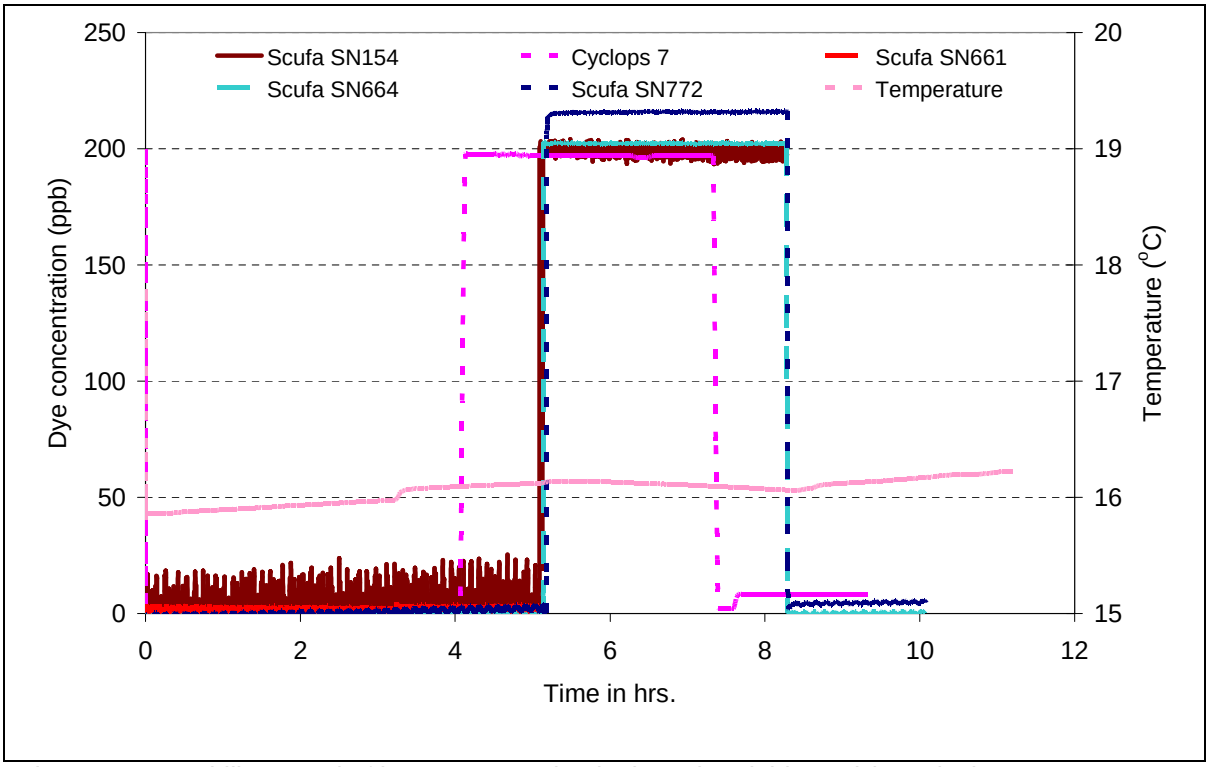

Figure 3-37. Stability tested of instruments using in the Lyby Field Pond (Sweden).

Figure 3-38. The in-door installation of instruments for stability tested.

Figure 3-39. The installation of Scufa instruments for stream stability tested.

3.8.6 Decay or absorbent test

As there are plenty of aquatic plants in the pond, they may absorb or decay the dye concentration. Both processes were considered as factors which may affect the operation of the dilution method (Dye, Rhodamine WT Tracing Technique). A decay test was set up with two different conditions, sunlight and dark condition, with two of the main four kinds of aquatic plants species used (Watercress and Myriophyllum heterophyllum coontail). The result showed there were contrasts between buckets with and without vegetation. Nevertheless, the study showed the same results for buckets in dark or sunlight conditions. Without taking into account the temperature effect on the Handheld (reading instrument), there was about 25% reduction and increase of dye concentration on the bucket with vegetation and without vegetation respectively, See Figure 3-40 & Figure 3-41. If we include the temperature effect on the instrument itself, the decay rate or absorbent rate (within around 3 to 4 Days) of vegetation on Dye (Rhodamine WT) was about 0% where the main effect may have been caused from the bio-film forming on the vegetation

during the dye measurement process, without filtering the sample, so the turbidity associated with the bio-film formation may have interfered with the reading.

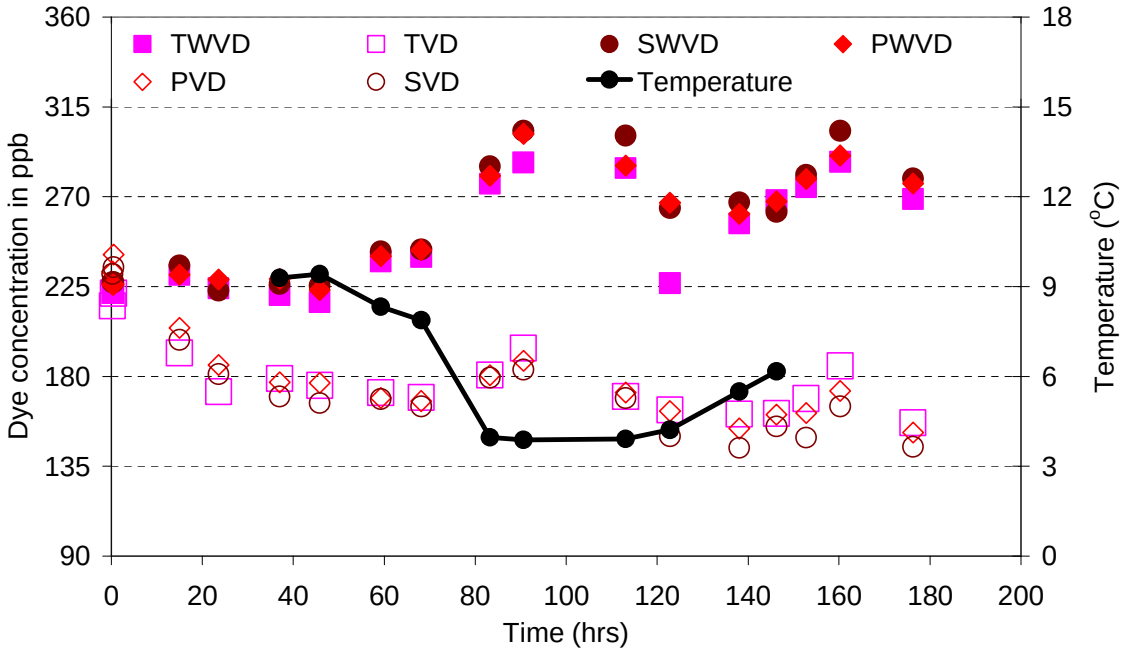

T = Tap water; P = Pond Water; S = Stream Water; WV= Without Vegetation; V = Vegetation; D = Dark; L = Sun Light

Figure 3-40. Decay and absorbence test based on dark condition.

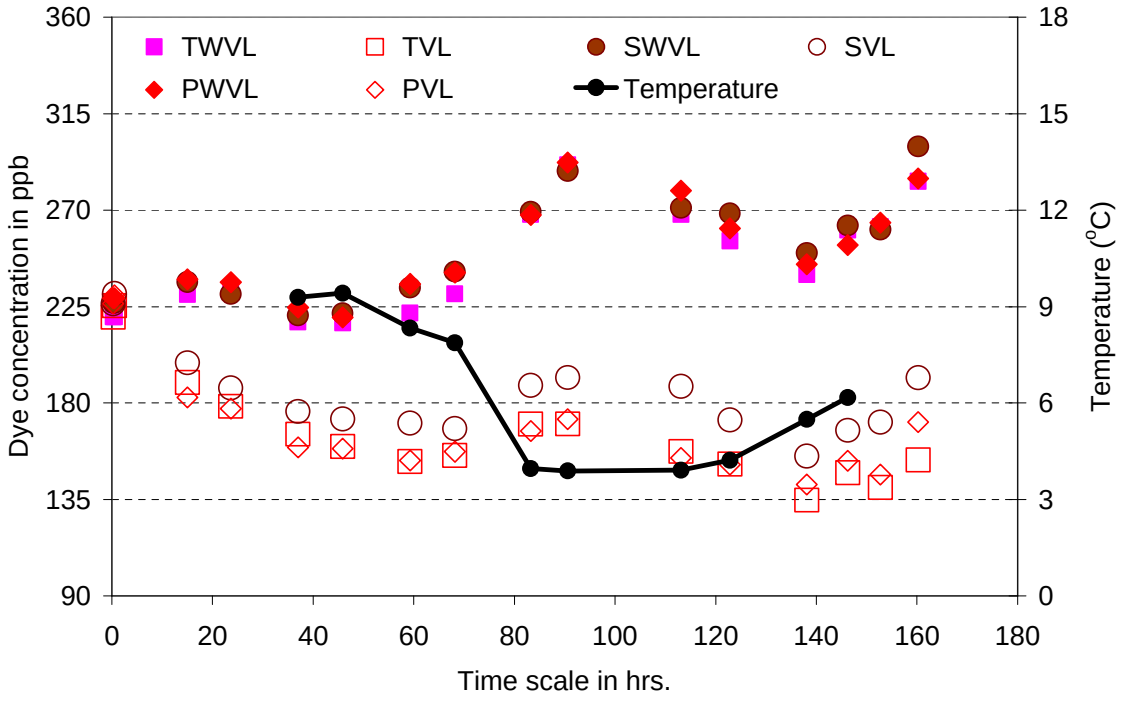

T = Tap water; P = Pond Water; S = Stream Water; WV= Without Vegetation; V = Vegetation; D = Dark; L = Sun Light

Figure 3-41. Decay and absorbent test based on sunlight condition.

3.8.7 Experimental Runs

Only three experiments were conducted within the flow rate range of 5-20 l/s and no experiments were conducted in the flow rate range of 20-40 l/s (as the inlet discharge based on water run-off from catchments area), in which overflow from the upper pond occurred through the inlet V-notch weir flume. The experiment was based on different kinds of vegetation density, with in 4four conditions (2 or 3 months based (Mar.-April, May-June, July-August, and Sep.-Nov., as Dec – Feb pond is frozen)). Eight configuration experiments were planned but only 3 experiments were conducted, see Table 3-3 and Appendix B. The field experimental runs were undertaken during the course of the experimental programme, in order to review *in situ* the design of new runs and number of runs

based on the results of work completed, which are based on the hydrograph of the inlet discharges. Table 3-3 shows the different run configurations undertaken.

Actual range of discharge, Q_{in} (l/s)	Vegetation Condition (Monthly based and support by photographs from the top of Constructed Hunting Tower).			
	Mar.-Apr.	May-June	July-Aug.	Sep.-Nov.
0 - 20	2	0	0	1

Table 3-3. Summary of field experimental running conditions.

CHAPTER: IV

4 Results (Laboratory Model)

4.1 Experiment results from physical Scale Pond with the same discharge

The main objective of this work was to provide sets of reliable data to enable comparison of the effect of discharges and vegetations condition on the Hydraulic Residence Time Distribution (HRTD), Hydraulic Retention Time (HRT or t_m as a centroid of HRTD) and Surface Velocity Profiles. Moreover, to understand how the effect of vegetation condition affected on the Nominal Retention Time (t_n= *V/Q*). The experiments were conducted from very low to very high discharge with 8 different vegetation configurations; there were triplicate experiment for higher discharge ranges from 28.69 to 45.90 ml/s but no PIV was conducted within this range of discharge. For lower range discharge (4.4 to 22.96 ml/s), 40 PIV studies performed with some limitation on double or triplicate repeats of the experimental run within this lower range of discharge. The data produced are considered

sufficient for the investigation of the effect of vegetation on the hydraulic behaviour as well as surface flow profiles to be determined.

A total of 145 runs have been conducted over a period of two years. Each run had a different experimental configuration. Both PIV technique and Rhodamine WT trace technique were utilised. Of the 145 runs conducted, only 40 were accompanied by PIV tests, with the rest using Rhodamine WT traces only. The detailed results of experimental runs for each configuration condition are presented below, starting from each fixed discharge ranging from 4.4 ml/ to 45.9 ml/s and each fixed discharge run with 7 different vegetation conditions. Moreover, starting from fixed vegetation, each vegetation ranged from non (0E) to highest density of both submerged and emerged vegetation (27EH) and each fixed vegetation was run with 9 different discharge.

4.1.1 Summary results from trace with discharge (Q_{in}) 4.4 ml/s with 7 vegetation conditions

i, *Trace with discharge 4.4 ml/s without vegetation condition (0E)*

The flow rate was fixed at 4.4 ml/s (in the field 7.5 l/s) and the controlled vegetations varied from no vegetation (0E) to only 11E (the length of emergent plants which grow toward the middle of the pond by 11%, at 1% of water and vegetation density, of the average pond cross-section) and then followed, step by step, to highest density of both emergent and submerge plants (22E, 27E, 27EL, 27EM and 27EH), Table 4-1. Dye recovery for all runs ranged from 75 to 123% with an average of 91%. There were some consistent differences between the HRTD plots of run number 1 and 2 at vegetation 0E and 11E (none or negligible

emergent plant) to run number 3 to 7 with both high density of emergent and submerged plant (22E, 27E, 27EL, 27EM and 27EH). Some parameters of hydraulic efficiency differed significantly between run 1 and 2 (0E and 11E) to run 3 to 7 (22E, 27E, 27EL, 27EM and 27EH), but none of the parameters of hydraulic efficiency differ significantly among high density vegetation cases such as run number 3 to 7, Figure 4-1. The relative hydraulic efficiency of actual residence time (t_m), relative of HRTD's centroid, e_m, varied from 0.75 to 1.15, at run 1 and 2 (0E and 11E) to 0.92 to 1.28 at run 3 to 7 (higher density of vegetation 22E, 27E, 27EL, 27EM and 27EH); The relative hydraulic efficiency e_o of the first dye arrival pond's outlet was 0.01 at run 1 and 2 (non- and less emergent plants, 0E and 11E) and 0.1 to 0.4 at run 3 to 7 with more higher density of vegetation. The relative hydraulic efficiency e_p of peak concentration varied from 0.01 to 0.02 at run 1 and 2 and 0.2 to 0.6 at run 3 to 7 (there was a possibility that a wind turbine affected run 6 which had a value of e_p = 0.17). The dimensionless relative time variance, σ^2, varied from 0.85 to 1.73 at run 1 and 2 and 0.61 to 1.45 at run 3 to 7.

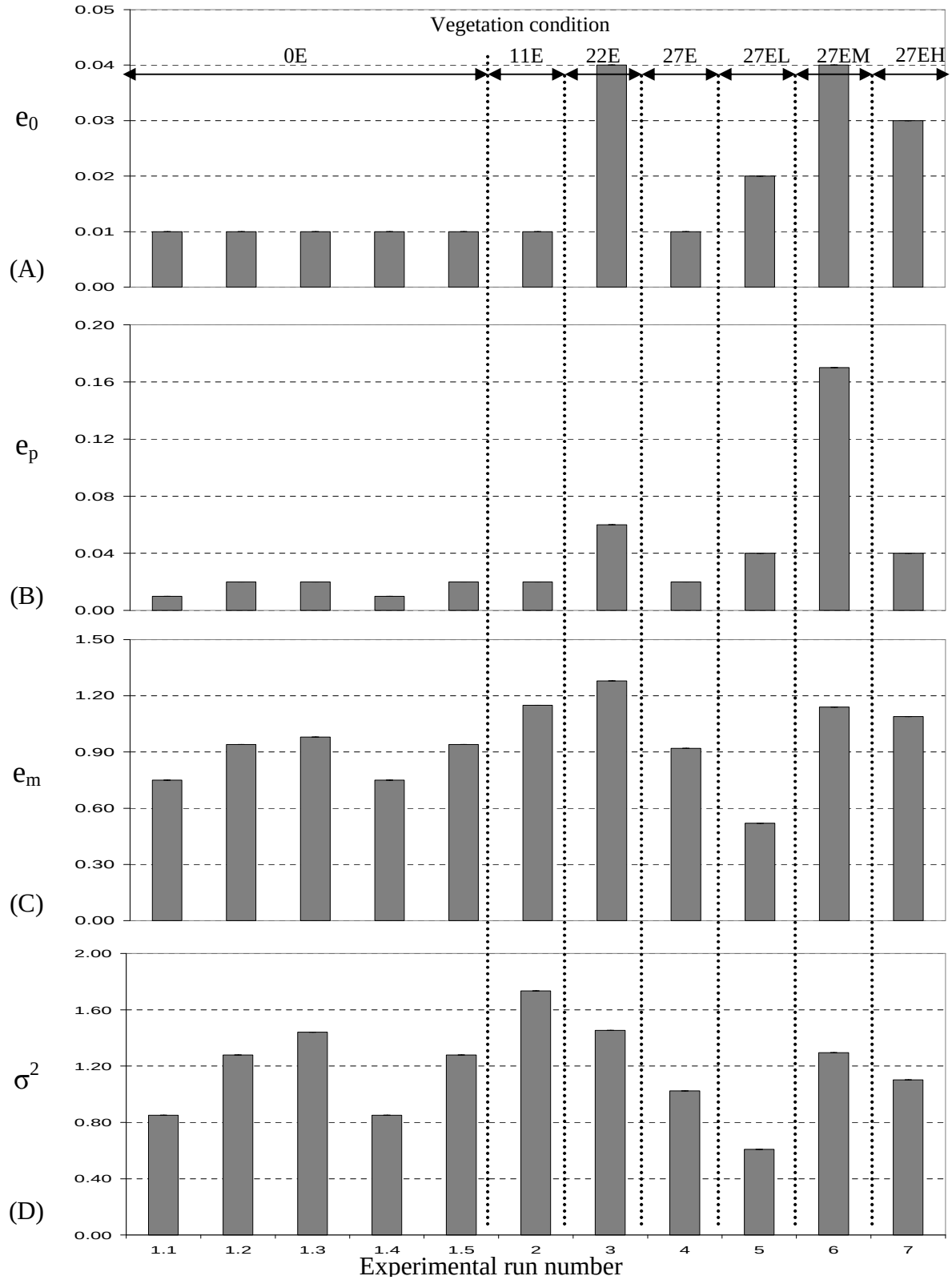

Figure 4-1. The residence time distribution (HRTD) characteristics under differing vegetation configuration. Comparisons are made at the same discharge (4.4 ml/s) and among different vegetation configurations for (A) first dye arrival at the pond outlet (e_0), (B) peak concentration time ($e_p = t_p / t_n$), (C) real residence time (Centroid of HRTD, $e_m = t_m / t_n$), (D) relative time variance (σ^2).

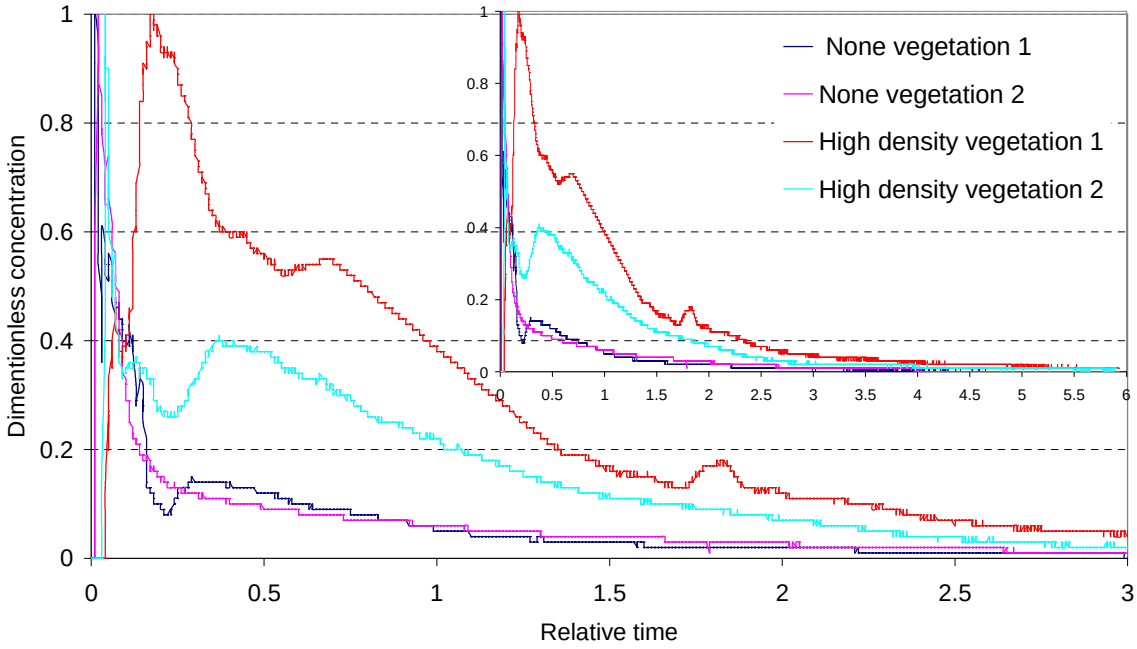

Figure 4-2. Comparison of four representative residence time distribution (HRTD) curves run with the same discharge (4.4 ml/s) at no vegetation to different vegetation configurations.

The overall results of HRTDs indicated that comparisons of run 1 to other runs (0E to different vegetation configurations) appeared to show distinctively different behaviour. Where the HRTDs of run 1 and 2 were unimodal, the HRTD for run 3 to 7 (more density vegetation 22E, 27E, 27D, 27EL, 27EM and 27EH) was usually bimodal, with the first peak typically arriving late and being more spread out than run 1 and 2 HRTD, Figure 4-2. These differences were reflected in the HRTD statistics, Figure 4-1. The average relative time of first dye arrival, e_0, was 0.01 for run with no and less emergent plants (run 1 and 2 at vegetation 0E and 11E), and 0.028 for the higher density vegetation configurations (run 3 to 7 at vegetation 22E, 27E, 27D, 27EL, 27EM and 27EH), Figure 4-1 A. The relative time to peak concentration of the HRTD curve, e_p, occurred at the average value of 0.017 for run with none and less emergent plants (run 1 and2 at vegetation 0E and 11E), and 0.04 for run with more higher density of vegetation configurations, Figure 4-1

B. The mean relative residence time, the relative HRTD centroid, e_m, was an average of 1.04 for run with no and little emergent plant (run 1 and 2 at vegetation 0E and 11E), and the average of 0.99 for the higher vegetation density configurations, Figure 4-1 C. The mean relative HRTD spread, σ^2, was an average of 1.43 for run with none or less plants (run 1 and 2 at vegetation 0E and 11E), and an average of 1.1 for the experimental runs with higher vegetation (run 2 to 7), Figure 4-1D. Each of these measurements of hydraulic efficiency is a function of nominal residence time (t_n= V/Q and normalise as t_n=1).

Repeat tests were conducted randomly among different vegetation configurations, with five repeat dye tracers conducted for run number 1, where there was no significant deference between all its HRTD results (Figure 4-1). Based on that result there was only one dye tracer experiment which was conducted for run 2 to 7 (other vegetation condition such as 11E, 22E, 27E, 27ED, 27EL, 27EM and 27EH). Table 4-1, shows the detail of HRTDs in all runs with none vegetation and all vegetation configurations based on 4.4 ml/s discharge (equal to 7.5 l/s in the Lyby pond).

Discharge, Qin (ml/s)	Vegetation Conditions	Run No.	$e_0 = t_0/t_n$	$e_p = t_p/t_n$	$e_m = t_m/t_n$	σ^2 (based on relative time)
4.4	0E	1.1	0.01	0.01	0.75	0.85
	0E	1.2	0.01	0.02	0.94	1.28
	0E	1.3	0.01	0.02	0.98	1.44
	0E	1.4	0.01	0.01	0.75	0.85
	0E	1.5	0.01	0.02	0.94	1.28
	Mean of 0E	1	0.01	0.02	0.94	1.14 (0.27)
	11E	2	0.01	0.02	1.15	1.73
	22E	3	0.04	0.06	1.28	1.45
	27E	4	0.01	0.02	0.92	1.02
	27EL	5	0.02	0.04	0.52	0.61
	27EM	6	0.04	0.17	1.14	1.30
	27EH	7	0.03	0.04	1.09	1.10

Table 4-1. HRTD Statistics of tracer runs at 4.4 ml/s with different vegetation configurations (0E, 11E, 22E, 27E, 27ED, 27EDL, 27EM and 27EH).

Surface flow profiles were obtained using PIV with fixed flow rate of 4.4 ml/s (in the field 7.5 l/s) and the controlled vegetation being varied from 0E, 11E and 11E and 22E, 27E, 27EL, 27EM and 27EH (see Table 4-1). There were some consistent differences between the surface flow profiles, mainly based on the presence or absence of vortices, of run number 1 and 2 at vegetation 0E or 11E to run 3 to 7 with higher vegetation density. Some of the surface flow profiles (vortices) differed significantly between run 1 and 2 (none and less vegetation), Figure 4-3, to run 3 to 7 with more higher density of vegetation but none of surface flow profiles differed significantly among run 3 to 7 at vegetation 22E, 27E, 27EL, 27EM and 27EH, Figure 4-4. Two main vortices were present, in section 1/3 and 2/3 of the physical scale pond and no channel flow in these section, at run 1 and 2, Figure 4-3. There was only one small vortex and the main channel flow was present in section 1/3 of the pond and in the remaining sections (2/3 and 3/3) of the physical scale pond respectively, at run 3 to 7 with vegetation 22E, 27E, 27EL, 27EM and 27EH, Figure 4-4.

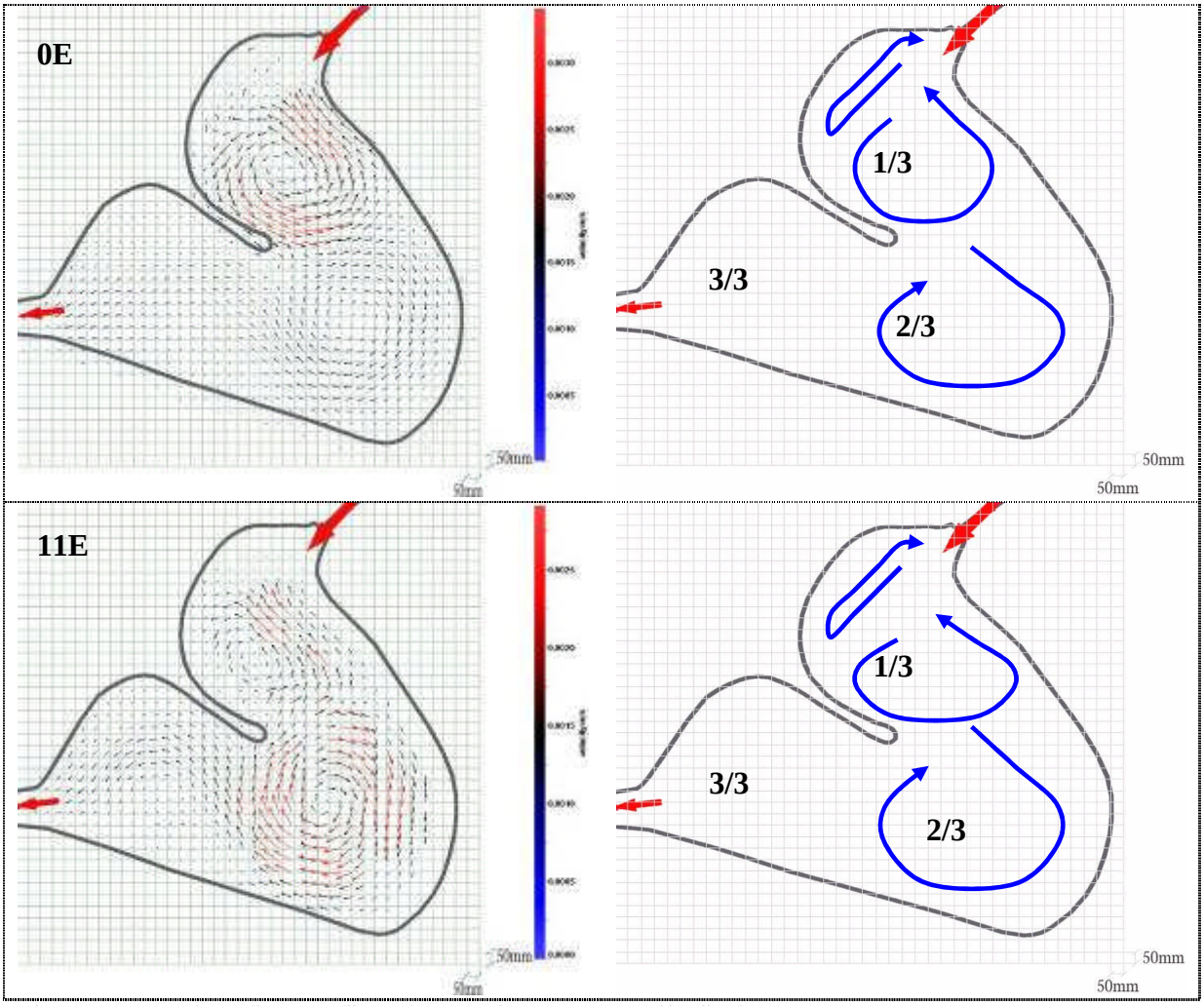

Figure 4-3. Surface flow profiles of 0E and 11E at 4.4 ml/s discharge.

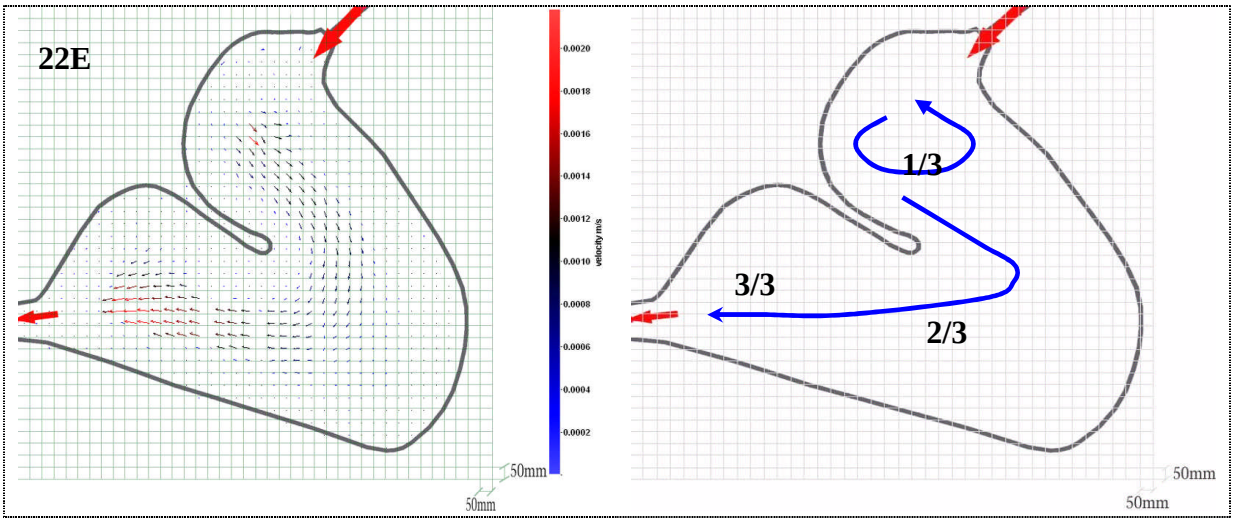

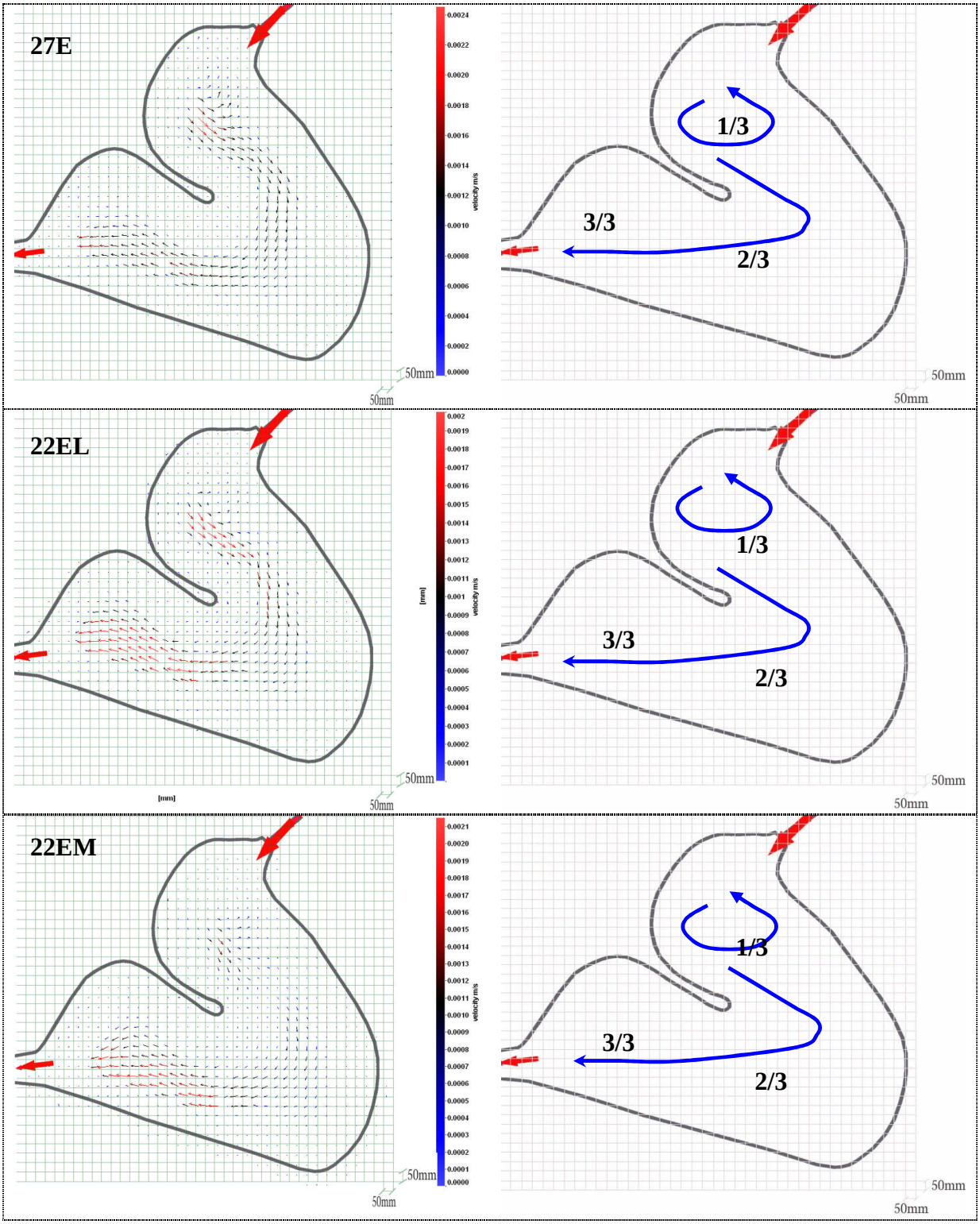

Figure 4-4. Surface flow profile of 22E, 27E, 27EL and 27EM at 4.4 ml/s discharge.

4.1.2 Summary results from trace with discharge (Q_{in}) 5.74 ml/s with 7 vegetation conditions

With the same controlled vegetation configurations as in section 4.1.1, the flow rate was changed and fixed at 5.74 ml/s (corresponding in the field to a value of 10 l/s), see Table 4-2. Dye recovery for all runs ranged from 60 to 119% with an average of 90%. No consistent trend was observed between the HRTD plots of run 8 to 16 with vegetation content varying between no vegetation (0E) to both high density of emergent and submerged plant (27EH), respectively. Some of the parameters for hydraulic efficiency fluctuated but did not have any significant difference whilst changing vegetation condition, Figure 4-5. For all runs, run 8 to 16 with no vegetation to the highest density of vegetation (0E to 27EH) respectively, e_m varied from 0.8 to 1.25 (δ = 0.16), e_o tended to reduce from 0.07 to 0.02, e_p varied from 0.08 to 0.16 and σ^2 was fluctuated and ranged from 0.42 to 2.52 (there was some problem on run 10.4 and 13.3, Table 4-2).

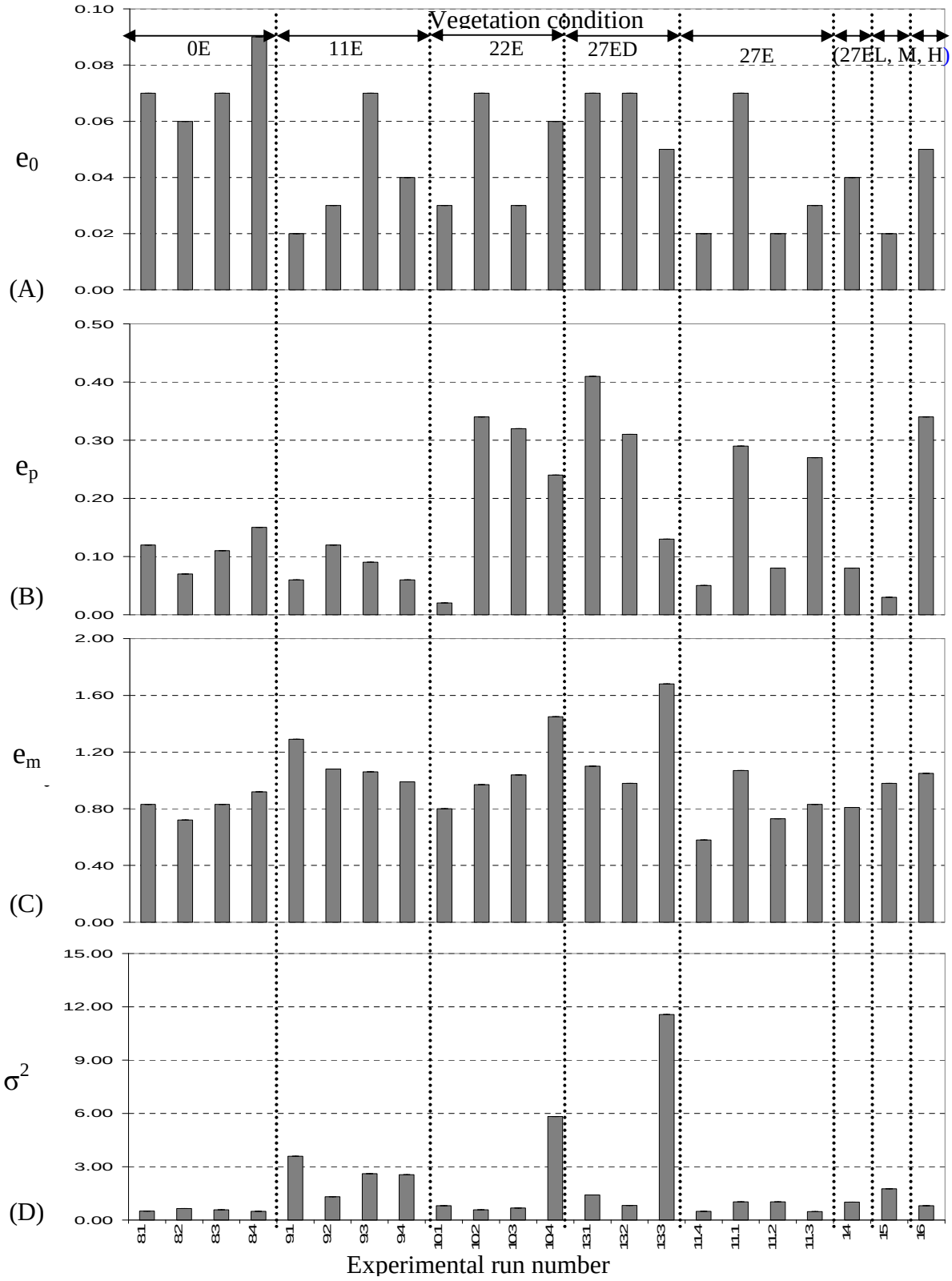

Figure 4-5. The residence time distribution (HRTD) characteristics under differing vegetation configuration. Comparisons are made at the same discharge (5.74 ml/s) and among different vegetation configurations for (A) first dye arrival at the pond outlet (e_0), (B) peak concentration time ($e_p = t_p / t_n$), (C) real residence time (Centroid of HRTD, $e_m = t_m / t_n$), (D) relative time variance (σ^2).

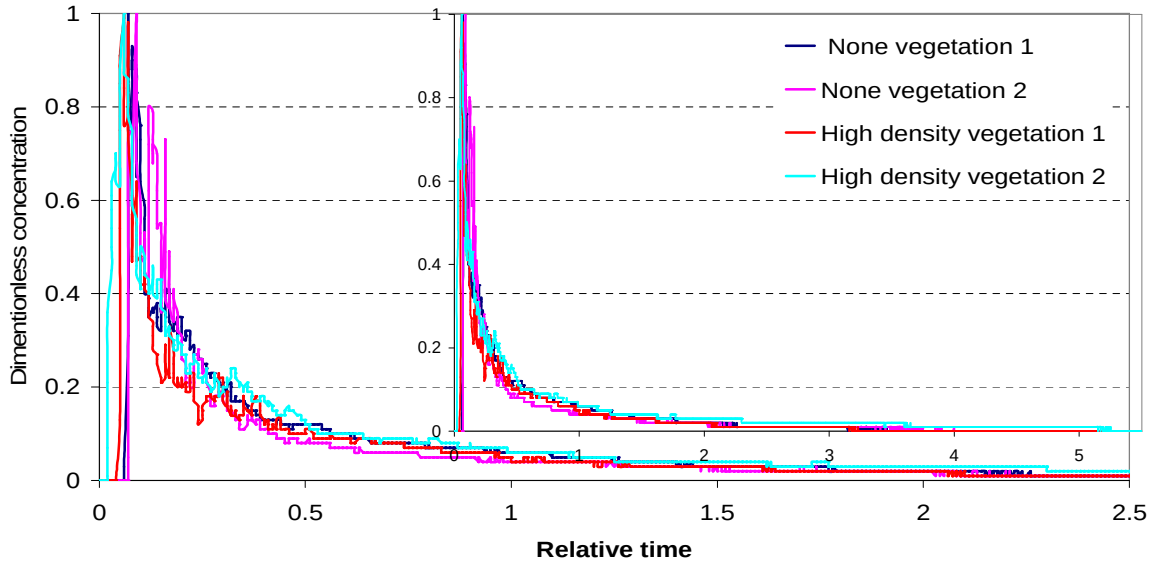

Figure 4-6. Comparison of four representative residence time distributions (HRTDs) curves of none vegetation to different vegetation configurations with Q = 5.74 ml/s.

The HRTDs were compared between each run from run number 8 to 16, as the vegetation configuration changed from no vegetation to different vegetation configurations, but no significant differences in HRTD were observed. In all cases the HRTDs were bimodal with the each first peak typically arriving early and being less spread out in its form. These similarities were reflected in the HRTD statistics, Figure 4-5. The mean value of overall first dye arrival, e_o, was 0.04 (δ = 0.02), Figure 4-5A. The time to peak concentration of the HRTD curves, e_p, occurred, with no consistent fluctuation among all runs where vegetation changed from none vegetation to highest vegetation condition, at the average value of 0.12 and mean value of 0.14 (δ = 0.12), Figure 4-5B. The relative mean residence time of all vegetation configurations, relative time HRTD centroid, e_m, with an average of 0.99 ,and mean value was 1.02 (δ = 0.16), Figure 4-5C. However, with the same experimental runs, run 8 to 16, σ^2 were slightly fluctuated but with no significantly difference, with an average σ^2 = 0.99.

The repeat tests were conducted randomly among different vegetation configurations, with four repeat dye tracers being conducted for run number 8, 9, 10, 11 and 13 where vegetation changed from 0E, 11E, 22E, 27E and 27ED, respectively. There were no significant differences observed between all their relative HRTD results, Figure 4-5 and then only one dye tracer was run for each run number 14 to 16 at 27EL, 27EM and 27EH vegetation configuration. Table 4-2, shows the details of the relative HRTDs in all runs (8 to 16) from no vegetation cases to all other vegetation configurations based on 5.74 ml/s discharge (equal to10 l/s in the Lyby pond).

Discharge, Qin (ml/s)	Vegetation Conditions	Run No.	$e_o = t_o/t_n$	$e_p = t_p/t_n$	$e_m = t_m/t_n$	σ^2 (based on relative time)
5.74	0E	8.1	0.07	0.12	0.83	0.51
	0E	8.2	0.06	0.07	0.72	0.65
	0E	8.3	0.07	0.11	0.83	0.58
	0E	8.4	0.09	0.15	0.92	0.49
	Mean of 0E (S.D)	8	0.07	0.12	0.83	0.56 (0.07)
	11E	9.1	0.02	0.06	1.29	3.59
	11E	9.2	0.03	0.12	1.08	1.32
	11E	9.3	0.07	0.09	1.06	2.61
	11E	9.4	0.04	0.06	0.99	2.55
	Mean of 11E	9	0.04	0.08	1.11	2.52 (0.93)
	22E	10.1	0.03	0.02	0.8	0.81
	22E	10.2	0.07	0.34	0.97	0.58
	22E	10.3	0.03	0.32	1.04	0.68
	22E	10.4	0.06	0.24	1.45	5.82
	Mean of 22E	10	0.05	0.15	1.07	0.69 (0.11)
	27ED	13.1	0.07	0.41	1.1	1.41
	27ED	13.2	0.07	0.31	0.98	0.82
	27ED	13.3	0.05	0.13	1.68	11.58
	Mean of 27ED	13	0.06	0.16	1.25	0.76 (0.31)
	27E	11.4	0.02	0.05	0.58	0.49
	27E	11.1	0.07	0.29	1.07	1.03
	27E	11.2	0.02	0.08	0.73	1.03
	27E	11.3	0.03	0.27	0.83	0.48
	Mean of 27E	11	0.04	0.11	0.80	0.42 (0.12)
	27EL	14	0.04	0.07	0.81	1.01
	27EM	15	0.02	0.08	0.98	1.76
	27EH	16	0.05	0.19	1.05	0.81

Table 4-2. HRTD statistics of tracer runs at 5.74 ml/s with different vegetation configurations (0E, 11E, 22E, 27E, 27ED, 27EL, 27EM and 27EH).

Surface flow profiles using PIV were obtained with fixed flow rate of 5.74 ml/s and controlled variations in vegetation. The experimental runs ranged from run number 8 to 16 where vegetation varied from 0E, 11E, 22E, 27E, 27ED, 27EL, 27EM and 27EH, respectively, Table 4-2. There were some consistent differences between the surface flow profiles, mainly based on the presence and forms of vortices (run 8 and 9 at vegetation 0E or 11E to run 10 to 16, with higher vegetation density). Some of the surface flow profiles (vortices) differed significantly between run 8 or 9 (vegetation 0E or 11E), Figure 4-7, to run 10 to 16 (for more higher density of vegetation) but none of surface flow profiles differed significantly among run 10 to 16 where vegetation ranged from 22E, 27E, 27ED, 27EL, 27EM and 27EH, Figure 4-8. Two main vortices appeared, in section 1/3 and 2/3 of the physical scale pond and no channel flow was observed in these section, at run 8 and 9 (vegetation 0E and 11E). There was only one small vortex and the main channel flow appeared in section 1/3 of the pond and in the remaining sections (2/3 and 3/3) of the physical scale pond respectively, at run 10 to 16 whilst vegetation range from 22E, 27E, 27ED, 27EL, 27EM and 27EH, respectively, Figure 4-8.

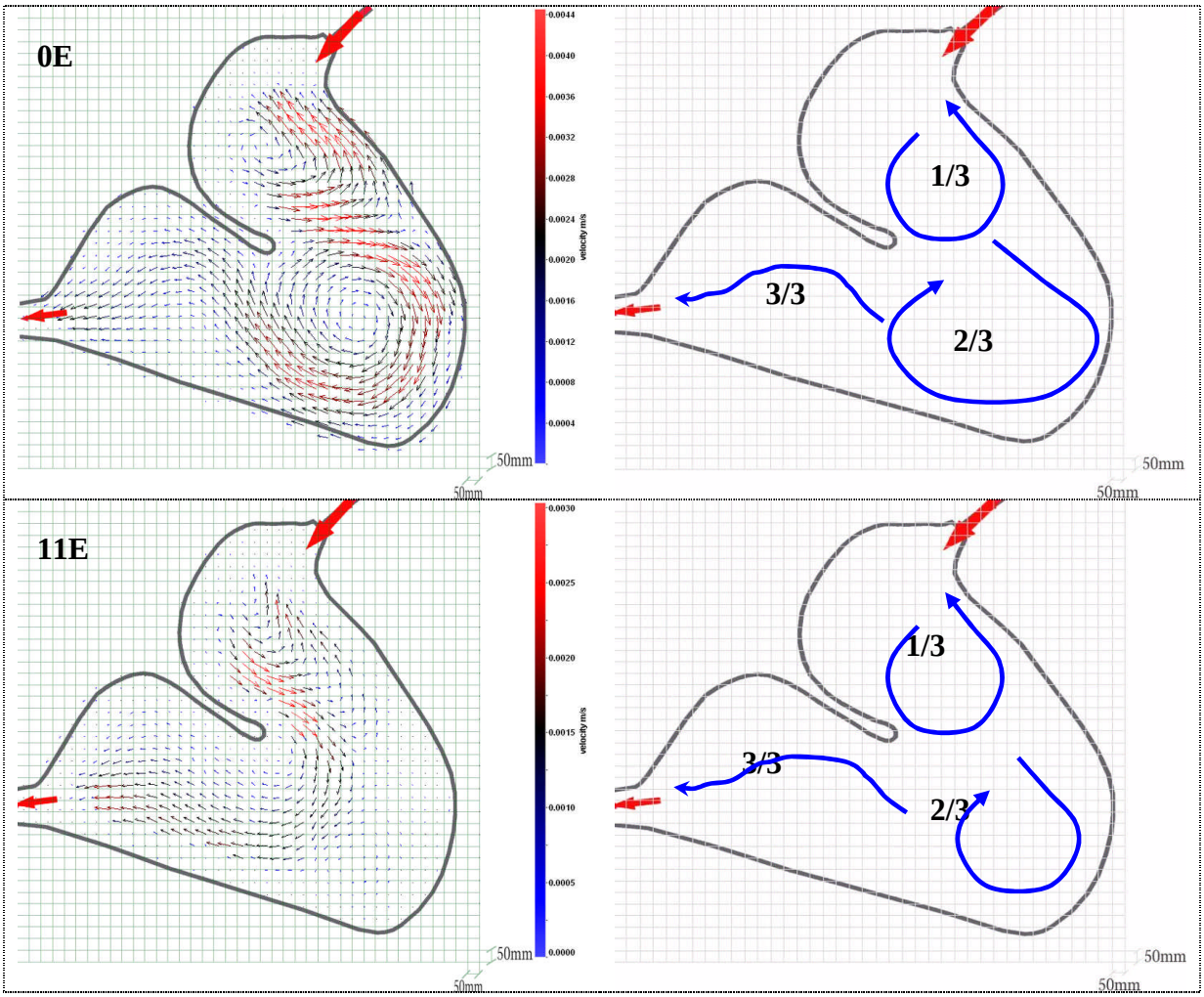

Figure 4-7. Surface flow profiles of 0E &11E vegetation at 5.74 ml/s discharge.

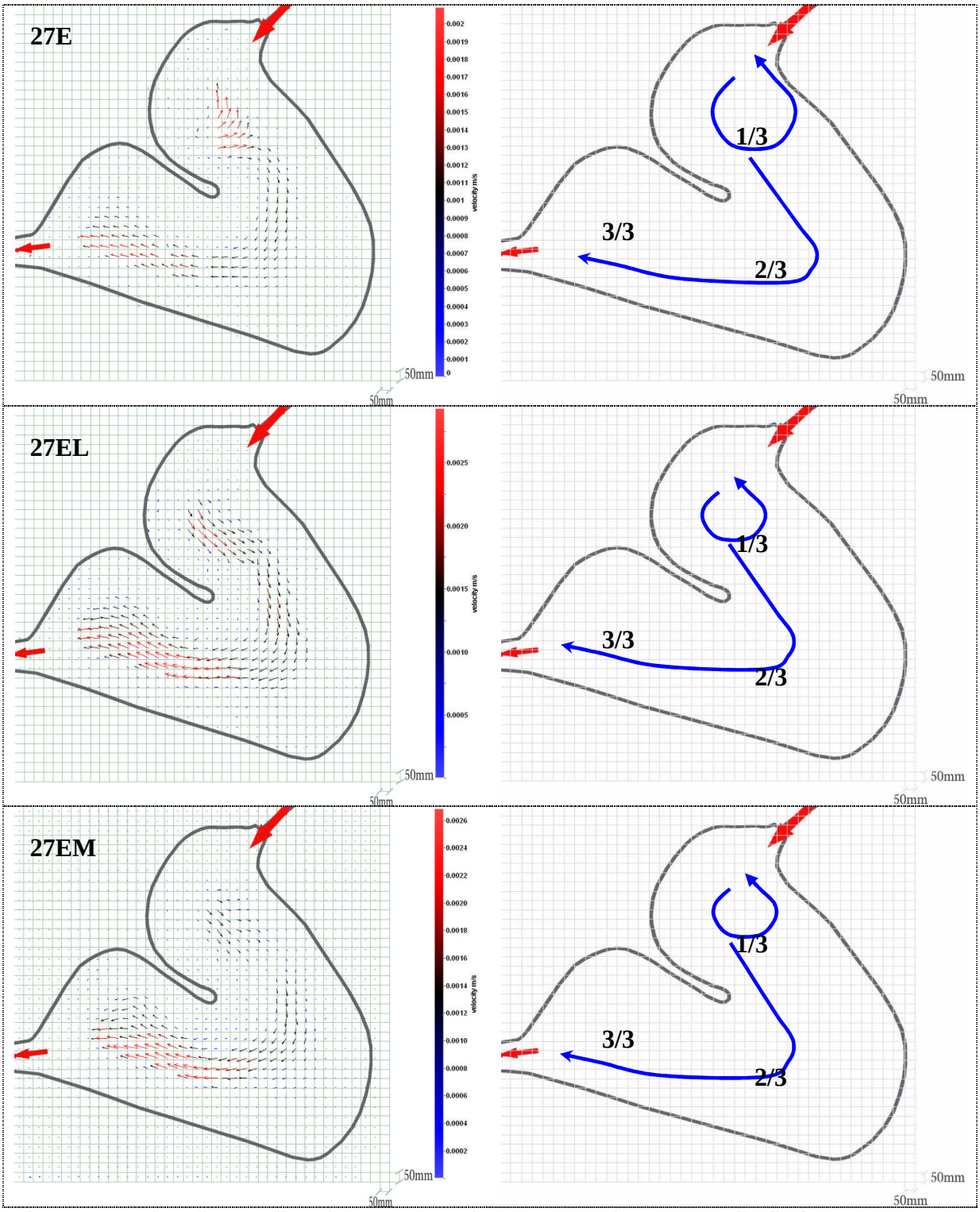

Figure 4-8.Surface flow profiles of 27E, 27EL and 27EM vegetation at 5.74 ml/s discharge.

4.1.3 Summary results from trace with discharge (Q_{in}) 11.48 ml/s with 7 vegetation conditions

With the same vegetation configurations as in section 4.1.2, the flow rate was changed from 5.74 to 11.48 ml/s (corresponding in the field to 20 l/s) see Table 4-3. Dye recovery for all runs (17 to 23) ranged from 60 to 134% with a mean value of 98% (δ = 0.17). There were no consistent differences measured between the relative HRTD plots of run number 17 to 23 where vegetation varied from 0E, 11E, 22E, 27E, 27ED, 27EL, 27EM and 27EH, respectively. Some of the parameters for hydraulic efficiency fluctuated but did not have any statistical significant difference as a result of changing vegetation conditions, Figure 4-9. Values of e_m varied from 0.53 to 1.12 (δ = 0.19), there was one spurious low value of e_m, because of an error on one trace (run 21); as expected it was affected by wind tunnel operation elsewhere in the laboratory during the experimental run. The mean value of e_m was 0.98, at run 17 to 23 from none vegetation to highest density of vegetation (0E to 27EH), Figure 4-9. The value of e_o fluctuated within the range from 0.03 to 0.07, where the mean value of e_o was 0.05 (δ = 0.01), for vegetation configuration changes from 0E to 27EH, Figure 4-9.

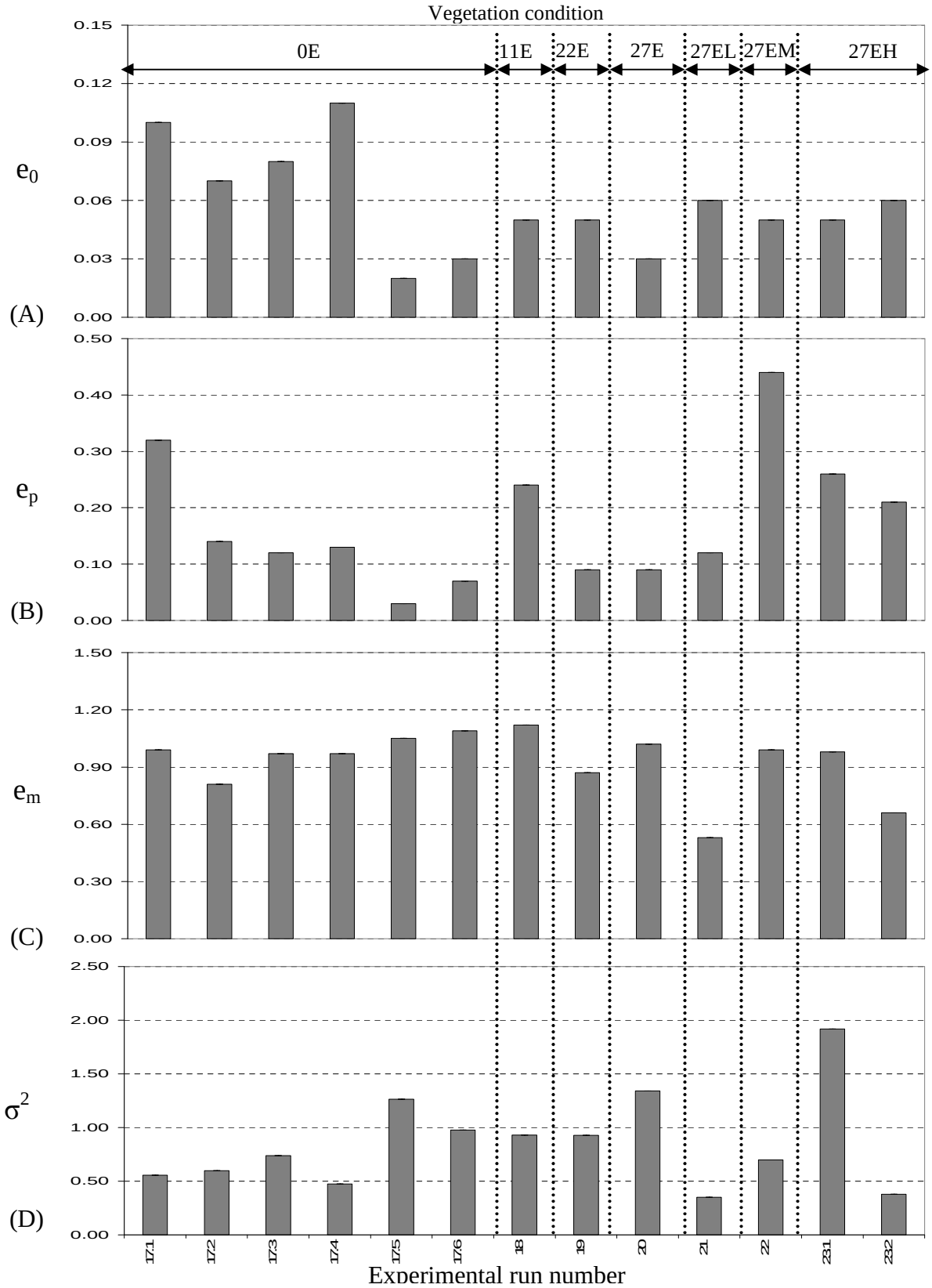

Figure 4-9. The residence time distribution (HRTD) characteristics under differing vegetation configuration. Comparisons are made at the same discharge (11.48 ml/s) and among different vegetation configurations for (A) first dye arrival at the pond outlet (e_0), (B) peak concentration time ($e_p = t_p / t_n$), (C) real residence time (Centroid of HRTD, , $e_m = t_m / t_n$), (D) relative time variance (σ^2).

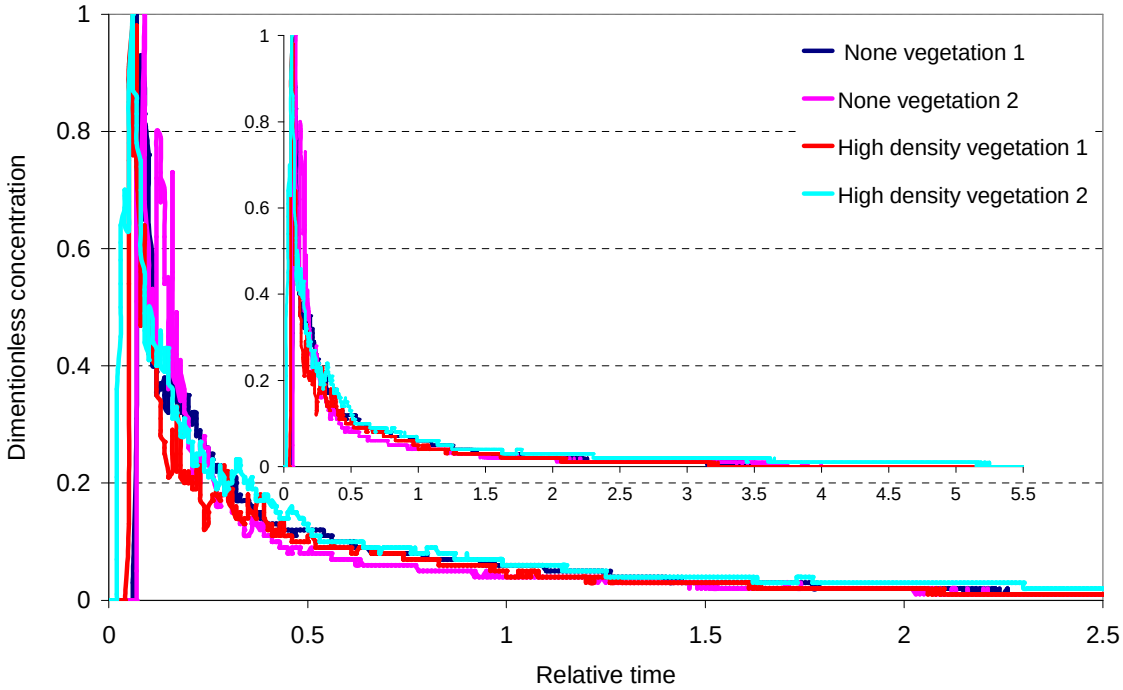

Figure 4-10. Comparison of four representative residence time distributions (HRTDs) curves of none vegetation to different vegetation configurations with Q = 11.48 ml/s.

As in section 4.1.2, relative HRTDs were compared between run 17 to 23 (from cases of no vegetation to different vegetation configurations), and appeared to show no significantly differences. All relative HRTDs were bimodal, with each first peak typically arriving early and being less spread out , as described for other experiments in section 4.1.2. These similarities were reflected in the HRTD statistics, Figure 4-10. The mean value of overall first dye arrival, e_o, was 0.05 (δ = 0.01) Figure 4-10A. The time to peak concentration of the HRTD curves, e_p, occurred, with none consistent fluctuation among run 17 to 23, from none vegetation to highest vegetation condition, at the average value of 0.19 and mean value of 0.14 (δ = 0.13), Figure 4-10B. The mean residence time of all runs with all vegetation configurations, relative HRTD centroid (t_m) was an average of 0.90 and mean value was 0.98 (δ = 0.19), Figure 4-10C.

Repeat tests were conducted randomly among different vegetation configurations; six repeat dye tracers were run for run number 17 with vegetation 0E (where there were no significant defences between all of the relative HRTD results, Figure 4-10), then only one dye tracer was run for each run number 18 to 23 with vegetation 11E, 22E,27E, 27EL, 27EM and 27EH, respectively. Table 4-3, shows the details of relative HRTD data in all runs (17 to 23) from no vegetation cases to all other vegetation configurations based on 11.48 ml/s discharge (corresponding to 20 l/s in the Lyby pond).

Discharge, Qin (ml/s)	Vegetation Conditions	Run No.	$e_o = t_o/t_n$	$e_p = t_p/t_n$	$e_m = t_m/t_n$	σ^2 (based on relative time)
11.48	0E	17.1	0.1	0.32	0.99	1.80
	0E	17.2	0.07	0.14	0.81	1.67
	0E	17.3	0.08	0.12	0.97	1.36
	0E	17.4	0.11	0.13	0.97	2.11
	0E	17.5	0.02	0.03	1.05	0.79
	0E	17.6	0.03	0.07	1.09	1.02
	Mean of 0E (S.D)	17	0.07(0.04)	0.23 (0.27)	0.98 (0.1)	1.46 (0.5)
	11E	18	0.05	0.24	1.12	1.08
	22E	19	0.05	0.09	0.87	1.08
	27E	20	0.03	0.09	1.02	0.75
	27EL	21	0.06	0.12	0.53	2.85
	27EM	22	0.05	0.44	0.99	1.43
	27EH	23.1	0.05	0.26	0.98	0.52
	27EH	23.2	0.06	0.21	0.66	2.64
	Mean of 27EH (S.D)	23	0.06 (0.01)	0.13 (0.03)	0.82 (0.23)	1.58 (1.5)

Table 4-3. HRTD statistics of tracer runs at 11.48 ml/s with different vegetation configurations (0E,11E, 22E, 27E, 27ED, 27EL, 27EM and 27EH).

Surface flow profiles from PIV measurements with a fixed flow rate of 11.48 ml/s (in the field 20 l/s) and vegetation varying from 0E to 11E and 22E, 27E, 27ED, 27EL, 27EM and 27EH (Table 4-3),showed some consistent differences (mainly based on vortices) between run number 17 or 18 with vegetation 0E or 11E to the

remaining run number 19 to 23 with more higher vegetation density. Some of the surface flow profiles (vortexes) differed significantly between run 17 or 18, with vegetation 0E or 11E, to run number 19 to 23 with more higher density of vegetation but none of surface flow profiles differed significantly between run 19 to 23 with vegetation 22E, 27E, 27ED, 27EL, 27EM and 27EH, Figure 4-12. There was only one main vortex observed in section 1/3 of the model pond and no channel flow in these section, at run number 17 and 18 with vegetation condition 0E and 11E, Figure 4-11. The main channel flow appeared in section 1/3, 2/3 and 3/3 at run 19 to 23 with vegetation 22E, 27E, 27ED, 27EL, 27EM and 27EH, respectively, Figure 4-12.

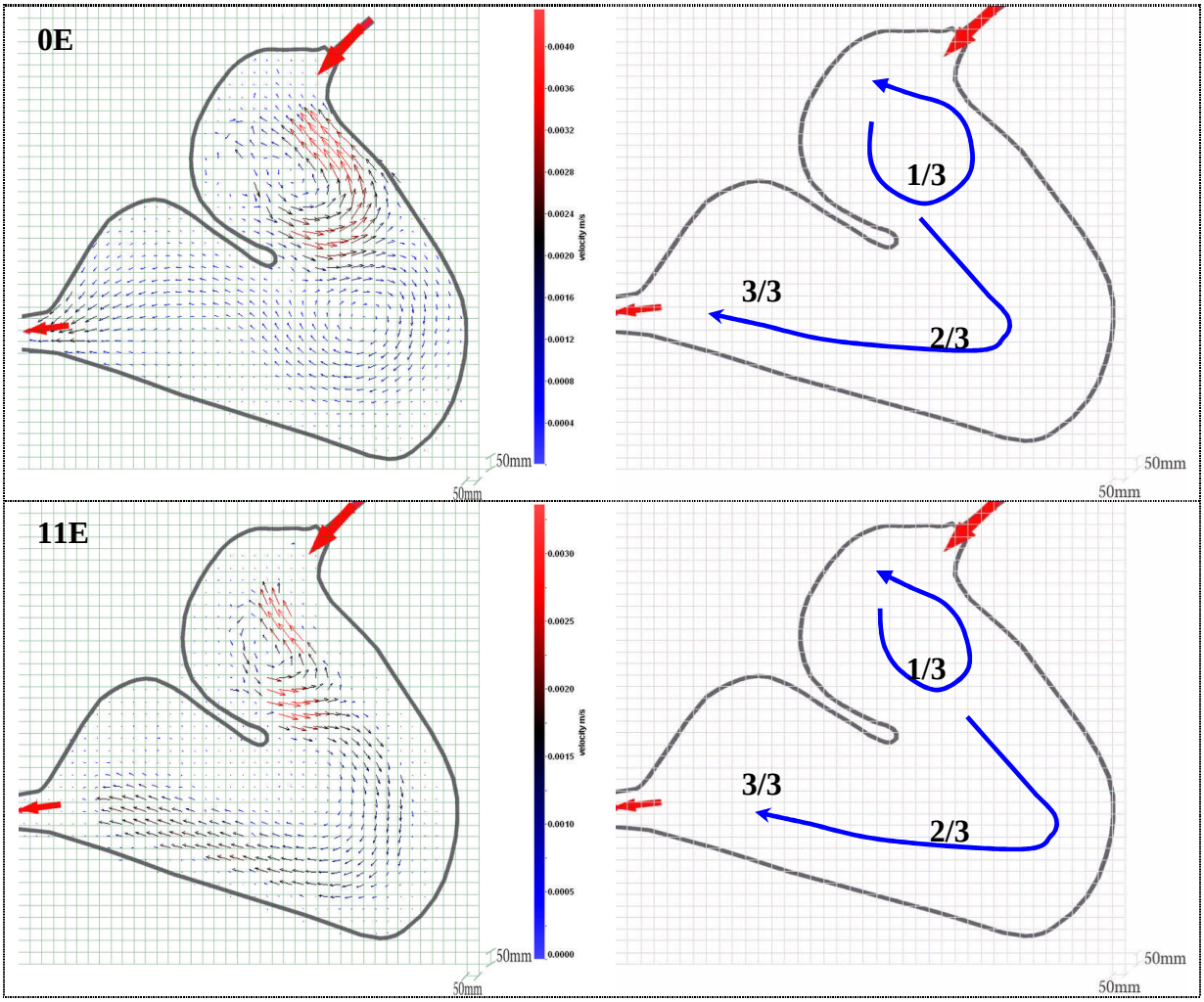

Figure 4-11. Surface flow profiles of 0E and 11E vegetation at 11.48 ml/s discharge.

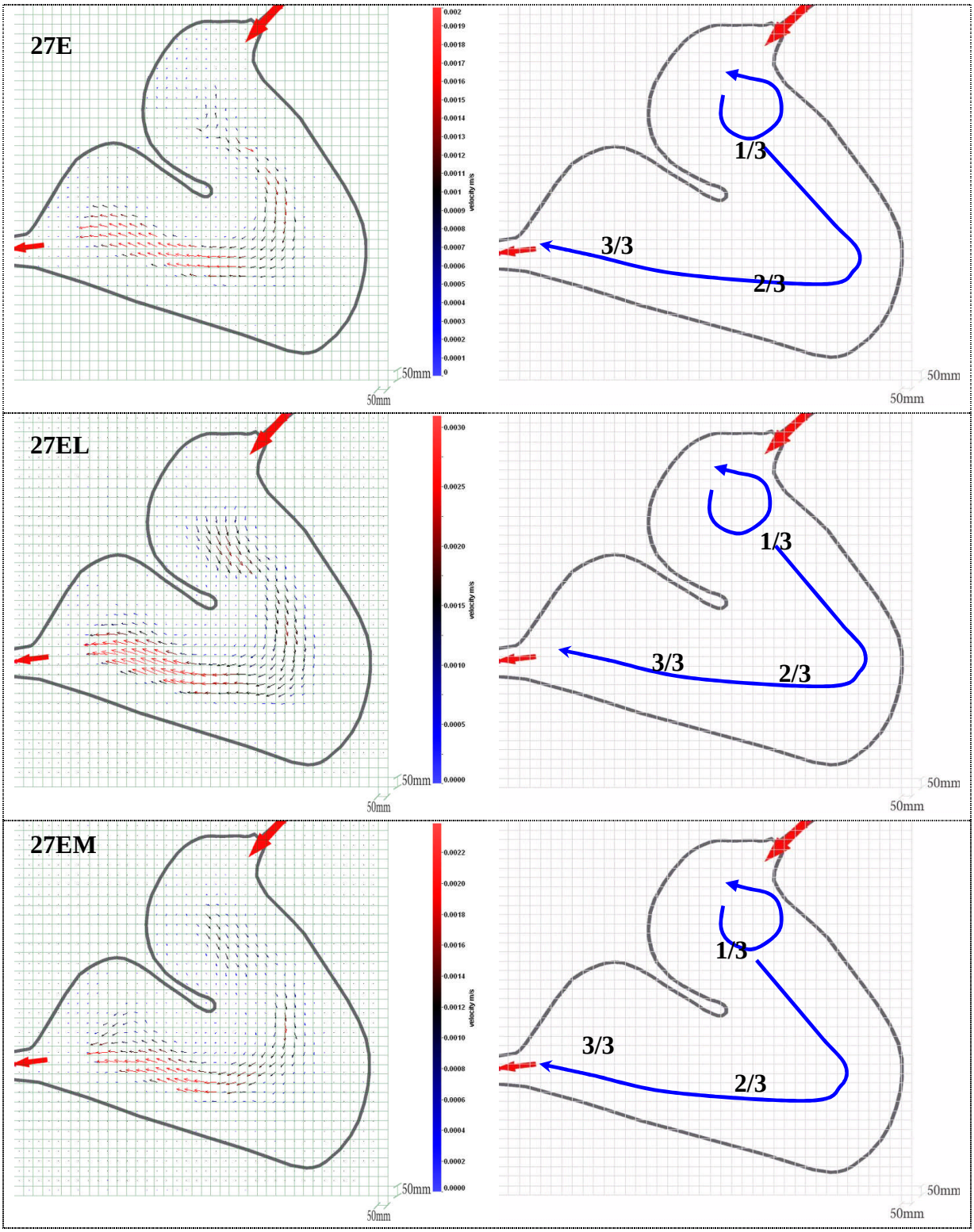
27E
0.002
0.0019
0.0018
0.0017
0.0016
0.0015
0.0014
0.0013
0.0012
0.0011
0.001
0.0009
0.0008
0.0007
0.0006
0.0005
0.0004
0.0003
0.0002
0.0001
0
velocity m/s
50mm
50mm
1/3
3/3
2/3
50mm
50mm
27EL
0.0030
0.0025
0.0020
0.0015
0.0010
0.0005
0.0000
velocity m/s
50mm
50mm
1/3
3/3
2/3
50mm
50mm
27EM
0.0022
0.0020
0.0018
0.0016
0.0014
0.0012
0.0010
0.0008
0.0006
0.0004
0.0002
0.0000
velocity m/s
50mm
50mm
1/3
3/3
2/3
50mm
50mm

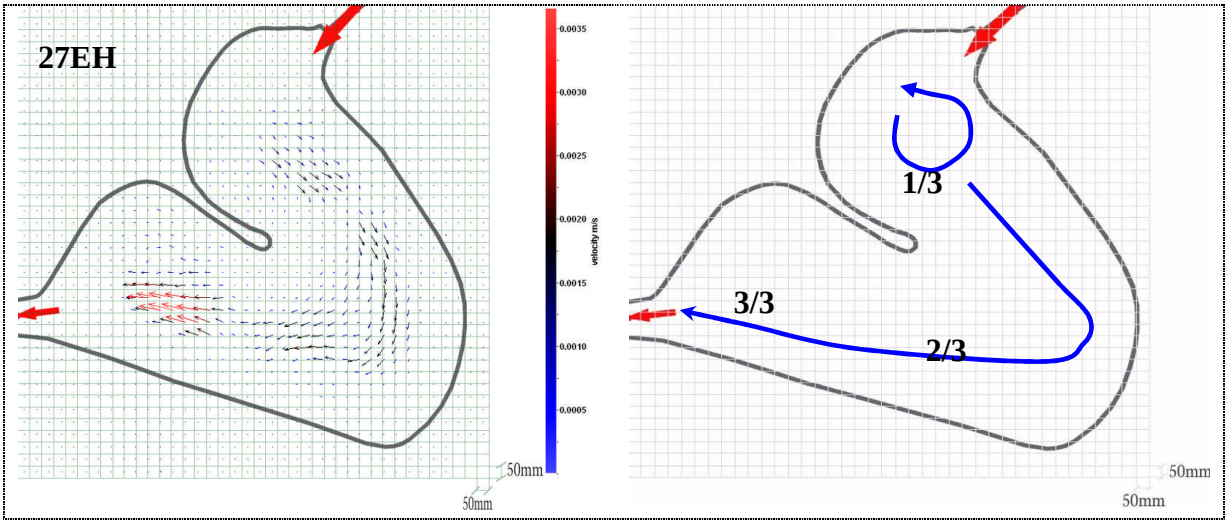

Figure 4-12. Surface flow profiles of 27E, 27EL, 27EM and 27EH vegetation at 11.48 ml/s discharge.

4.1.4 Summary results from trace with discharge (Q_{in}) 17.21 ml/s with 7 vegetation condition

With the same vegetation configurations as in the previous discharge condition, the flow rate was changed from 11.48 to 17.21 ml/s (in the field 30 l/s) see Table 4-4. Dye recovery for all runs (24 - 28) ranged from 68 to 111% with an average of 87%. There were some consistent differences between the relative HRTD plots of run number 24 to 28 with vegetation range from 0E, 11E, 22E, 27E, 27ED, 27EL, 27EM and 27EH, respectively. Some of the parameters for hydraulic efficiency fluctuated and reduced but did not show any statistically significant differences for changing vegetation conditions, Figure 4-13. The effective relative centroid, e_m, varied from 0.69 to 1.23 (δ = 0.17), where the mean of e_m is 0.95, between the no vegetation case to the highest density of vegetation (run 24 to 30 with vegetation 0E to 27EH), Figure 4-13 C. The effective relative time to peak, $e_{o,}$ was tended to reduce from 0.14 to 0.06, where the mean value of e_o is 0.09 (δ = 0.03), whilst vegetation configuration changed from 0E to 27EH, Figure 4-13 B.

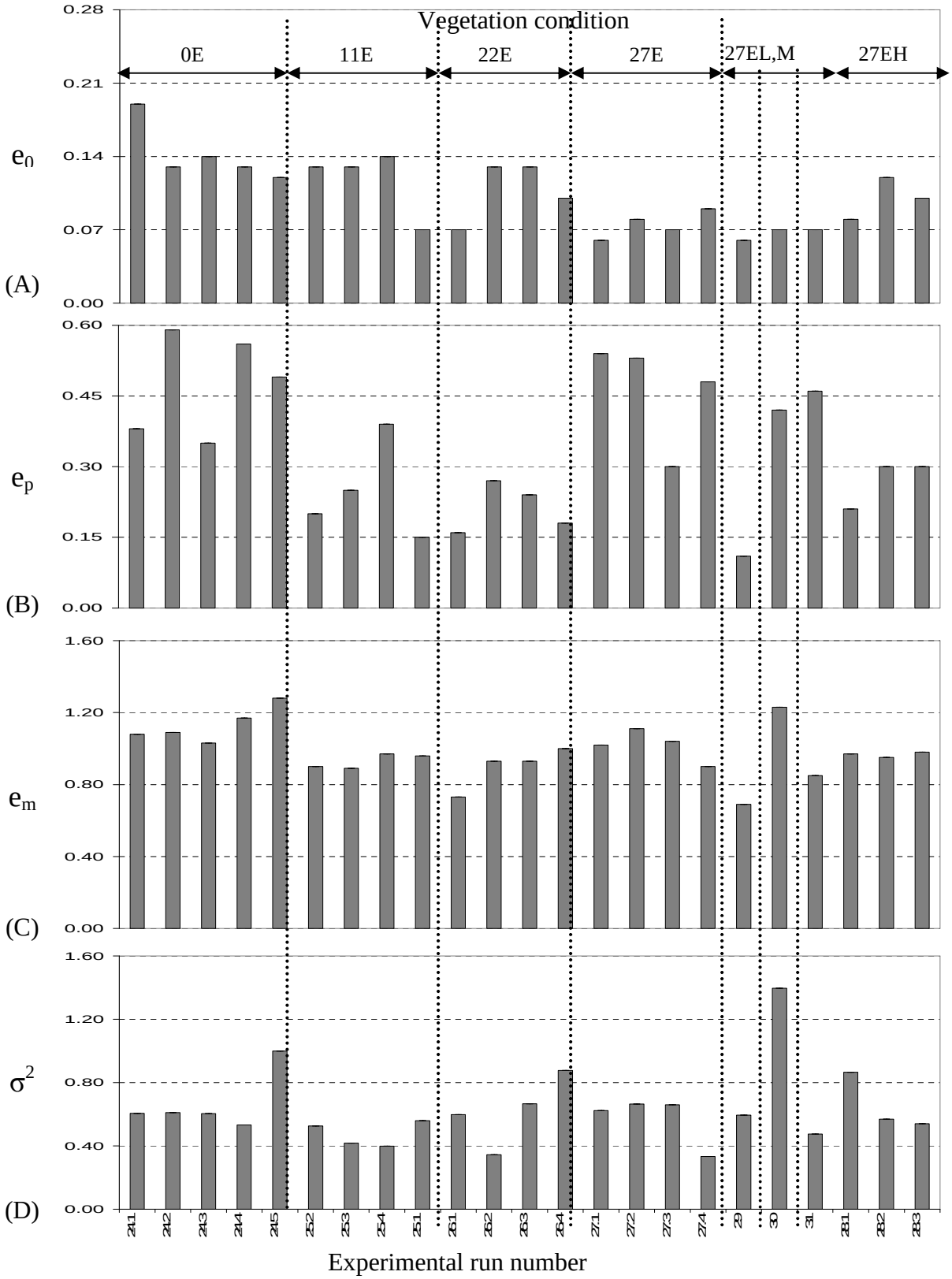

Figure 4-13. The residence time distribution (HRTD) characteristics under differing vegetation configuration. Comparisons are made at the same discharge (17.21 ml/s) and among different vegetation configurations for (A) first dye arrival at the pond outlet (e_0), (B) peak concentration time ($e_p = t_p / t_n$), (C) real residence time (Centroid of HRTD, $e_m = t_m / t_n$), (D) relative time variance (σ^2).

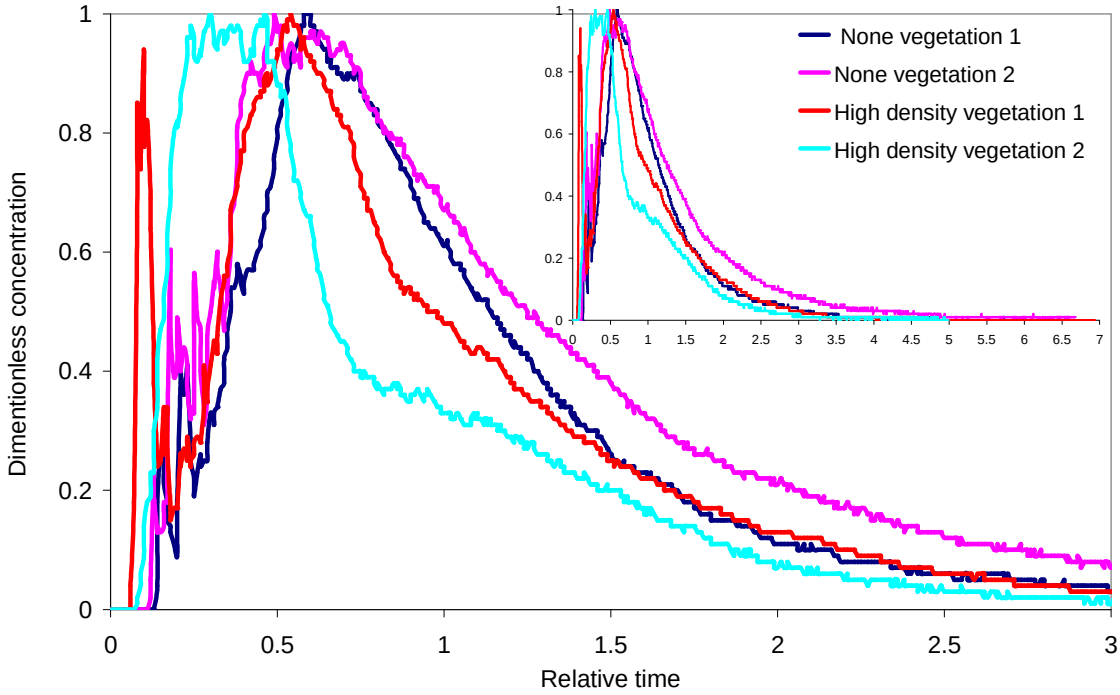

Figure 4-14. Comparison of four representative residence time distributions (HRTDs) curves of no vegetation to different vegetation configurations with Q = 17.21 ml/s.

The HRTDs for the no vegetation cases and the different vegetation configurations appeared distinctively different from each other and distinctively different from the cases with the previous discharges (4.4, 5.74 and 11.48 ml/s). Where most of relative HRTD of all vegetation configuration was usually bimodal, with the first peak typically arriving late and being more spread out than the previous discharge with the same vegetation configuration HRTD, Figure 4-14. These bimodal shapes were reflected in the HRTD statistics, Figure 4-13. The average of relative effective of first dye arrival, e_o, for all runs (24 to 28) and all vegetation configurations was 0.09. The time to peak concentration of the HRTD curve, e_p, occurred at the average value of 0.33. The mean residence time, HRTD centroid, e_m, was an average of 0.95, where each of these measurements of hydraulic efficiency is relative to the nominal residence time (t_n= V/Q).

Repeat tests were conducted randomly among different vegetation configurations; five repeat dye tracers were conducted for run number 24 with no vegetation (0E), four repeat tests for run number 25 to 27 with vegetation 11E to 27E and three repeat tests for run number 28 with vegetation 27ED. Where there was no significant difference between all relative HRTD results, Figure 4-13, then only one dye tracer was conducted for each run number 25 to 27 with vegetation 27EL, 27EM and 27EH. Table 4-4, shows the details of relative HRTDs in all runs from no vegetation to all other vegetation configurations based on 17.21 ml/s discharge (equal to 30 l/s in the Lyby pond).

Discharge, Qin (ml/s)	Vegetation Conditions	Run No.	$e_o = t_o/t_n$	$e_p = t_p/t_n$	$e_m = t_m/t_n$	σ^2 (based on relative time)
17.21	0E	24.1	0.19	0.38	1.08	1.65
	0E	24.2	0.13	0.59	1.09	1.64
	0E	24.3	0.14	0.35	1.03	1.66
	0E	24.4	0.13	0.56	1.17	1.88
	0E	24.5	0.12	0.49	1.28	1.00
	Mean of 0E (S.D)	24	0.14 (0.03)	0.47 (0.11)	1.13 (0.1)	1.57 (0.33)
	11E	25.2	0.13	0.2	0.9	1.90
	11E	25.3	0.13	0.25	0.89	2.40
	11E	25.4	0.14	0.39	0.97	2.51
	11E	25.1	0.07	0.15	0.96	1.79
	Mean of 11E (S.D)	25	0.12 (0.04)	0.25 (0.12	0.93 (0.04)	2.15 (0.39)
	22E	26.1	0.07	0.16	0.73	1.67
	22E	26.2	0.13	0.27	0.93	2.91
	22E	26.3	0.13	0.24	0.93	1.50
	22E	26.4	0.1	0.18	1	1.14
	Mean of 22E (S.D)	26	0.11 (0.03)	0.21 (0.05	0.90 (0.12)	1.81 (0.77)
	27E	27.1	0.06	0.54	1.02	1.61
	27E	27.2	0.08	0.53	1.11	1.51
	27E	27.3	0.07	0.3	1.04	1.52
	27E	27.4	0.09	0.48	0.9	3.01
	Mean of 27E (S.D)	27	0.08 (0.01)	0.46 (0.11)	1.02 (0.09)	1.91 (0.73)
	27EL	29	0.06	0.11	0.69	1.68
	27EM	30	0.07	0.42	1.23	0.72
	27EH	31	0.07	0.46	0.85	2.11
	27ED	28.1	0.08	0.21	0.97	1.16
	27ED	28.2	0.12	0.3	0.95	1.76
	27ED	28.3	0.1	0.3	0.98	1.85
	Mean of 27ED (S.D)	28	0.1 (0.02)	0.27 (0.05)	0.97 (0.02)	1.59 (0.38)

Table 4-4. HRTD statistics of tracer runs at 17.21 ml/s with different vegetation configurations (0E,11E, 22E, 27E, 27ED, 27EL, 27EM and 27EH).

Surface flow velocity profiles obtained from the PIV measurements with a fixed flow rate of 17.21 ml/s (in the field 20 l/s) and vegetation conditions varied from 0E to 11E and 22E, 27E, 27ED, 27EL, 27EM and 27EH are summarised in Table 4-4. As before, some consistent differences were observed between the surface flow profiles, mainly based on the presence or absence of vortices (see run number 24 or 25 with vegetation 0E or 11E to run number 26 to 28 with higher vegetation density). Some of the surface flow profiles (with particular regard to the vortices) differed significantly between run 24 ro 25 (no or less vegetation density) to run 26 to 28 (more or higher vegetation density), but none of surface flow profiles differed significantly between runs 26 to 28 at vegetation 22E, 27E, 27ED, 27EL, 27EM and 27EH, Figure 4-16. With runs 24 and 25 (vegetation 0E and 11E), only one main vortex was observed, in section 1/3 of the physical scale pond and no channel flow in this section, Figure 4-15. There was one very small vortex close to the inlet (in section 1/3) but most of the flow domain consisted of the main channel flow in sections 1/3, 2/3 and 3/3 of the physical scale pond, at runs 26 to 28 (with vegetation configuration 22E, 27E, 27ED, 27EL, 27EM and 27EH), Figure 4-16.

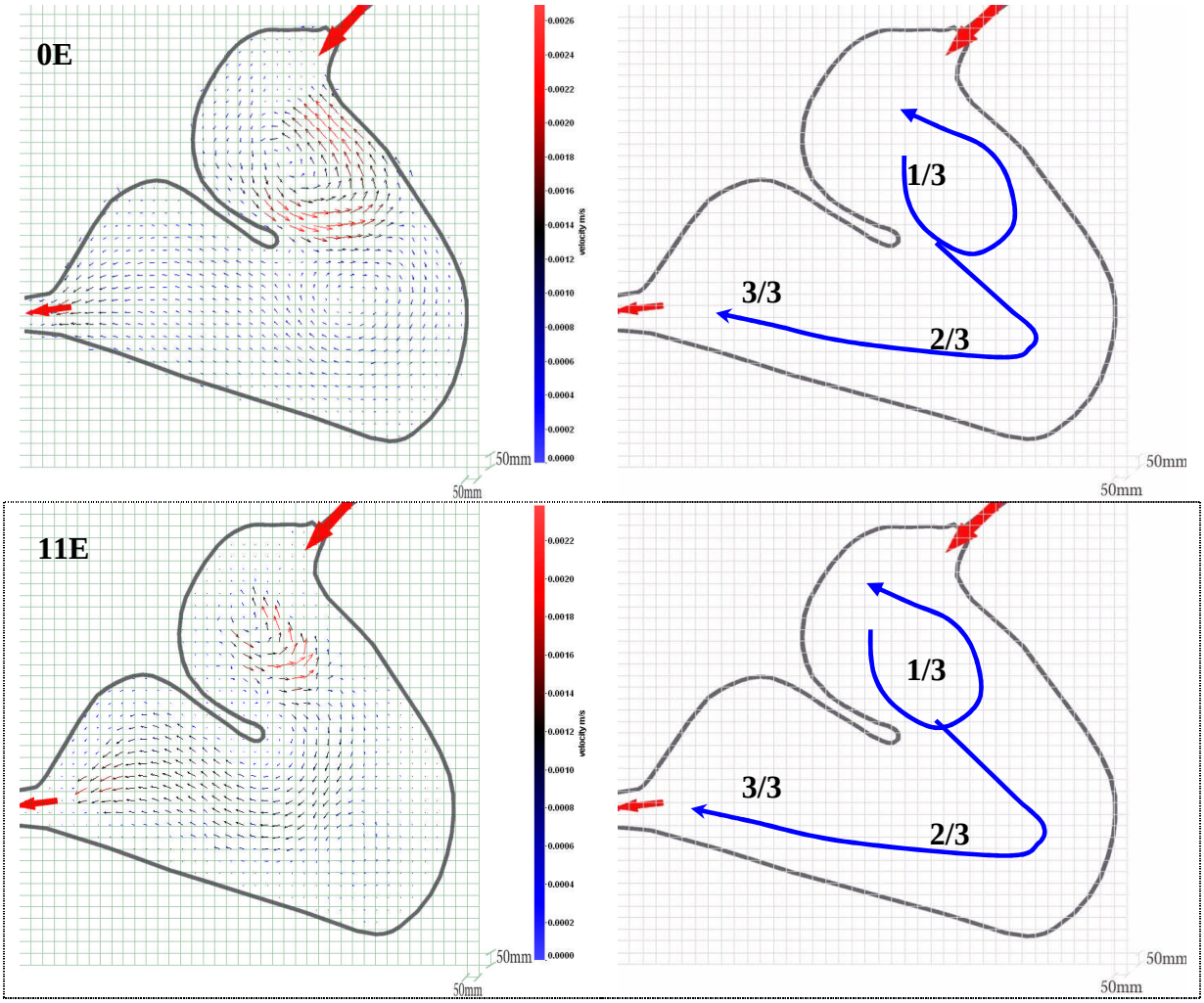

Figure 4-15. Surface flow profiles of 0E and 11E vegetation at 17.21 ml/s discharge.

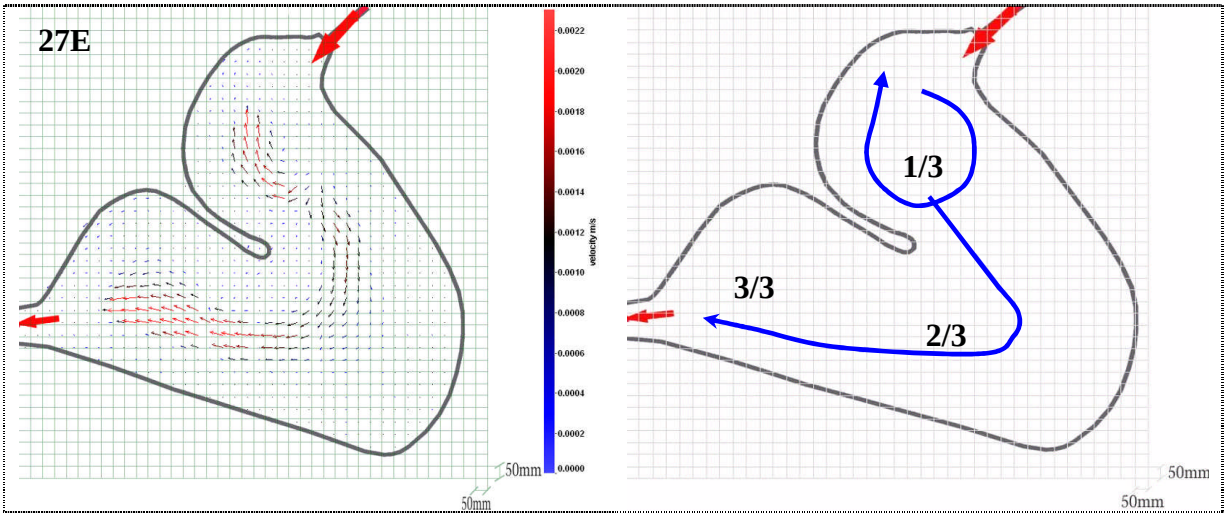

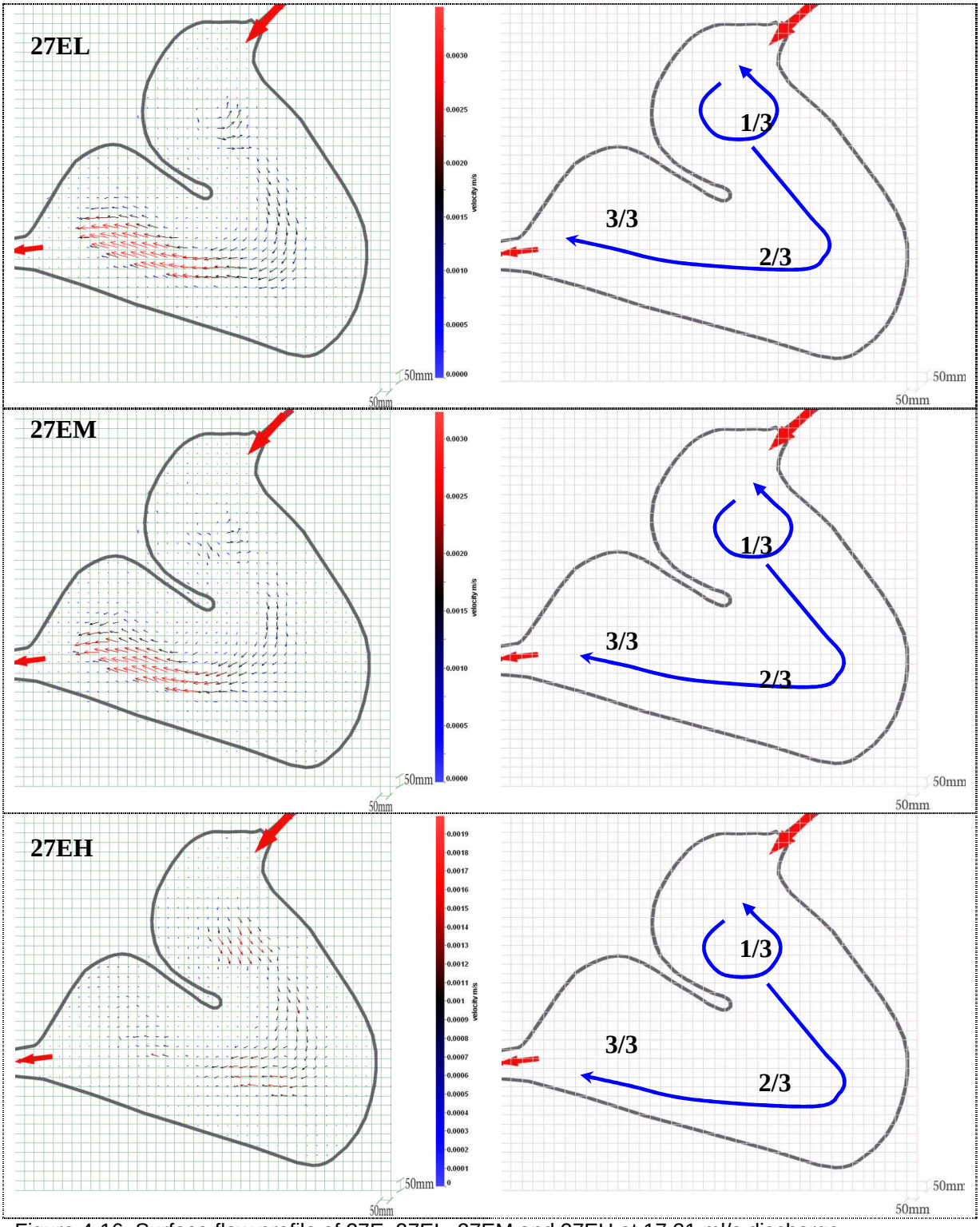

Figure 4-16. Surface flow profile of 27E, 27EL, 27EM and 27EH at 17.21 ml/s discharge

4.1.5 Summary results from trace with discharge (Q_{in}) 22.96 ml/s with 7 vegetation conditions

Changing the flow rate from 17.21 to 22.96 ml/s (in the field 40 l/s) and vegetation configuration showed the same behaviour as above. Mass dye recovery for all runs ranged from 66% to 107% with an average of 87%. There were no consistent differences between the relative HRTD plots of run numbers 32 to 38 with vegetation 0E, 11E, 22E, 27E, 27ED, 27EL, 27EM and 27EH respectively. None of the parameters for hydraulic efficiency differed significantly between runs 32 to 38 with vegetation 0E ,11E, 22E, 27E, 27ED, 27EL, 27EM and 27EH, respectively, Figure 4-17. The relative hydraulic efficiency of the real residence time, e_m, varied from 0.96 to 1.07 where the relative hydraulic efficiency of first dye arrival, e_o, varied from 0.05 to 0.1.

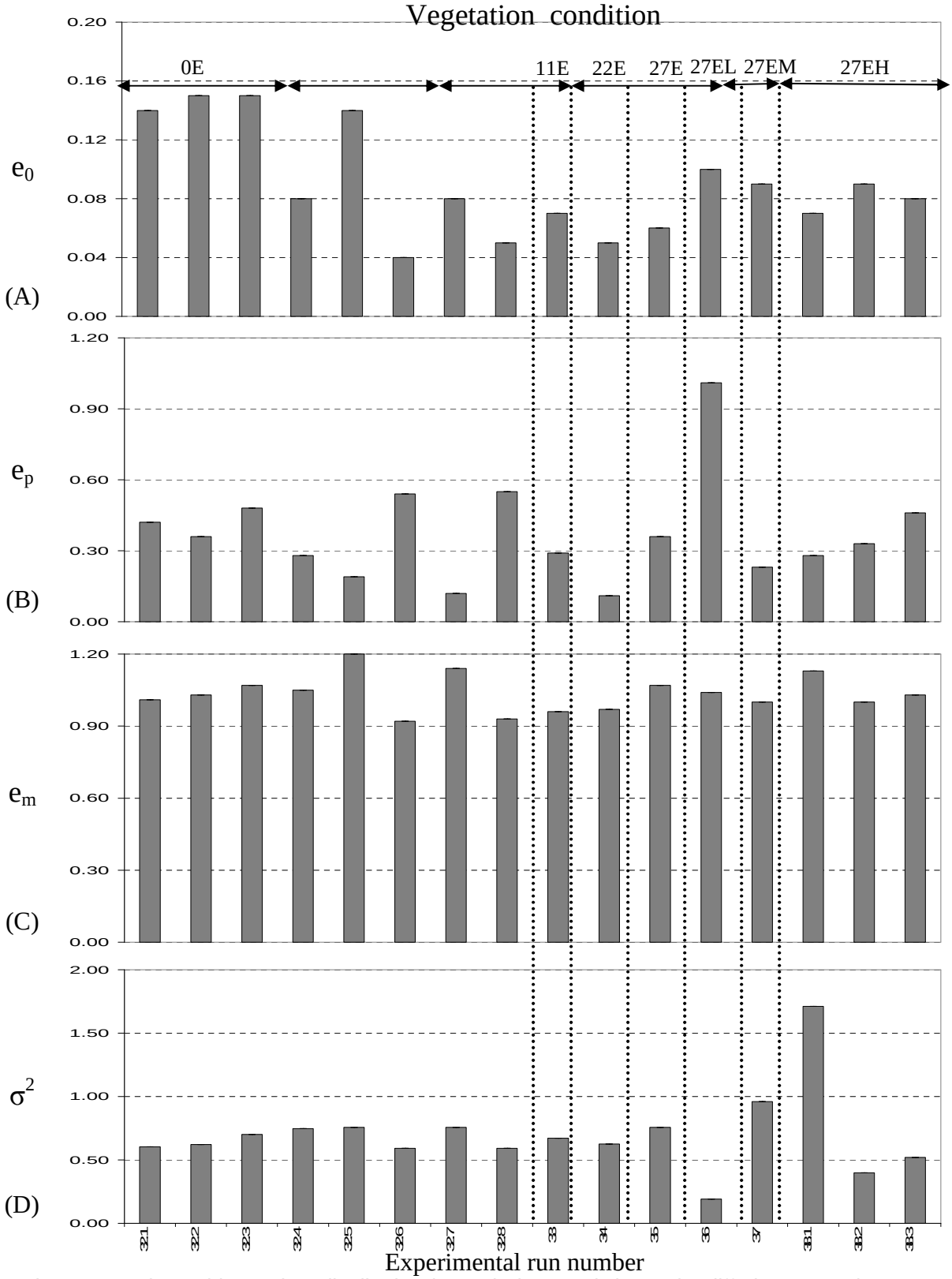

Figure 4-17 The residence time distribution (HRTD) characteristics under differing vegetation configuration. Comparisons are made at the same discharge (22.96 ml/s) and among different vegetation configurations for (A) first dye arrival at the pond outlet (e_0), (B) peak concentration time ($e_p = t_p / t_n$), (C) real residence time (Centroid of HRTD, $e_m = t_m / t_n$), (D) relative time variance (σ^2).

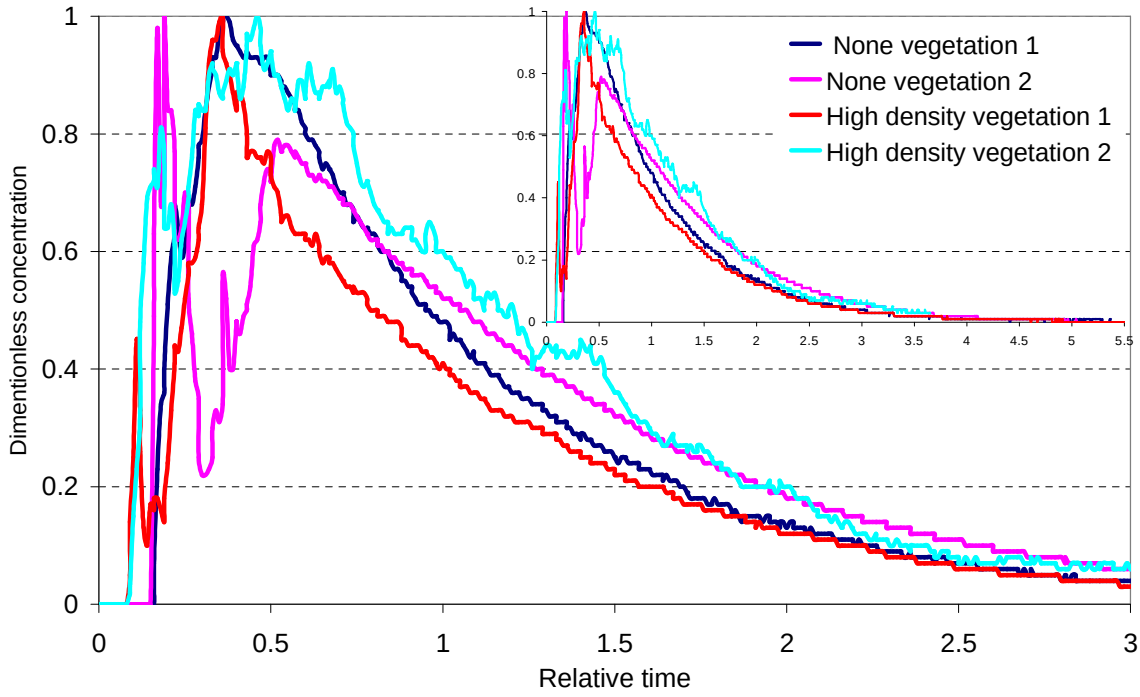

Figure 4-18. Comparison of four representative residence time distributions (HRTDs) curves of none vegetation to different vegetation configurations with Q = 22.96 ml/s.

The relative HRTDs compared between runs 32 to 38 (or between no (0E) vegetation to other different vegetation configurations) showed no distinctive differences. Where most of HRTD of all vegetation configurations were usually bimodal, with the first peak typically arriving late and being more spread out (similar to the previous condition with discharge 17.21 ml/s), Figure 4-18. These bimodal shapes were reflected in the relative HRTD statistics, Figure 4-17. The average of the relative first dye arrival, e_o, for all runs with all vegetation configuration was 0.08, Figure 4-17 A. The relative time to peak concentration of the HRTD curve, e_p, occurred also at the average value of 0.39. (Figure 4-17 B). The relative mean residence time, as measured by the relative HRTD centroid, e_m, was an average of 1.02, Figure 4-17 C.

Again, as with the previous discharge with the same vegetation condition, repeat tests were conducted randomly among different vegetation configurations; eight

repeat dye tracers were conducted for run 32 with 0E vegetation condition, where there were no significant differences between all the relative HRTD results, Figure 4-16, then only one dye tracer was run for each run (33 to 38) with vegetation 11E, 22E, 27E, 27EL, 27EM and 27EH, respectively. Figure 4-18, shows the details of relative HRTDs in all runs from no vegetation cases to all other vegetation configurations based on 22.96 ml/s discharge (equal to 40 l/s in the Lyby pond).

Discharge, Q_{in} (ml/s)	Vegetation Conditions	Run No	$e_o = t_o/t_n$	$e_p = t_p/t_n$	$e_m = t_m/t_n$	σ^2 (based on relative time)
22.96	0E	32.1	0.14	0.42	1.01	0.42
	0E	32.2	0.15	0.36	1.03	0.36
	0E	32.3	0.15	0.48	1.07	0.48
	0E	32.4	0.08	0.28	1.05	0.28
	0E	32.5	0.14	0.19	1.2	0.19
	0E	32.6	0.04	0.54	0.92	0.54
	0E	32.7	0.08	0.12	1.14	0.12
	0E	32.8	0.05	0.55	0.93	0.55
	Mean of 0E (S.D)	32	0.10 (0.05)	0.20 (0.05)	1.04 (0.1)	1.51 (0.17)
	11E	33	0.07	0.29	0.96	0.29
	22E	34	0.05	0.11	0.97	0.11
	27E	35	0.06	0.36	1.07	0.36
	27EL	36	0.1	1.01	1.04	1.01
	27EM	37	0.09	0.23	1	0.23
	27EH	38.1	0.07	0.28	1.13	0.28
	27EH	38.2	0.09	0.33	1	0.33
	27EH	38.3	0.08	0.46	1.03	0.46
	Mean of 27EH (S.D)	38	0.08 (0.01)	0.21 (0.05)	1.05 (0.07)	1.68 (0.99)

Table 4-5. HRTD statistics of tracer runs at 22.96 ml/s with different vegetation configurations (0E,11E, 22E, 27E, 27ED, 27EL, 27EM and 27EH).

Surface flow profiles measured from the PIV experiments with a fixed Q_{in} value of of 22.96 ml/s (in the field 40 l/s) and vegetation varied from no vegetation to the highest vegetation density (0E to 27EH), Table 4-5. As in previous runs, some consistent differences were seen between the surface flow profiles, mainly based on the patterns of vortices (see run 32 or 33 (vegetation 0E or 11E) to the other

runs ranging from 34 to 38, with higher vegetation density). Some of the surface flow vortex patterns differed significantly between runs 32 or 33 (vegetation 0E or 11E) to runs number 34 to 38 (with higher density of vegetation) but none of surface flow profiles differed significantly between runs 34 to 38 at vegetation 22E, 27E, 27ED, 27EL, 27EM and 27EH, respectively, Figure 4-20. Regarding runs 32 and 33 with 0E and 11E vegetation configurations, the results show that there was only one main vortex which was appeared, in section 1/3, very small vortexes existed in 2/3 of physical scale pond and no channel flow in this section. For runs with higher density vegetation, from 22E to 27EH, there was one very small vortex was appeared close to the inlet (in section 1/3) but mostly main channel flow was appeared, in section 1/3, 2/3 and 3/3 of the physical scale pond, Figure 4-20.

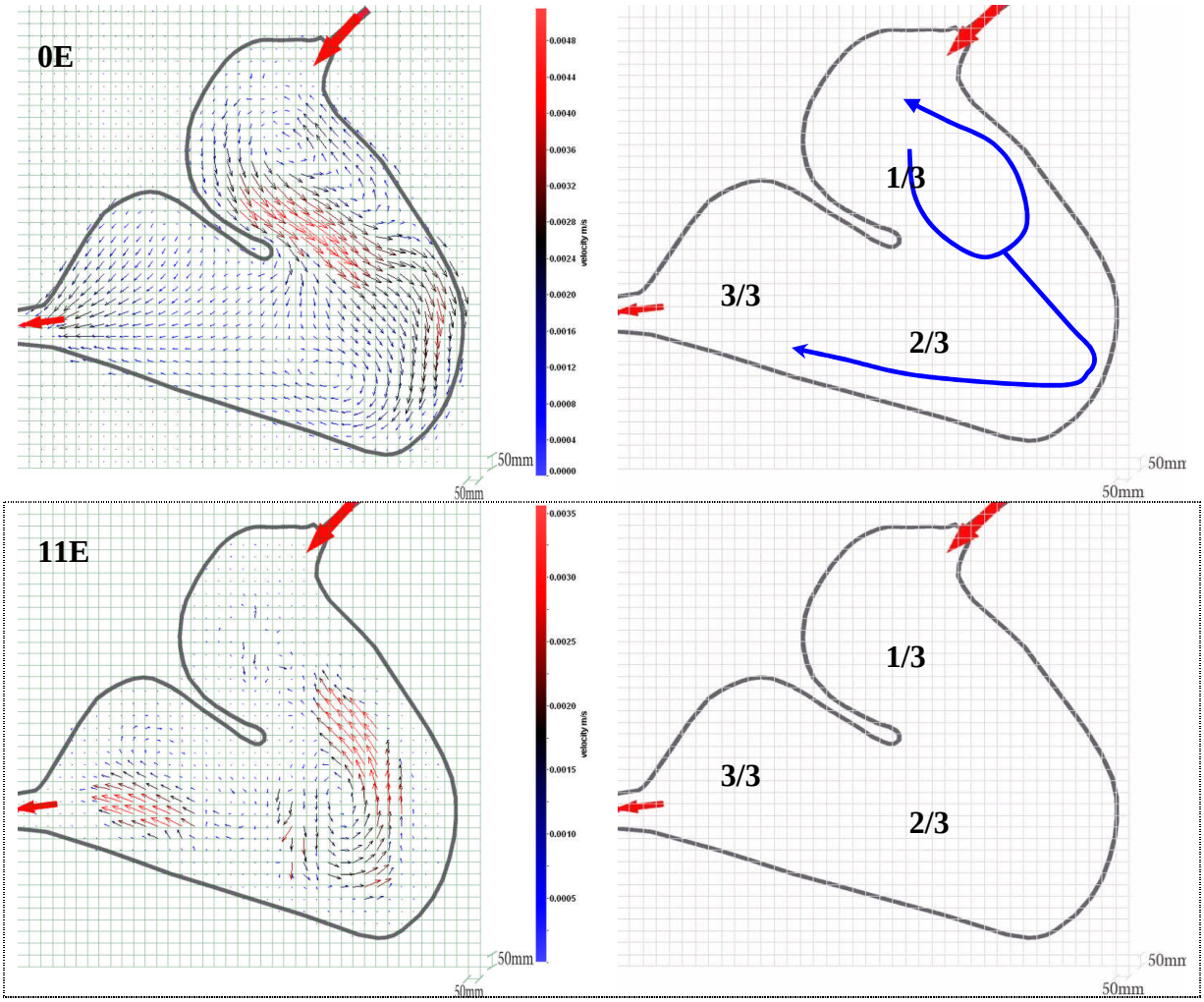

Figure 4-19. Surface flow profiles of none vegetation and 11E at 22.96 ml/s discharge.

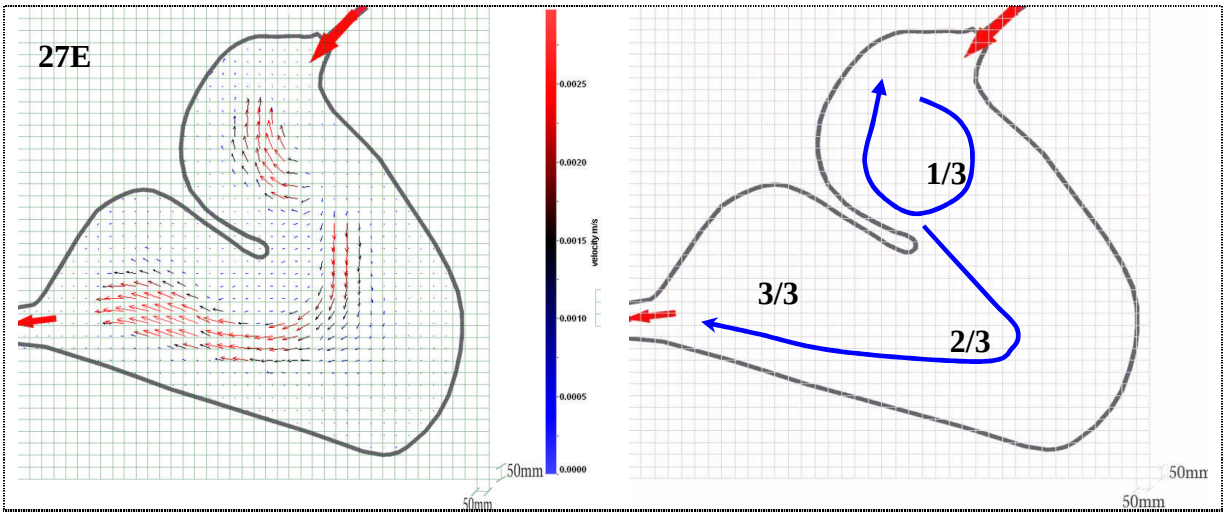

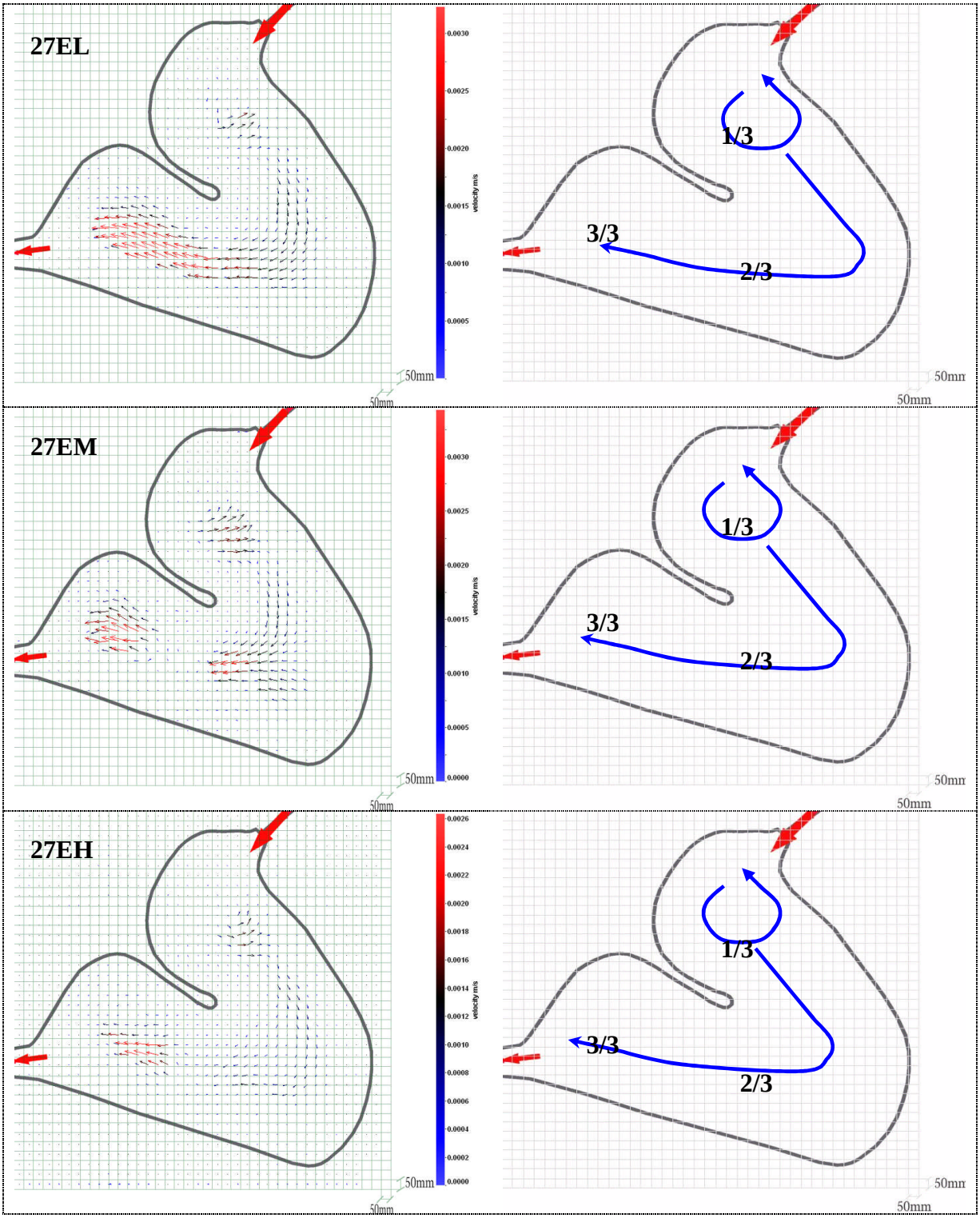

Figure 4-20. Surface flow profiles of 27E, 27EL, 27EM and 27EH at 22.96 ml/s discharge.

4.1.6 Summary results from trace with discharge (Q_{in}) 28.69 ml/s with 4 vegetation conditions

Further experiments were run by changing the flow rate from 22.96 to 28.69 l/s (in the field the latter vale corresponds to 50 l/s), with the vegetation configurations remaining the same as above, but only ranging from 0E, 11E, 22E and 27E (no vegetation and emergent plants). Dye recovery for all runs (run 39 to 42) ranged from 72% to 119% with an average of 90%. There was no consistent difference between the HRTD plots of experimental runs 39 to 42 with vegetation 0E, 11E, 22E and 27E, respectively. The results show that none of the parameters for hydraulic efficiency differed significantly between runs 39 to 42 whilst vegetation changed from 0E ,11E, 22E and 27E, respectively, Figure 4-21. The relative hydraulic efficiency of the real HRTDs centroid, e_m, varied from 0.90 to 1.13, where the relative hydraulic efficiency of first dye arrival, e_o, varied from 0.13 to 0.16.

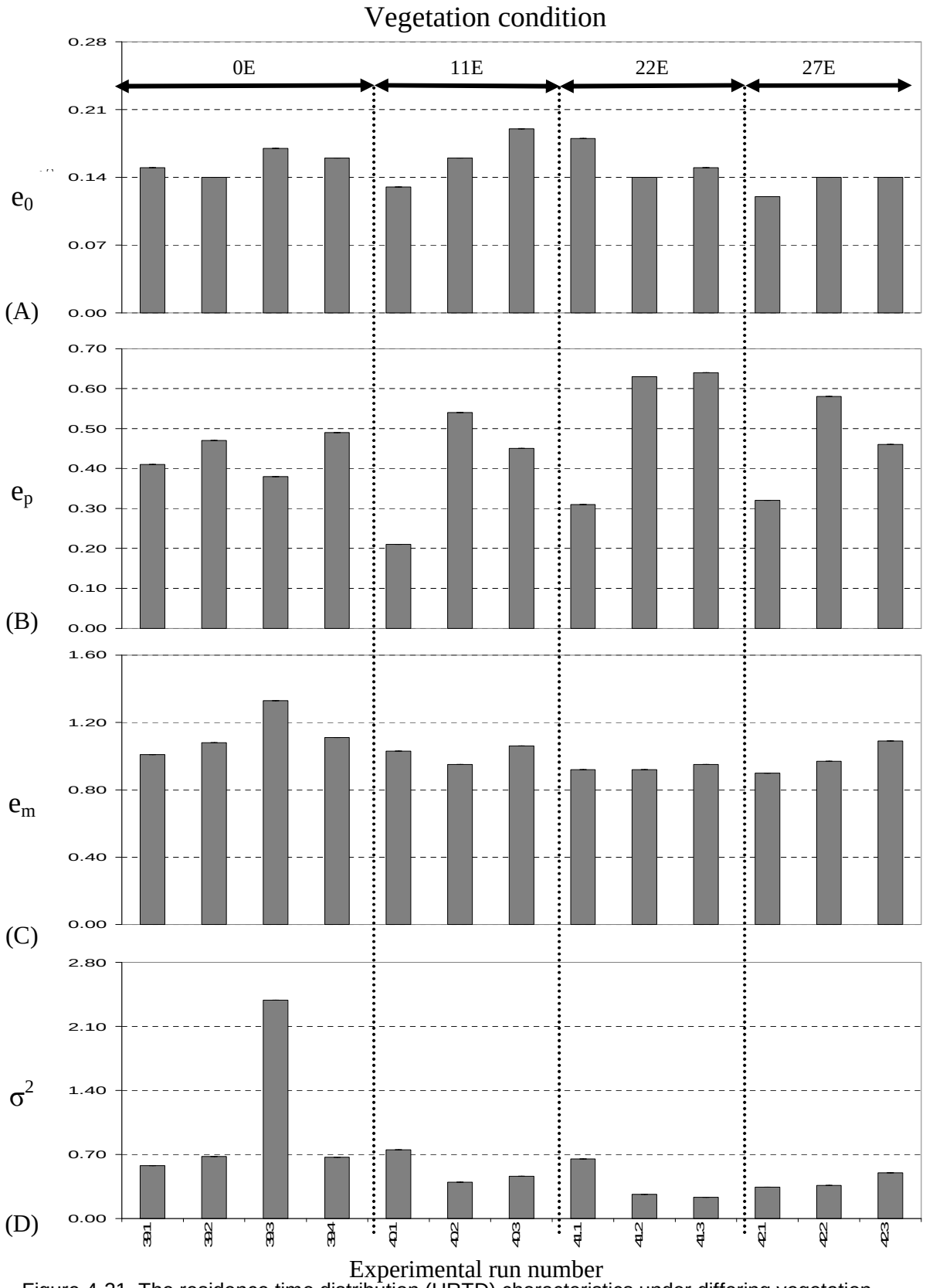

Figure 4-21. The residence time distribution (HRTD) characteristics under differing vegetation configuration. Comparisons are made at the same discharge (28.69 ml/s) and among different vegetation configurations for (A) first dye arrival at the pond outlet (e_0), (B) peak concentration time ($e_p = t_p / t_n$), (C) real residence time (Centroid of HRTD, $e_m = t_m / t_n$), (D) relative time variance (σ^2).

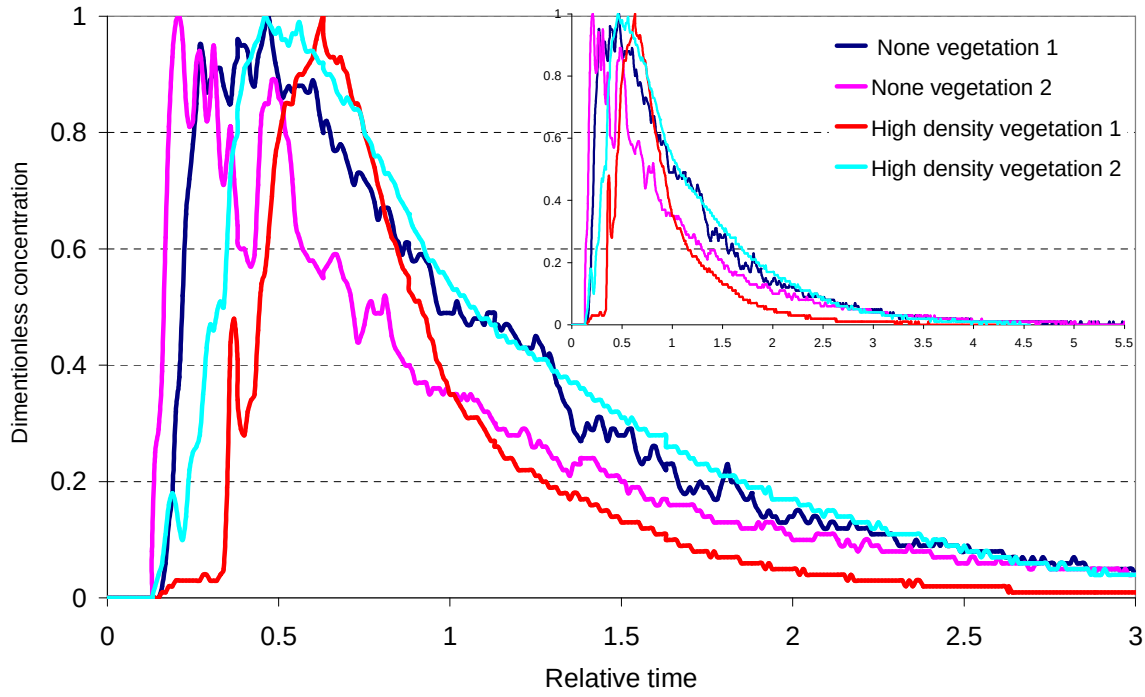

Figure 4-22. Comparison of four representative residence time distributions (HRTDs) curves of none vegetation to high emergent vegetation configurations with Q = 28.69 ml/s.

The HRTDs comparisons between run 39 and others (no vegetation to different emergent vegetation configurations) appeared not distinctively different. Where the HRTD of all vegetation configurations were usually bimodal, with the first peak typically arriving late and being more spread out, Figure 4-22. These bimodal shapes were reflected in the HRTD statistics, Figure 4-21. The relative average and mean of first dye arrival, e_o, for all vegetation configurations was 0.08, Figure 4-21 A. The relative time to peak concentration of the HRTD curve, e_p, occurred at the average value of 0.45 of t_n for all runs and all vegetation configurations, Figure 4-21 B. The relative mean residence time, HRTD centroid, e_m, was an average of 1.02, Figure 4-21 C.

As with the previous discharge cases, the repeat tests were conducted randomly among different runs and different vegetation configurations; four repeat dye tracers were conducted for run 39 at 0E (no) vegetation condition, where there

were no significant differences between all HRTD results, Figure 4-21, then only three repeated dye tracers were conducted for run numbers 40 to 42 with vegetation 11E, 22E and 27E, respectively. Table 4-6, shows the detailed results of HRTDs in all runs from no vegetation to all other emergent vegetation configurations based on 28.69 ml/s discharge (equal to 50 l/s in the Lyby pond).

Due to time constraints and also the changes from full scale to distorted scale, there was no PIV measurement for surface flow profiles on the high discharge such as 28.69, 34.43, 40.15 and 45.90 ml/s.

Discharge, Qin (ml/s)	Vegetation Conditions	Run No.	$e_o = t_o/t_n$	$e_p = t_p/t_n$	$e_m = t_m/t_n$	σ^2 (based on relative time)
28.69	0E	39.1	0.15	0.41	1.01	1.73
	0E	39.2	0.14	0.47	1.08	1.47
	0E	39.3	0.17	0.38	1.33	0.42
	0E	39.4	0.16	0.49	1.11	1.49
	Mean of 0E (S.D)	39	0.16 (0.01)	0.27 (0.02)	1.13 (0.14)	1.28 (0.59)
	11E	40.1	0.13	0.21	1.03	1.33
	11E	40.2	0.16	0.54	0.95	2.53
	11E	40.3	0.19	0.45	1.06	2.16
	Mean of 11E (S.D)	40	0.16 (0.03)	0.29 (0.11)	1.01 (0.06)	2.01 (0.61)
	22E	41.1	0.18	0.31	0.92	1.54
	22E	41.2	0.14	0.63	0.92	3.79
	22E	41.3	0.15	0.64	0.95	4.32
	Mean of 22E (S.D)	41	0.16 (0.02)	0.36 (0.11)	0.93 (0.02)	3.22 (1.48)
	27E	42.1	0.12	0.32	0.9	2.92
	27E	42.2	0.14	0.58	0.97	2.78
	27E	42.3	0.14	0.46	1.09	2.00
	Mean of 27E (S.D)	42	0.13 (0.01)	0.32 (0.03)	0.99 (0.10)	2.56 (0.49)

Table 4-6. HRTD statistics of tracer runs at 28.69 ml/s with vegetation configuration range from 0E,11E, 22E and 27E.

4.1.7 Summary results from trace with discharge (Q_{in}) 34.43 ml/s with 7 vegetation conditions

The controlled flow rate was changed from 28.69 to 34.43 ml/s (corresponding to a field value of 60 l/s) and the vegetation configurations remained the same as for the previous discharge, but the vegetation only ranged from 0E, 11E, 22E, 27E and 27ED (which covered only no vegetation and the highest emergent plants). Dye recovery for all runs (run 43 to 47) ranged from 75% to 116% with an average of 97%. There was no consistent difference between the relative HRTD plots of runs 43 to 47 with vegetation 0E, 11E, 22E, 27E and 27ED, respectively, Figure 4-23. None of the parameters for hydraulic efficiency differed significantly between runs 43 to 47, Figure 4-23. The relative hydraulic efficiency of real residence time, e_m, varied from 1.00 to 1.09, Figure 4-23 C, where the relative hydraulic efficiency of first dye arrival, e_0, varied from 0.13 to 0.22, Figure 4-23 A.

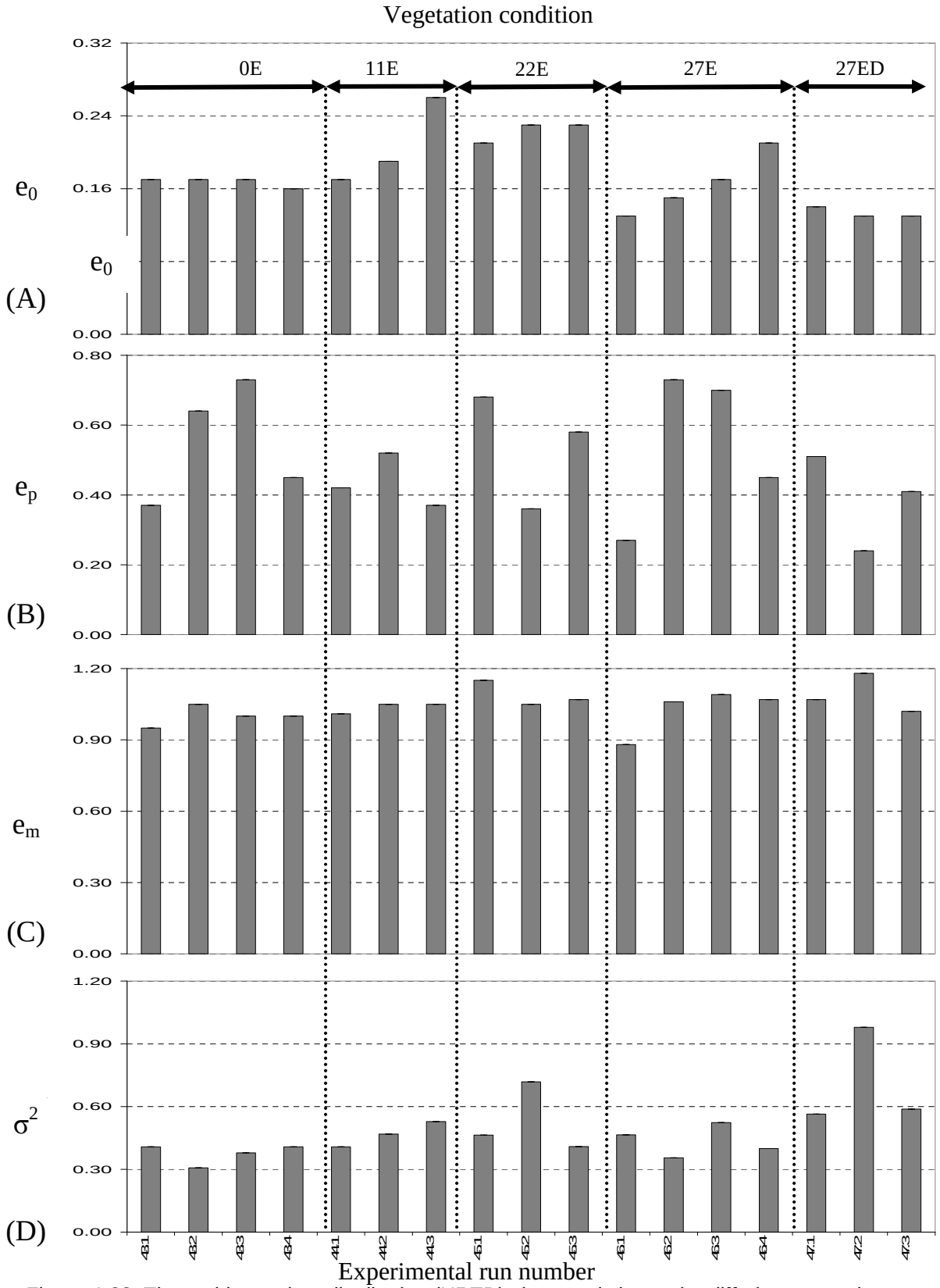

Figure 4-23. The residence time distribution (HRTD) characteristics under differing vegetation configuration. Comparisons are made at the same discharge (34.43 ml/s) and among different vegetation configurations for (A) first dye arrival at the pond outlet (e_0), (B) peak concentration time ($e_p = t_p / t_n$), (C) real residence time (Centroid of HRTD, $e_m = t_m / t_n$), (D) relative time variance (σ^2).

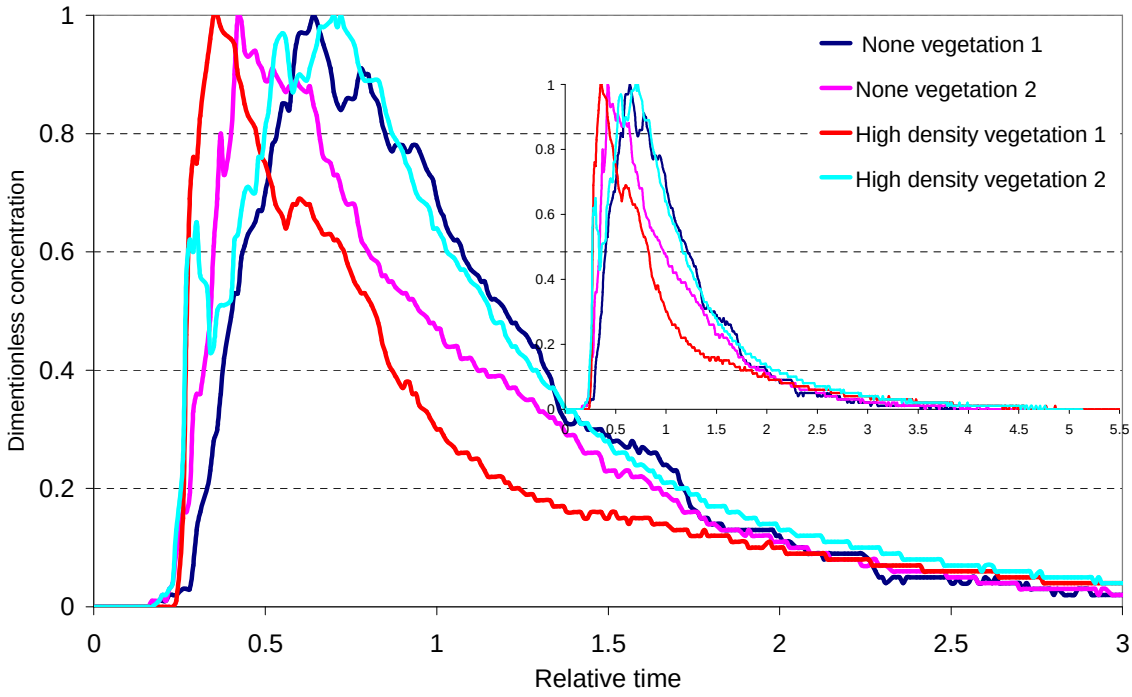

Figure 4-24. Comparison of four representative residence time distributions (HRTDs) curves of none vegetation to highest emergent vegetation configurations with Q = 34.43 ml/s.

The relative HRTDs, at the same discharge, compared between no vegetation to different highest emergent vegetation configurations appeared not distinctively different. The HRTD of all vegetation configurations usually showed the same behaviour, with a bimodal shape, with the first peak typically arriving late and being more spread out, Figure 4-24. These bimodal shapes were reflected in the relative HRTD statistics in Figure 4-23 where the average and mean of relative first dye arrival, e_o, for all vegetation configurations was 0.18, the relative time to peak concentration of the HRTD curve, e_p, occurred at the average value of 0.49 of all vegetation configurations with the same discharge (Q = 34.43 ml/s). The relative mean residence time, the relative HRTD centroid, e_m, was an average of 1.05. The mean relative HRTD spread,σ^2, was an average of1.02 to 3.26.

Repeat tests were conducted randomly among different vegetation configurations; four repeat dye tracers were conducted for run 43, as 0E (no) vegetation condition,

where there were no significant differences between of all its relative HRTD results, Figure 4-23, then only three repeated dye tracer tests were conducted for each run from 44 to 47 with vegetation 11E, 22E, 27e and 27ED, respectively. Table 4-7, shows the detail of relative HRTDs in all runs, 43 to 47, from none vegetation to all other emergent vegetation configurations based on 34.43 ml/s discharge (equal to 60 l/s in the Lyby pond).

Discharge, Qin (ml/s)	Vegetation Conditions	Run No.	$e_o = t_o/t_n$	$e_p = t_p/t_n$	$e_m = t_m/t_n$	σ^2 (based on relative time)
34.43	0E	43.1	0.17	0.3	0.95	2.46
	0E	43.2	0.17	0.42	1.05	3.26
	0E	43.3	0.17	0.36	1	2.64
	0E	43.4	0.16	0.28	1	2.45
	Mean of 0E (S.D)	43	0.17 (0.00)	0.34 (0.06)	1.00 (0.04)	2.70 (0.38)
	11E	44.1	0.17	0.35	1.01	2.46
	11E	44.2	0.19	0.35	1.05	2.14
	11E	44.3	0.26	0.35	1.05	1.89
	Mean of 11E (S.D)	44	0.21 (0.05)	0.35 (0.00)	1.04 (0.02)	2.16 (0.28)
	22E	45.1	0.21	0.43	1.15	2.16
	22E	45.2	0.23	0.3	1.05	1.39
	22E	45.3	0.23	0.41	1.07	2.45
	Mean of 22E (S.D)	45	0.22 (0.01)	0.38 (0.07)	1.09 (0.05)	2.00 (0.55)
	27E	46.1	0.13	0.2	0.88	2.15
	27E	46.2	0.15	0.34	1.06	2.82
	27E	46.3	0.17	0.34	1.09	1.91
	27E	46.4	0.21	0.37	1.07	2.51
	Mean of 27E (S.D)	46	0.17 (0.02)	0.31 (0.08)	1.03 (0.11)	2.35 (0.47)
	27ED	47.1	0.14	0.28	1.07	1.78
	27ED	47.2	0.13	0.23	1.18	1.02
	27ED	47.3	0.13	0.26	1.02	1.70
	Mean of 27ED (S.D)	47	0.13 (0.01)	0.26 (0.03)	1.09 (0.08)	1.50 (0.41)

Table 4-7. HRTD statistics of tracer runs at 34.43 ml/s with vegetation configuration range from 0E,11E, 22E, 27E and 27ED.

4.1.8 Summary results from trace with discharge (Q_{in}) 40.15 ml/s with 4 vegetation conditions

The controlled flow rate was changed from 34.43 to 40.15 ml/s (in the field 70 l/s) and the vegetation configuration remained the same as above but only ranged between 0E, 11E, 22E and 27E (no vegetation and high density of emergent plants). Dye recovery for all runs ranged from 74% to 103% with an average of 91%. There was no consistent difference between the relative HRTD plots of run 48 to 51 where vegetation ranged from 0E, 11E, 22E and 27E, respectively. None of the parameters for relative hydraulic efficiency differed significantly between runs 48 to 51, Figure 4-25. The relative hydraulic efficiency of real residence time, e_m, varied from 0.99 to 1.11, Figure 4-25 C, where the relative hydraulic efficiency of first dye arrival, $e_{0,}$ varied from 0.10 to 0.22, Figure 4-25 A.

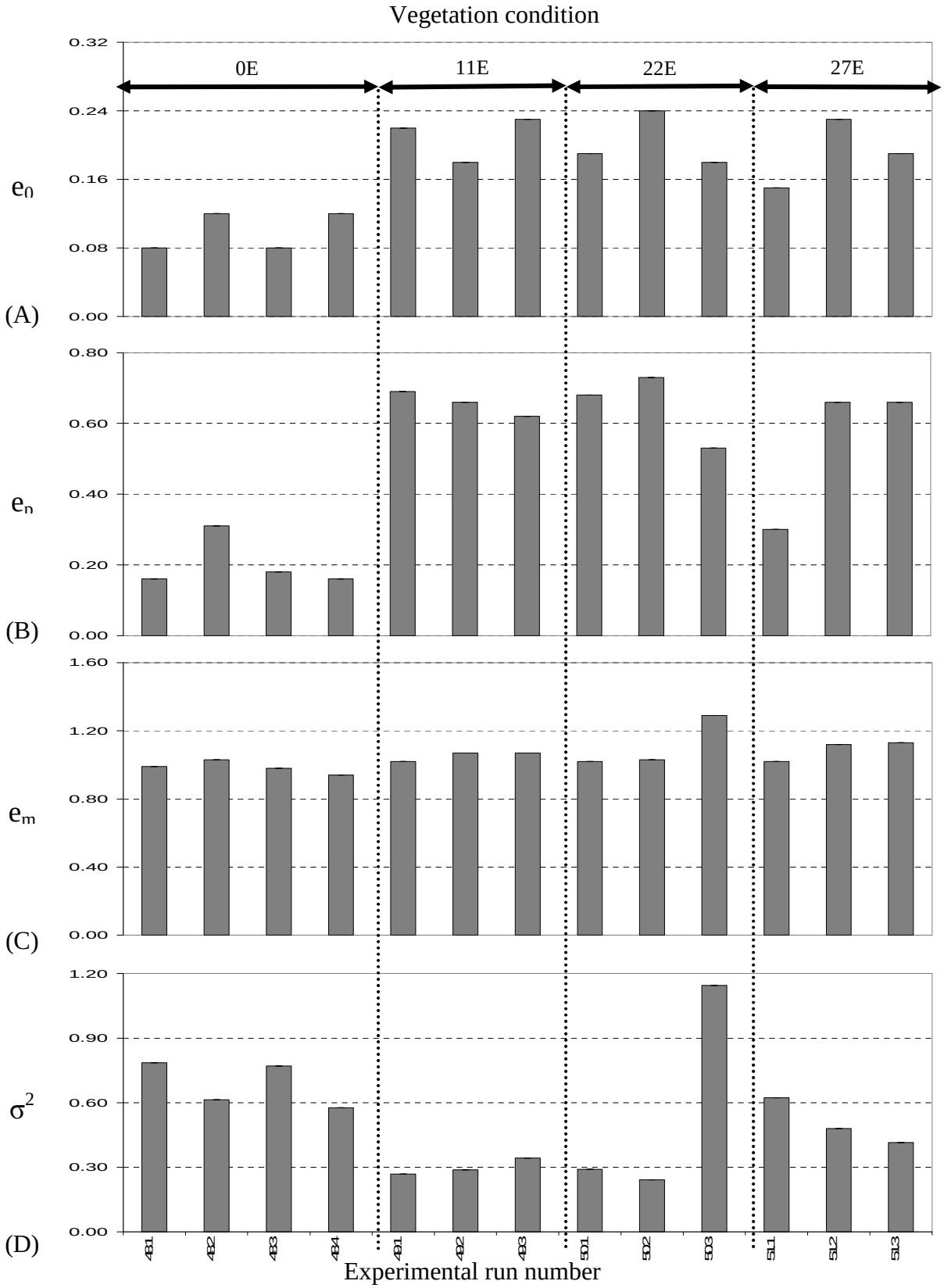

Figure 4-25. The residence time distribution (HRTD) characteristics under differing vegetation configuration. Comparisons are made at the same discharge (40.15 ml/s) and among different vegetation configurations for (A) first dye arrival at the pond outlet (e_0), (B) peak concentration time ($e_p = t_p / t_n$), (C) real residence time (Centroid of HRTD, $e_m = t_m / t_n$), (D) relative time variance (σ^2).

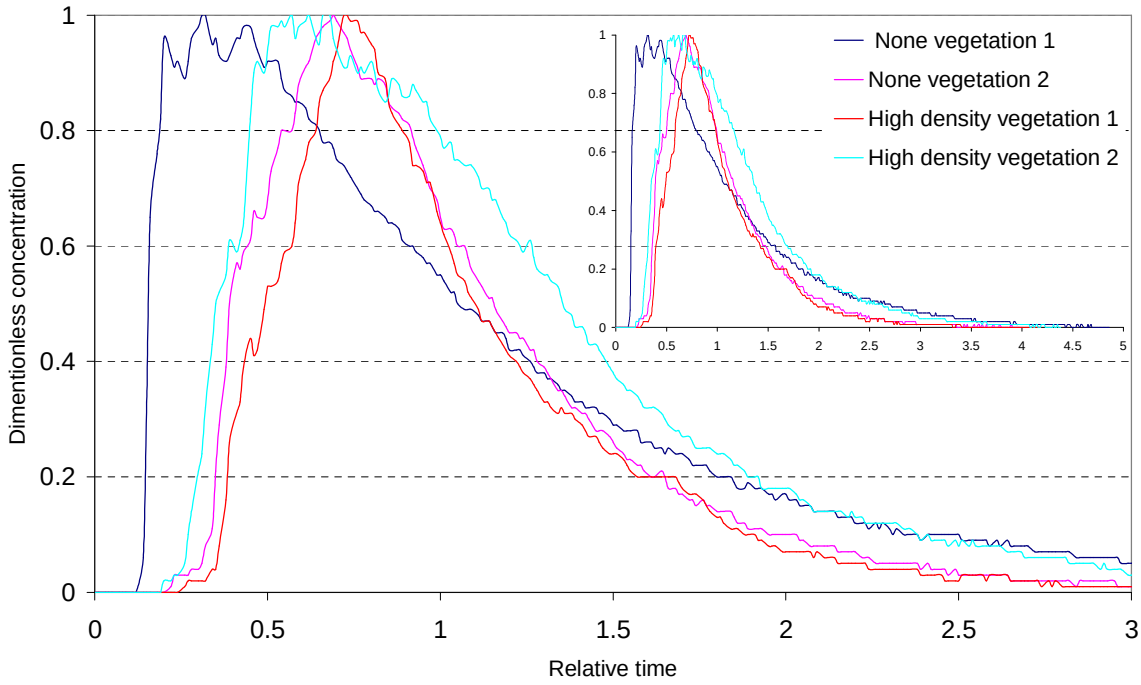

Figure 4-26. Comparison of four representative residence time distributions (HRTDs) curves of none vegetation to highest emergent vegetation configurations with Q = 40.15 ml/s.

The relative HRTDs of discharge 40.15 ml/s, when compared with cases varying between no vegetation and different high density emergent plant configurations again appeared not distinctively different. Where relative HRTD of all runs 48 to 51 and all vegetation configurations usually still showed a bimodal shape, with the first peak typically arriving late and being more spread out, Figure 4-26. These bimodal shapes were reflected in the HRTD statistics, Figure 4-25. The relative average and mean of first dye arrival, e_o, for runs and all vegetation configurations was 0.18. The relative time to peak concentration of the relative HRTD curve, e_p, occurred at the average value of 0.51 for all vegetation configurations. The relative mean residence time, relative HRTD centroid (t_m) was an average of 1.06.

As in previous discharges, the repeat tests were conducted randomly among different vegetation different configurations; four repeat dye tracers were conducted for run 48 at 0E (none) vegetation condition, where there were no

significant differences observed of all its relative HRTD results (Figure 4-25), then only three repeated dye tracer was conducted for each run 49 to 51 with vegetation 11E, 22E and 27E, respectively. Table 4-8, shows the details of the relative HRTDs in all runs from no vegetation to all other emergent vegetation configurations based on 40.15 ml/s discharge (equal to70 l/s in the Lyby pond).

Discharge, Qin (ml/s)	Vegetation Conditions	Run No.	$e_o = t_o/t_n$	$e_p = t_p/t_n$	$e_m = t_m/t_n$	σ^2 (based on relative time)
40.15	0E	48.1	0.08	0.14	0.99	1.27
	0E	48.2	0.12	0.22	1.03	1.63
	0E	48.3	0.08	0.15	0.98	1.30
	0E	48.4	0.12	0.16	0.94	1.73
	Mean of 0E (S.D)	48	0.10 (0.02)	0.17 (0.04)	0.99 (0.04)	1.48 (0.23)
	11E	49.1	0.22	0.42	1.02	3.72
	11E	49.2	0.18	0.46	1.07	3.46
	11E	49.3	0.23	0.43	1.07	2.91
	Mean of 11E (S.D)	49	0.21 (0.03)	0.44 (0.02)	1.05 (0.03)	3.37 (0.41)
	22E	50.1	0.19	0.45	1.02	3.44
	22E	50.2	0.24	0.47	1.03	4.13
	22E	50.3	0.18	0.41	1.29	0.87
	Mean of 22E (S.D)	50	0.20 (0.03)	0.44 (0.03)	1.11 (0.15)	2.82 (1.72)
	27E	51.1	0.15	0.24	1.02	1.61
	27E	51.2	0.23	0.37	1.12	2.08
	27E	51.3	0.19	0.41	1.13	2.41
	Mean of 27E (S.D)	51	0.19 (0.04)	0.34 (0.09)	1.09 (0.06)	2.03 (0.41)

Table 4-8. HRTD statistics of tracer runs at 40.15 ml/s with vegetation configuration range from 0E,11E, 22E and 27E.

4.1.9 Summary results from trace with discharge (Q_{in}) 45.9 ml/s with 5 vegetation conditions

At the controlled flow rate of 45.90 ml/s (in the field 80 l/s), experiments were conducted with vegetation configurations remaining the same as above but only ranging from 0E, 11E, 22E and 27E (*i.e* between cases of no vegetation and high density of emergent plants). Dye recovery for all runs 51 to 55 ranged from 78% to 121%, with an average of 100%. Again, there was no consistent difference between the relative HRTD plots of runs 51 to 55 within the vegetation range from 0E, 11E, 22E, 27E and 27ED, respectively. None of the parameters for hydraulic efficiency differed significantly between 0E, 11E, 22E, 27E and 27ED, Figure 4-27. The relative hydraulic efficiency e_m of the real residence time varied from 1.01 to 1.15, Figure 4-27 B, where the relative hydraulic efficiency of first dye arrival, e_o, varied from 0.15 to 0.24, Figure 4-27 A.

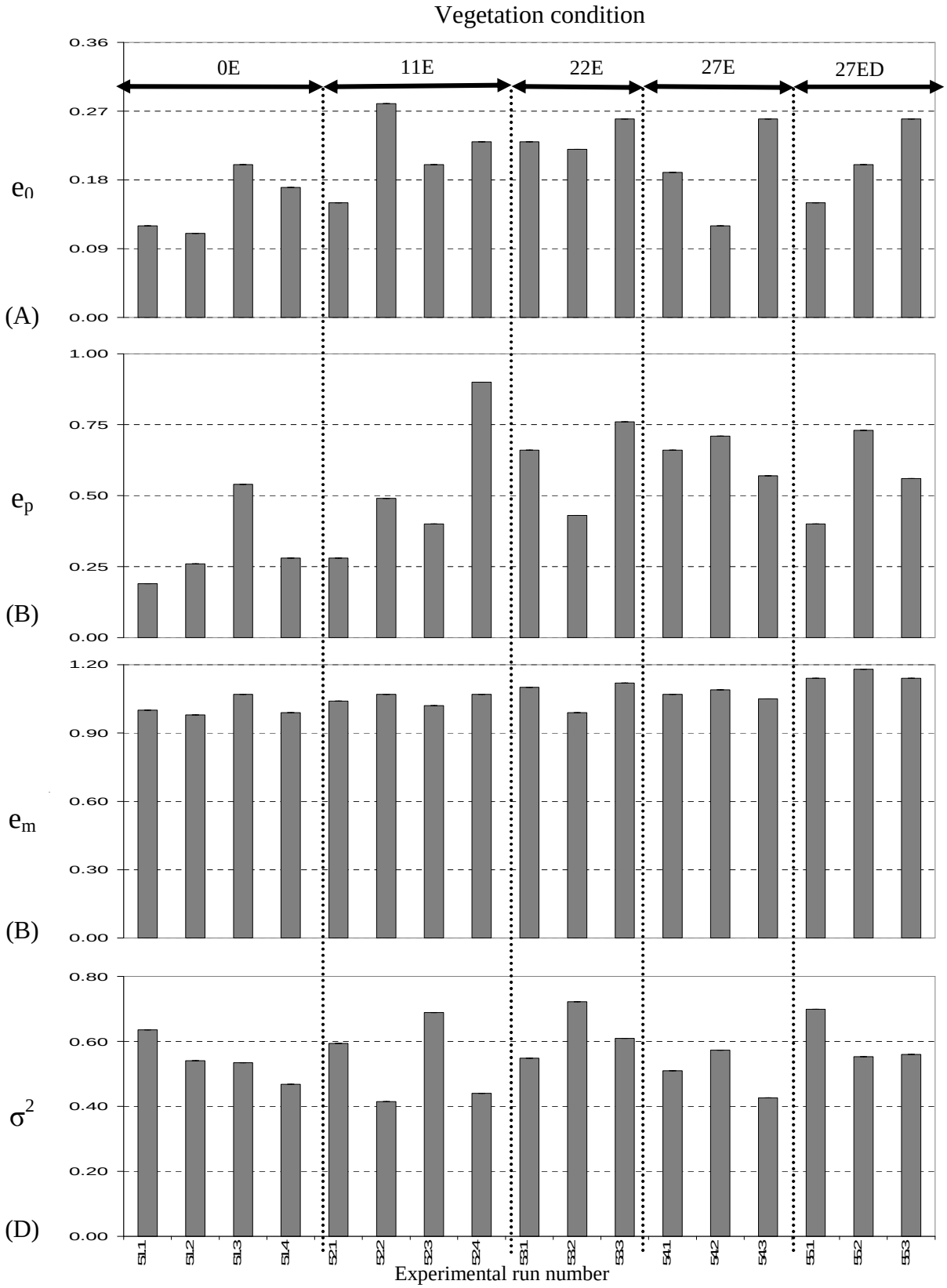

Figure 4-27. The residence time distribution (HRTD) characteristics under differing vegetation configuration. Comparisons are made at the same discharge (45.9 ml/s) and among different vegetation configurations for (A) relative first dye arrival at the pond outlet (e_0), (B) relative peak concentration time ($e_p = t_p / t_n$), (C) relative residence time (Centroid of HRTD, $e_m = t_m / t_n$), (D) relative time variance (σ^2).

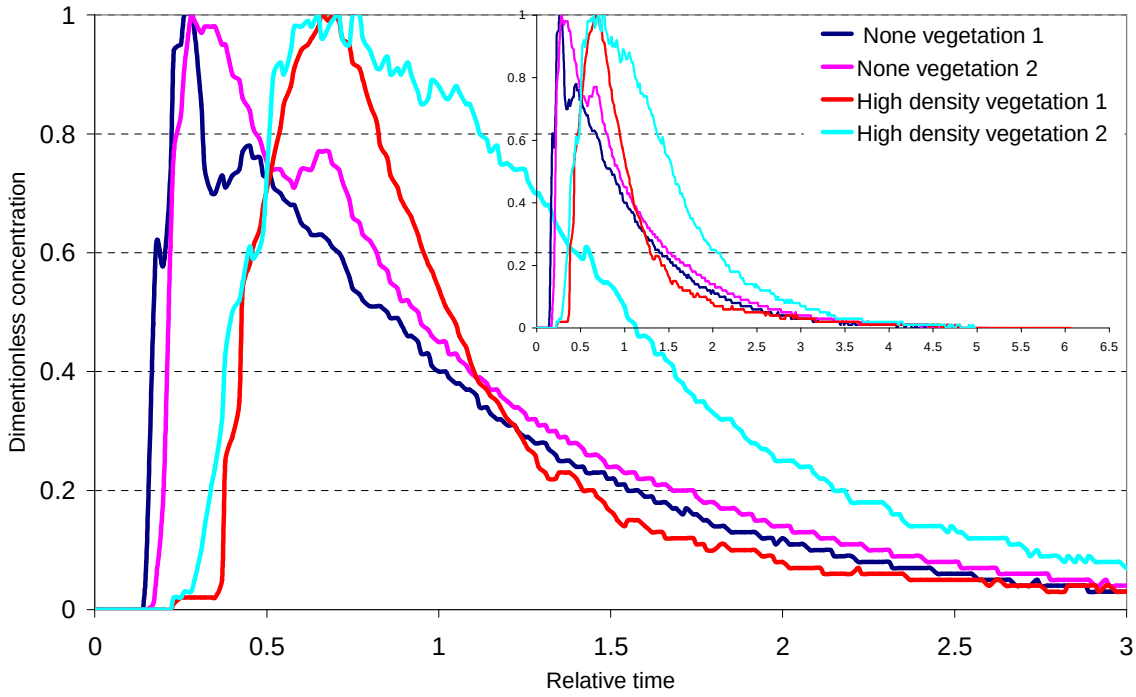

Figure 4-28. Comparison of four representative residence time distributions (HRTDs) curves of none vegetation to highest emergent vegetation configurations with Q = 45.90 ml/s.

The relative HRTDs when compared between cases of no vegetation to different high density of emergent plant configurations did not appear to be distinctively different. The relative HRTDs of all vegetation configurations is seen still to show a bimodal shape, with the first peak typically arriving late and being more spread out, Figure 4-28. These bimodal shapes were reflected in the relative HRTD statistics, Figure 4-27. The relative average and mean of first dye arrival, e_o, for all runs and all vegetation configurations was delayed to 0.20. The relative time to peak concentration of the HRTD curve, e_p, occurred at the average value of 0.53 for all runs and all vegetation configurations. The average relative mean residence time, HRTD centroid, e_m, was 1.07.

Repeat tests were conducted randomly among different vegetation configurations; four repeat dye tracers were conducted for run 51 and 52 with 0E and 11E vegetation condition (where there were no significant defences of all its relative HRTD results, Figure 4-27) then only three repeated dye tracers were developed for runs 53 to 55 with vegetation 22E, 27E, and 27ED, respectively. Table 4-9 shows the detail of HRTDs in all runs from no vegetation to all other emergent vegetation configurations based on 40.15 ml/s discharge (equal to 70 l/s in the Lyby pond).

Discharge, Qin (ml/s)	Vegetation Conditions	Run No.	$e_o = t_o/t_n$	$e_p = t_p/t_n$	$e_m = t_m/t_n$	σ^2 (based on relative time)
45.9 0	0E	51.1	0.12	0.17	1	1.57
	0E	51.2	0.11	0.22	0.98	1.85
	0E	51.3	0.2	0.29	1.07	1.87
	0E	51.4	0.17	0.26	0.99	2.14
	Mean of 0E (S.D)	51	0.15 (0.04)	0.24 (0.05)	1.01 (0.04)	1.86 (0.23)
	11E	52.1	0.15	0.26	1.04	1.68
	11E	52.2	0.28	0.4	1.07	2.41
	11E	52.3	0.2	0.31	1.02	1.45
	11E	52.4	0.23	0.34	1.07	2.27
	Mean of 0E (S.D)	52	0.22 (0.05)	0.33 (0.06)	1.05 (0.02)	1.95 (0.46)
	22E	53.1	0.23	0.45	1.1	1.82
	22E	53.2	0.22	0.31	0.99	1.38
	22E	53.3	0.26	0.32	1.12	1.64
	Mean of 0E (S.D)	53	0.24 (0.02)	0.36 (0.08)	1.07 (0.07)	1.62 (0.22)
	27E	54.1	0.19	0.34	1.07	1.96
	27E	54.2	0.12	0.34	1.09	1.74
	27E	54.3	0.26	0.28	1.05	2.34
	Mean of 0E (S.D)	54	0.19 (0.07)	0.32 (0.03)	1.07 (0.02)	2.02 (0.30)
	27ED	55.1	0.15	0.31	1.14	1.43
	27ED	55.2	0.2	0.36	1.18	1.81
	27ED	55.3	0.26	0.34	1.14	1.78
	Mean of 0E (S.D)	55	0.20 (0.06)	0.34 (0.03)	1.15 (0.02)	1.67 (0.21)

Table 4-9. HRTD statistics of tracer runs at 40.15 ml/s with vegetation configuration range from 0E,11E, 22E, 27E and 27ED.

4.2 Experimental results from Physical Scale Pond with the same vegetation

4.2.1 Summary results from trace without vegetation (0E) and different Q_{in}

A range of experiments were conducted by fixing the vegetation in one specific condition (in this case the condition was fixed at no vegetation (0E)), whilst the discharge varied from 4.4, 5.74, 11.48, 17.21, 22.96, 28.69, 34.43, 40.15 to 45.9 ml/s, Table 4-10. Dye recovery for all 43 runs ranged from 74 to 127% with an average of 100% of mass dye recovery. There were some consistent differences between the relative HRTD plots at low discharges (defined arbitrarily as 4.4, 5.74 and 11.48 ml/s) and high discharges (17.21, 22.96, 28.69, 34.43, 40.15 and 45.90 ml/s). Some parameters of the hydraulic efficiency differed significantly between cases of low to high discharge but some parameters for hydraulic efficiency did not differ significantly, Figure 4-29. The relative hydraulic efficiency of the actual residence time, e_m, varied and increased from 0.83 to 0.98 as the flow changed between low discharge (from 4.4 to 11.48 ml/s) to 0.99 to 1.13 at higher discharge (17.21 to 45.90 l/s). The relative hydraulic efficiency of first dye arrival at the outlet, e_o, was increase from 0.01 to 0.07 at low discharges and 0.10 to 0.17 at higher discharge respectively. These indicated that increase the discharge led to the elimination or minimisation of short circuiting in the pond.

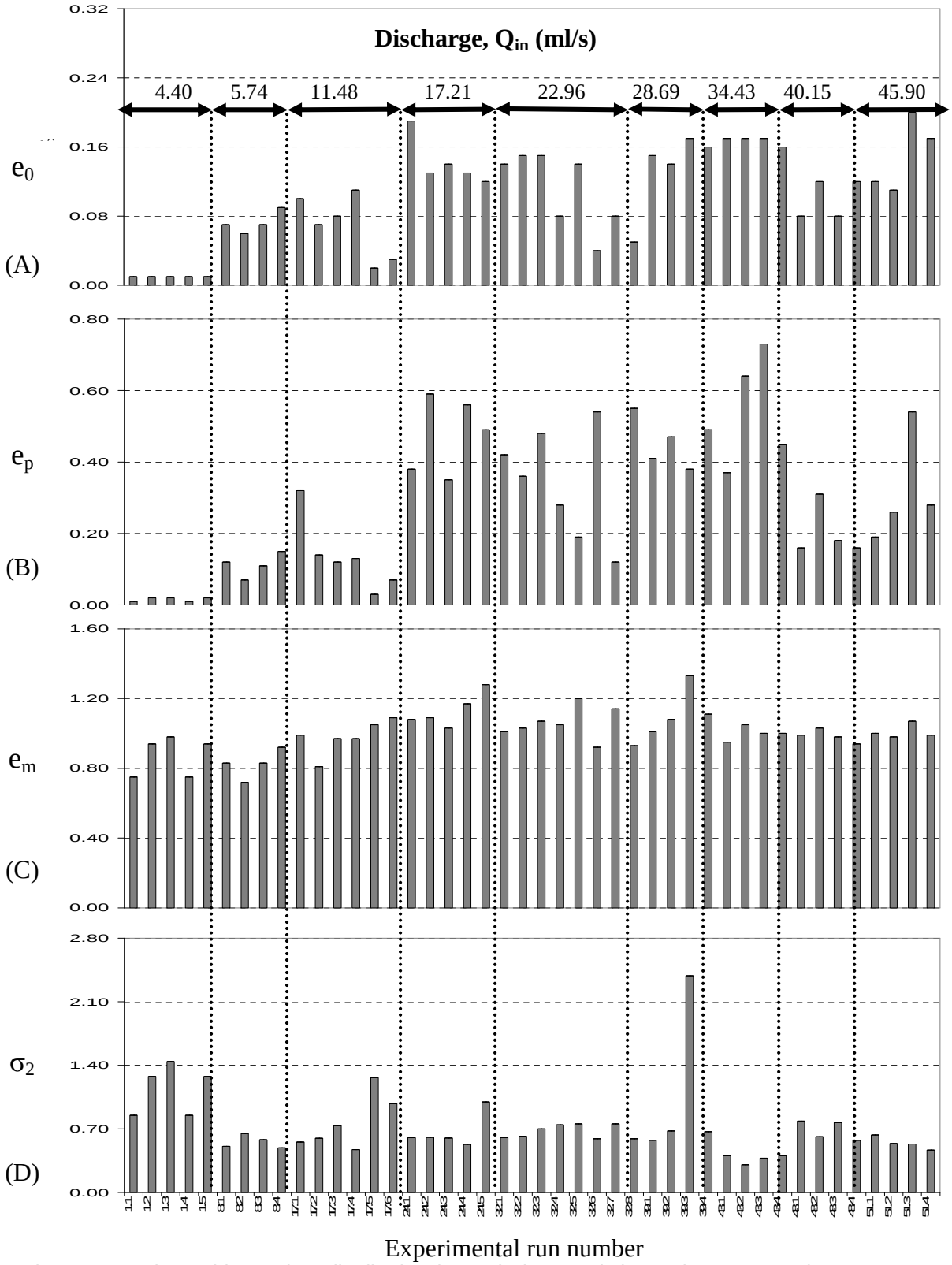

Figure 4-29. The residence time distribution (HRTD) characteristics under 0Evegetation configuration. Comparisons are made at the same non vegetation and among different discharge configurations for (for (A) relative first dye arrival at the pond outlet (e_0), (B) relative peak concentration time ($e_p = t_p / t_n$), (C) relative residence time (Centroid of HRTD, $e_m = t_m / t_n$), (D) relative time variance (σ^2).

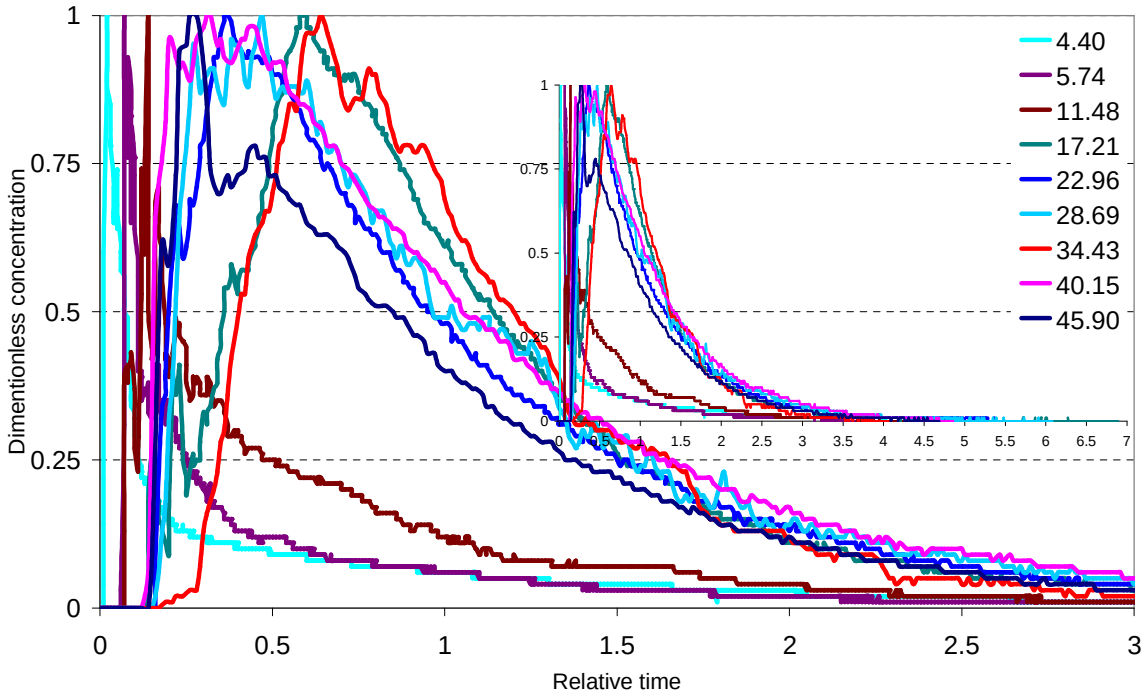

Figure 4-30. Comparison of four representative residence time distribution (HRTD) curves run at 0E with discharge range from 4.4 to 45.9 ml/s.

The relative HRTDs compared between low and higher discharge configurations appeared to be distinctively different. Where the relative HRTD of less discharge tended to be unimodal in the shape of the distribution curve, the relative HRTD for the higher discharge usually tended to become bimodal in shape, with the first peak typically arriving late and being more spread out than the lower discharge's relative HRTD, Figure 4-30. These differences were reflected in the HRTD statistics, Figure 4-29. The average of relative first dye arrival, e_o, was 0.05 for lower discharge and 0.14 for higher discharge configurations. The relative time to peak concentration of the HRTD curve, e_p, occurred at the average value of 0.09 for the low discharge configurations and 0.39 for high discharge configurations. The mean relative residence time, relative HRTD centroid, e_m, had an average value of 0.89 for low discharge configurations and 1.05 of t_n for the high discharge configurations. Each of these measurements of hydraulic efficiency is a time function of the nominal residence time (t_n= V/Q).

Twelve repeat dye tracers were conducted for the run with a discharge condition of 22.96 ml/s (where there were no significant defences of all its HRTD results, Figure 4-29), then only six dye tracer runs were conducted for runs with 11.48 ml/s discharge. Five dye tracers were run for each 4.4 and 17.21 ml/s discharge conditions, four dye tracer was run for each of 5.74, 34.43 and 40.15 ml/s discharge conditions, and only three dye tracer was run for the 45.90 ml/s discharge condition. Table 4-10, shows the detail of HRTDs in all runs with and without vegetation configuration.

Vegetation Condition	Discharge, Qin (ml/s)	Run No.	$e_o = t_o/t_n$	$e_p = t_p/t_n$	$e_m = t_m/t_n$	σ^2 (based on relative time)
0E (no vegetation)	4.4	1.1	0.01	0.03	0.75	0.85
	4.4	1.2	0.01	0.03	0.94	1.28
	4.4	1.3	0.01	0.02	0.98	1.44
	4.4	1.4	0.01	0.02	0.75	0.85
	4.4	1.5	0.01	0.02	0.94	1.28
	Mean of 4.4 (S.D)	1	0.01	0.02	0.87	1.14 (0.27)
	5.74	8.1	0.07	0.12	0.83	0.51
	5.74	8.2	0.06	0.08	0.72	0.65
	5.74	8.3	0.07	0.11	0.83	0.58
	5.74	8.4	0.09	0.16	0.92	0.49
	Mean of 5.74 (S.D)	8	0.07	0.12	0.83	0.56 (0.07)
	11.48	17.1	0.1	0.77	0.99	0.56
	11.48	17.2	0.07	0.12	0.81	0.60
	11.48	17.3	0.08	0.12	0.97	0.74
	11.48	17.4	0.11	0.19	0.97	0.47
	11.48	17.5	0.02	0.07	1.05	1.26
	11.48	17.6	0.03	0.08	1.09	0.98
	Mean of 11.48 (S.D)	17	0.07	0.23	0.98	0.77 (0.30)
	17.21	24.1	0.19	0.28	1.08	0.60
	17.21	24.2	0.13	0.32	1.09	0.61
	17.21	24.3	0.14	0.27	1.03	0.60
	17.21	24.4	0.13	0.43	1.17	0.53
	17.21	24.5	0.12	0.3	1.28	1.00
	Mean of 17.21 (S.D)	24	0.14	0.32	1.13	0.67 (0.19)
	22.96	32.1	0.14	0.25	1.01	0.60
	22.96	32.2	0.15	0.26	1.03	0.62
	22.96	32.3	0.15	0.26	1.07	0.70
	22.96	32.4	0.08	0.2	1.05	0.75
	22.96	32.5	0.14	0.21	1.2	0.76
	22.96	32.6	0.04	0.14	0.92	0.59
	22.96	32.7	0.08	0.14	1.14	0.76
	22.96	32.8	0.05	0.15	0.93	0.59
	Mean of 22.96 (S.D)	32	0.10	0.20	1.04	0.67 (0.08)
	28.69	39.1	0.15	0.24	1.01	0.58
	28.69	39.2	0.14	0.27	1.08	0.68
	28.69	39.3	0.17	0.27	1.33	2.39
	28.69	39.4	0.16	0.3	1.11	0.67
	Mean of 28.69 (S.D)	39	0.16	0.27	1.13	1.08 (0.87)
	34.43	43.1	0.17	0.3	0.95	0.41
	34.43	43.2	0.17	0.42	1.05	0.31
	34.43	43.3	0.17	0.36	1	0.38
	34.43	43.4	0.16	0.28	1	0.41
	Mean of 34.43 (S.D)	43	0.17	0.34	1.00	0.37 (0.05)
	40.15	48.1	0.08	0.14	0.99	0.79
	40.15	48.2	0.12	0.22	1.03	0.61
	40.15	48.3	0.08	0.15	0.98	0.77
	40.15	48.4	0.12	0.16	0.94	0.58
	Mean of 4.4 (S.D)	48	0.1	0.17	0.99	0.69 (0.11)
	45.9	51.1	0.12	0.17	1	0.64
	45.9	51.2	0.11	0.22	0.98	0.54
	45.9	51.3	0.2	0.29	1.07	0.53
	45.9	51.4	0.17	0.26	0.99	0.47
	Mean of 4.4 (S.D)	51	0.15 (0.04)	0.24 (0.05)	1.01 (0.04)	0.54 (0.07)

Table 4-10 HRTD statistics of tracer runs at 0E with discharge range from 4.4 to 45.9 ml/s.

Surface flow profiles from the PIV measurements were obtained by holding fixed the (no) vegetation configuration (0E) and varying the discharge from low to high (4.4 up to 22.96 ml/s). No PIV data were collected for high discharge cases ranging from 28.96 to 45.90 ml/s, Table 4-10 , and no consistent difference between the surface flow profiles (in terms of the vortex patterns) were seen for discharge values ranging between 4.4 and 22.96 ml/s. There were two main vortexes observed in sections 1/3 and 2/3 of the model pond and no channel flow in these sections, at discharge rates ranging from 4.4 to 22.96 ml/s, Figure 4-40.

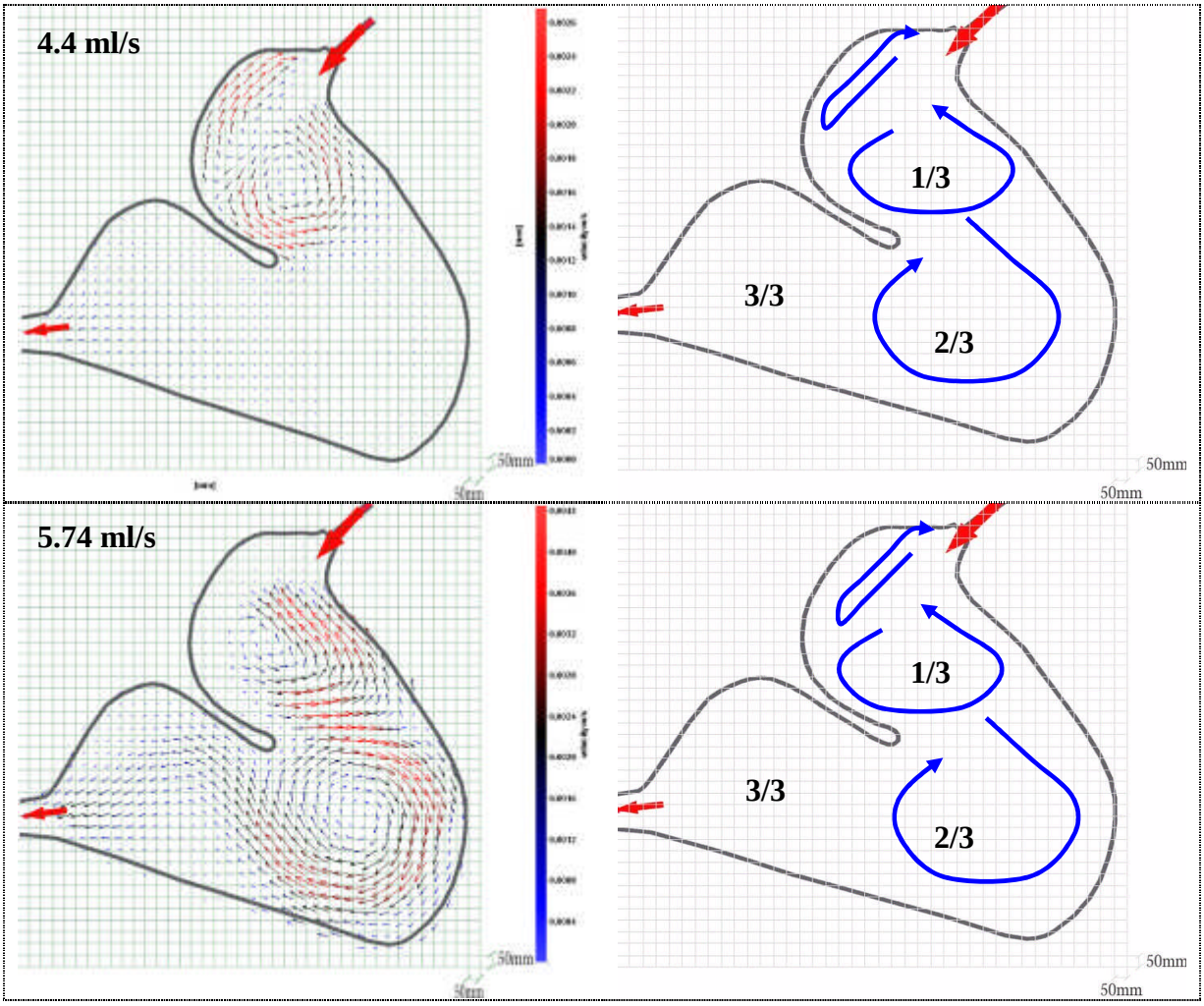

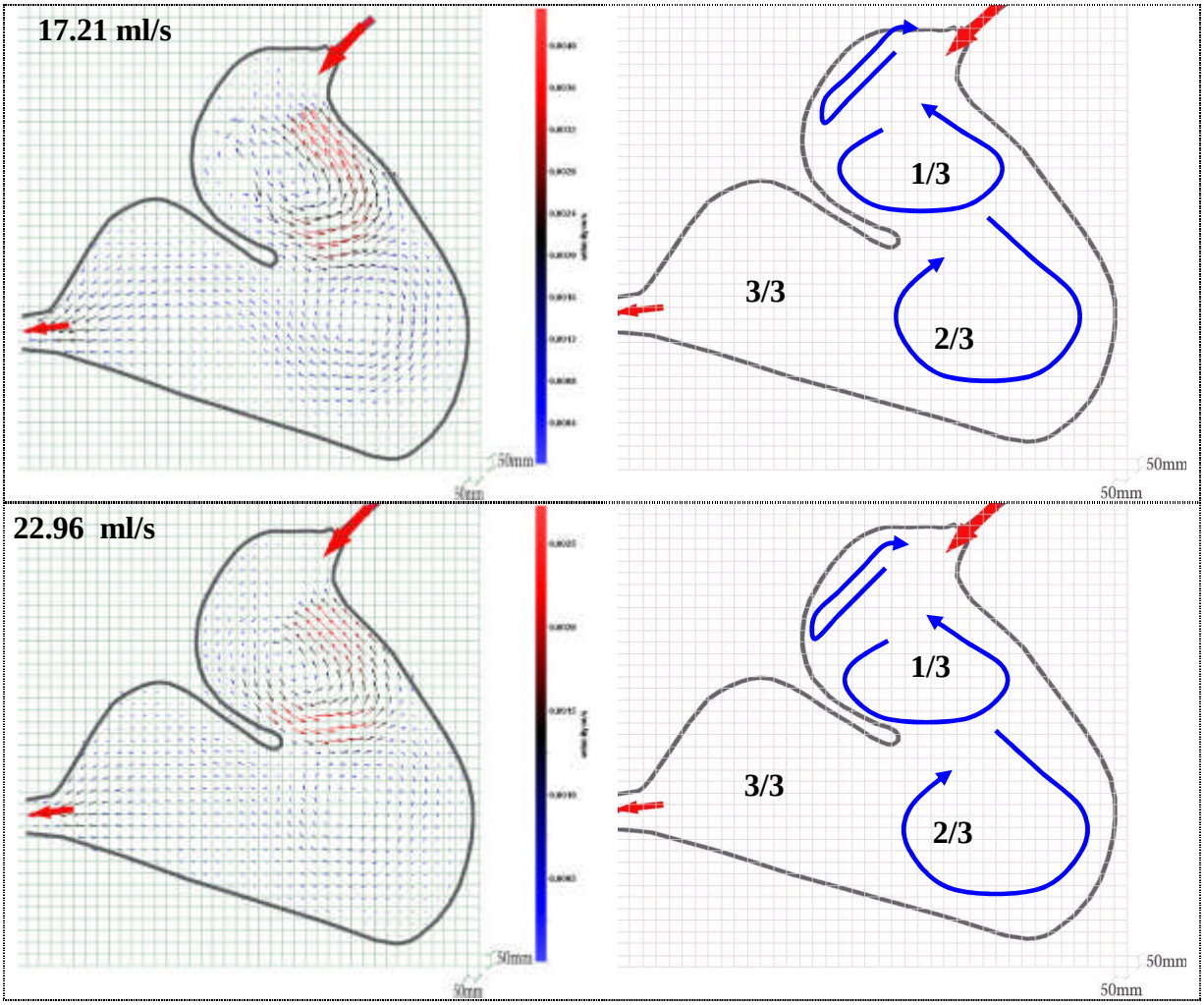

Figure 4-31. Surface flow profiles of discharge 4.4, 5.74, 17.21 and 22.96 ml/s at 0E vegetation configuration.

4.2.2 Summary results from trace with 11E vegetation and different Q_{in}

A range of experiments was conducted with a fixed vegetation condition; in this case, the condition was fixed at 11E vegetation, whilst the discharge varied from 4.4 to 45.9 ml/s, Table 4-11. Dye recovery for all 24 runs ranged from 67 to 105% with an average of 93%. There were some consistent differences between the relative HRTD plots of low discharges to and high discharges (4.4 to 45.9 ml/s) but some were not significantly different. Some of the parameters for relative hydraulic efficiency differed significantly between lower discharges to higher discharge but some parameters for hydraulic efficiency did not differ significantly, Figure 4-32. The mean relative residence time, relative HRTD centroid, e_m, varied

and fluctuated from 0.92 to 1.15, between the lowest and highest discharge values (4.4 to 45.90 l/s). The mean relative time of the first dye arrival at the outlet, e_o, was exponential increase from 0.01 to 0.24 whilst discharge increase from 4.4 to 45.9 ml/s respectively.

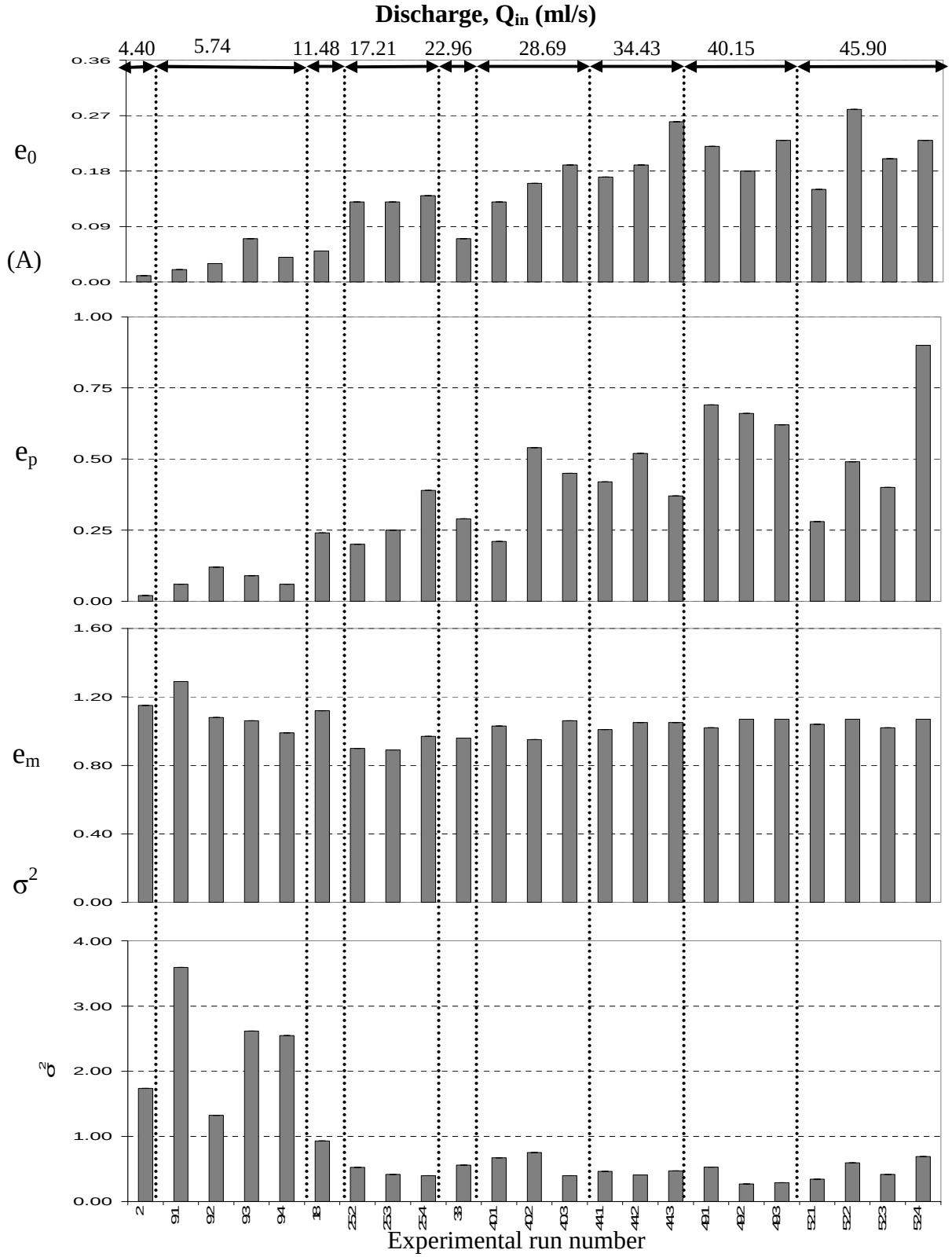

Figure 4-32. The residence time distribution (HRTD) characteristics under 11Evegetation configuration. Comparisons are made at the same 11E vegetation and among different discharge configurations for for (A) relative first dye arrival at the pond outlet (e_0), (B) relative peak concentration time ($e_p = t_p / t_n$), (C) relative residence time (Centroid of HRTD, $e_m = t_m / t_n$), (D) relative time variance (σ^2).

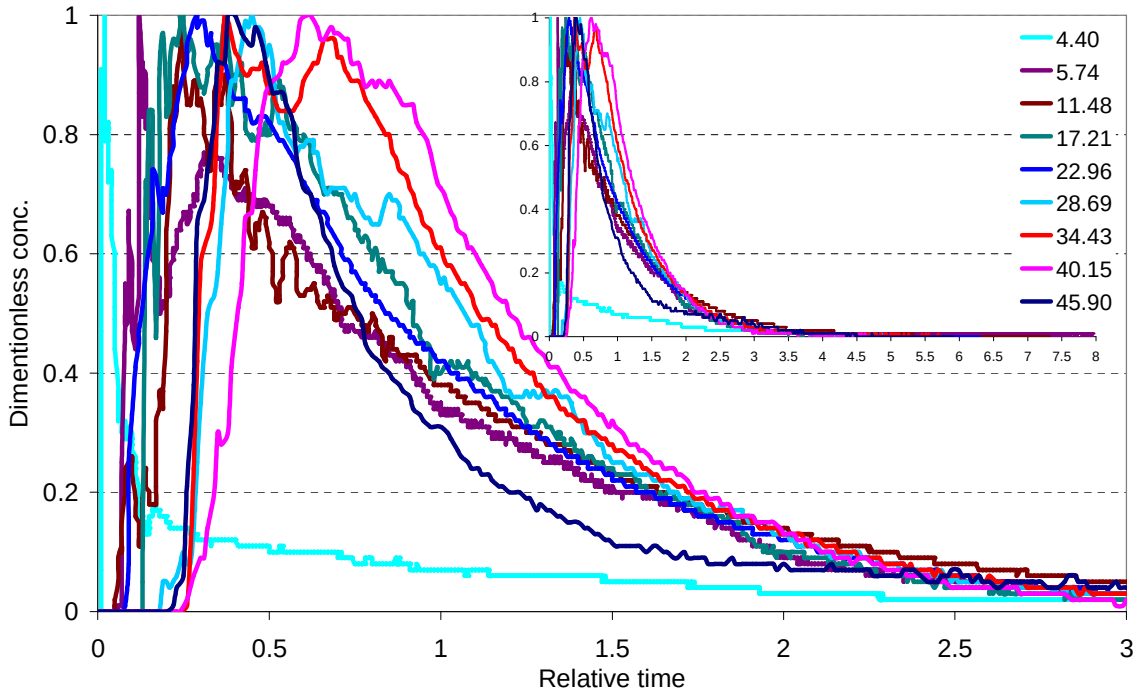

Figure 4-33. Comparison of four representative residence time distribution (HRTD) curves run at 11E vegetation and a discharge range from 4.4 to 45.9 ml/s.

The relative HRTDs between low and higher discharge configurations appeared distinctively different from each other. Where the relative HRTD of the smallest discharge tended to be unimodal in shape, the relative HRTD for the higher discharge usually tended to have a bimodal shape, with the first peak typically arriving late and being more spread out than lower discharge HRTD, Figure 4-33. These differences were reflected in the HRTD statistics, Figure 4-32. The average of relative first dye arrival, e_o, was exponentially increased from 0.01 to 0.24 whilst discharge increase from lowest to highest (4.4 to 45.9 ml/s). The relative time to peak concentration of the HRTD curve, e_p, was significantly and rapidly increased from 0.02 to 0.66 while the discharge increased from 4.4 to 45.9 ml/s. On the other hand, the increase of discharge from very low to very high did not affect the relative mean residence time, relative HRTD centroid, e_m. It looked very much the same with mean and average values of 1.05 with very small standard deviation of 0.07 (δ).

Four repeat dye tracers were run for the 5.74 and 45.9 ml/s discharge conditions, where there were no significant defences of all its relative HRTD results (Figure 4-32), then only three repeat dye tracer runs were made for discharge of 17.21, 28.69, 34.43 and 40.15 ml/s; only one dye tracer was run for each discharge of 4.4, 11.48 and 22.96 ml/s. Table 4-11, shows the details of mean of relative HRTDs in all runs with 11E vegetation configuration.

Vegetation Condition	Discharge, Qin (ml/s)	Run No.	$e_o = t_o/t_n$	$e_p = t_p/t_n$	$e_m = t_m/t_n$	σ^2 (based on relative time)
11E	4.4	2	0.01	0.03	1.15	0.58
	5.74	9.1	0.02	0.04	1.29	0.28
	5.74	9.2	0.03	0.14	1.08	0.76
	5.74	9.3	0.07	0.09	1.06	0.38
	5.74	9.4	0.04	0.06	0.99	0.39
	Mean of 5.74 (S.D)	9	0.04 (0.02)	0.08 (0.04)	1.11 (0.13)	0.45 (0.21)
	11.48	18	0.05	0.22	1.12	1.08
	17.21	25.2	0.13	0.21	0.9	1.90
	17.21	25.3	0.13	0.2	0.89	2.40
	17.21	25.4	0.14	0.34	0.97	2.51
	Mean of 17.21 (S.D)	25	0.13 (0.01)	0.25 (0.08)	0.92 (0.04)	2.27 (0.33)
	22.96	33	0.07	0.18	0.96	1.79
	28.69	40.1	0.13	0.2	1.03	1.49
	28.69	40.2	0.16	0.3	0.95	1.33
	28.69	40.3	0.19	0.36	1.06	2.53
	Mean of 28.69 (S.D)	40	0.16 (0.03)	0.29 (0.08)	1.01 (0.06)	1.78 (0.65)
	34.43	44.1	0.17	0.35	1.01	2.16
	34.43	44.2	0.19	0.35	1.05	2.46
	34.43	44.3	0.26	0.35	1.05	2.14
	Mean of 34.43 (S.D)	44	0.21 (0.05)	0.35 (0.00)	1.04 (0.02)	2.25 (0.18)
	40.15	49.1	0.22	0.42	1.02	1.89
	40.15	49.2	0.18	0.46	1.07	3.72
	40.15	49.3	0.23	0.43	1.07	3.46
	Mean of 40.15 (S.D)	49	0.21 (0.03)	0.44 (0.02)	1.05 (0.02)	3.03 (0.99)
	45.9	52.1	0.15	0.26	1.04	2.91
	45.9	52.2	0.28	0.4	1.07	1.68
	45.9	52.3	0.2	0.31	1.02	2.41
	45.9	52.4	0.23	0.34	1.07	1.45
	Mean of 45.9 (S.D)	52	0.24 (0.05)	0.35 (0.36)	1.05 (0.02)	1.85 (0.67)

Table 4-11. HRTD statistics of tracer runs at 11E vegetation at discharge ranged from 4.4 to 45.9 ml/s.

Surface flow profiles were derived from the PIV data with the fixed case of 11E vegetation configuration and varying discharge between low to high values (4.4 up to 22.96 ml/s). No PIV was conducted at the high discharge range from 28.96 to

45.90 ml/s), Table 4-11, and no consistent difference was found between the surface vortex flow profiles for the discharge range 4.4 and 22.96 ml/s, where two main vortices appeared in sections 1/3 and 2/3 of the physical scale pond with no channel flow in these section, Figure 4-34. On the other hand, at discharge values of 5.74, 11.48 and 17.21 ml/s, there was only one main vortex seen in section 1/3 of the model pond and no channel flow was observed in this section, Figure 4-34.

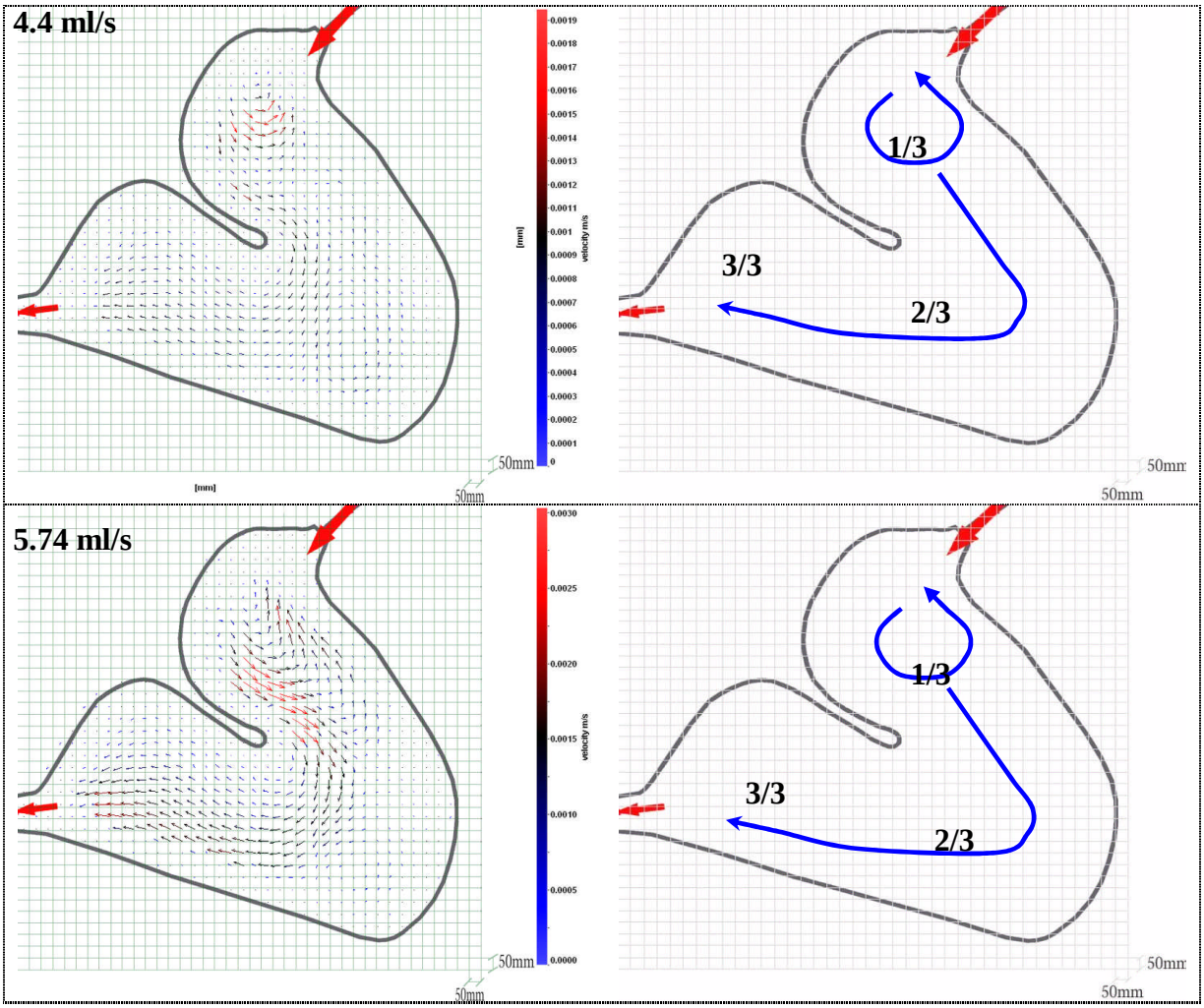

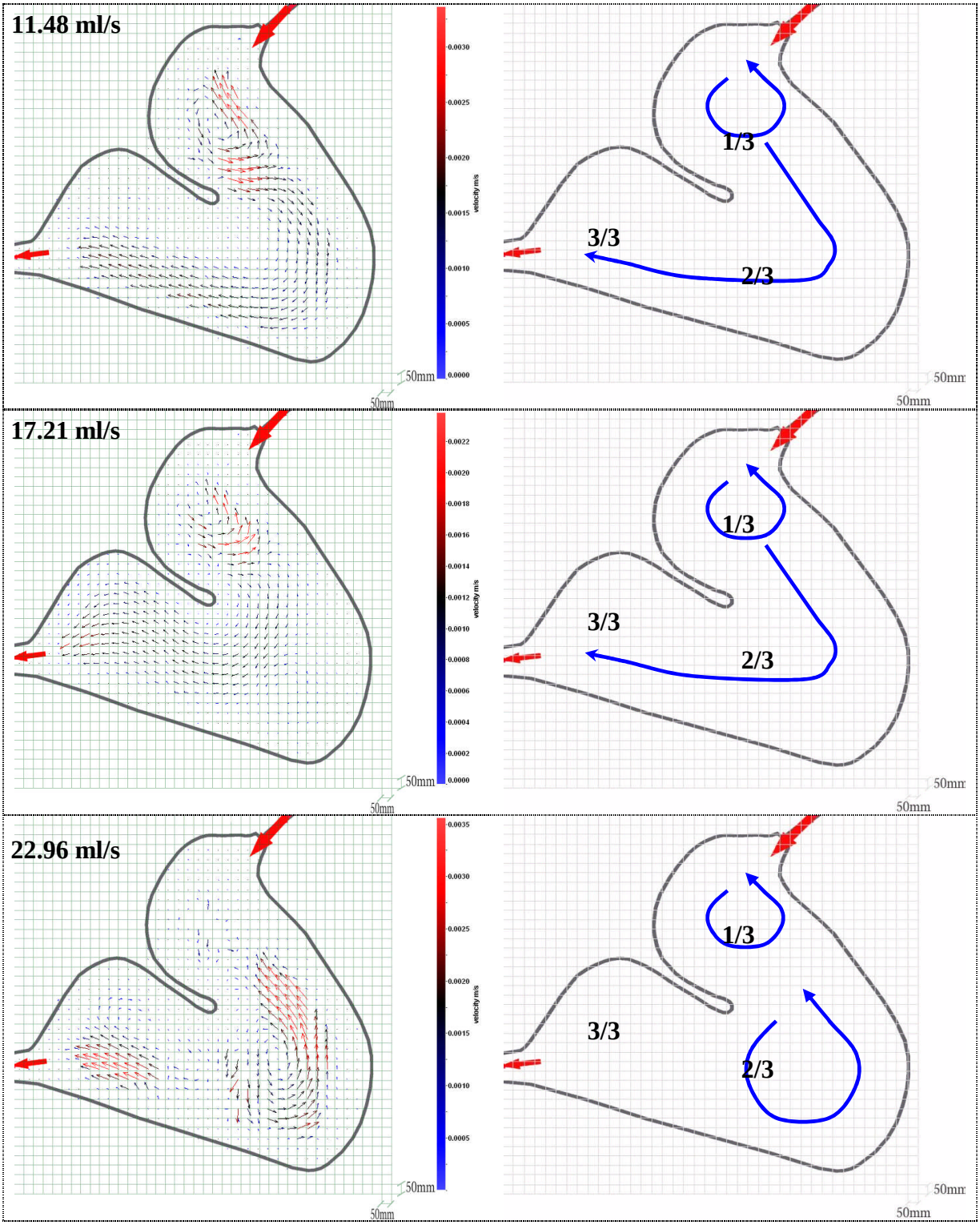

Figure 4-34. Surface flow profiles based on discharge 4.4, 5.74, 11.48, 17.21 and 22.96 ml/s Vegetation.

4.2.3 Summary results from trace with 22E vegetation and different Q_{in}

A range of experiments was conducted with a fixed vegetation condition, in this case, the condition was fixed at 11E vegetation, whilst the discharge varied from 4.4 to 45.9 ml/s, Table 4-12. Dye recovery for all 23 runs ranged from 73 to 123% with an average of 86%. There were some consistent differences between the relative HRTD plots of low to high discharges (4.4 to 45.9 ml/s) but some were not significantly different. Some of the parameters for hydraulic efficiency differed significantly between lower discharge to higher discharge but some parameters for hydraulic efficiency did not differ significantly, Figure 4-35. The mean relative residence time, relative HRTD centroid, e_m, varied and fluctuated from 0.87 to 1.28, between the lowest and highest discharge values (4.4 to 45.90 l/s). The mean relative time of the first dye arrival at the outlet, e_o, was exponential increase from 0.04 to 0.24 whilst discharge increase from 4.4 to 45.9 ml/s respectively

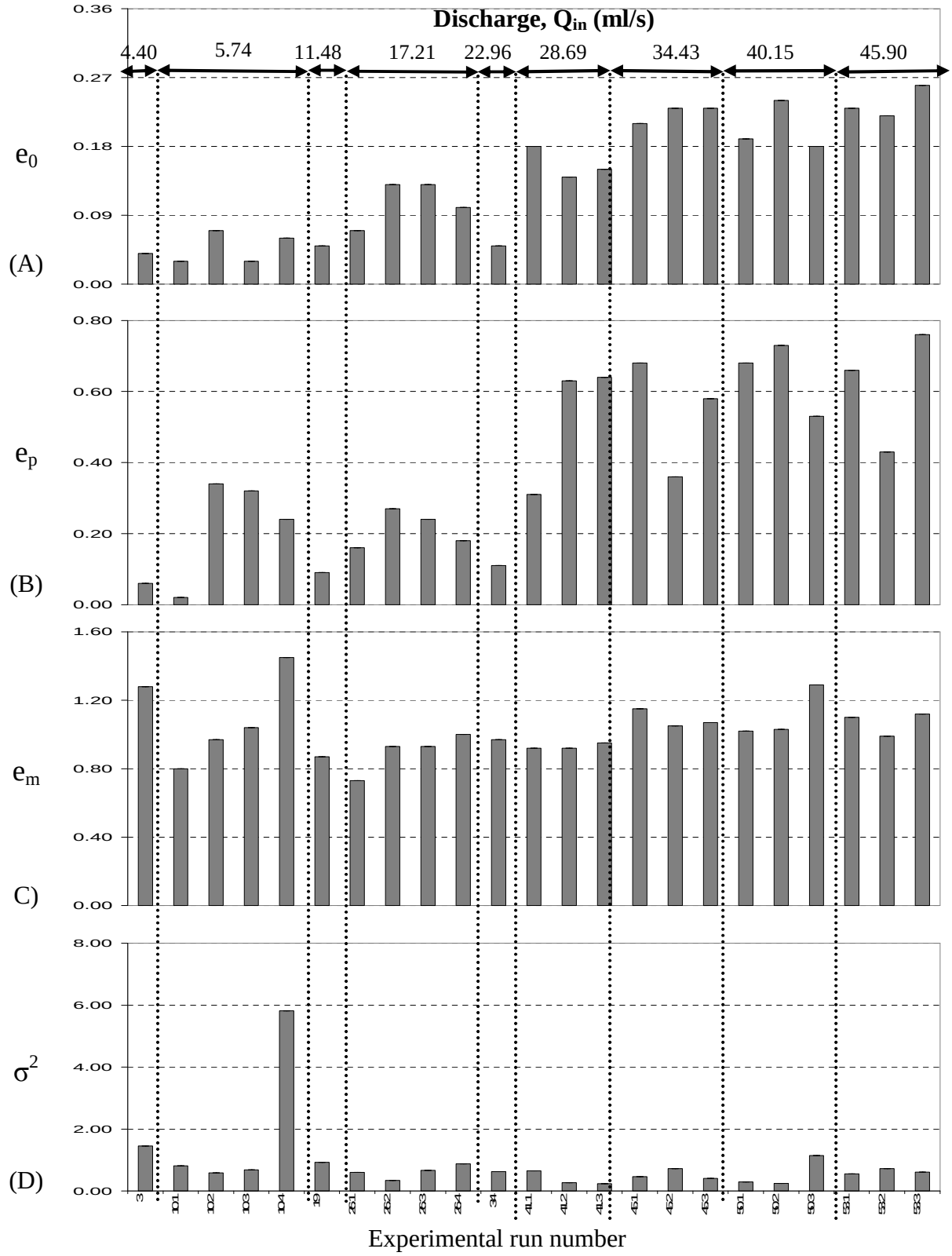

Figure 4-35. The residence time distribution (HRTD) characteristics under 22Evegetation configuration. Comparisons are made at the same 22E vegetation and among different discharge configurations for for (A) relative first dye arrival at the pond outlet (e_0), (B) relative peak concentration time ($e_p = t_p / t_n$), (C) relative residence time (Centroid of HRTD, $e_m = t_m / t_n$), (D) relative time variance (σ^2).

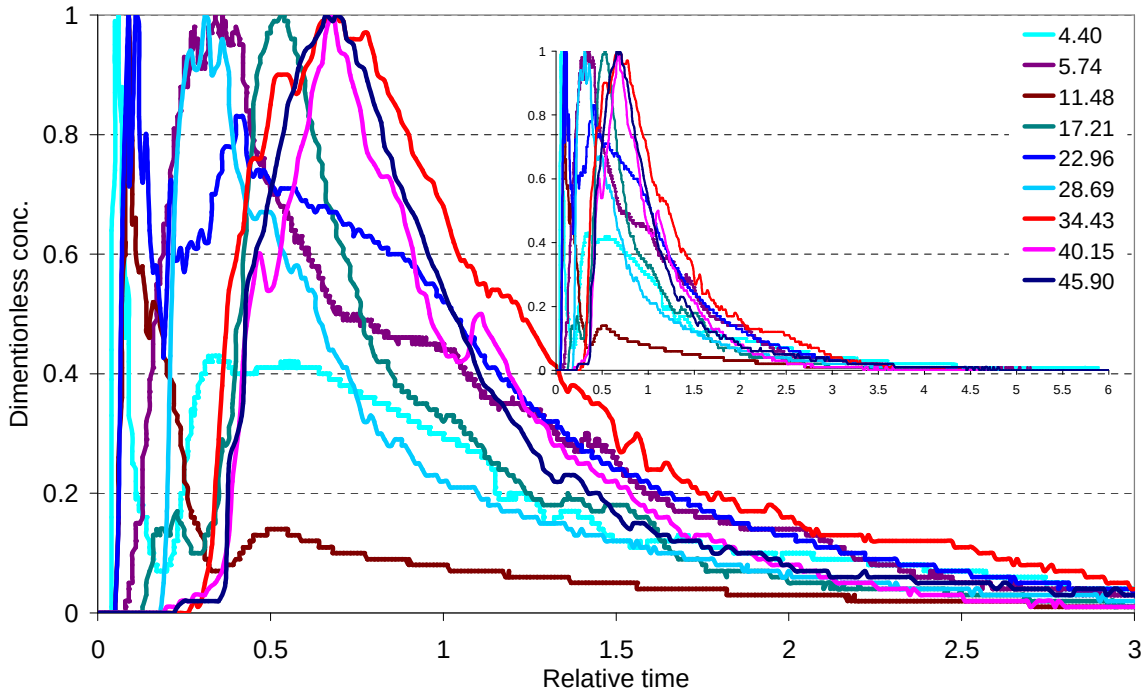

Figure 4-36. Comparison of four representative residence time distribution (HRTD) curves run at 22E with discharge range from 4.4 to 45.9 ml/s.

The relative HRTDs between low and higher discharge configurations appeared distinctively different from each other. Where the relative HRTD of the smallest discharge tended to be unimodal in shape, the relative HRTD for the higher discharge usually tended to have a bimodal, with the first peak typically arriving late and being more spread out than lower discharge HRTD, Figure 4-36. These differences were reflected in the HRTD statistics, Figure 4-35. The average relative time of first dye arrival, e_o, was exponentially increased from 0.04 to 0.24 whilst discharge increase from lowest to highest (4.4 to 45.9 ml/s). The relative time to peak concentration of the relative HRTD curve, e_p, was significantly and rapidly increased from 0.06 to 0.65 while the discharge increased from 4.4 to 45.9 ml/s. On the other hand, the increase of discharge from very low to very high did not affect on the relative mean residence time, relative HRTD centroid, $e_{m.}$ It was

looked very much the same with relative mean and average values (e_m) of 1.05 with very small standard deviation of 0.13 (δ).

Four repeat dye tracers were run for the 5.74 and 17.21 ml/s discharge conditions, where there were no significant defences of all its HRTD results, Figure 4-35, then only three repeat dye tracer runs were made for discharge ranged from 28.69 to 45.9 ml/s; and only one dye tracer was run for each discharge of 4.4, 11.48 and 22.96 ml/s . Table 4-12, shows the details of relative mean HRTDs in all runs with 22E vegetation configuration.

Vegetation Condition	Discharge, Qin (ml/s)	Run No.	$e_o = t_o/t_n$	$e_p = t_p/t_n$	$e_m = t_m/t_n$	σ^2 (based on relative time)
22E	4.4	3	0.04	0.08	1.28	0.69
	5.74	10.1	0.03	0.03	0.8	1.23
	5.74	10.2	0.07	0.21	0.97	1.71
	5.74	10.3	0.03	0.21	1.04	1.47
	5.74	10.4	0.06	0.14	1.45	0.17
	Mean of 5.74 (S.D)	10	0.05 (0.02)	0.15 (0.09)	1.07 (0.28)	1.15 (0.68)
	11.48	19	0.05	0.09	0.87	1.08
	17.21	26.1	0.07	0.12	0.73	1.67
	17.21	26.2	0.13	0.37	0.93	2.91
	17.21	26.3	0.13	0.21	0.93	1.50
	17.21	26.4	0.1	0.17	1	1.14
	Mean of 17.21 (S.D)	26	0.11 (0.03)	0.22 (0.11)	0.90 (0.12)	1.81 (0.77)
	22.96	34	0.05	0.12	0.97	1.60
	28.69	41.1	0.18	0.24	0.92	1.54
	28.69	41.2	0.14	0.42	0.92	3.79
	28.69	41.3	0.15	0.43	0.95	4.32
	Mean of 28.69 (S.D)	41	0.16 (0.02)	0.36 (0.11)	0.93 (0.02)	3.22 (1.48)
	34.43	45.1	0.21	0.43	1.15	2.16
	34.43	45.2	0.23	0.3	1.05	1.39
	34.43	45.3	0.23	0.41	1.07	2.45
	Mean of 34.43 (S.D0	45	0.22 (0.01)	0.38 (0.07)	1.09 (0.05)	2.00 (0.55)
	40.15	50.1	0.19	0.45	1.02	3.44
	40.15	50.2	0.24	0.47	1.03	4.13
	40.15	50.3	0.18	0.41	1.29	0.87
	Mean of 40.15 (S.D)	50	0.20 (0.03)	0.44 (0.03)	1.11 (0.15)	2.82 (1.12)
	45.9	53.1	0.23	0.45	1.1	1.82
	45.9	53.2	0.22	0.31	0.99	1.38
	45.9	53.3	0.26	0.32	1.12	1.64
	Mean of 45.9 (S.D)	53	0.24 (0.02)	0.36 (0.08)	1.07 (0.07)	1.62 (0.22)

Table 4-12 HRTD statistics of tracer runs at 22E vegetation at discharge range from 4.4 to 45.9 ml/s.

Surface flow profiles were derived from the PIV data with fixed case of 22E vegetation configuration and varying discharge between low to high values (4.4 up

to 22.96 ml/s). No PIV was conducted at the high discharge range from 28.96 to 45.90 ml/s), Table 4-13, and no consistent difference was found between the surface vortex flow profiles for the discharge range 4.4 to 22.96 ml/s, where one small vortex appeared appeared. very close to inlet. in section 1/3 of the model pond and no channel flow was observed in this section and clearly there was channel flow upward from the small vortex (section 1/3) toward the pond outlet, Figure 4-37.

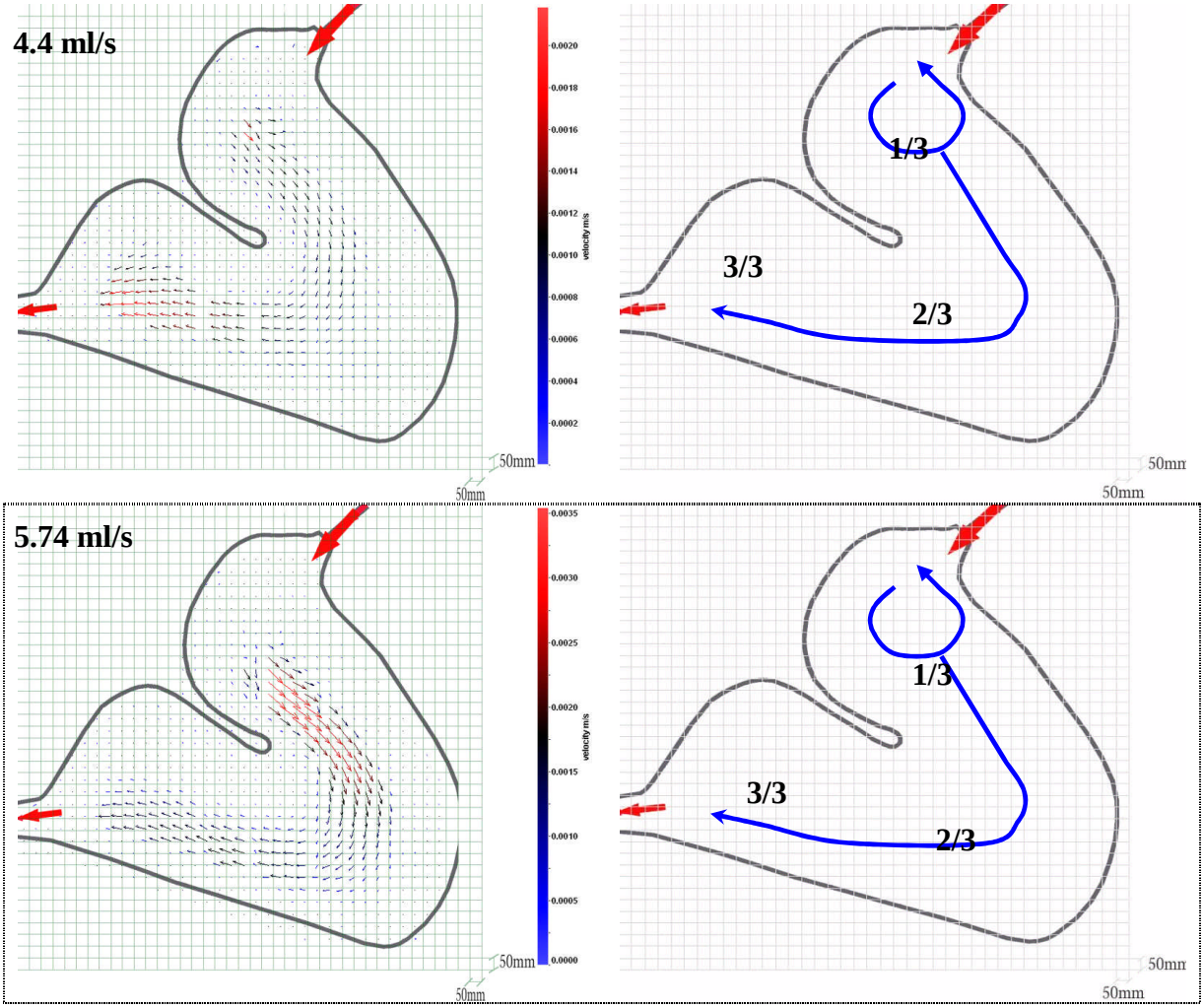

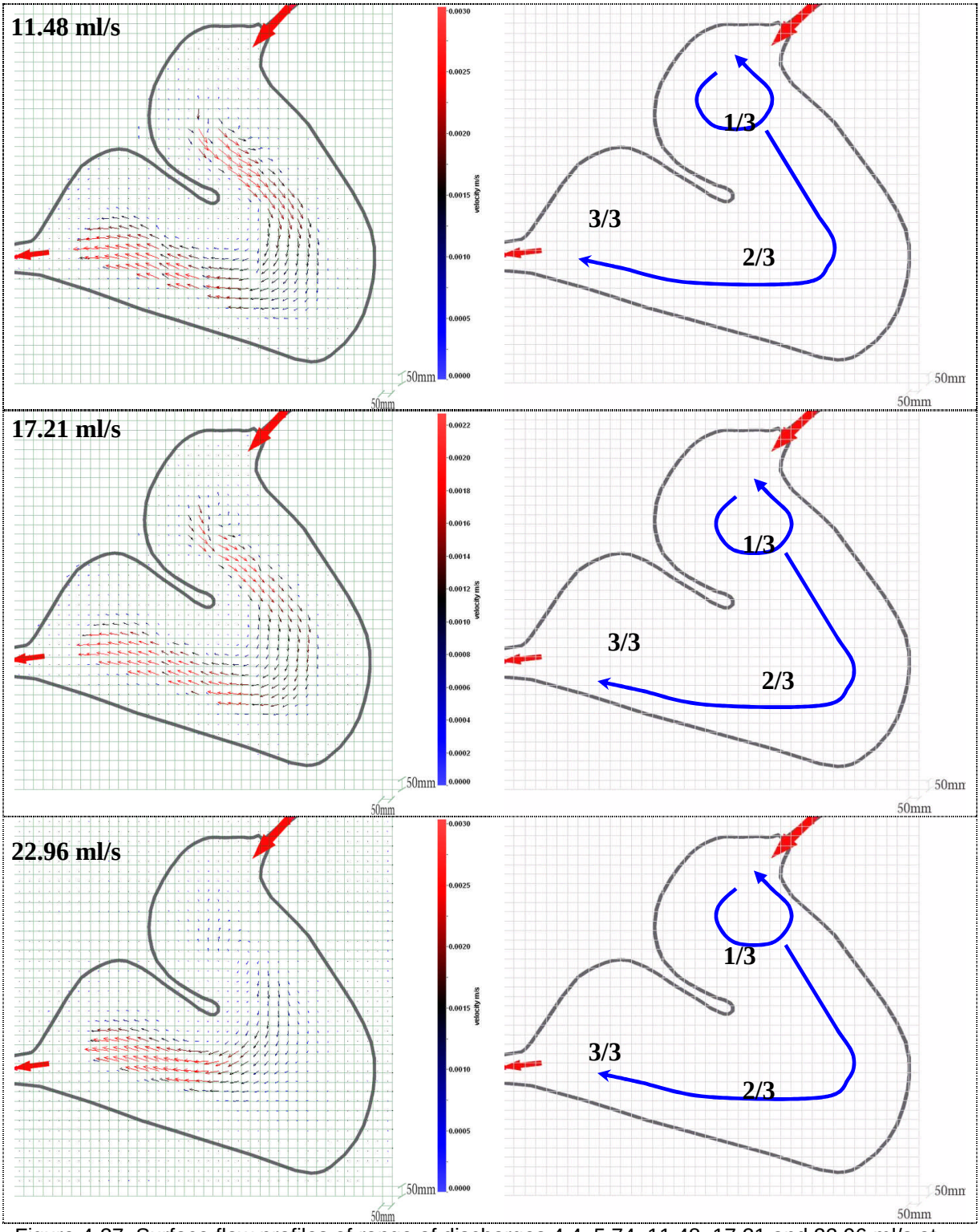

Figure 4-37. Surface flow profiles of range of discharges 4.4, 5.74, 11.48, 17.21 and 22.96 ml/s at 22E Vegetation.

4.2.4 Summary results from trace with 27E vegetation and different Q_{in}

A range of experiments was conducted with fixed vegetation condition, in this case, the condition was fixed at 27E vegetation, whilst the discharge varied from 4.4 to 45.9 ml/s, Table 4-13. Dye recovery for all 24 runs ranged from 60 to 102% with an average of 83%. There were some consistent differences between the relative HRTD plots of low to high discharges (4.4 to 45.9 ml/s) but some were not significantly different. Some parameters of hydraulic efficiency differed significantly between lower discharge to higher discharge but some parameters of hydraulic efficiency did not differ significantly, Figure 4-38. The mean relative residence time, relative HRTD centroid, e_m, varied and fluctuated from 0.80 to 1.09, between the lowest and highest discharge values (4.4 to 45.90 l/s). The mean relative time of the first dye arrival at the outlet, e_o, was exponential increase from 0.01 to 0.19 whilst discharge increase from 4.4 to 45.9 ml/s respectively.

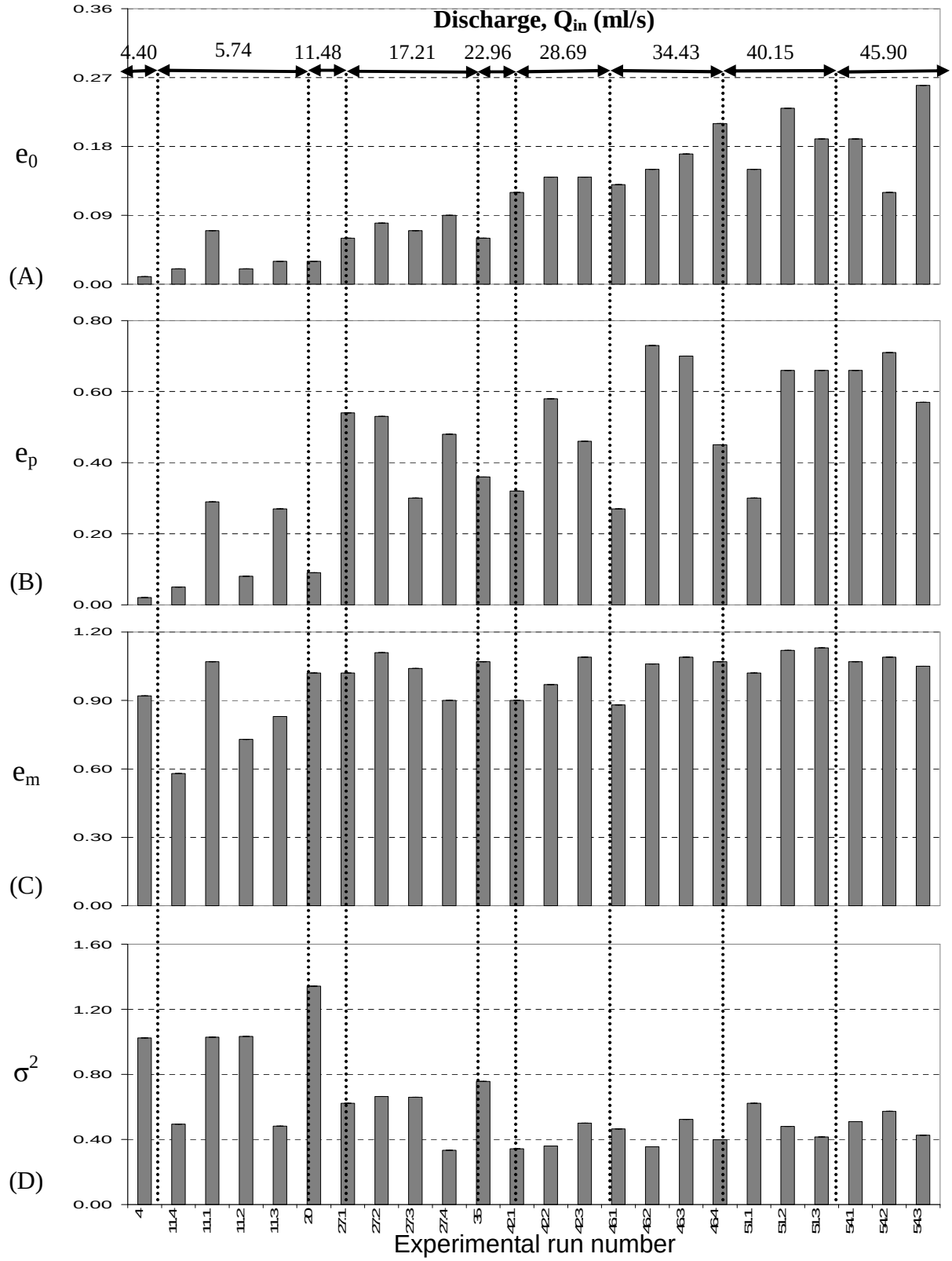

Figure 4-38. The residence time distribution (HRTD) characteristics under 27Evegetation configuration. Comparisons are made at the same 27E vegetation and among different discharge configurations for for (A) relative first dye arrival at the pond outlet (e_0), (B) relative peak concentration time ($e_p = t_p / t_n$), (C) relative residence time (Centroid of HRTD, $e_m = t_m / t_n$), (D) relative time variance (σ^2).

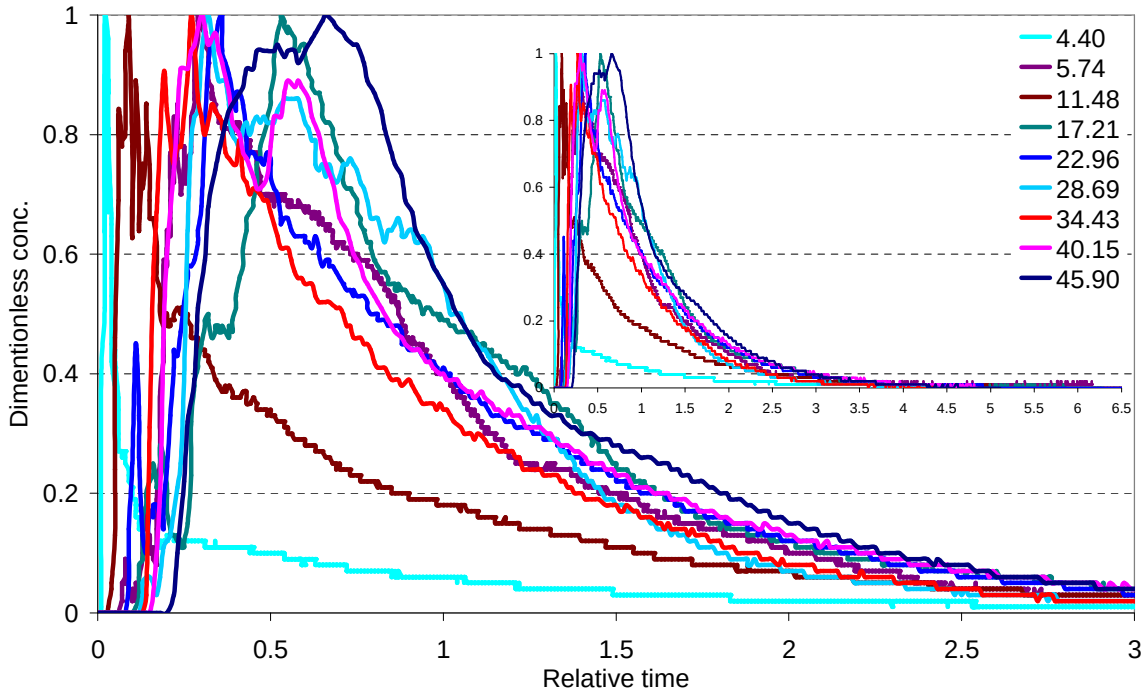

Figure 4-39. Comparison of four representative residence time distribution (HRTD) curves run at 27E with discharge range from 4.4 to 45.9 ml/s.

The relative HRTDs between low and higher discharge configurations appeared distinctively different from each other. Where the relative HRTD of the smallest discharge tended to be unimodal in shape, the relative HRTD for the higher discharge usually tended to have a bimodal, with the first peak typically arriving late and being more spread out than lower discharge HRTD, Figure 4-39. These differences were reflected in the relative HRTD statistics The relative time average of first dye arrival, e_o, was exponentially increased from 0.01 to 0.19 whilst discharge increase from lowest to highest (4.4 to 45.9 ml/s). The relative time to peak concentration of the relative HRTD curve, e_p, was significantly and rapidly increased from 0.02 to 0.65 while the discharge increased from 4.4 to 45.9 ml/s. On the other hand, the increase of discharge from very low to very high (4.4 to 45.9 ml/s) did not affect on the relative mean residence time, relative HRTD

centroid, $e_{m.}$ It looked very much the same with mean and average values of 1.02 with very small variation of standard deviation of 0.09 (δ).

Four repeated dye tracers were run for the 5.74, 17.21 28.69 and 34.43 ml/s discharge conditions, where there were no significant difference of all its repeated relative HRTD results, Figure 4-38, then only three repeated dye tracer runs were made for discharge ranged from 40.15 to 45.9 ml/s; only one dye tracer was run for each discharge of 4.4, 11.48 and 22.96 ml/s. Table 4-13, shows the details of mean HRTDs in all runs with 27E vegetation configuration.

Vegetation Condition	Discharge, Qin (ml/s)	Run No	$e_o = t_o/t_n$	$e_p = t_p/t_n$	$e_m = t_m/t_n$	σ^2 (based on relative time)
27E	4.4	4	0.01	0.03	0.92	0.98
	5.74	11.4	0.02	0.04	0.58	2.03
	5.74	11.1	0.07	0.23	1.07	0.97
	5.74	11.2	0.02	0.04	0.73	0.97
	5.74	11.3	0.03	0.13	0.83	2.08
	Mean of 5.74 (S.D)	11	0.04 (0.02)	0.11 (0.09)	0.80 (0.21)	1.51 (0.62)
	11.48	20	0.03	0.08	1.02	0.75
	17.21	27.1	0.06	0.14	1.02	1.61
	17.21	27.2	0.08	0.31	1.11	1.51
	17.21	27.3	0.07	0.24	1.04	1.52
	17.21	27.4	0.09	0.28	0.9	3.01
	Mean of 17.21 (S.D)	27	0.08 (0.01)	0.24 (0.07)	1.02 (0.09)	1.91 (0.73)
	22.96	35	0.06	0.25	1.07	1.32
	28.69	42.1	0.12	0.29	0.9	2.92
	28.69	42.2	0.14	0.32	0.97	2.78
	28.69	42.3	0.14	0.34	1.09	2.00
	Mean of 28.69 (S.D)	42	0.13 (0.01)	0.32 (0.03)	0.99 (0.10)	2.56 (0.49)
	34.43	46.1	0.13	0.2	0.88	2.15
	34.43	46.2	0.15	0.34	1.06	2.82
	34.43	46.3	0.17	0.34	1.09	1.91
	34.43	46.4	0.21	0.37	1.07	2.51
	Mean of 34.43 (S.D)	46	0.17 (0.03)	0.31 (0.08)	1.03 (0.10)	2.35 (0.40)
	40.15	51.1	0.15	0.24	1.02	1.61
	40.15	51.2	0.23	0.37	1.12	2.08
	40.15	51.3	0.19	0.41	1.13	2.41
	Mean of 40.15(S.D)	51	0.19 (0.04)	0.34 (0.09)	1.09 (0.06)	2.03 (0.41)
	45.9	54.1	0.19	0.34	1.07	1.96
	45.9	54.2	0.12	0.34	1.09	1.74
	45.9	54.3	0.26	0.28	1.05	2.34
	Mean of 45.9 (S.D)	54	0.19 (0.07)	0.32 (0.03)	1.07 (0.02)	2.02 (0.30)

Table 4-13. HRTD statistics of tracer runs at 27E vegetation at discharge range from 4.4 to 45.9 ml/s.

Surface flow profiles were derived from the PIV data with the fixed case of 27E vegetation configuration and varying discharge between low to high values (4.4 up to 22.96 ml/s. No PIV was conducted at the high discharge range from 28.96 to 45.90 ml/s), Table 4-13, and no consistent difference was found between the surface vortex flow profiles for the discharge range from 4.4 to 11.48 ml/s, where one small vortex (clock wise) appeared, very close to inlet, in section 1/3 of the model pond with no channel flow in this section then there was channel flow upward from the small vortex (section 1/3) toward the pond outlet. On the other hand at the discharge values of 17.21 to 22.96 ml/s, there was only one main vortex seem in section 1/3, as same as in low discharge, but this vortex appeared to change from clockwise to anti clockwise, Figure 4-40.

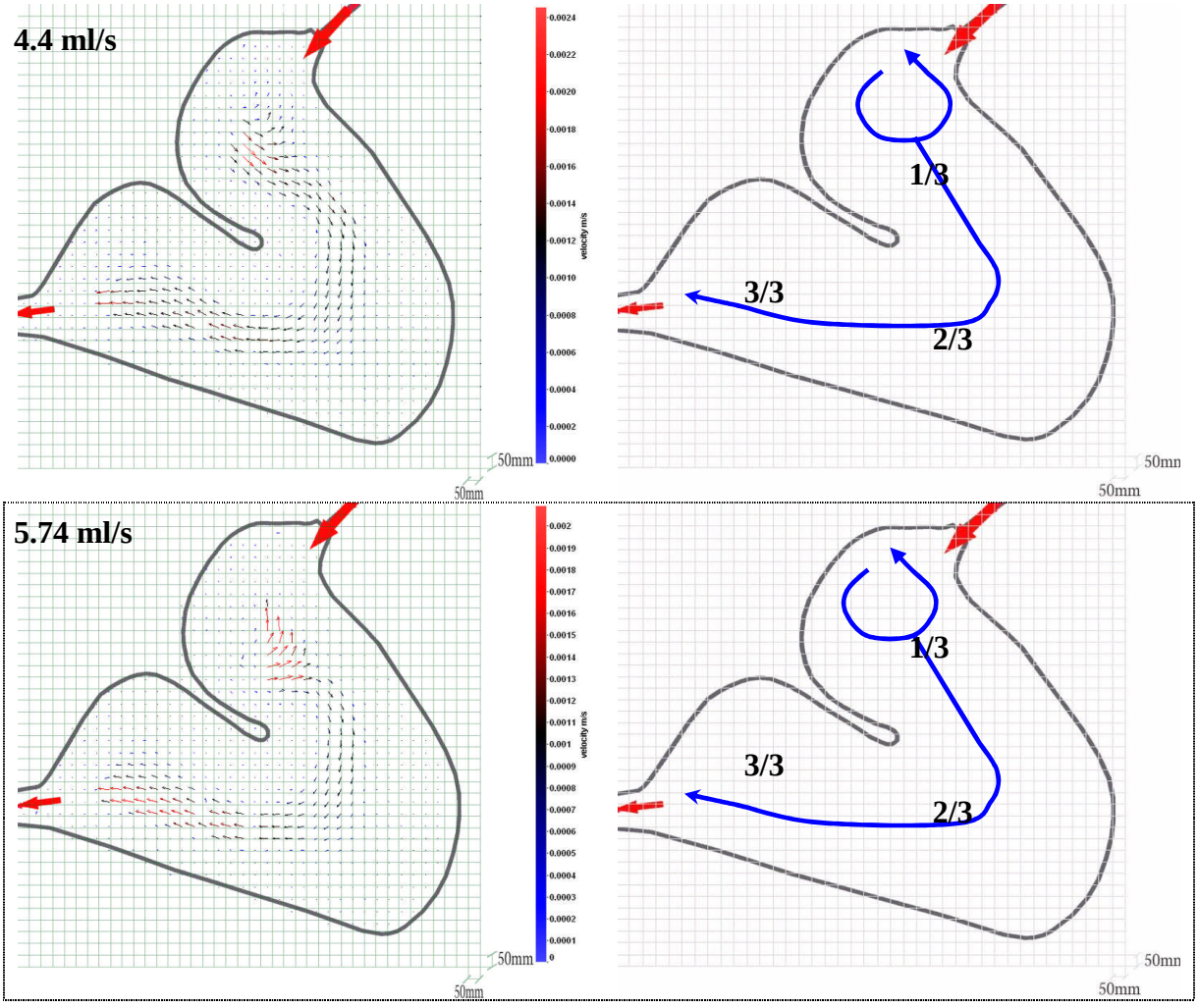

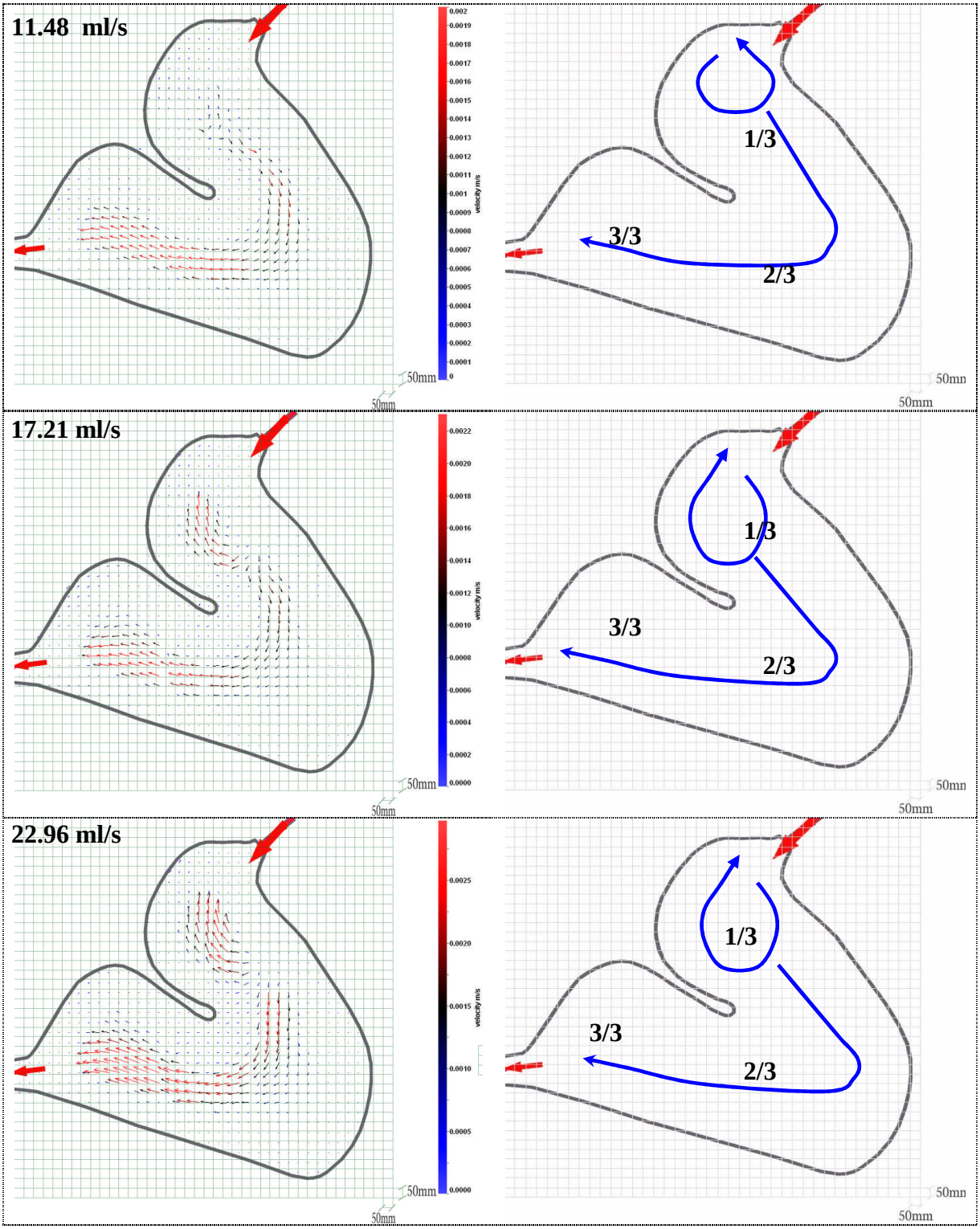

Figure 4-40. Surface flow profiles of range of discharges 4.4, 5.74, 11.48, 17.21 and 22.96 ml/s at 27E vegetation.

4.2.5 Summary results from trace with 27EL vegetation and different Q_{in}

A range of experiments was conducted with fixed vegetation condition, in this case, the condition was fixed at 27EL vegetation, whilst the discharge was kept varied from 4.4 to 22.96 ml/s Dye recovery for all 5 runs ranged from 60 to 85% with an average of 69%. There were some consistent differences between the relative HRTD plots of low to high discharges (4.4 to 22.96 ml/s). Some of the parameters for relative hydraulic efficiency differed significantly between lower discharge to higher discharge, Figure 4-41. The mean relative residence time, relative HRTD centroid, e_m, varied with exponential increasing from 0.5 to 0.81, between the lowest to highest discharge values (4.4 to 17.21 l/s, except with discharge 22.96 ml/s where there was affected by wind tunnel). The mean relative time of the first dye arrival at the outlet, e_o, was slightly exponential increase from 0.02 to 0.06 whilst discharge increase from 4.4 to 17.21 ml/s respectively.

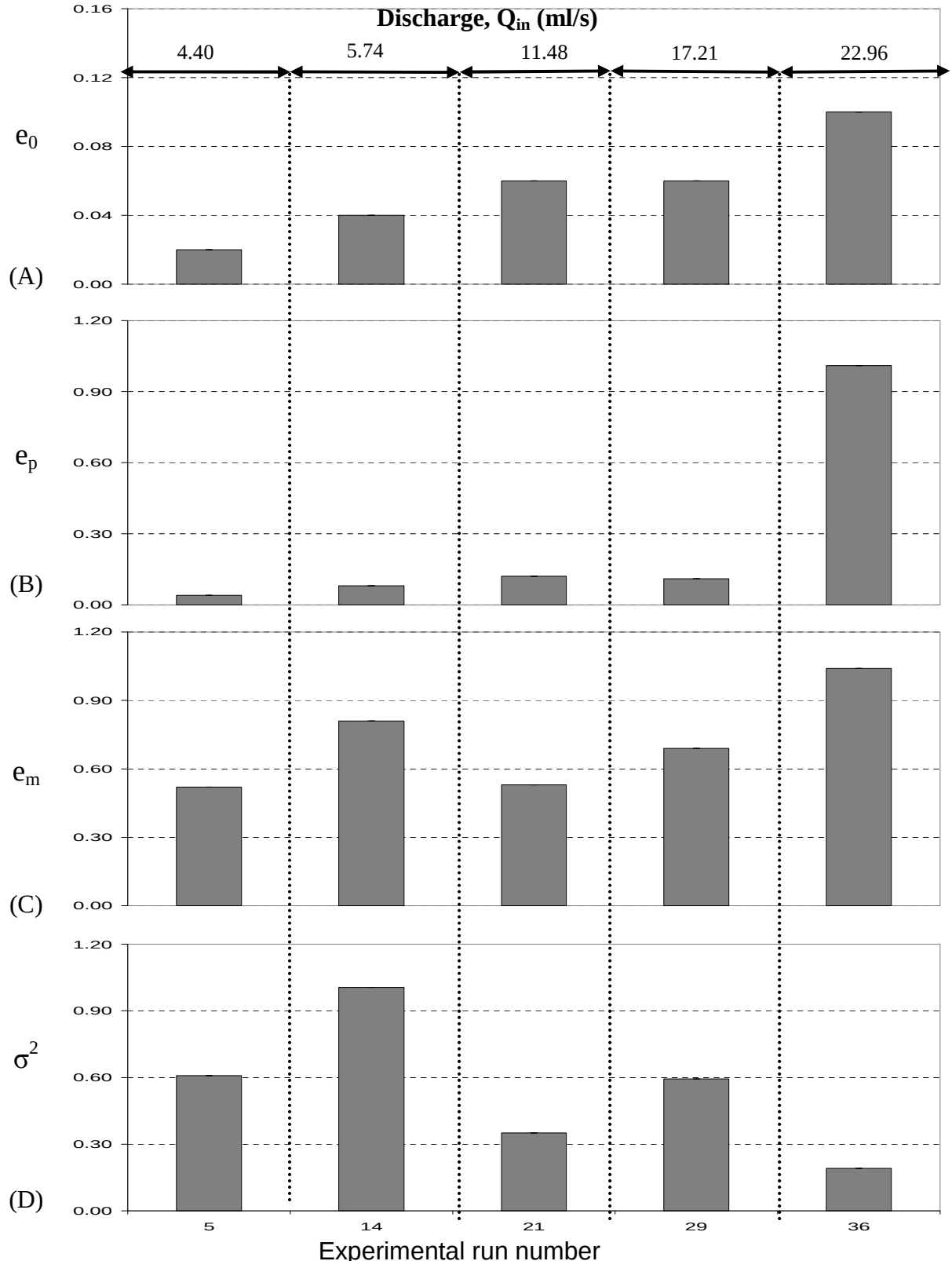

Figure 4-41. The residence time distribution (HRTD) characteristics under 27EL vegetation configuration. Comparisons are made at the same 27EL vegetation and among different discharge configurations for for (A) relative first dye arrival at the pond outlet (e_0), (B) relative peak concentration time ($e_p = t_p / t_n$), (C) relative residence time (Centroid of HRTD, $e_m = t_m / t_n$), (D) relative time variance (σ^2).

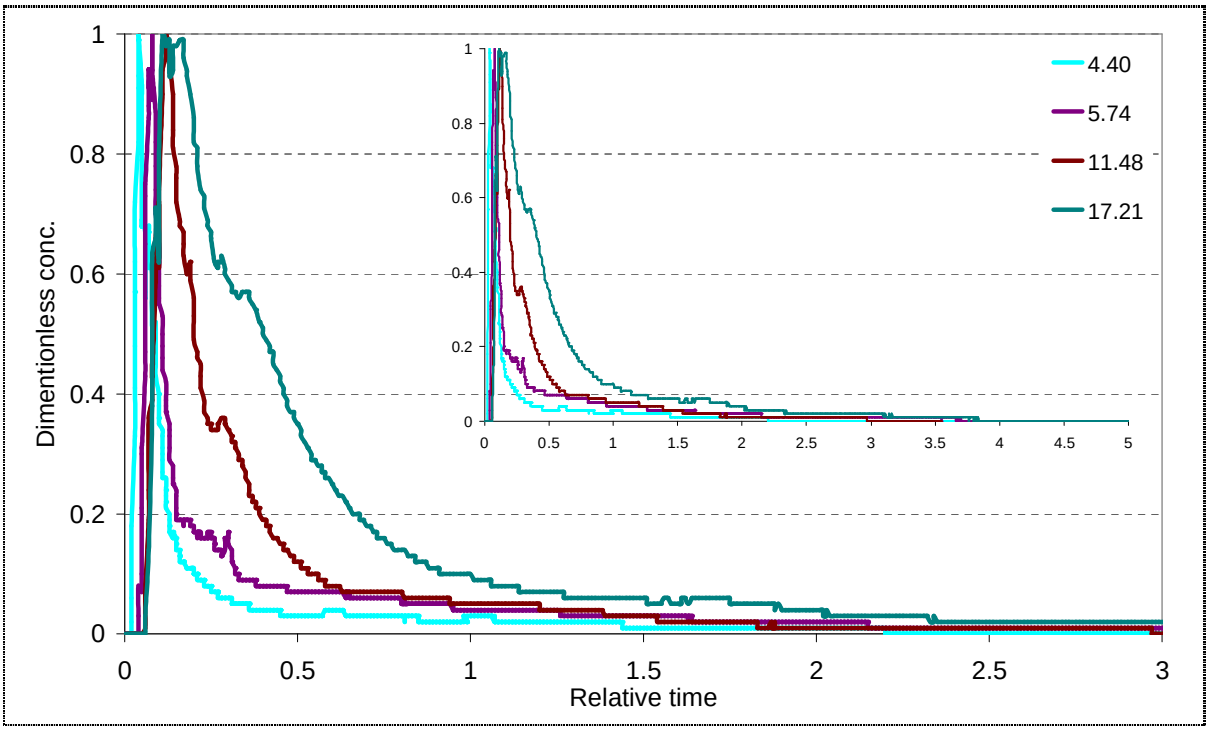

Figure 4-42. Comparison of four representative residence time distribution (HRTD) curves run at 27EL vegetation at discharge range from 4.4 to 45.9 ml/s.

The relative HRTDs between low and higher discharge configurations appeared distinctively different from each other. Where the relative HRTD of the smallest discharge tended to be unimodal in shap, the HRTD for the higher discharge was usually tended to have a bimodal, with the first peak typically arriving late and being more spread out than lower discharge HRTD, Figure 4-42. These differences were reflected in the HRTD statistics, Figure 4-41. The relative time average of first dye arrival, e_o, was only slightly exponential increased from 0.02 to 0.06 whilst discharge increase from lowest to highest (4.4 to 17.21 ml/s). The relative time to peak concentration of the relative HRTD curve, e_p, was significantly and rapidly increased from 0.04 to 0.12 whilst the discharge increased from 4.4 to 17.21 ml/s. On the other hand, the increase of discharge from very from 4.4 to 17.21 seems to exponentially increase in the relative mean residence time, relative

HRTD centroid, e_m. It was looked very much the same with mean and average values of 0.61 with standard deviation of 0.14 (δ).

Due to the experience from previous and repeated runs appeared with no significant differences of all its relative HRTD results; so only one dye tracer run was conducted for each discharge such as 4.4, 5.74, 11.48 and 17.21 ml/s discharge, Figure 4-41 and Table 4-14 , shown the details of relative mean HRTDs in all runs with 27EL vegetation configuration.

Vegetation Condition	Discharge, Qin (ml/s)	Run No.	$e_o = t_o/t_n$	$e_p = t_p/t_n$	$e_m = t_m/t_n$	σ^2 (based on relative time)
27EL	4.4	5	0.02	0.03	0.52	1.64
	5.74	14	0.04	0.07	0.81	0.99
	11.48	21	0.06	0.09	0.53	2.85
	17.21	29	0.06	0.1	0.69	1.68
	22.96	36	0.1	0.38	1.04	5.24

Table 4-14. HRTD statistics of tracer runs at 27EL with discharge range from 4.4 to 45.9 ml/s.

Surface flow profiles were derived from the PIV data with the fixed case of 27EL vegetation configuration and varying discharge between low to high values (4.4 up to 17.21 ml/s). No PIV was conducted at the high discharge range from 28.96 to 45.90 ml/s), and no consistent difference was found between the surface vortex flow profiles for the discharge range from 4.4 to 17.21 ml/s, where one small vortex (anti-clock wise) appeared, very close to inlet, at in section 1/3 of the model pond with no channel flow in this section but there was channel flow upward from the small vortex (section 1/3) toward the pond outlet, Figure 4-43.

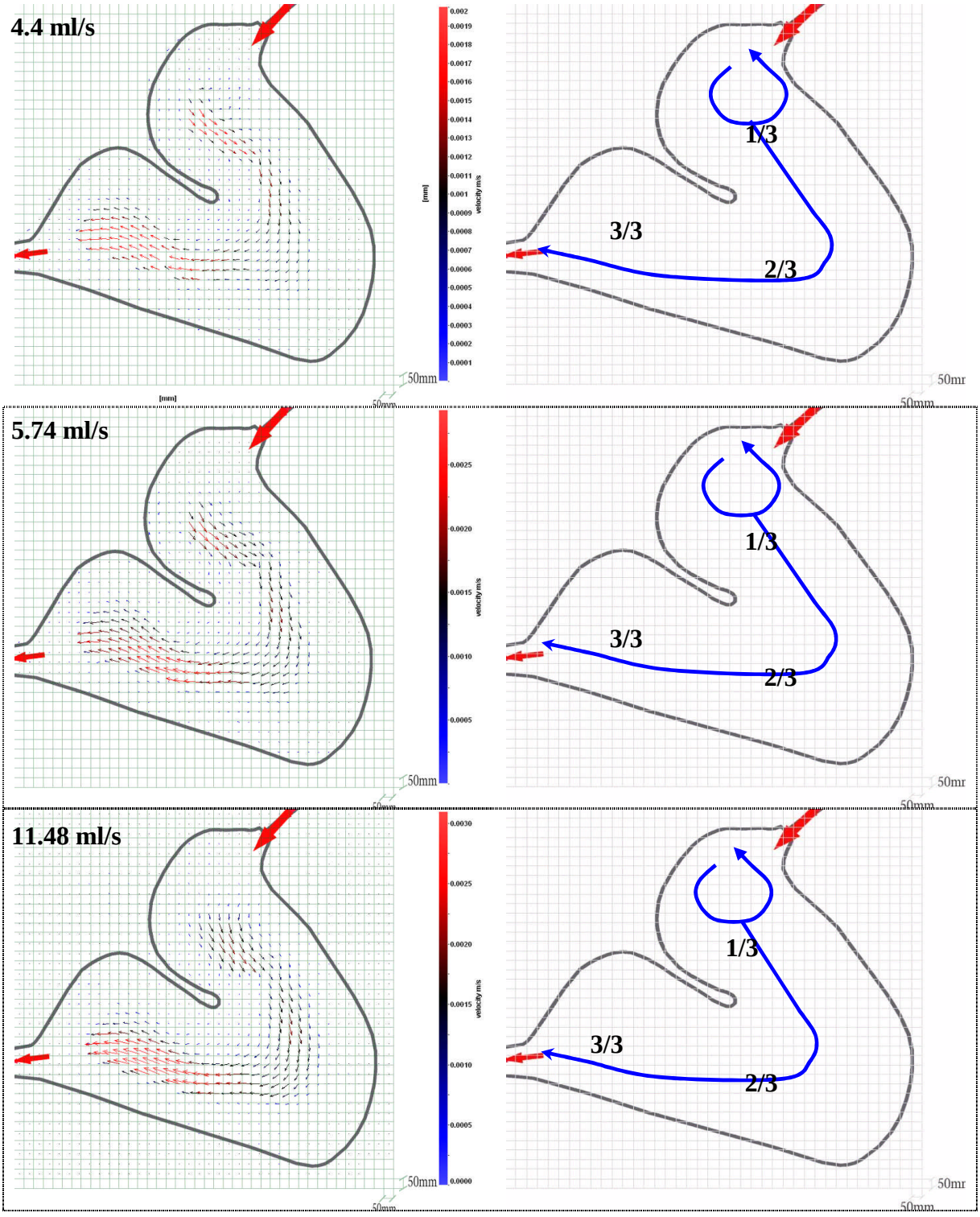
4.4 ml/s
1/3
3/3
2/3
50mm
5.74 ml/s
1/3
3/3
2/3
50mm
11.48 ml/s
1/3
3/3
2/3
50mm

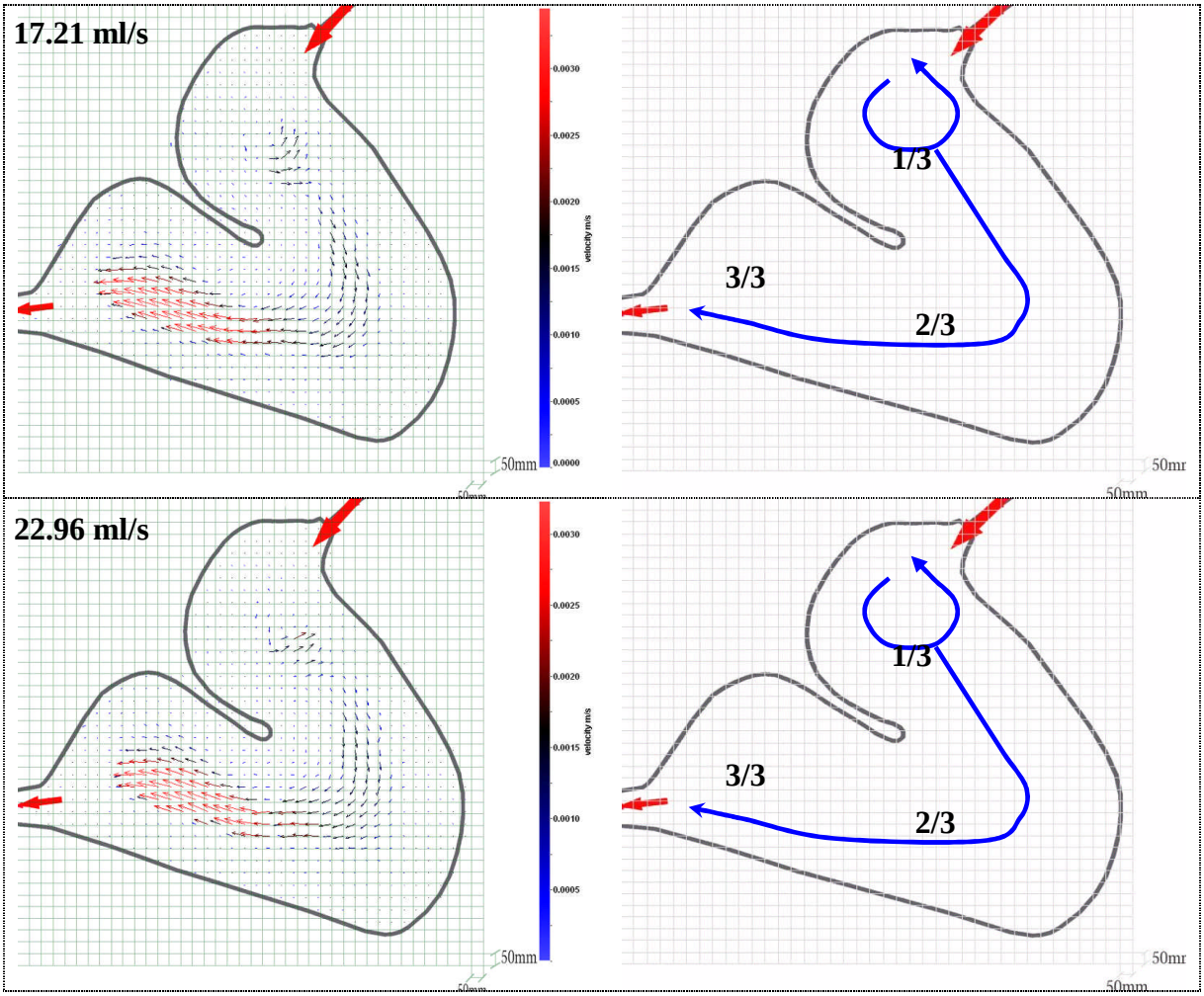

Figure 4-43. Surface flow profiles of, 4.4, 5.74, 11.48 , 17.21 and 22.96 ml/s at 27EL vegetation.

4.2.6 Summary results from trace with 27EM vegetation and different Q_{in}

A range of experiments was conducted with fixed vegetation condition, in this case, the condition was fixed at 27EM vegetation, whilst the discharge varied from 4.4 to 22.96 ml/s, Table 4-15. Dye recovery for all 5 runs ranged from 68 to 134 % with an average of 98%. There were some consistent differences between the relative HRTD plots of lower to high discharges (4.4 to 22.96 ml/s) but some were not significantly different. Some of the parameters for relative hydraulic efficiency differed significantly between lower discharge to higher discharge but some parameters for hydraulic efficiency did not differ significantly The mean relative residence time, relative HRTD centroid, e_m, slightly varied and fluctuated from 0.98

to 1.23, between the lowest and highest discharge values (4.4 to 22.96 l/s). The mean relative time of the first dye arrival at the outlet, e_o, was slightly exponentially increasing from 0.02 to 0.09 whilst discharge increased from 4.4 to 22.96 ml/s respectively.

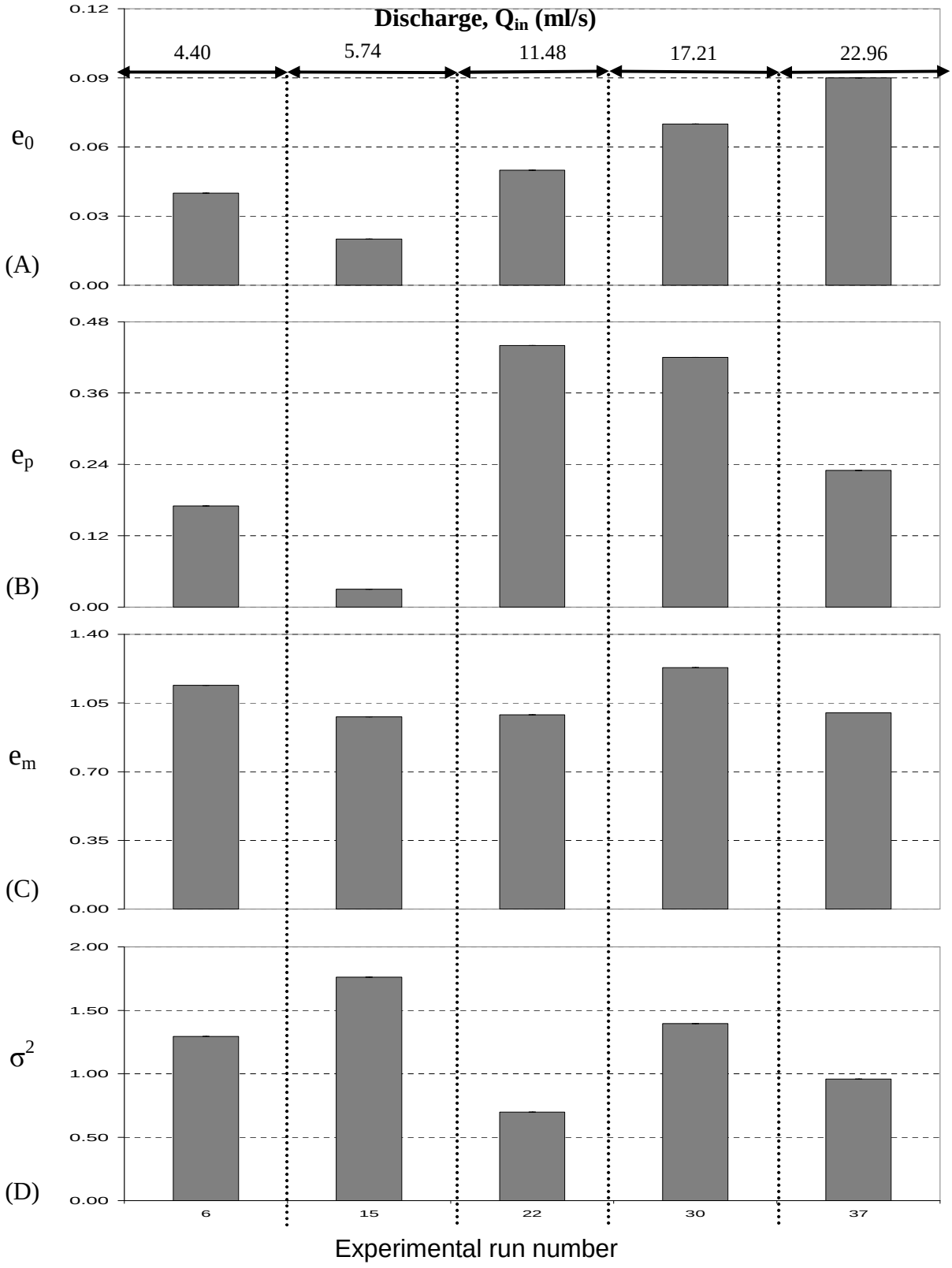

Figure 4-44. The residence time distribution (HRTD) characteristics under 27EM vegetation configuration. Comparisons are made at the same 27EM vegetation and among different discharge configurations for for (A) relative first dye arrival at the pond outlet (e_0), (B) relative peak concentration time ($e_p = t_p / t_n$), (C) relative residence time (Centroid of HRTD, $e_m = t_m / t_n$), (D) relative time variance (σ^2).

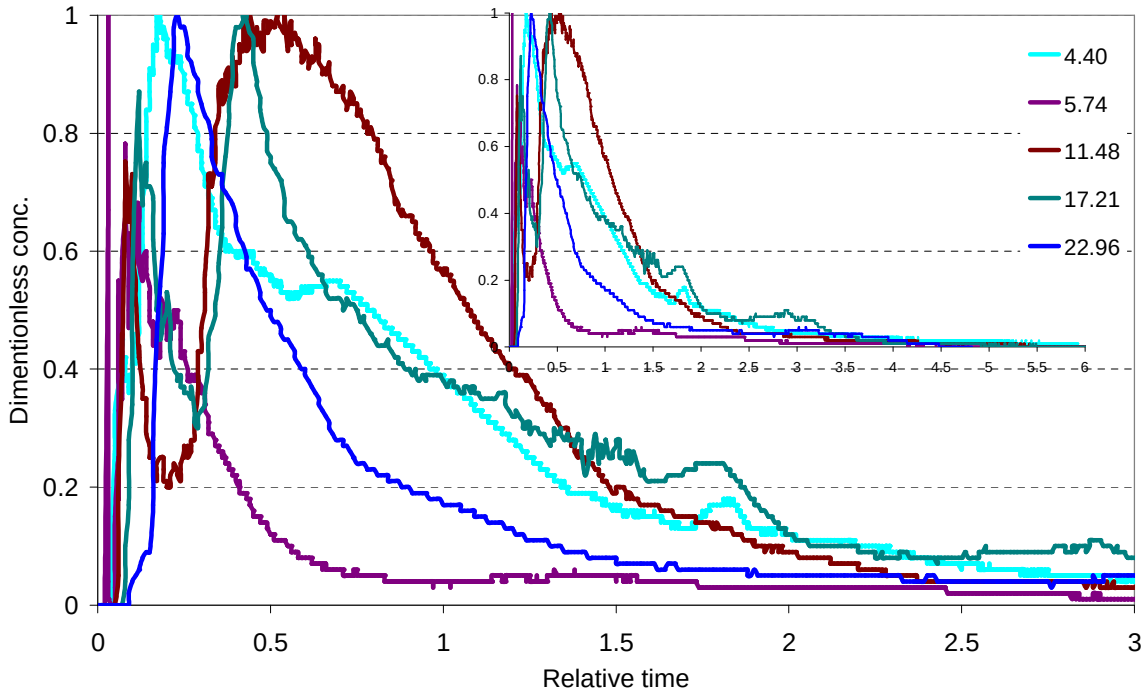

Figure 4-45. Comparison of four representative residence time distribution (HRTD) curves run at 27EM with discharge range from 4.4 to 45.9 ml/s.

The relative HRTDs between low and higher discharge configurations appeared distinctively different from each other. Where the relative HRTD from smallest to to highest discharge values tended to randomly spread out with the first peak typically arriving early or late randomly, Figure 4-45. These fluctuations and differences were reflected in the relative HRTD statistics, Figure 4-44. The relative average of first dye arrival, e_o, was very small exponentially increased from 0.02 to 0.09 whilst discharge increase from lowest to highest (4.4 to 22.96 ml/s). The relative time to peak concentration of the HRTD curve, e_p, significantly fluctuated where equal to 0.03, 0.17 and 0.23 at discharge 5.74, 4.4 and 22.96 ml/s respectively. The time to peak becomes similar for two discharges 11.48 and 17.21 ml/s where e_p equal to 0.44 and 0.42 respectively. On the other hand, the increased of discharge from very from 4.4 to 22.96 ml/s seems did not affect and just fluctuate from one to another; on the relative mean residence time, HRTD

centroid, e_m. It was looked very much the same with mean and average values of 1.00 (which equal to the nominal residence time, t_n) with standard deviation of 0.11 (δ).

Due to the experience from previous and repeated runs where there were no significant differences of all its relative HRTD results, so in this specific vegetation configuration and different discharges, only one dye tracer was run for each discharge range from 4.4 to 22.96 ml/s. Figure 4-44 and Table 4-15, shown the details of mean HRTDs in all runs with 27EM vegetation configuration.

Vegetation condition.	Discharge, Qin (ml/s)	Run No.	$e_o = t_o/t_n$	$e_p = t_p/t_n$	$e_m = t_m/t_n$	σ^2 (based on relative time)
27EM	4.4	6	0.04	0.14	1.14	0.77
	5.74	15	0.02	0.08	0.98	0.57
	11.48	22	0.05	0.17	0.99	1.43
	17.21	30	0.07	0.16	1.23	0.72
	22.96	37	0.09	0.19	1.00	1.04

Table 4-15. HRTD statistics of tracer runs at 27EM vegetation at discharge range from 4.4 to 22.96 ml/s.

The same as previous runs surface flow profiles were derived from the PIV data with the fixed case of 27EM vegetation configuration and and varying discharge between low to high values (4.4 up to 22.96 ml/s), Table 4-5. No consistent difference was found between the surface vortex flow profiles for the discharge range from (4.4 to 22.96 ml/s), where only one small vortex (anti-clock wise) appeared, very close to inlet, at in section 1/3 of the model pond with no channel flow in this section but there were channel flow upward from the small vortex (in section 1/3) through to pond outlet, Figure 4-46.

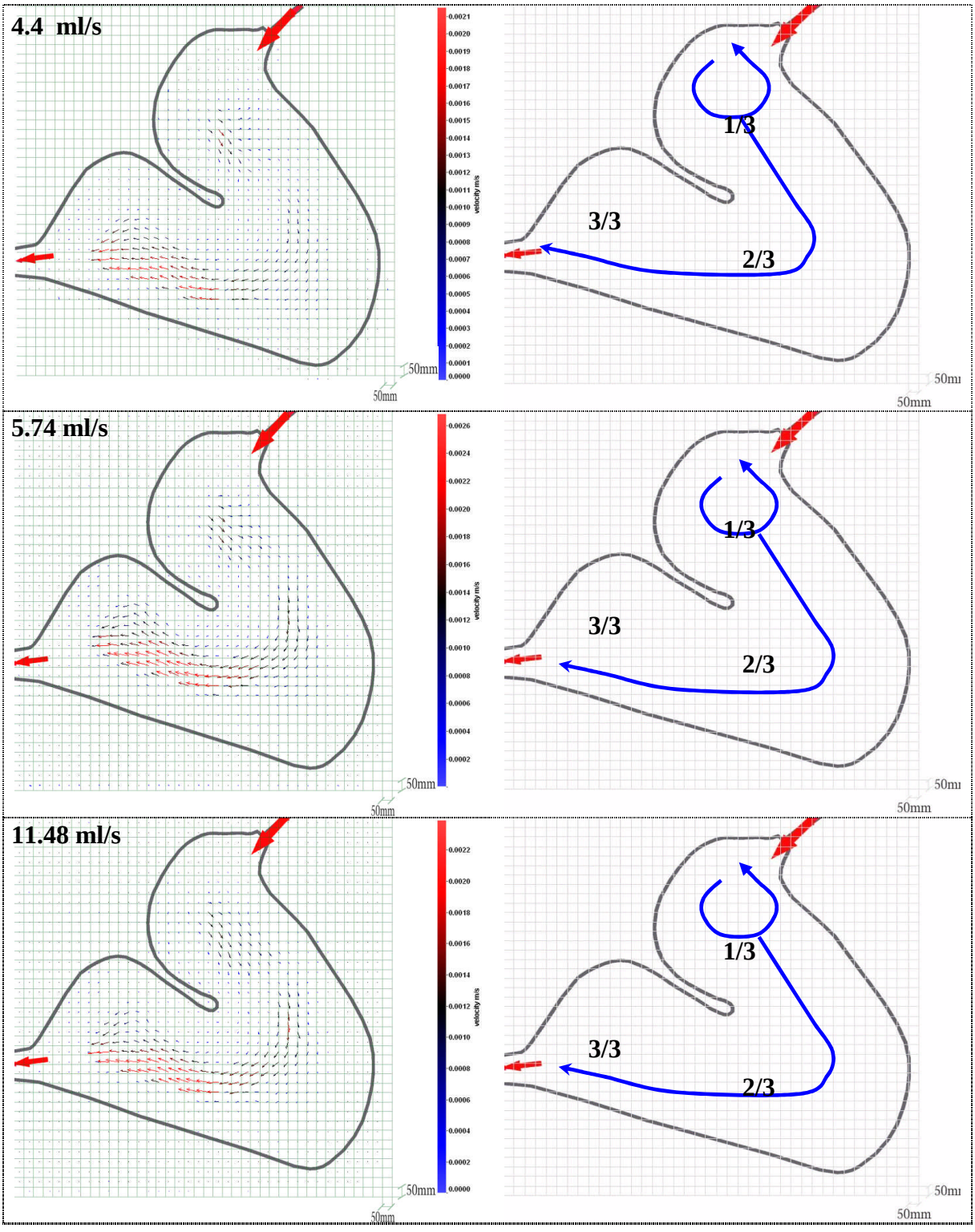
4.4 ml/s
1/3
3/3
2/3
50mm
50mm
5.74 ml/s
1/3
3/3
2/3
50mm
50mm
11.48 ml/s
1/3
3/3
2/3
50mm
50mm

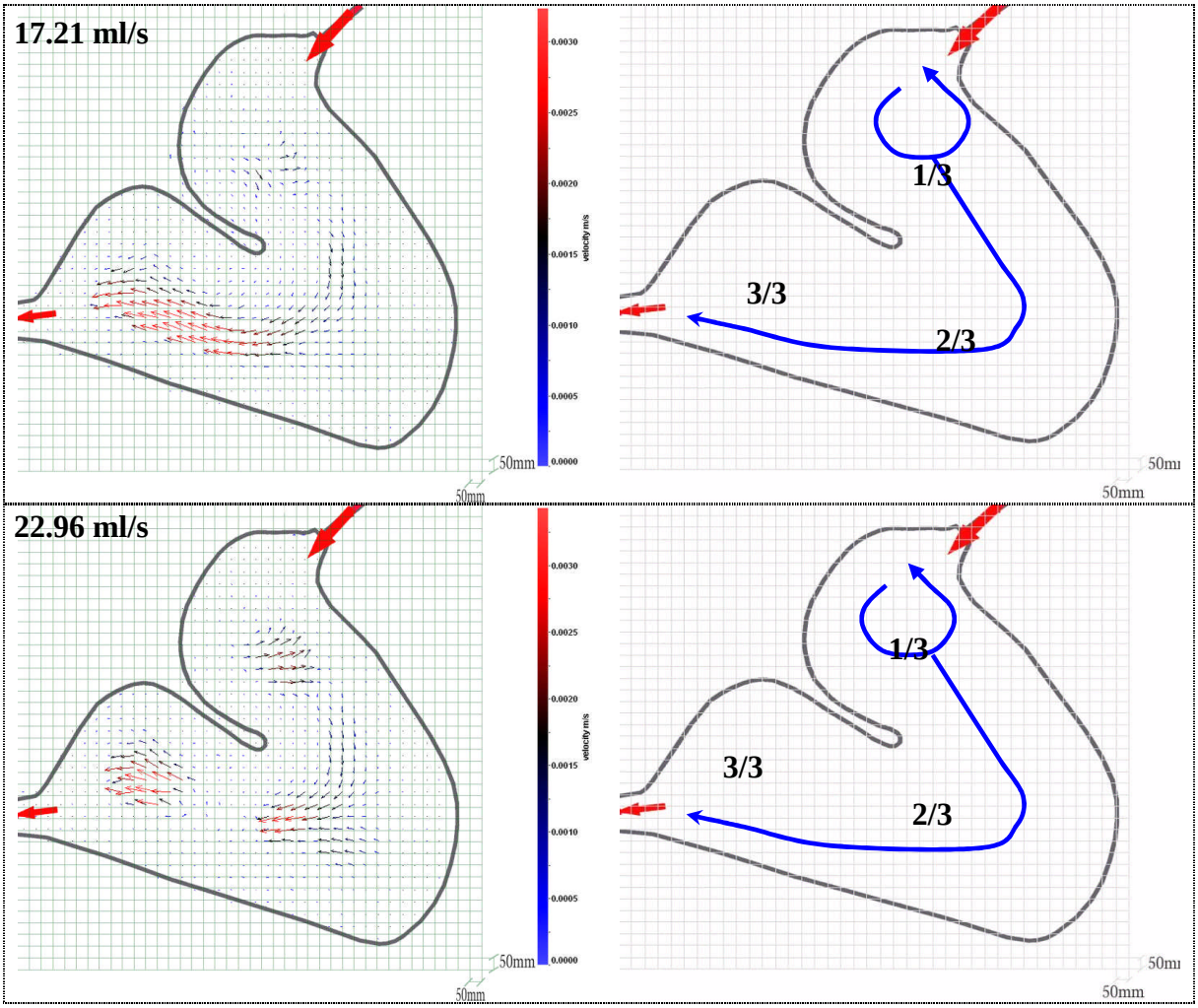

Figure 4-46.Surface flow profiles of 4.4, 5.74, 11.48, 17.21 and 22.96 ml/s at 27EM vegetation.

4.2.7 Summary results from trace with 27EH vegetation and different Q_{in}

A range of experiments was conducted with fixed vegetation condition, in this case, the condition was fixed at 27EH vegetation, whilst the discharge varied from 4.4 to 22.96 ml/s, Figure 4-47. Mass dye recovery for all 8 runs ranged from 78 to 97 % with an average of 87%. There were some consistent differences between the relative HRTD plots of lower discharge to high discharge (4.4 to 22.96 ml/s) but some was not significantly different. Some of the parameters for hydraulic efficiency differed significantly between lower discharge to higher discharge but some parameters for hydraulic efficiency did not differ significantly, Figure 4-47. The mean relative residence time, relative HRTD centroid, e_m, slightly varied and

fluctuated from 0.82 to 1.09, between the lowest and highest discharge values (4.4 to 22.96 l/s), Figure 4-47 B. The mean relative time of the first dye arrival at the outlet, e_o, was slightly exponential increase from 0.03 to 0.08 whilst discharge increased from 4.4 to 22.96 ml/s, Figure 4-47 A.

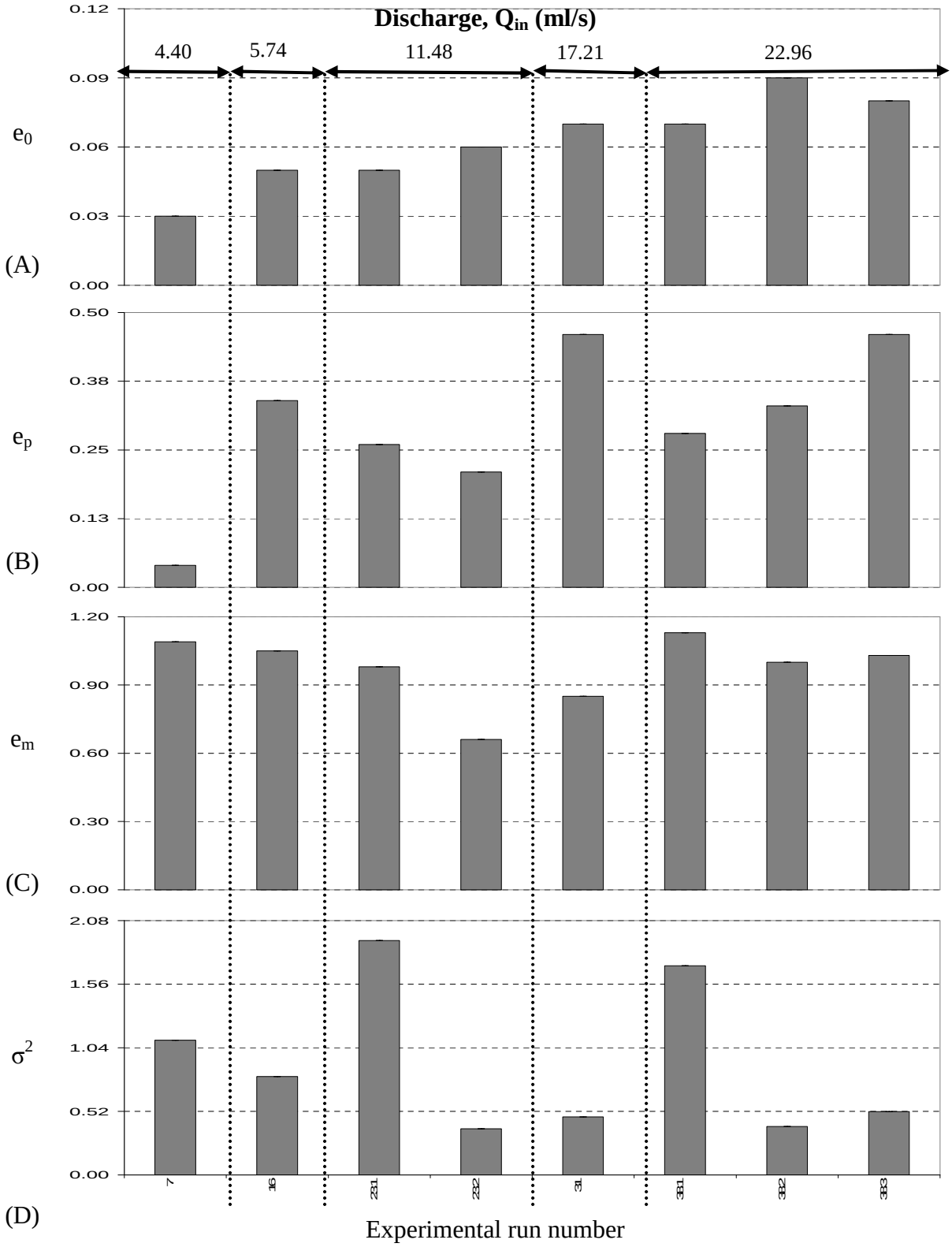

Figure 4-47. The residence time distribution (HRTD) characteristics under 27EH vegetation configuration. Comparisons are made at the same 27EH vegetation and among different discharge configurations for for (A) relative first dye arrival at the pond outlet (e_0), (B) relative peak concentration time ($e_p = t_p / t_n$), (C) relative residence time (Centroid of HRTD, $e_m = t_m / t_n$), (D) relative time variance (σ^2).

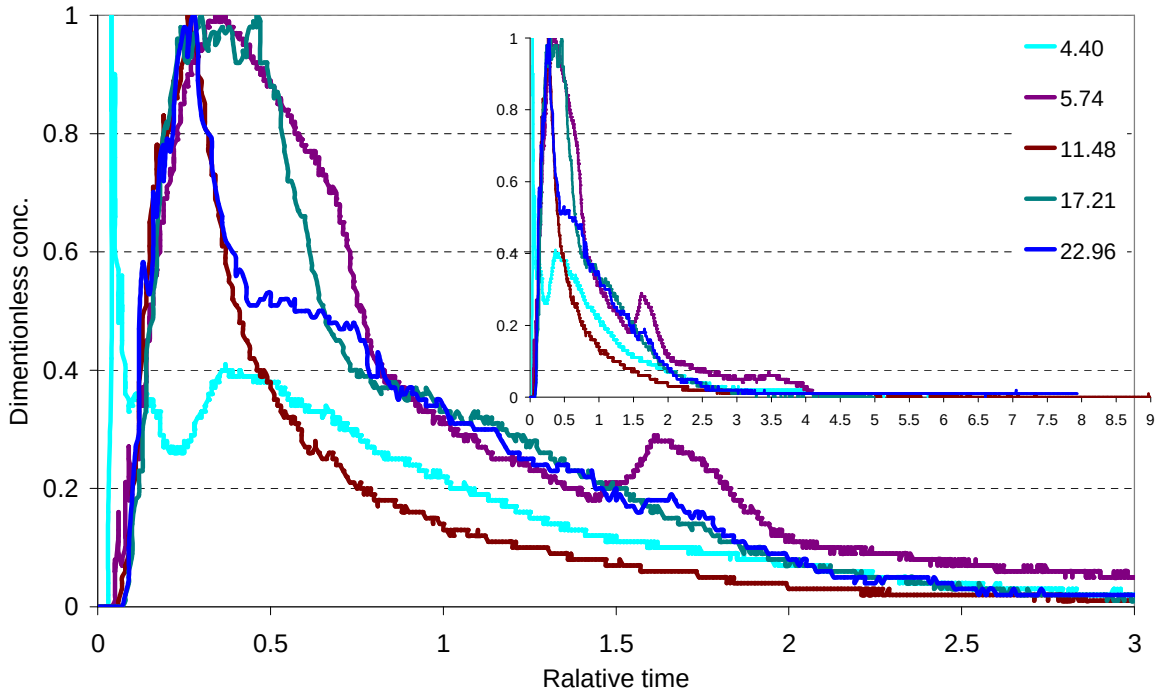

Figure 4-48. Comparison of four representative residence time distribution (HRTD) curves run at 27EH with discharge range from 4.4 to 45.9 ml/s.

The relative HRTDs compared between low and higher discharge configurations appeared distinctively different from each other. Where the HRTD of the smallest discharges (4.4 and 5.74 ml/s) tended to be unimodal in shape, the relative HRTD for the higher discharges (11.48, 17.21 and 26.96 ml/s) usually tended to have a bimodal, with the first peak typically arriving late and being more spread out than lower discharge HRTD, Figure 4-48. The relative time average of first dye arrival, e_o, was exponentially increased from 0.03 to 0.08 whilst discharge increase from lowest to highest (4.4 to 22.96 ml/s), Figure 4-47 A. The relative time to peak concentration of the HRTD curve, e_p, significantly increase with fluctuation where range from 0.04 to 0.46 whilst the discharge increased from 4.4 and 22.96 ml/s, Figure 4-47 C. On the other hand, the increase of discharge from very from 4.4 to 22.96 ml/s did not seem to affect and just fluctuate from one to another, on the relative mean residence time, HRTD centroid, e_m. It was looked very much the

same with mean and average values of 1.05 (very similar to nominal residence time, t_n), with standard deviation of 0.13 (δ), Figure 4-47 B.

Due to the experience from previous and repeated runs shown no significant differences of all its HRTD results; so in this specific vegetation configuration with different range discharge, there were only three repeat dye tracers runs was conducted for discharge at 22.96 ml/s, two repeat dye tracer runs for discharge at 11.48 ml/s and only one dye tracer run for each discharge at 4.4, 5.74 and 17.21 ml/s. Figure 4-47 and Table 4-16, shown the details of mean HRTDs in all runs with 27EH vegetation configuration.

Vegetation Condition	Discharge, Qin (ml/s)	Run No.	$e_o = t_o/t_n$	$e_p = t_p/t_n$	$e_m = t_m/t_n$	σ^2 (based on relative time)
27EH	4.4	7	0.03	0.07	1.09	0.91
	5.74	16	0.05	0.19	1.05	1.24
	11.48	23.1	0.05	0.15	0.98	0.52
	11.48	23.2	0.06	0.11	0.66	2.64
	Mean of 11.48 (S.D)	23	0.06 (0.01)	0.13 (0.03)	0.82 (0.23)	1.58 (1.50)
	17.21	31	0.07	0.19	0.85	2.11
	22.96	38.1	0.07	0.17	1.13	0.58
	22.96	38.2	0.09	0.26	1	2.52
	22.96	38.3	0.08	0.19	1.03	1.93
	Mean of 22.96 (S.D)	38	0.08 (0.01)	0.21 (0.05)	1.05 (0.07)	1.68 (0.99)

Table 4-16. HRTD statistics of tracer runs at 27EH vegetation at discharge range from 4.4 to 22.96 ml/s.

Surface flow profiles were derived from the PIV data with the fixed case of 27EH vegetation configuration and varying discharge between low to high values (4.4 up to 22.96 ml/s). No PIV was conducted at the high discharge range above 22.96 ml/s, Table 4-16, and no consistent difference was found between the surface flow profiles (primarily the presence and patterns of vortices); only one small vortex ,

(again anti-clock wise in sense) was observed very close to inlet at in section 1/3 of the model pond (no channel flow in this section), but there was channel flow upward from the small vortex (section 1/3) to warded pond outlet, Figure 4-49.

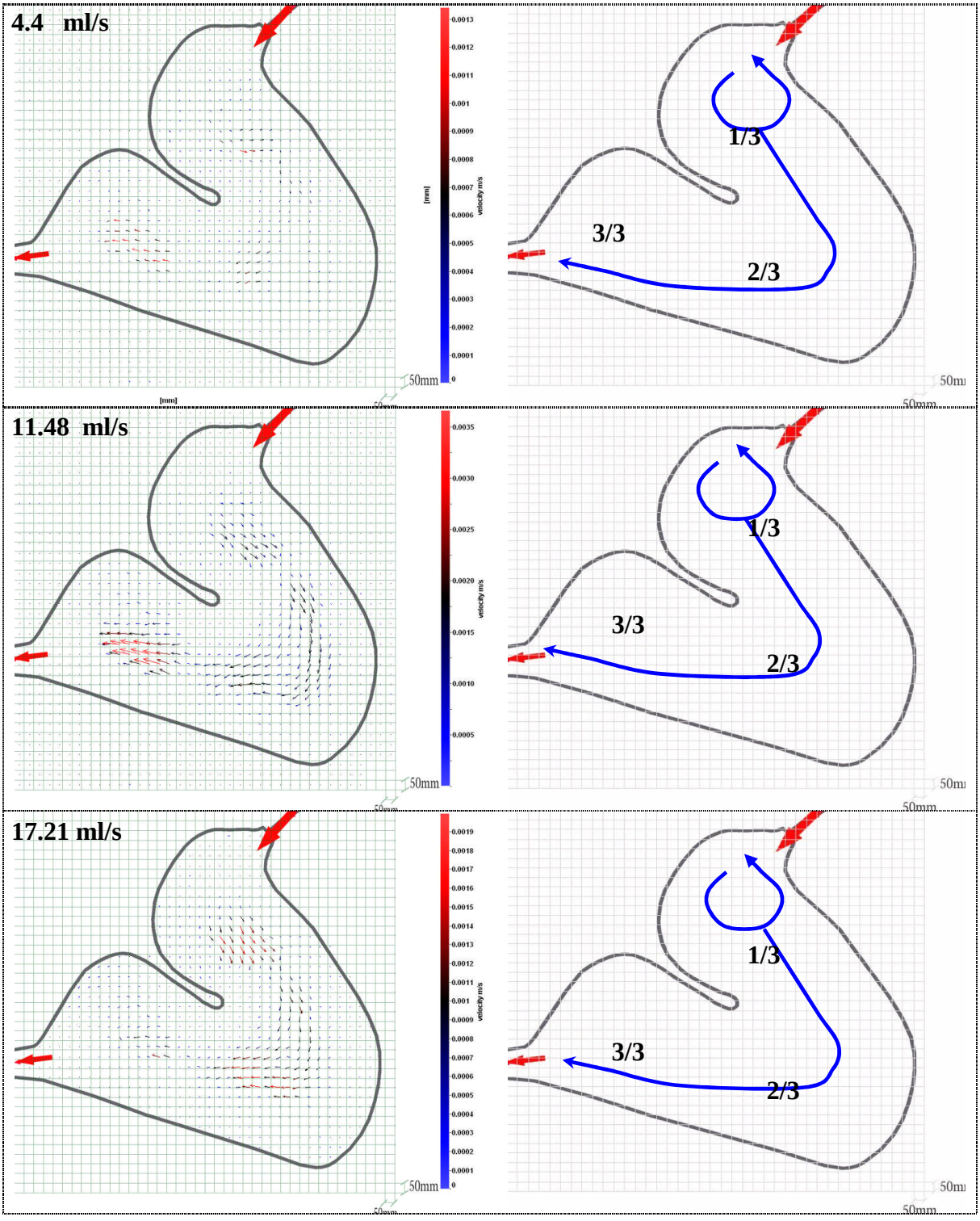

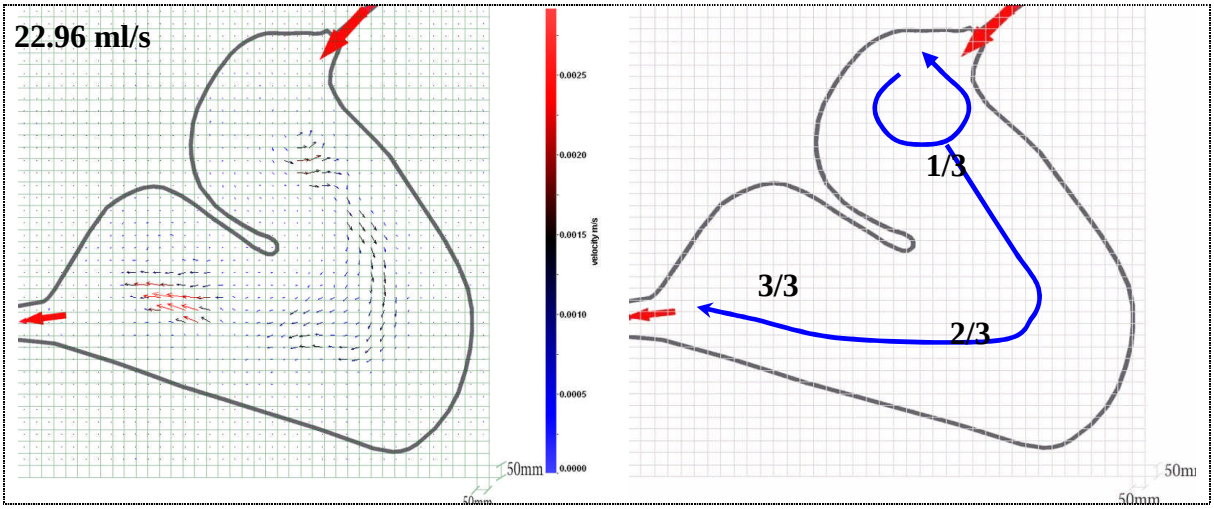

Figure 4-49. Surface flow profiles of 4.4, 11.48, 17.21 and 22.96 ml/s at 27EH vegetation.

4.2.8 Summary results from traces with 27ED vegetation and different Q_{in}

A range of experiments was conducted in which the vegetation was fixed on one specific condition (in this case, 27ED) and the discharge was varied from 5.74 to 45.90 ml/s, Figure 4-50. Dye recovery for all 12 runs ranged from 98 to121 % with an average of 108%. There were some consistent differences between the HRTD plots of low to high discharges (5.74 to 45.90 ml/s) but some were not significantly different. Some of the parameters for hydraulic efficiency differed significantly between lower discharges to higher discharge but some parameters for hydraulic efficiency did not differ significantly. The mean relative residence time, relative HRTD centroid, e_m, varied slightly within the range from 0.82 to 1.09, at random discharge from low to highest discharge (5.74 to 45.90 l/s), Figure 4-50 B. The mean relative time of the first dye arrival at the outlet, e_o showed a rapid increase from 0.02 to 0.37 for increases in discharge from 5.74 to 45.90 ml/s respectively, Figure 4-50 C.

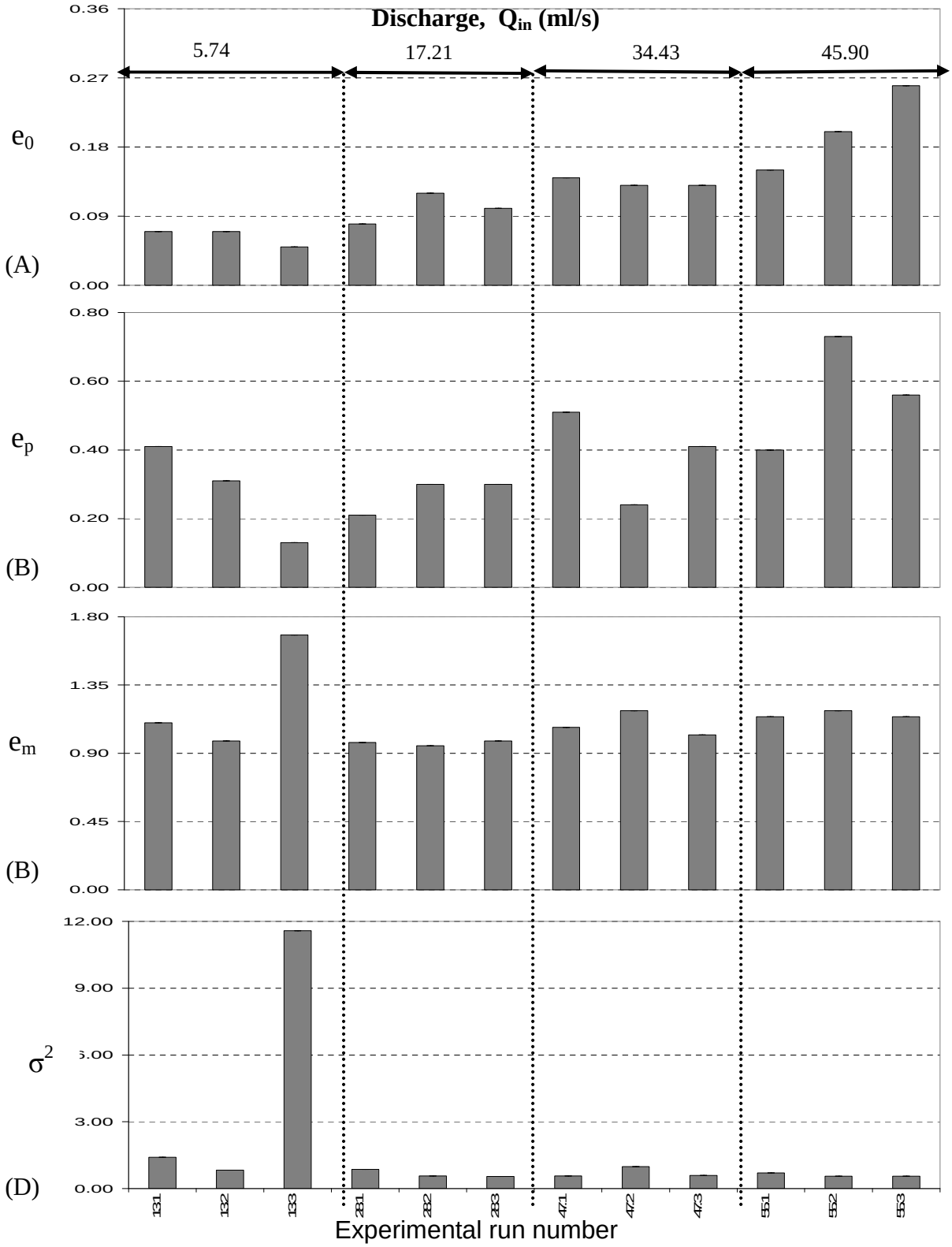

Figure 4-50. The residence time distribution (HRTD) characteristics under 27ED vegetation configuration. Comparisons are made at the same 27ED vegetation and among different discharge configurations for for (A) relative first dye arrival at the pond outlet (e_0), (B) relative peak concentration time ($e_p = t_p / t_n$), (C) relative residence time (Centroid of HRTD, $e_m = t_m / t_n$), (D) relative time variance (σ^2).

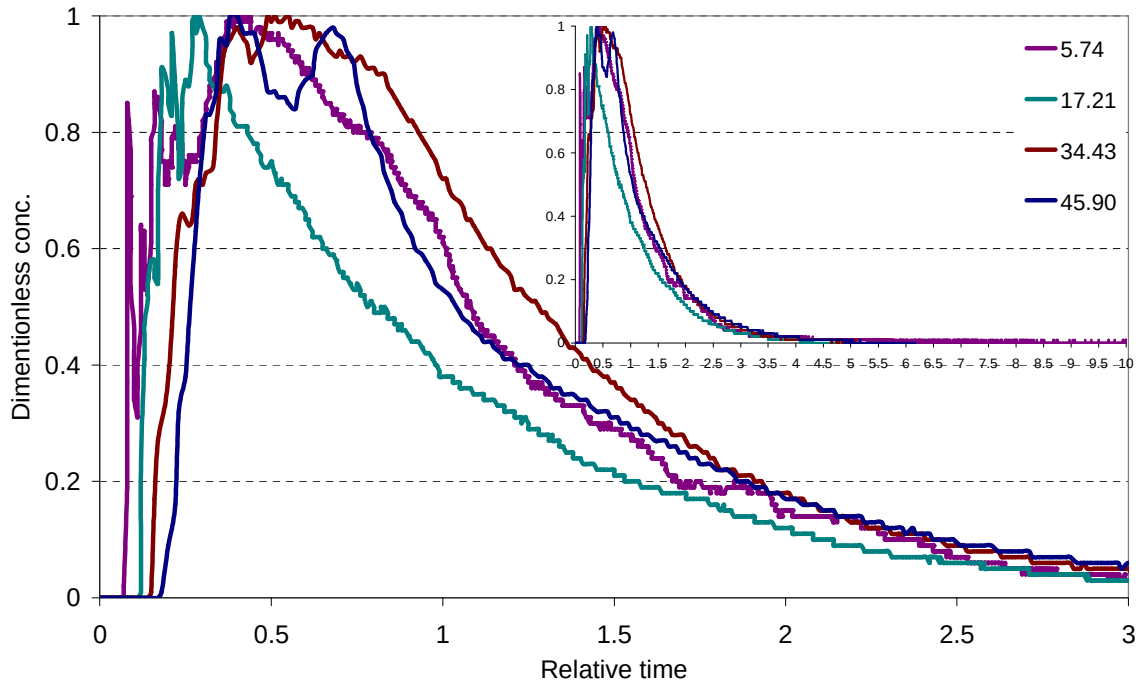

Figure 4-51. Comparison of four representative residence time distribution (HRTD) curves run at 27ED with discharge range from 4.4 to 45.9 ml/s.

The HRTDs, when compared between low and higher discharge configurations, did not show significant differences, with the relative HRTDs from less to higher discharge tending to randomly spread out with the first peak typically arriving early or late randomly, Figure 4-51. These consistent fluctuations were reflected in the relative HRTD statistics, Figure 4-50. The average of first dye arrival, e_o, varied and increased sharply from 0.06 to 0.20 in response to increases in the discharge from lowest to highest (5.74 to 45.9 ml/s) values. The time to peak concentration of the HRTD curve, e_p, was also significantly increased from 0.27 to 0.56 at low to high discharge (5.74 to 45.9 ml/s) respectively, Figure 4-50 C. On the other hand, the increase of discharge from 5.74 to 45.9 ml/s did not seem to produce systematic changes to the relative mean residence time, relative HRTD centroid, e_m. It looked very much the same with a mean value of 1.12 (12% higher than the nominal residence time t_n), with standard deviation of 0.12 (δ), Figure 4-50 B.

Due to the experience gained from previous runs where there were no significant differences in all relative HRTD results from the repeat runs, only three repeat dye tracers were run for all of the discharge range from 5.74 to 45.9 ml/s. Figure 4-50 and Table 4-17, show the details of the relative mean HRTDs in all runs with 27ED vegetation configuration. No PIV measurements were taken for the 27ED configuration but, based on dye observation during the dye tracer; the flow profile appeared similar to the 27E vegetation configuration where 27ED is the double density of emergent plant at 27E.

Vegetation Condition	Discharge, Qin (ml/s)	Run No.	$e_o = t_o/t_n$	$e_p = t_p/t_n$	$e_m = t_m/t_n$	σ^2 (based on relative time)
27ED	5.74	13.1	0.07	0.17	1.1	0.71
	5.74	13.2	0.07	0.18	0.98	1.22
	5.74	13.3	0.05	0.12	1.68	0.09
	5.74 (S.D)	13	0.06 (0.01)	0.28 (0.14)	1.25 (0.37)	0.67 (0.57)
	17.21	28.1	0.08	0.17	0.97	1.16
	17.21	28.2	0.12	0.19	0.95	1.76
	17.21	28.3	0.1	0.23	0.98	1.85
	17.21 (S.D)	28	0.10 (0.02)	0.27 (0.05)	0.97 (0.02)	1.59 (0.38)
	34.43	47.1	0.14	0.28	1.07	1.78
	34.43	47.2	0.13	0.23	1.18	1.02
	34.43	47.3	0.13	0.26	1.02	1.70
	Mean of 34.43 (S.D)	47	0.13 (0.01)	0.39 (0.14)	1.09 (0.08)	1.50 (0.41)
	45.9	55.1	0.15	0.31	1.14	1.43
	45.9	55.2	0.2	0.36	1.18	1.81
	45.9	55.3	0.26	0.34	1.14	1.78
	Mean of 45.90 (S.D)	55	0.20 (0.06)	0.56 (0.17)	1.15 (0.02)	1.67 (0.21)

Table 4-17. HRTD statistics of tracer runs at 27ED vegetation at discharge range from 5.74 to 45.9 ml/s.

4.3 Conclusion of the results from the model pond experiments

a) Results from the distorted, physical scale pond have been demonstrated for its specific 3-D natural shape, with the actual residence time being approximately equal to the theoretical residence time, ($t_m = t_n \pm 15\%$ or $e_m = 1 \pm 15\%$), whenever changing discharge from 4.4 to 45.90 ml/s or changing vegetation from no vegetation to the highest density of both submerged and emerged vegetation (0E to 27EH). This result for t_m or e_0 being almost equal to t_n contrasts with the results of previous researchers, both in field and laboratory, who measured always $t_m < t_n$,. There are three reasons that may influence the result, namely (i) the effect of vegetation (though this reason can be ruled out due to all experiment runs without vegetation also showing t_m being equal to t_n, (ii) the natural pond's shape (but this also may not be realistic as the surface flow profiles revealed by PIV showed that the advections in the pond were introduced by the discharge and pond geometry) and (iii) the scale down of the model is a distorted scale (1:30 for X and Y and 1:15 for Z) is a unique natural shape. Moreover, the problem of trace's background reduction may also cause uncertainty in the distribution of dye mass; more investigations need to be done to compare the results of the laboratory scale tests to the field result and also more experiment should be conducted on non-distorted scale models with a precise strategy of background deduction.

b) Values of other parameters, notably the first dye arrival time, t_o, or the relative first dye arrival at the pond outlet, e_o and the peak concentration (t_p) or relative peak concentration, e_p, were found to be a function of discharge and, to a much lesser extent, the magnitude of analogue emergent and submerged vegetation. For instance, the result indicated that changes in the flow rate from

4.4 to 45.9 ml/s resulted in increases in e_o and e_p of 10 and 19 times of its value at discharge 4.4 ml/s respectively, whereas the pond with the highest density of submerged plant and the highest coverage (27% of pond cross section) of emergent plants only exhibited increases in e_o and e_p of 1.5 and 1.8 of its value of without vegetation respectively compared to the pond without either emergent or submerged plants.

c) It has been demonstrated for a specific distorted physical scale model pond with a “natural” shape that the time to complete a trace or time to have a complete HRTD is approximately equal 5 times of its theoretical residence time ($t_{end} = t_n \pm 1$) and this parameter is largely insensitive to changes in vegetation and discharge.

d) Even though the defined t_m tend to be equal to t_n which percentile of cumulative mass falls with in 60 – 65%, some traces still indicated that up to 75% of cumulative mass distribution had been passed through the outlet within the period of t_n.

e) The PIV investigation has shown that, for all discharge conditions and only with no vegetation and little emerged plant from the pond’s edge (11E, which corresponds to 11% of the average pond cross section and is 1m from the pond edge of the real full scale field pond), well mixed conditions existed before the water reached the outlet. This is due to the appearance of few vortices in section 1 (closed to the inlet) and the middle of pond. In contrast, with more vegetation, only one vortex formed close to the inlet at section 1/3; this may result in short circuiting of the outflow but, as explained above, t_o or e_o are only affected

by discharge when low discharge conditions exist and when short circuiting may due to water surface tension .

CHAPTER: V

5 Results (Field Studies)

5.1 Results from Lyby field pond test

5.1.1 Results of trace on 23 March 2008 at Lyby field pond

The experiment commenced at Lyby pond on 23 March 2008, a time of year when all the vegetation had died out but the stem of the emergent plant still existed. The trace was conducted by using 100 ml of neat dye (l/l) mixed with 1.9 l of water and then gradually poured from the inlet flume for about 10 minutes and discharged to the pond. To observe the effect of vegetation and discharge on HRTD, HRT, and C%, the raw data output from scufa SN154 was plotted as time spend against dye concentration and the background concentration was deducted; the method of deducted background concentration in the laboratory scale experiment was also applied for the field data. Figure 5-1 shows the raw data and after deduction background where the trace took about 160 hours to finish and the average discharge was 9 l/s.

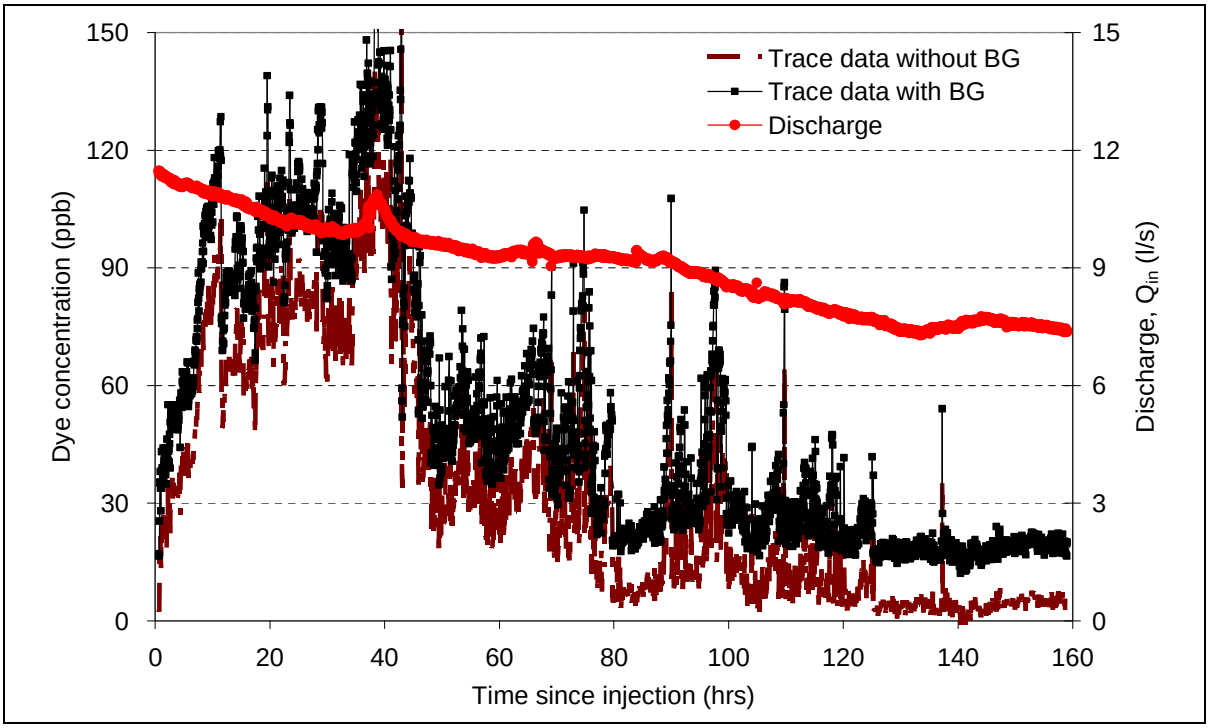

Figure 5-1. HRTD with and without background deduction of trace on 23 March 2008.

From the HRTD, pond volume and trace average discharge values, t_m and t_n were calculated to give a value of t_m that is approximately 2/3 of t_n. Mass recovery calculations showed that the concentration *C* of this trace was about 186% of the original Rhodamine WT injected at the inlet. Clearly this is not possible and this problem was finally attributed to the presence of leeches on the instrument sensor. The leeches affected the fluorescent reading on the instrument, resulting in a spurious increase in the mass recovery. As in the laboratory model experiments, for the purposes of comparison, concentrations *C* have been assumed to be 100% of the mass of dye passing through the outlet and the percentage of dye mass passed through the outlet defined the mass dye distribution parameters such as t_0, t_{25}, t_{55}, t_{95}, t_{peak} and the final observed concentration, Figure 5-2 & Table 5-1.

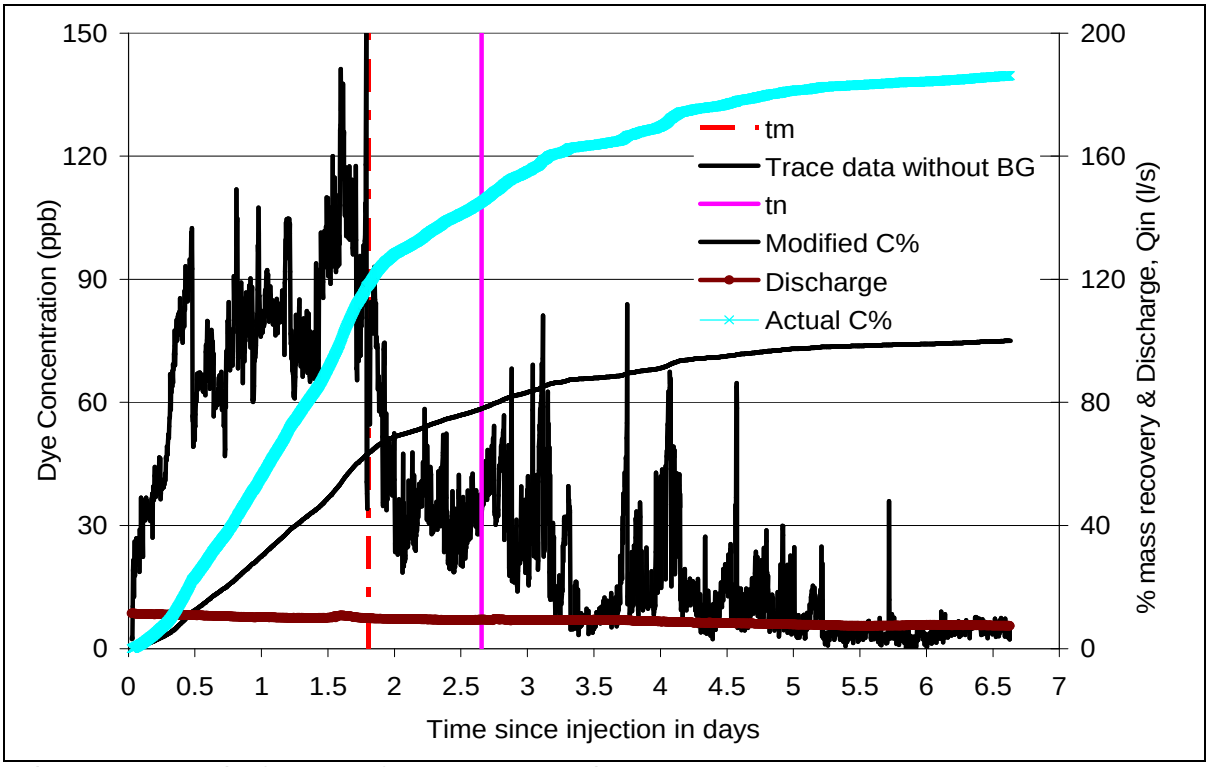

Figure 5-2. Result of HRTD of trace on 23 March 2008.

As the main purpose is to compare results from field experiment to field experiment, as well as from field experiment to the laboratory experiments, the results for time and concentration are expressed in dimensionless form. The same as in laboratory experiment, the HRTD was made dimensionless based on peak concentration (t_p =1) and HRT (nominal residence time, t_n =1), Figure 5-3. Moreover, from the assumption *of* C equal to 100% and equation 2.1, 2.2,2.3, 2.4 and 2.6 in section 2, the results of t_n, HRTD, t_m, e_o, e_p and e_m of this experimental run have been calculated, Table 5-1.

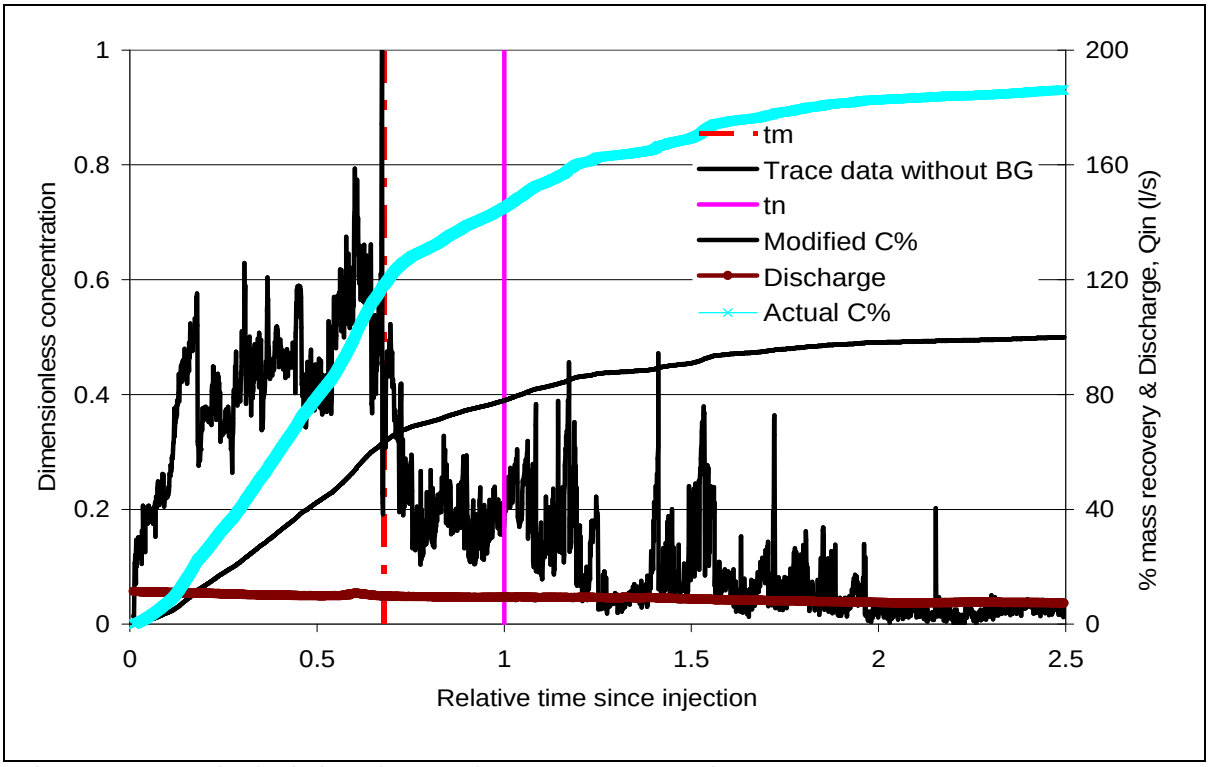

Figure 5-3. Result of relative of HRTD for trace on 23 March 2008.

Averaged Discharge, Qin (ml/s)	Vegetation Conditions	Run Dated.	Calculated from data value						Theory	Normalize or relative time			
			t_0	t_{25}	t_p	t_{55}	t_m	t_{95}	t_n (=1)	e_0	e_p	e_m	σ^2
			(hrs)							t_0/t_n	t_p/t_n	t_m/t_n	as relative time
9	Only emergent plant	23 Mar. 2008	0.6	52	21	38	43	108	64	0.01	0.33	0.68	0.26

Table 5-1. Summary result of trace on 23 March 2008.

With an average flow rate of about 9 l/s and only emergent plant in the pond, the results from the trace in Table 5-1 indicated that the first dye arrived very fast at the pond's outlet, with approximately 1% of its nominal residence time t_n. The relative hydraulic efficiency of peak concentration, e_p, was only 33% of its t_n. value. The relative hydraulic efficiency of the actual residence time, e_m, was just 68% of its t_n value, indicating that the level of mixing in the pond was not high in general;

moreover, the relative time of variance also indicate relatively low levels of mixing in the system, with the value of σ^2 being only 0.26. In Overall, this experiment took about 2.5 times of nominal residence time to complete a trace or a completed value of HRTD, Figure 5-3.

5.1.2 Results of trace on 17 November 2008 at Lyby field pond

This experiment was conducted on 17 November 2008 with all the vegetation in maximum density (both submerged and emergent plants). The trace was conducted by using 100 ml of neat dye (l/l) gradually poured from the inlet flume for about 10 minutes and discharged to the pond. The same method of deducted background was applied in this study and Figure 5-4 shows the raw data and after deducting background where the trace took about 120 hours to complete with the averaged discharge value of 11.5 l/s.

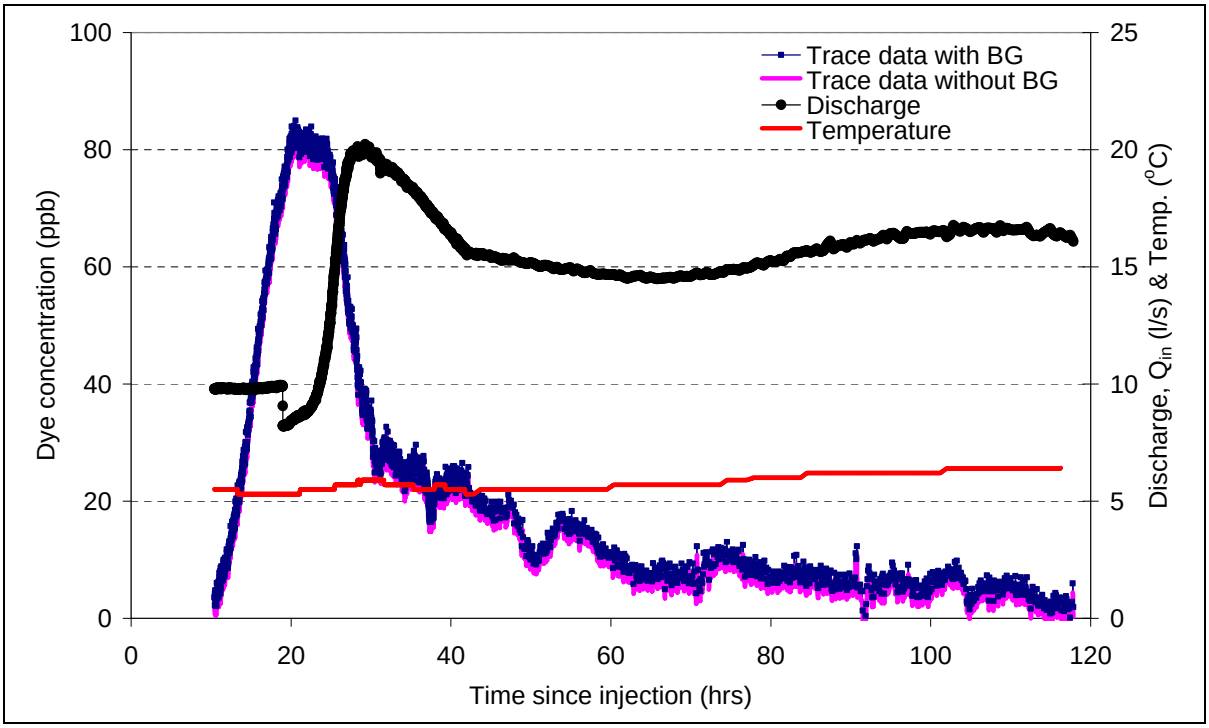

Figure 5-4. HRTD with and without background deduction of trace on 17 November 2008.

Mass recovery of the trace was determined, with the concentration *C* of this trace being about 90% of the original Rhodamine WT injected at the inlet. To simplify the comparison, *C* has been assumed to be only 100% of the mass dye passed through the outlet such that the percentage % of dye mass passed through the outlet could define the mass dye distribution parameters such as t_0, t_{25}, t_{55}, t_{95}, t_{peak} and the final observed concentration, Figure 5-5 & Table 5-2.

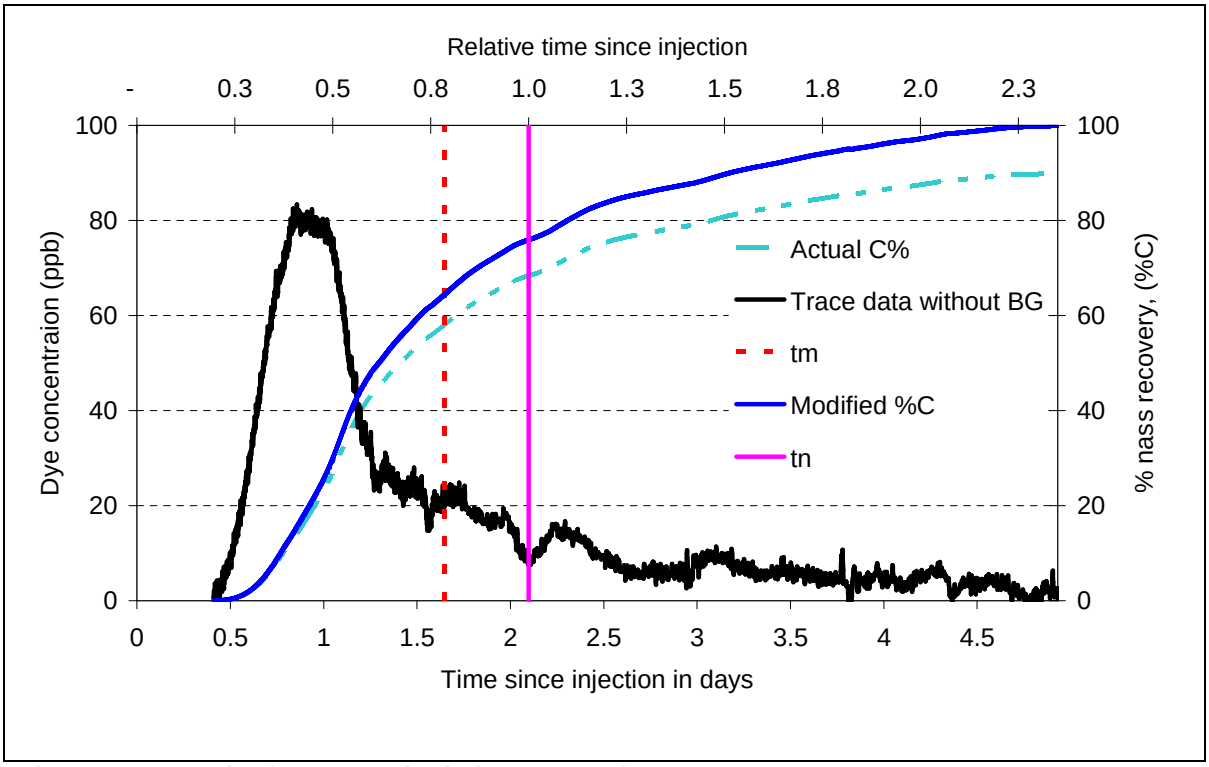

Figure 5-5. Result of HRTD and relative HRTD of trace on 17 Nov. 2008.

HRTD was made dimensionless based on peak concentration (t_p = 1) and HRT (nominal residence time, t_n =1), Figure 5-5. The results of the trace in Table 5-2 indicated that the first dye arrived at the pond's outlet after only about 2% of its nominal residence time t_n. The relative hydraulic efficiency of peak concentration, e_p, was nearly 50% of its t_n. The relative hydraulic efficiency of actual residence time, e_m, was closed to 80% of it's t_n this also indicated that there was not completely well mix but this trace is more mixing than the previous trace due to the more vegetation covered as well as higher discharge. However, the relative time of variance was indicated similar to trace on 23 March 2008 where σ^2 was only 0.22. Moreover, the result also indicated the same as trace on March 2008 where it took the same 2.5 times of nominal residence time to complete a trace or a completed of HRTD, Figure 5-5.

Averaged Discharge, Qin (ml/s)	Vegetation Conditions	Run Dated.	Calculated from data value						Theory	Normalize or relative time			
			t_0	t_{25}	t_p	t_{55}	t_m	t_{95}	t_n (=1)	e_0	e_p	e_m	σ^2
			(hrs)							t_0/t_n	t_p/t_n	t_m/t_n	as relative time
11.5	Full vegetation cover	17 Nov. 2008	9.9	23.8	21.6	33.5	39.5	92	50.4	0.20	0.47	0.78	0.26

Table 5-2. Summary result of trace on 17 November 2008.

5.1.3 Results of trace on 17 April 2009 at Lyby field pond

This experiment was conducted on 17 March 2009 when all the vegetation had died out but the stems of emergent plants still existed in the same state as the trace on 23 March 2008. The trace was conducted by using 198 ml of neat dye (l/l) gradually poured from the inlet flume for 10 minutes, as in the other experiments. The same method of deducting the background level was applied in this study where Figure 5-6 shows the raw data and after the deduction of the background. The trace took about 650 hours to complete with very low discharge (the averaged discharge was only about 1.6 l/s).

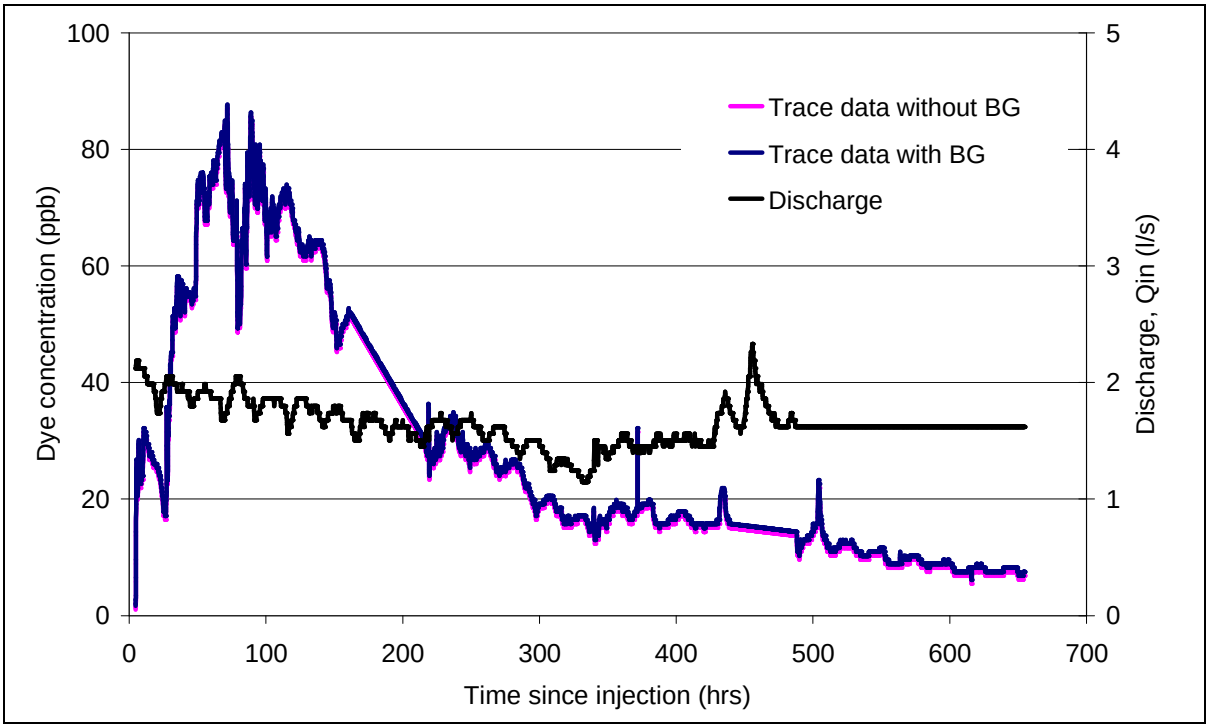

Figure 5-6. HRTD with and without background deduction of trace on 17 March 2009.

Mass recovery of this trace was very low (about 60% of the original Rhodamine WT injected at the inlet) because it was very long trace and the instruments were evidently affected by sunlight and/or the build up of sediment, respectively. With the assumption that *C*(%) is 100% of the mass of dye passed through the outlet then the percentage of dye mass passed through the outlet defined the mass dye distribution parameters such as t_0, t_{25}, t_{55}, t_{95}, t_{peak} and the last observed concentration, Figure 5-7 & Table 5-3.

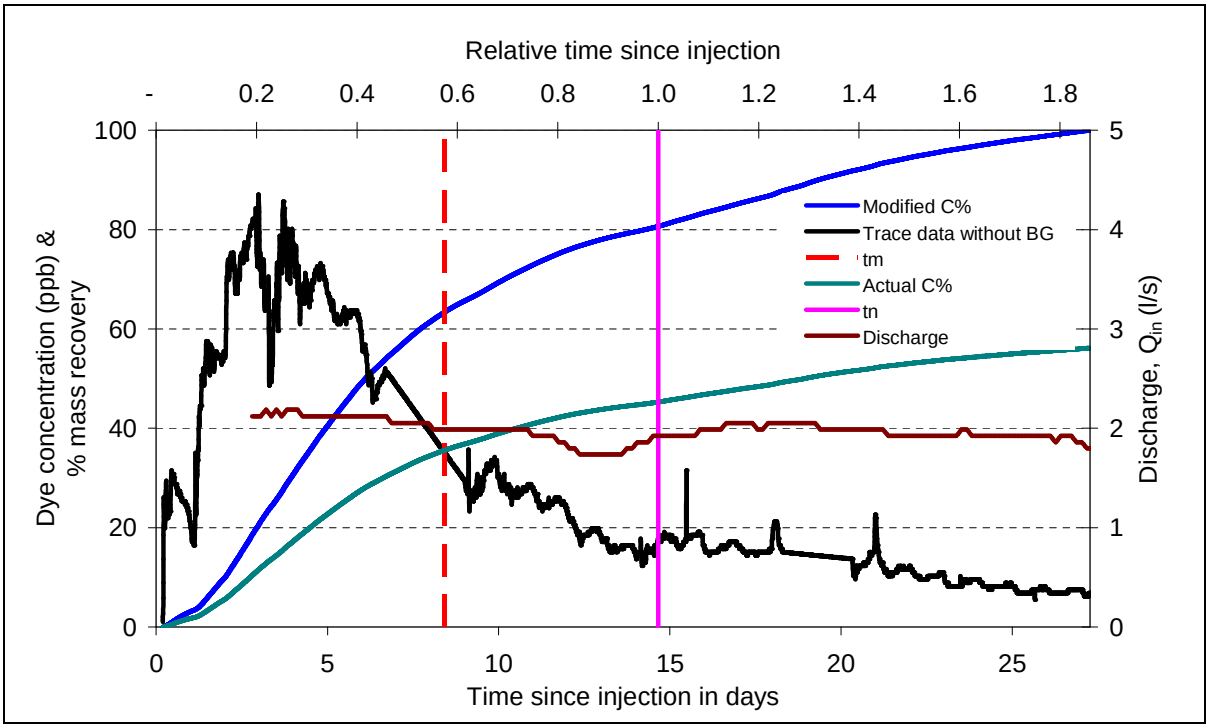

Figure 5-7. HRTD with and without background deduction of trace on 17 March 2009.

HRTD was made dimensionless and Figure 5-7) & Table 5-3 indicated that the first dye arriving at pond's outlet was the same as on the trace on March 2008, within about 1% of its nominal residence time t_n. The relative hydraulic efficiency of peak concentration, e_p, was only 37% of its t_n. The relative hydraulic efficiency of actual residence time, e_m, was just 58% of its t_n, indicating also that there was not complete mixing, as in the experiment on March 2008 where the trace had a similar vegetation condition. However, the relative time of variance was completely different from previous two traces where σ^2 was only 0.08. Moreover, the result also indicated the same as previous traces, where it took nearly the same 2.5 times of nominal residence time to complete a trace or a completed of HRTD, Figure 5-7.

Averaged Discharge, Qin (ml/s)	Vegetation Conditions	Run Dated.	Calculated from data value						Theory	Normalize or relative time			
			t_0	t_{25}	t_p	t_{55}	t_m	t_{95}	t_n (=1)	e_0	e_p	e_m	σ^2
			(hrs)							t_0/t_n	t_p/t_n	t_m/t_n	as relative time
1.6	Full submerged plants	17 Mar.. 2009	4.6	82.4	71.8	165	202	537	351	0.01	0.37	0.58	0.08

Table 5-3. Summary result of trace on 17 March 2009.

5.1.4 Summary results from the Lyby field pond experimental runs

All complete three traces from the Lyby pond which have average flow rates varying from 1.6 to 11.5 l/s and vegetations that varied seasonally from high density in November (in both emergent and submerged vegetation), low density in March (as very low density of submerged plants but still high density of emergent plant because all the dead stem of emergent plants remained) followed by medium density in April and May where both emergent and submerged started to grow again, Table 5-4. Dye recovery for all runs ranged from 56 to 186% with an average of 105%. There were some consistent differences between the HRTD plots of low and medium plants in March and April to high density vegetation, this statement being based on the assumption that flow rate does not have an effect on HRTD. Some of the parameters for hydraulic efficiency differed significantly between low and medium vegetation (March and April) to high density of emergent and submerged vegetation (in November) but none of the parameters for hydraulic efficiency differed significantly between low density of plant (in March) to medium vegetation density (in April), Figure 5-9. The value of e_m varied from 0.58 to 0.68, at low and medium density plant in March and April, to 0.78 at high density of vegetation in November, Figure 5-9B. The value of e_o was 0.01 at low and medium vegetation in March and April and 0.4 at high density of vegetation in

November, Figure 5-9 A. The relative hydraulic efficiency of peak concentration, e_p, varied from 0.33 to 0.47 (run 1 and 3 with low discharge) and e_p varied from 0.33 to 0.37 at low and medium vegetation (during March and April) and 0.47 at high density of vegetation in November, Figure 5-9 C. The relative time variance, σ^2, was varied from 0.08 to 0.26, σ^2 was 0.26 at run 1, 0.16 at run 2, and 0.08 at run 3, Figure 5-9 D. These relative time variances did not reflect the previous hydraulic efficiency, this property may have been caused by the delay of the tail in run 3 as it was very low discharge (1.6 l/s) and the trace lasted more than 6 weeks.

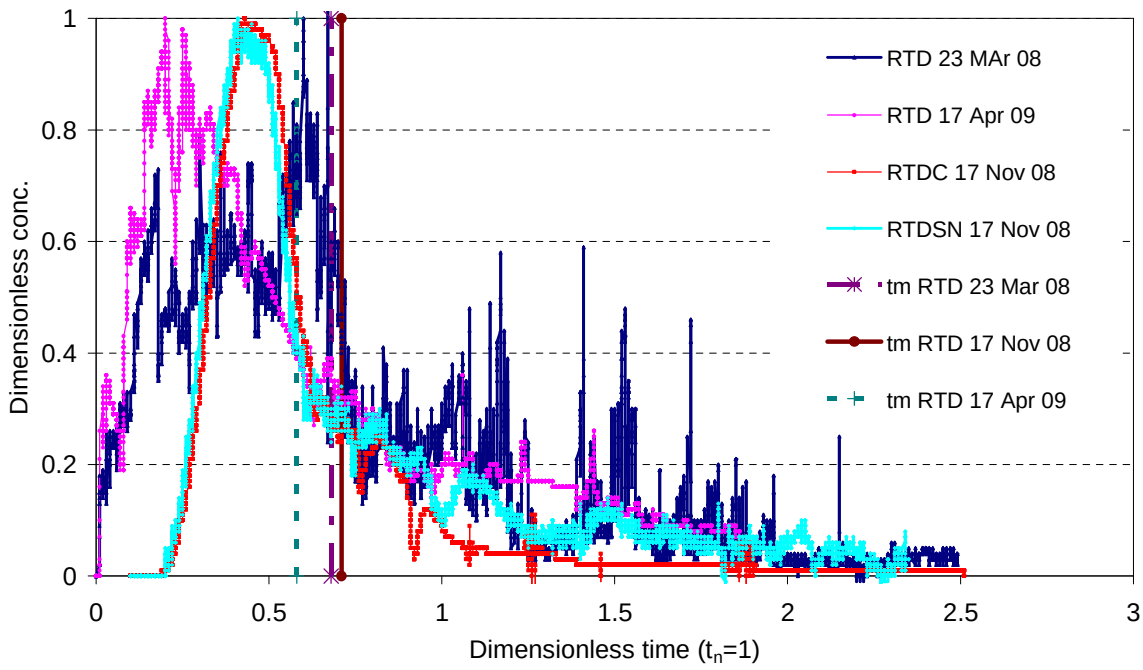

Figure 5-8 Comparison of three representative residence time distribution (HRTDs) curves run at different discharge and vegetation configurations.

The HRTDs, when compared between low, medium and high vegetation density cases, appeared distinctively different. Where the HRTDs of run 1 and 3 at low and medium vegetation were unimodal, the HRTD for run 2 at high density vegetation was bimodal, with the first peak typically arriving late and being more

spread out than for the low and medium vegetation cases HRTD, Figure 5-8. These differences were reflected in the HRTD statistics, Figure 5-9. The average of first dye arrival, e_o, was 0.01 for run 1 and 3 at low and medium vegetation and 0.02 for run 3 at high density vegetation configurations. The time to peak concentration of the HRTD curve, e_p, occurred at the average value of 0.35 for run 1 and 3 at low and medium vegetation configuration and 0.47 for run 2 at high density vegetation configurations. The relative mean residence time, relative HRTD centroid, e_m, had an average of 0.63 for run 1 and 3 at less and medium vegetation configurations in March and April and the average of 0.71 for run 2 at high density vegetation configurations in November.

Two double measurements dye tracers were measured for high vegetation condition in November where there was no significant difference in all its HRTD results, then only one measure of dye tracer was measured for low and medium vegetation density in March and April. Table 5-4, shows the details of HRTDs in all runs with different discharge and vegetation configurations..

Average Discharge, Q_{in} l/s	Tracer Injection date	Veg. Condition	Run No.	$e_o = t_o/t_n$	$e_p = t_p/t_n$	$e_m = t_m/t_n$	σ^2 (m^2/day)	σ^2 (Nom.)
9	23/03/08	Only Emergent	1	0.01	0.33	0.68	1.86	0.26
11.5	17/11/08	Full vegetation	2	0.20	0.47	0.78	0.74	0.16
1.6	17/04/09	Emergent and little Submerge	3	0.01	0.37	0.58	17.93	0.08

Table 5-4. HRTD statistics of three Lyby pond field tracer runs based on seasonal variation of vegetation.

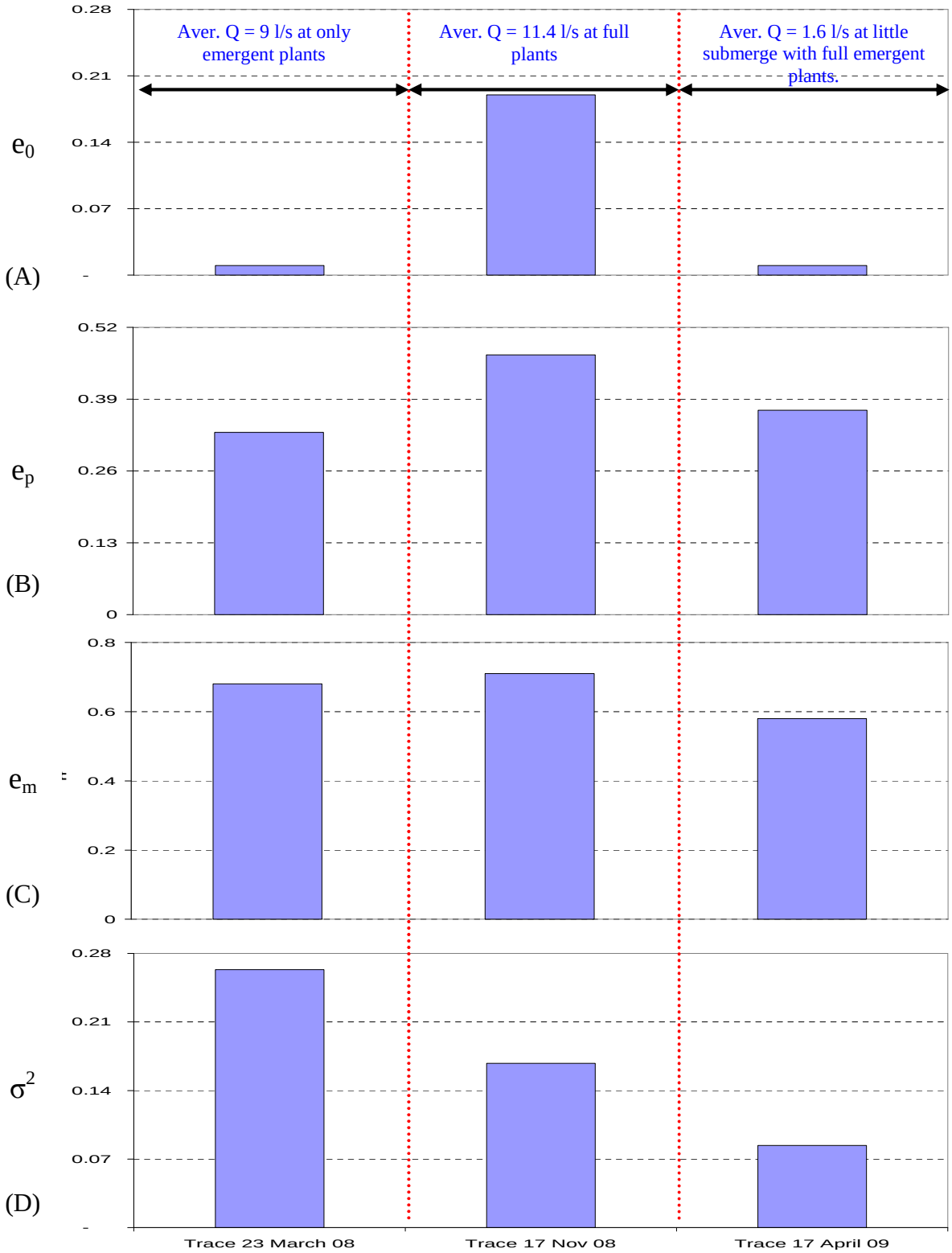

Figure 5-9. The residence time distribution (HRTD) characteristics of the three Lyby Pond traces. Comparisons are made at the averaged discharge of 9, 11.4 and 1.6 l/s and among different vegetation configurations for (A) relative first dye arrival at the pond outlet (e_0), (B) relative peak concentration time ($e_p = t_p / t_n$), (C) relative residence time (Centroid of HRTD, e_m (= t_m / t_n), (D) relative time variance (σ^2).

CHAPTER: VI

6 Summary of Results, Discussion and Conclusion

Discussion

The aim of this thesis was the assessment of the effect of vegetation and discharge on the residence time distribution (HRTD) of a natural pond shape in both a field and a laboratory scale surface pond as shown in Figure 3-8, Figure 3-25 and Figure 3-35. Two main objectives could be defined:

(i) to study the above effects in a naturally shaped physical scale model in a controlled environment where cotton pipes and sisal grasses were used as artificial emergent and submerged plants (Figure 3-8) and the discharge was controlled by a peristaltic pump, with discharges ranging from very low (4.4 ml/s) to very high (45.90 ml/s), as shown in Table 3-1. The study investigated the effects of different discharge and vegetation configurations on pond surface flow profiles, residence time distribution (as actual residence time, as t_m or e_m), short

circuiting (as first arrival time, t_o or e_o), variance (σ^2) and surface flow field were investigated.

(ii) to study the above processes in the Lyby field pond in Sweden where vegetation and discharge conditions were varying seasonally and the discharge was controlled by an earth overspill weir structure (Figure 3-25): the same investigations as for the physical scale model were carried out, with the exception of surface flow profiles.

In both cases a dye tracer technique was used to determine the distribution and movement of contaminants within the ponds under varying conditions.

The HRTD of the distorted scale model (scaled down by X:Y:Z, 30:30:15) was found to be significantly different from the HRTD of the Lyby field pond (Sweden) (Figure 5-9, Figure 6-1 and Figure 6-2) that it was built to model.

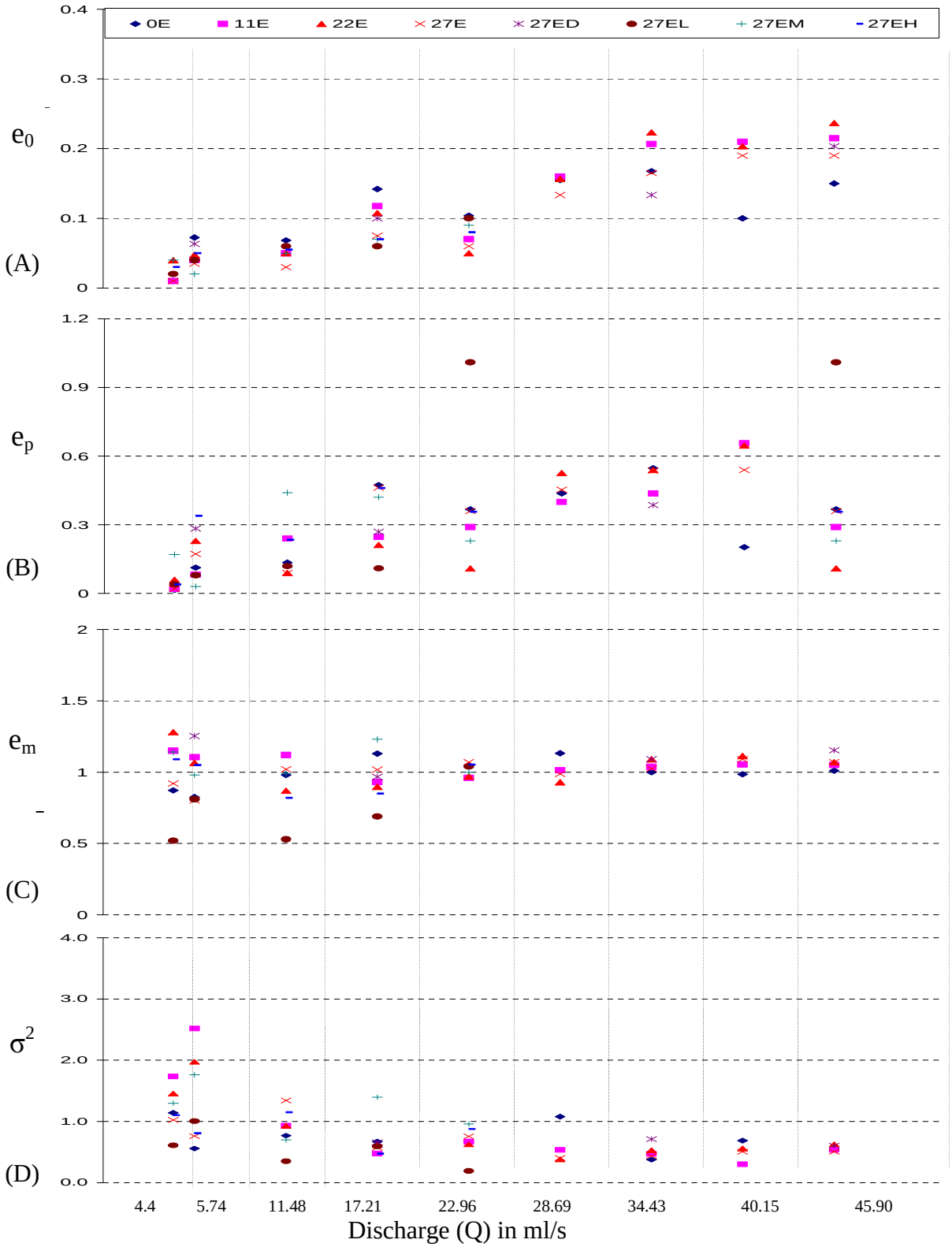

Figure 6-1. The HRTD characteristics under different discharges and vegetation configurations. Comparisons are made at the same each discharge with different vegetation configurations for (A) relative time first dye arrival at the pond outlet (e_0), (B) relative peak concentration time (e_p) ; (C) relative real residence time (relative centroid of HRTD,(e_m), , (D) relative time variance (σ^2).

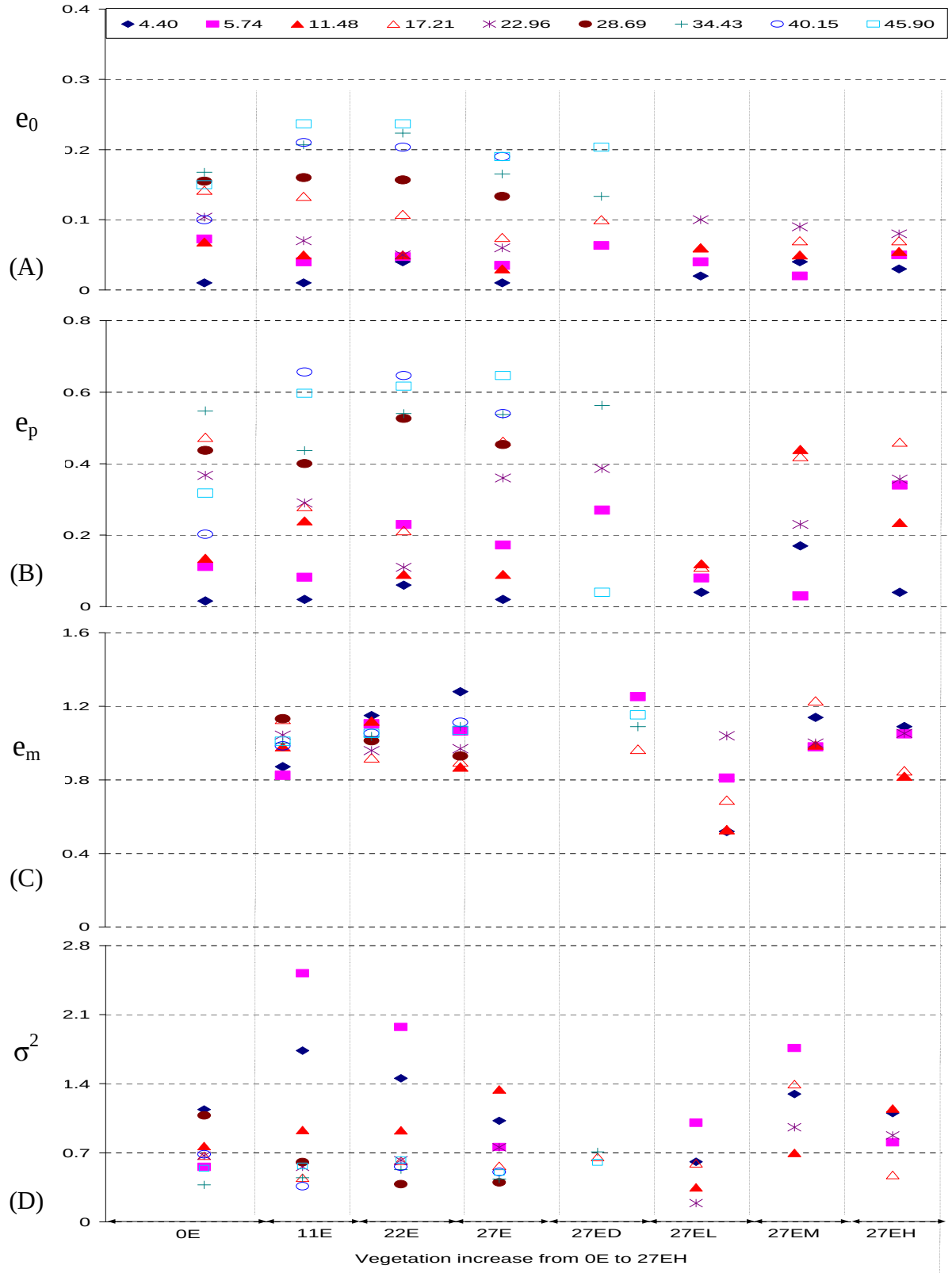

Figure 6-2. The HRTD characteristics under different discharges and vegetation configurations. Comparisons are made at the same each vegetation condition with different discharge configurations for (A) relative time first dye arrival at the pond outlet (e_0), (B) relative peak concentration time; (C) relative real residence time (relative centroid of HRTD,(e_m), (e_p), (D) relative time variance (σ^2).

In particular the sensitivity to changes in vegetation and flow rate of HRTD in the field and in the distorted laboratory scale pond were different. Furthermore, the hydraulic efficiency metrics of both field and laboratory ponds were different over a wide range of flow rate and vegetation configurations, the relative centroid, e_m, ranged from 58 % to 78 % of the nominal retention time for the Lyby field pond afford the low discharges (runs 1, 2 and 3) whereas e_m ranged from 66 % to 125 % of nominal retention time (runs 1 to 23) for the distorted laboratory scale model,(Figure 5-9, Figure 6-3, Figure 6-4 and Table 6-1.

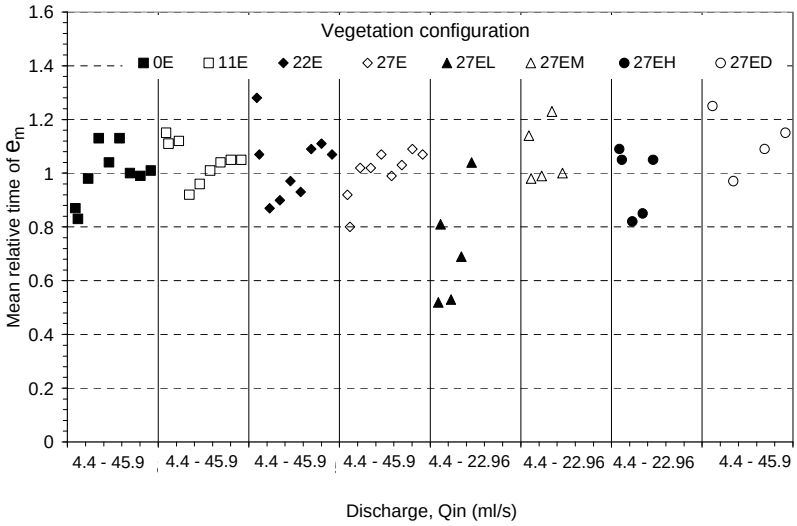

Figure 6-3. Summary of mean relative HRTD of em of fixed different vegetations.

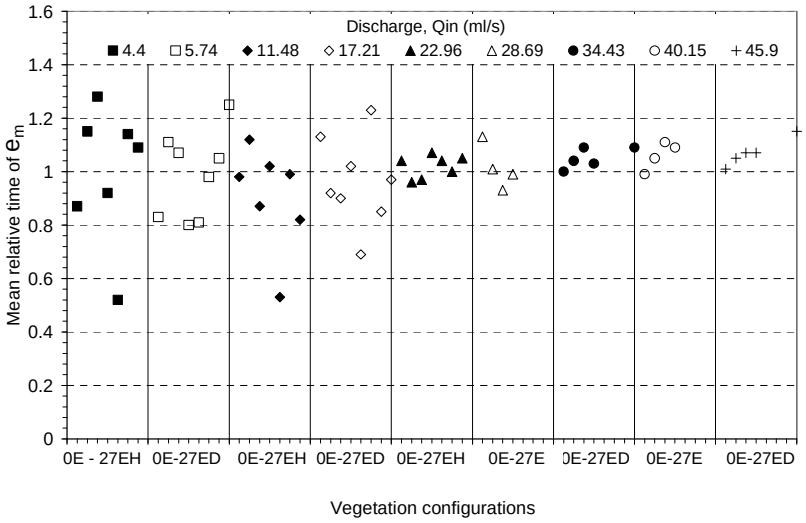

Figure 6-4. Summary of mean relative HRTD of e_m,of fixed different discharges.

Discharge, Qin (ml/s)	Vegetation Conditions	Run No.	$e_o = t_o/t_n$	$e_p = t_p/t_n$	$e_m = t_m/t_n$	σ^2 (based on relative time)
4.4	0E (S.D)	1	0.01 (0.0)	0.02	0.94 (0.11)	1.14 (0.27)
	11E	2	0.01	0.02	1.15	1.73
	22E	3	0.04	0.06	1.28	1.45
	27E	4	0.01	0.02	0.92	1.02
	27EL	5	0.02	0.04	0.52	0.61
	27EM	6	0.04	0.17	1.14	1.30
	27EH	7	0.03	0.04	1.09	1.10
5.74	0E (S.D)	8	0.07	0.12	0.83 (0.08)	0.56 (0.07)
	11E (S.D)	9	0.04	0.08	1.11 (0.13)	2.52 (0.93)
	22E (S.D)	10	0.05	0.15	1.07 (0.28)	0.69 (0.11)
	27ED (S.D)	13	0.06	0.16	1.25 (0.37)	0.76 (0.31)
	27E (S.D)	11	0.04	0.11	0.80 (0.21)	0.42 (0.12)
	27EL	14	0.04	0.07	0.81	1.01
	27EM	15	0.02	0.08	0.98	1.76
	27EH	16	0.05	0.19	1.05	0.81
11.48	0E (S.D)	17	0.07(0.04)	0.23	0.98 (0.1)	1.46 (0.5)
	11E	18	0.05	0.24	1.12	1.08
	22E	19	0.05	0.09	0.87	1.08
	27E	20	0.03	0.09	1.02	0.75
	27EL	21	0.06	0.12	0.53	2.85
	27EM	22	0.05	0.44	0.99	1.43
	27EH	23.1	0.05	0.26	0.98	0.52
	27EH	23.2	0.06	0.21	0.66	2.64
	27EH (S.D)	23	0.06	0.13	0.82 (0.23)	1.58 (1.5)
17.21	0E (S.D)	24	0.14	0.47	1.13 (0.1)	1.57 (0.33)
	11E (S.D)	25	0.12	0.25	0.93 (0.04)	2.15 (0.39)
	22E (S.D)	26	0.11	0.21	0.90 (0.12)	1.81 (0.77)
	27E (S.D)	27	0.08	0.46	1.02 (0.09)	1.91 (0.73)
	27EL	29	0.06	0.11	0.69	1.68
	27EM	30	0.07	0.42	1.23	0.72
	27EH	31	0.07	0.46	0.85	2.11
	27ED (S.D)	28	0.1 (0.02)	0.27	0.97 (0.02)	1.59 (0.38)
22.96	0E (S.D)	32	0.10	0.20	1.04 (0.1)	1.51 (0.17)
	11E	33	0.07	0.29	0.96	0.29
	22E	34	0.05	0.11	0.97	0.11
	27E	35	0.06	0.36	1.07	0.36
	27EL	36	0.1	1.01	1.04	1.01
	27EM	37	0.09	0.23	1	0.23
	27EH (S.D)	38	0.08	0.21	1.05 (0.07)	1.68 (0.99)
28.69	0E (S.D)	39	0.16	0.27	1.13 (0.14)	1.28 (0.59)
	11E (S.D)	40	0.16	0.29	1.01 (0.06)	2.01 (0.61)
	22E (S.D)	41	0.16	0.36	0.93 (0.02)	3.22 (1.48)
	27E (S.D)	42	0.13	0.32	0.99 (0.10)	2.56 (0.49)
34.43	0E (S.D)	43	0.17	0.34	1.00 (0.04)	2.70 (0.38)
	11E (S.D)	44	0.21	0.35	1.04 (0.02)	2.16 (0.28)
	22E (S.D)	45	0.22	0.38	1.09 (0.05)	2.00 (0.55)
	27E (S.D)	46	0.17	0.31	1.03 (0.11)	2.35 (0.47)
	27ED (S.D)	47	0.13	0.26	1.09 (0.08)	1.50 (0.41)
40.15	0E (S.D)	48	0.10	0.17	0.99 (0.04)	1.48 (0.23)
	11E (S.D)	49	0.21	0.44	1.05 (0.03)	3.37 (0.41)
	22E (S.D)	50	0.20	0.44	1.11 (0.15)	2.82 (1.72)
	27E (S.D)	51	0.19	0.34	1.09 (0.06)	2.03 (0.41)
45.90	0E (S.D)	51	0.15	0.24	1.01 (0.04)	1.86 (0.23)
	0E (S.D)	52	0.22	0.33	1.05 (0.02)	1.95 (0.46)
	0E (S.D)	53	0.24	0.36	1.07 (0.07)	1.62 (0.22)
	0E (S.D)	54	0.19	0.32	1.07 (0.02)	2.02 (0.30)
	0E (S.D)	55	0.20	0.34	1.15 (0.02)	1.67 (0.21)

Table 6-1. Summary mean results of laboratory experiment with fixed different discharge.

The measurement of short-circuiting, e_o, was found to be 0.2 in the field, but 0.01 in the lab, reflecting more frequently short-circuiting than in the lab possibly due to the small size of the physical scale model, (Figure 6-5, Figure 6-6, Figure 5-9 and Table 6-2).

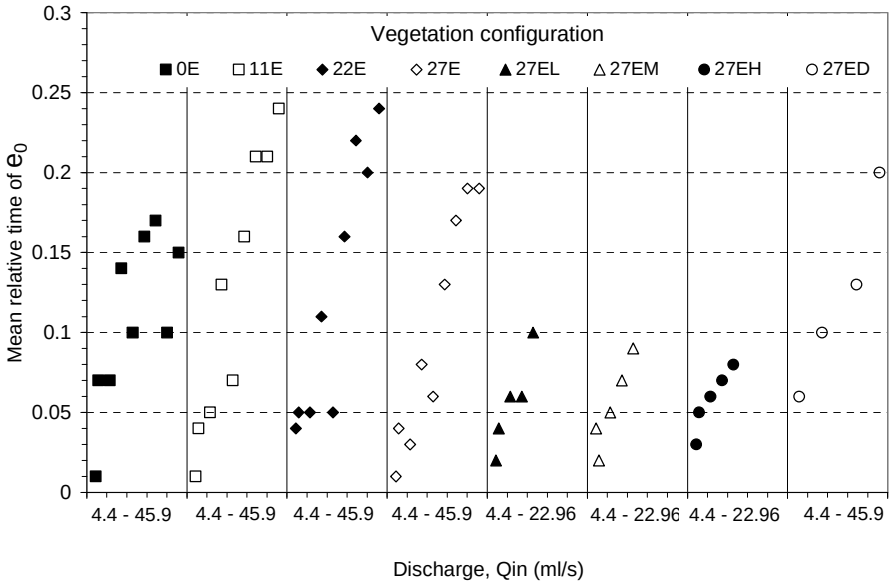

Figure 6-5. Summary of mean relative HRTD of, e_o. of fixed different vegetations.

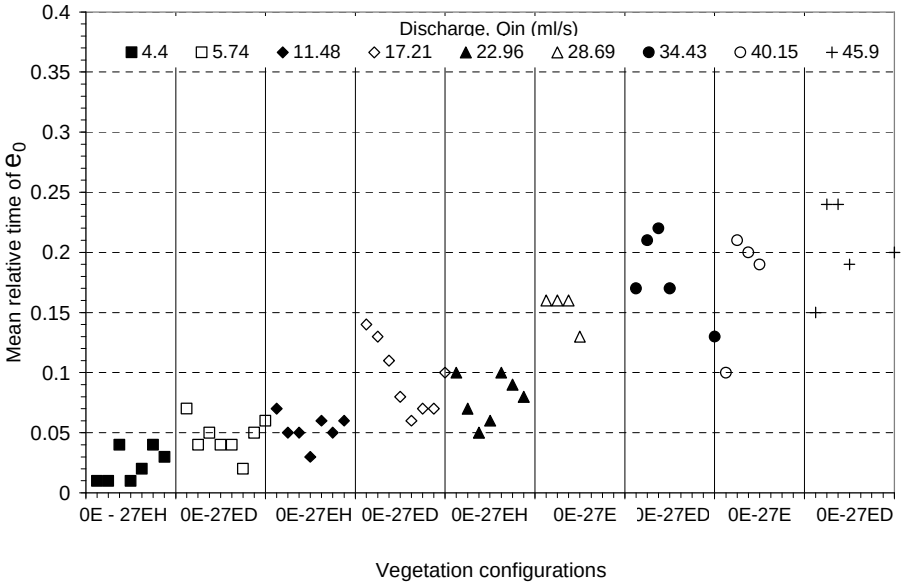

Figure 6-6. Summary of mean relative HRTD of e_o.of fixed different discharges.

Vegetation Condition	Discharge, Qin (ml/s)	Run No.	$e_o = t_o/t_n$	$e_p = t_p/t_n$	$e_m = t_m/t_n$	σ^2 (based on relative time)
OE	4.4 (S.D)	1	0.01	0.02	0.87	1.14 (0.27)
	5.74 (S.D)	8	0.07	0.12	0.83	0.56 (0.07)
	11.48 (S.D)	17	0.07	0.23	0.98	0.77 (0.30)
	17.21 (S.D)	24	0.14	0.32	1.13	0.67 (0.19)
	22.96 (S.D)	32	0.10	0.20	1.04	0.67 (0.08)
	28.69 (S.D)	39	0.16	0.27	1.13	1.08 (0.87)
	34.43 (S.D)	43	0.17	0.34	1.00	0.37 (0.05)
	4.4 (S.D)	48	0.1 (0.02)	0.17	0.99	0.69 (0.11)
	4.4 (S.D)	51	0.15	0.24	1.01	0.54 (0.07)
11E	4.4	2	0.01	0.03	1.15	0.58
	5.74 (S.D)	9	0.04	0.08	1.11	0.45 (0.21)
	11.48	18	0.05	0.22	1.12	1.08
	17.21 (S.D)	25	0.13	0.25	0.92	2.27 (0.33)
	22.96	33	0.07	0.18	0.96	1.79
	28.69 (S.D)	40	0.16	0.29	1.01	1.78 (0.65)
	34.43 (S.D)	44	0.21	0.35	1.04	2.25 (0.18)
	40.15 (S.D)	49	0.21	0.44	1.05	3.03 (0.99)
	45.9 (S.D)	52	0.24	0.35	1.05	1.85 (0.67)
22E	4.4	3	0.04	0.08	1.28	0.69
	5.74 (S.D)	10	0.05	0.15	1.07	1.15 (0.68)
	11.48	19	0.05	0.09	0.87	1.08
	17.21 (S.D)	26	0.11	0.22	0.90	1.81 (0.77)
	22.96	34	0.05	0.12	0.97	1.60
	28.69 (S.D)	41	0.16	0.36	0.93	3.22 (1.48)
	34.43 (S.D0	45	0.22	0.38	1.09	2.00 (0.55)
	40.15 (S.D)	50	0.20	0.44	1.11	2.82 (1.12)
	45.9 (S.D)	53	0.24	0.36	1.07	1.62 (0.22)
27E	4.4	4	0.01	0.03	0.92	0.98
	5.74 (S.D)	11	0.04	0.11	0.80	1.51 (0.62)
	11.48	20	0.03	0.08	1.02	0.75
	17.21 (S.D)	27	0.08	0.24	1.02	1.91 (0.73)
	22.96	35	0.06	0.25	1.07	1.32
	28.69 (S.D)	42	0.13	0.32	0.99	2.56 (0.49)
	34.43 (S.D)	46	0.17	0.31	1.03	2.35 (0.40)
	40.15(S.D)	51	0.19	0.34	1.09	2.03 (0.41)
	45.9 (S.D)	54	0.19	0.32	1.07	2.02 (0.30)
27EL	4.4	5	0.02	0.03	0.52	1.64
	5.74	14	0.04	0.07	0.81	0.99
	11.48	21	0.06	0.09	0.53	2.85
	17.21	29	0.06	0.1	0.69	1.68
	22.96	36	0.1	0.38	1.04	5.24
27EM	4.4	6	0.04	0.14	1.14	0.77
	5.74	15	0.02	0.08	0.98	0.57
	11.48	22	0.05	0.17	0.99	1.43
	17.21	30	0.07	0.16	1.23	0.72
	22.96	37	0.09	0.19	1.00	1.04
27EH	4.4	7	0.03	0.07	1.09	0.91
	5.74	16	0.05	0.19	1.05	1.24
	11.48 (S.D)	23	0.06	0.13	0.82	1.58 (1.50)
	17.21	31	0.07	0.19	0.85	2.11
	22.96 (S.D)	38	0.08	0.21	1.05	1.68 (0.99)
	5,74 (S.D)	13	0.06	0.28	1.25	0.67 (0.57)
	17.21 (S.D)	28	0.10	0.27	0.97	1.59 (0.38)
	34.43 (S.D)	47	0.13	0.39	1.09	1.50 (0.41)
	45.90 (S.D)	55	0.20	0.56	1.15	1.67 (0.21)

Table 6-2. Summary mean results of laboratory experiment with fixed different vegetation.

The variance, σ^2 , of the mixing scale, variance, ranged from 0.008 to 0.26 for the Lyby field pond but 0.42 to 2.52 for the distorted physical scale, (Figure 6-7, Figure 6-8 and Table 6-1). The relative time to peak, e_p, varied from 0.33 to 0.47 for the field pond but 0.02 to 0.23 for the laboratory model, (Figure 6-9, Figure 6-10 and Table 6-2).

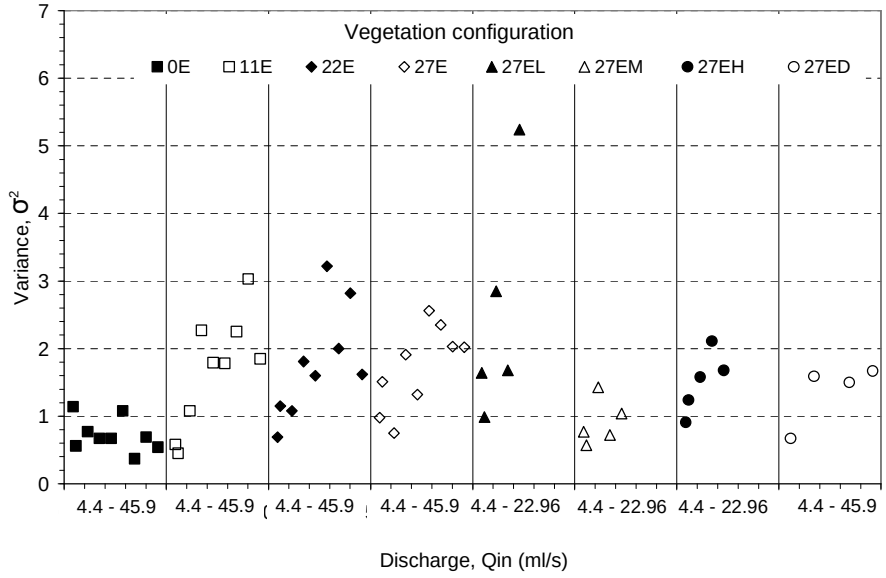

Figure 6-7. Summary of mean relative HRTD of σ^2 of fixed different vegetations.

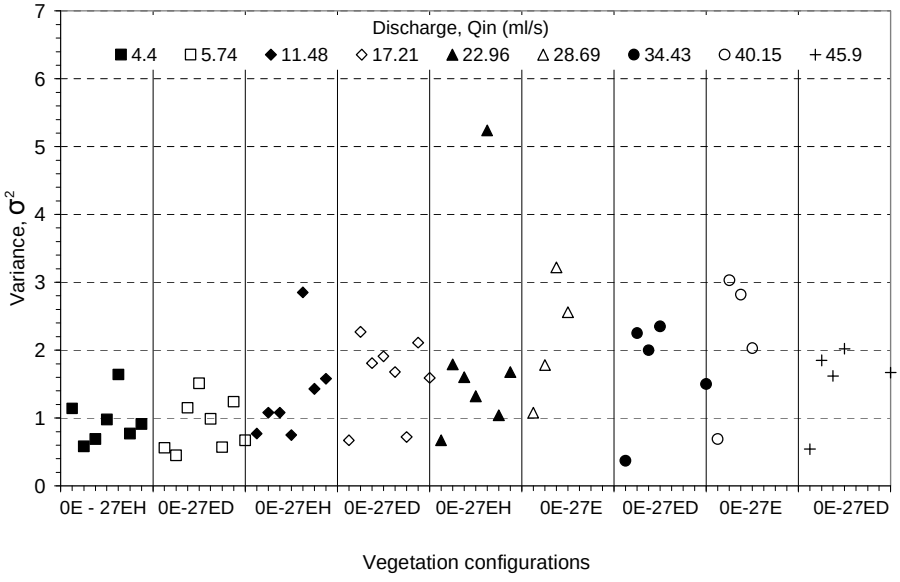

Figure 6-8. Summary of mean relative HRTD of σ^2 of fixed different discharges.

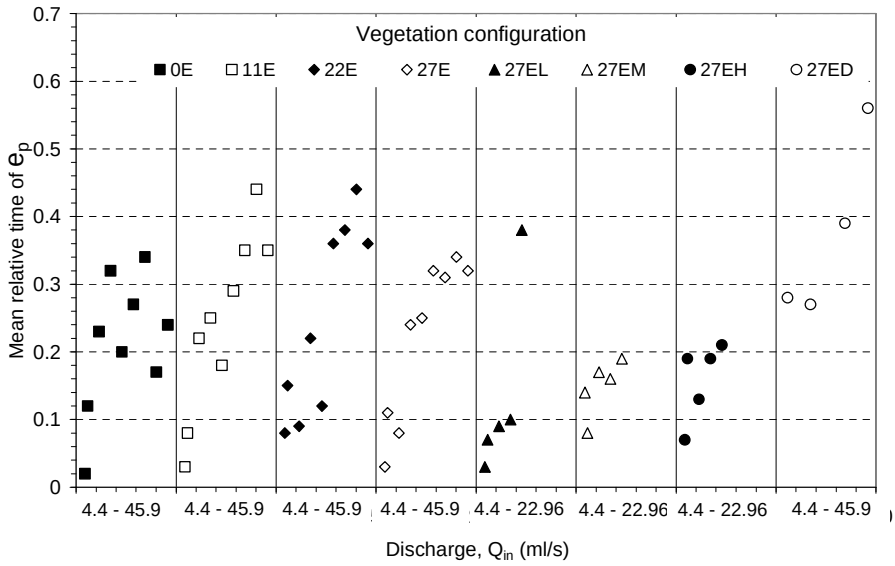

Figure 6-9. Summary of mean relative HRTD of e_p of fixed different vegetations.

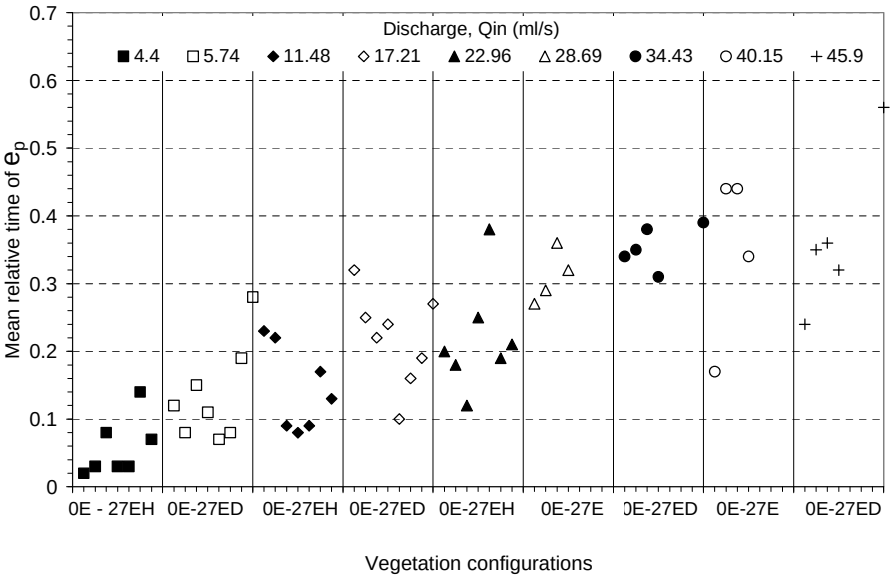

Figure 6-10. Summary of mean relative HRTD of e_p of fixed different discharges.

Both ponds, however, exhibited similar values of e_0. These observations illustrate significantly different hydraulic efficiencies between the field and model ponds. Each metric of hydraulic efficiency used in this study has unique implications on optimised treatment effectiveness. Further research may therefore consider not to use distorted physical scale models but instead conduct more tracer experiments

on the field pond, conducted, at least repeated for two years cycle, with different seasonal variation of vegetation and discharge.

Due to the distorted scaling, the laboratory model may not fully represent the full scale, so the following discussion will be mainly discussed separately between results from distorted physical scale model and from Lyby field pond.

The results from physical scale pond indicated that the HRTD of a natural shape model is not significantly sensitive to changes in vegetation and/or flow rate. If this result is characteristic of natural ponds in general, then it indicates that a natural shape physical model provides the best optimisation of the actual pond residence time where change in flow rate (as a factor of 1 to 9) and/or change in vegetation (none to fully emergent plant and to fully emergent with submerged plants). In this study, a total of 55 configuration within 145 laboratory tests was enough to optimise and stabilise the hydraulic efficiency and measured by the relative centroid, e_m, at mean value of 1.02 (S.D = 0.15), (see Figure 6-1**,** Figure 6-4 & Table 6-1). Small, not statistically significant changes in e_o, e_p and σ^2 were observed when changing from non-vegetation to fully emergent and submerged plants. However, changing the natural shape physical scale pond's discharge by a factor of 1, is enough to elicit a significant exponential changes in some e_o, e_p (increasing) and σ^2 (decreasing) (see Figure 6-2, Figure 6-9, Figure 6-3, Figure 6-7 and Table 6-2).

Although this study illustrates no significant effect of vegetation on the HRTD in the laboratory model, the range of validity of application to field ponds needs to be considered. The distribution density of emergent plants may be different in a field

pond than that of the cotton pipe analogue used in the laboratory model; the distribution of submerged plants in a field pond may different from that of the sisal grass analogue used in the laboratory model. Thus vegetation effects on the HRTD may be greater in naturally environmental conditions at the field than under laboratory conditions used in this study. Further tracer tests in the field would be needed to test this conjecture, although we note that water surface tension that may dominate at very low flow or with full of vegetation conditions, are difficult to isolate and measure with HRTD analysis because of the shorter retention times and scales involved in the physical scale experiment. On the other hand, variations of discharge are more likely to remain more or less within the range tested in this study.

From Equation 3.10 and 3.12 where $S_q = S_L S_Y^{3/2}$ and $S_T = \frac{S_L}{S_Y^{1/2}}$

Physical Scale Pond		From physical scale to field by scaling up 30:30:30			From physical scale to field by scaling up 15:15:15		
t_n in day (lab.'s pond volume 179l)	Discharge at lab. scale pond (Q) in ml/s	Predicted discharge (Q) from lab. to field pond in l/s	Expected field t_n in day	Estimate Field Pond's Volume in m^3	Predicted discharge (Q) from lab. to field pond in l/s	Expected field t_n in day	Estimate Field Pond's Volume in m^3
0.73	2.84	13.99	4.00	4835.45	28.72	4.62	11456.00
0.55	3.78	18.66	3.00	4835.45	38.30	3.46	11456.00
0.47	4.40	21.69	2.58	4835.45	44.52	2.98	11456.00
0.36	5.74	28.30	1.98	4835.45	58.08	2.28	11456.00
0.18	11.48	56.59	0.99	4835.45	116.17	1.14	11456.00
0.12	17.21	84.84	0.66	4835.45	174.15	0.76	11456.00
0.09	22.96	113.18	0.49	4835.45	232.34	0.57	11456.00
0.07	28.69	141.43	0.40	4835.45	290.32	0.46	11456.00
0.06	34.43	169.72	0.33	4835.45	348.41	0.38	11456.00
0.05	40.15	197.92	0.28	4835.45	406.29	0.33	11456.00
0.05	45.90	226.26	0.25	4835.45	464.48	0.29	11456.00

Table 6-3. Proposed the estimated discharges and pond volume based on scale up by 30 or 15 times.

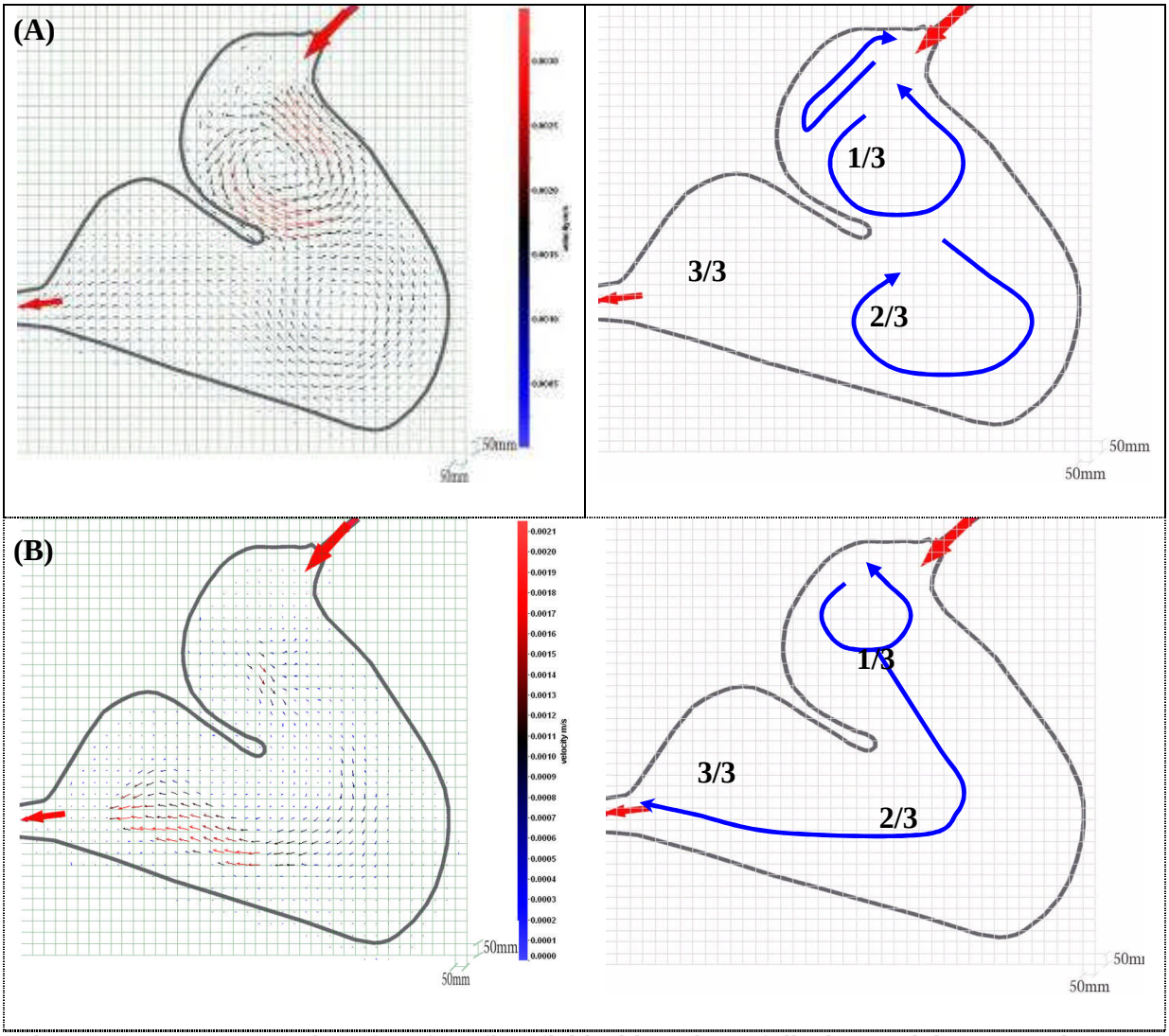

Figure 6-11. Representative of surface flow field with variety of discharge, (A): None or less vegetation; (B): High density vegetation.

Design and management implications

The study of the physical scale pond shows that vegetation effects on hydraulic efficiency may not be important for this specific natural physical pond shape. The e_m (t_m) parameter remained in the range of 1±0.15 (0.85 with low flow rate and 1.15 while high flow rate) for a range of vegetation conditions (non to highest density in either emerged or submerged plants). Moreover, by changing discharge from 25% to 200% of the designed physical scale pond (4.4 to 45.9 ml/s), result in linearity of relative HRTD centroid, e_m (t_m), which Y = 0.0025X + 0.9293 while

vegetation changed from not vegetation to highest density vegetation (0E to 27EH). However, the result in general in every discharges (4.4 to 45.9 ml/s) with changing vegetation from 0E to 27EH, the relative HRTD of e_m, e_o and e_p linear increased 0.015, 1.5 and 1.8 times respectively. On the other hand the results in general in any vegetation conditions (0E to 27EH) with changing discharge from 25% to 200% of the designed nominal residence time (4.4 to 45.9 ml/s) the relative HRTD of e_m, e_o and e_p linear increased by 0.46, 10 and 9 times respectively. The result indicated that the actual vegetation used in the physical scale pond has no significant effect on relative HRTD of e_o and e_p but the variation of discharge didn't significant effect. However, both, variation of vegetation and discharge applied in the physical scale model did not show any significant effect on the relative HRTD centroid where e_m linear increase by 0.5 and 0.46 times by changing vegetation from 0E to 27EH and discharge from 4.4 to 45.9 ml/s respectively. This reflects the result of the relative HRTD of variance, $\sigma^2_{,}$ where, both with fully variation of vegetation and discharge, the spread is fluctuated increasing between 2.2 to 3.3 times.

The results of surface flow profile with variation of discharge and vegetation indicated that 3 vortices appeared with none (0E) or less (11E) vegetation but there is only one small vortex appeared with more vegetation density (22E to 27EH), Figure 6-11. The surface flow results did not reflect on the relative HRTD where by theory when there are more vortices exist mean there will be the increase of mixing activities but the relative HRTD centroid, e_m, only linear increase by 0.5 and 0.46 times by changing vegetation from 0E to 27EH and discharge from 4.4 to 45.9 ml/s respectively. This lead to the prediction that the

pond surface flow profile did not represent all the flow file with different depth due to the result of pond with natural shape at different depth in different location. The depth of a treatment wetland is an important design consideration because of its effect on the retention time (Kadlec and Knight, 1996), the ecology (Batzer and Resh, 1992; Mitsch and Gosselink, 2000), and the hydrologic effectiveness, a measure of compliance with h minimum prescribed retention time in a stormwater treatment wetland (Wong and Somes, 1995). If the results of this study are representative of other ponds with natural shape, the effect of vegetation on hydraulic efficiency should not be a factor considered during pond design and management.

With the specific natural pond shape in this study, the effect of flow rate on hydraulic efficiency, in terms of relative centroid is not significant, this result also appeared the same as vegetation as the relative centroid (t_m) is minimal different from its nominal residence time (t_n).. The hydraulic efficiency parameters, e_o and e_p, exhibited smaller changes due to flow rate than due to vegetation. This occurred in any vegetation conditions (0E to 27EH) with changing discharge from 25% to 200% of the designed nominal residence time (4.4 to 45.9 ml/s) the relative HRTD of e_m, e_o and e_p linear increased by 0.46, 10 and 9 times respectively. However, in every discharges (4.4 to 45.9 ml/s) with changing vegetation from 0E to 27EH. This illustrates that the decrease of short-circuiting at higher flow rate but the actual residence times were remain no significant difference. The relationship between flow rate and retention time is expected to have a much greater influence on treatment efficiency (Kadlec and Knight, 1996) than the relationship between flow rate and hydraulic efficiency.

The results of this study demonstrate that different hydraulic efficiency metrics can respond uniquely to the same treatment. In general, short-circuiting is never desirable in a treatment pond or wetland because treatment area is effectively lost (Thackston et al., 1987; Kadlec, 1994). This may not be of concern in pond ecology, but it is of practical concern regarding the performance of a treatment wetland. The centroid of the normalized HRTD, e_m, represents the fraction of the pond that is not short-circuited. Short-circuiting, quantified by e_m, is therefore an unquestionably important factor to be resolved from HRTD analysis

CONCLUSION

It has been demonstrated for a specific laboratory model pond with a “natural” shape the actual residence time is approximately equal to the theoretical residence time, ($t_m = t_n \pm 15\%$ or $e_m = 1 \pm 15\%$), and this parameter is largely insensitive to changes in vegetation and discharge.

However, the values of other parameters, notably the relative first dye arrival at the pond outlet, e_o and the relative peak concentration, $e_{p,}$ were found to be a function of (i) discharge; and to a much lesser extent (ii) magnitude of emergent and submerge vegetation. Change the flow rate from 4.4 to 45.9 ml/s, resulted in increases in e_o and e_p of 10 and 19 times of its value at discharge 4.4 ml/s respectively; whereas the pond with the highest density of submerged plant and the highest coverage (27% of pond cross section) of emergent plants only exhibited increases in e_o and e_p of 1.5 and 1.8 of its value of without vegetation respectively compared to the pond without either emergent or submerged plants.

In comparison, studies of a similarly shaped natural treatment pond, Lyby pond, revealed rather different hydraulic parameters (t_m = 0.5 t_n or e_m = 0.5) from the laboratory models as well as differences in the sensitivity of these parameters to changes in vegetation and discharge rates. These differences reflect in part (i) scaling differences between the two ponds; (ii) differences between analogue and natural vegetation. Further study should focus on an undistorted model which should be based faithfully on the field dimension data.

With regard to the issue of distortion in laboratory models, it is noted, in general, that the scaling differences between the two ponds resulted in the distorted scale model having a larger horizontal scale than vertical scale (30 and 15) when compared with the field site. That is, the distorted model had a relatively exaggerated vertical scale making it effectively much deeper than the field site. In general, distorted models are used widely within the field of hydraulics, without serious problems and they may be considered when departure from geometric similitude serves some definite objective; however, Wornock (1950) identified that distorted models may affect different factors such as velocity, flow details and wave properties; velocities may not be correctly reduced in magnitude and direction, some flow details may not be in similitude, wave refraction and diffraction may not be correctly reproduced and there is potential for unknown scale effects to influence model results as to determining the appropriated degree of distortion can often be very difficult. (Steven (1993) has indicated an example on the river flow models where they often need to be constructed using distorted length scales because the physical dimensions of a typical river cross-section

would geometrically scale in such a way that the model water depth be less than a few centimetres deep. In an undistorted model this would allow surface tension effects in the mode thus invalidating model results. So the main objective of model distortion is to avoid surface tension effects). The disadvantages of using distorted models may be summarised as:

- velocities may not be correctly reduced in magnitude and direction.
- some flow details will not be in similitude
- wave refraction and diffraction may not be correctly reproduced
- there are unfavourable psychological effects on the observer accustomed to viewing geometrically correct models
- there is potential for unknown scale effects to influence model results.
- determining the appropriate degree of distortion can often be difficult.

In the present case, where the discrepancies found between results from model and field data have been ascribed partially to distortion effects, the evidence comes from two directions. Firstly, the exaggerated (higher) depth in the model may be associated with preferentially increased jetting in the upper part of the model, as compared with the field site and, secondly, the distortion can affect the vortex patterns in the flow in such a way as to influence significantly the transport properties of the basin. Evidence for these conclusions come from unpublished CFD (*Fluent*) studies carried out for the full-scale natural pond at Lyby by Stovin (personal communication), where vortex patterns generated in the CFD studies were significantly different from those seen in the laboratory model, with and without vegetation.

The differences between analogue (in the model experiments) and natural vegetation (in the prototype pond) may also play a significant role in determining the discrepancies between the results. The different root and stem structures, irregularity of flow barriers, vegetation material properties (for example, the non-rigidity of the cotton threads and the rigidity of the cattail stems), bio-absorption processes, variety and the non-homogeneity of vegetation distribution may all be expected to play a role in generating discrepancies of the types discussed above. Several authors have investigated aspects of this problem. For example, Struve *et al* (2003) used laboratory flume and two dimensional depth-integrated numerical modeling to study the influence of model mangrove trees on the hydrodynamics in a flume. The study, and others by the same author(s) (Wu *et al*., 2001) highlighted the role of drag but the range of Reynolds numbers covered and, more importantly, the very high vegetation blockage factor used in the study mean that the applicability of the results is limited for the present study.

Tanino & Nepf (2008, 2009) have investigated much smaller vegetation elements than the mangroves considered above, with correspondingly much smaller values of the relevant Reynolds numbers. Tanino and Nepf (2008) used laser-induced fluorescence to measure the lateral dispersion of passive solutes in random arrays of rigid, emergent cylinders of solid volume fraction $\emptyset = 0.010 – \emptyset = 0.35$. Such densities correspond to those observed in aquatic plant canopies and complement those in packed beds of spheres, where $\emptyset > 0.5$. The paper focussed on pore Reynolds numbers greater than 250, for which the laboratory experiments demonstrated that the spatially averaged turbulence intensity and the lateral dispersion coefficient normalized by the mean velocity in the fluid volume and the

cylinder diameter, *d*, are independent of Reynolds number. The experiments indicated that only turbulent eddies with mixing length scale greater than *d* contribute significantly to net lateral dispersion, and that neighbouring cylinder centres must be farther than *r** from each other for the pore space between them to contain such eddies. These results provide insight into the interpretation of the present studies with vegetation (in particular, the conditions under which eddies form around the vegetation elements and the structure of such eddies) but the direct application of the findings of Tanino & Nepf (2008, 2009) to the present work is also limited because of the differences in material (reed beds) and the different ranges of blockage factors used.

At first sight, changes in the external environment during the course of a field experiment might also be expected to lead to discrepancies between the measurements and the results from the controlled laboratory experiments. For example, the field data in the Chapter 6 show that temperature and the inlet discharges were occasionally not constant during some of the trace experiments. However, in fact, from the three field experiments conducted, two had relatively constant conditions; on the 23 March 2008 trace, the discharge decreased from 11 to 7.5 l/s but over a period of over 6 days 12 hours, during which time the temperature changed by 2^{o}C only. On the 17 March 2009 trace experiment, the discharge was quite stable (about 2 l/s for a period of 30 days) even though the problem of mass recovery happened (only 60%) recovered. These findings seem to indicate that physical changes in the external conditions played a minor role in the discrepancies (particularly the mass recover, where the growth of algae on the sensor is assumed to have had a strong effect). In the third case (17 November,

2008), the discharge started to increase gradually up to its highest value due to a sudden, huge rainfall; for this case, it is not surprising that this change could affect the flow considerably.

The mass recovery problem mentioned above is attributed to the following three possible factors:

(i) Algae grow in the pond and affect the reading. This explanation an be rejected because the start and the end background reading were checked to make sure that the gradient of the background readings were negligible every time the trace started and ended.

(ii) Algae and/or biofilms absorb dye and release it slowly during the next trace. This cause was ruled out because it was ensured for all of the traces that the start and end background gradient was negligible.

(iii) The systematic effect of build up of sediment (coating) on the flow through sensors. This is proposed as the most possible reason for the effect on the mass balance, the problem of mass balance occurred when there were long traces which took more than 2 days to be completed.

The comparisons discussed so far have been primarily in terms of the HRTDs from the model and field data. However, the work presented in this dissertation also demonstrates the importance of variances as the key residence time parameters (KRTP, in both dimensional and/or dimensionless) as well as the actual residence time (t_m, or e_m), the first dye arrival (t_o, e_o), the time to peak (t_p, e_p)

and the dispersion variance (σ^2). These are essential KRTP which should be used to understand the flow behaviours as well as the comparisons between laboratory result to field results, mathematical simulation results or computation fluid dynamic results.

There was a common finding between laboratory and field data on the first arrival of dye, e_o, where e_o equals to 1% of its relative nominal retention time (t_n = 1) at very low discharge with no or little vegetation. On the other hand, comparison, studies of a similarly shaped natural treatment pond (Lyby) and its distorted physical scale model revealed rather different times to complete a trace or time to have a complete HRTD. The laboratory experiment took about two times that of the field experiment, where in the field it took only about 2.5 times of its nominal retention time (t_n) but in the laboratory may took about 6 times of its nominal retention time (t_n). These differences reflect in part (i) scaling differences between the two ponds; (ii) differences between analogue and natural vegetation

Note, finally, that the above result and interpretation did not take into account the uncertainties associated with, for instance, the accuracy of measurement of the loss of dye due to vegetation in the field or in the laboratory; the problem of the trace's background removal may also cause uncertainty in the distribution of dye mass.

CHAPTER: VII

7 Recommendation

7.1 Lessons learn from the current study for further work

Throughout many experimental runs conducted in field and distorted physical scale pond. There are few tips that need to be considered for further work, firstly the extension of the current study on the scale model but we should not use as distorted scale; Secondly, more traces should be conducted in the field pond at least 24 traces within two years period which the instrument should be improve out of the interference from such leaches.

The understanding gained from the current study of pond shape, discharge, and vegetation effects shows that more investigations should be done through a combination of field measurements, full scale laboratory experiment, numerical simulations and computational fluid dynamics (CFD). PIV alone is not sufficient to

explain in detail the 3D flow field in the side of the pond but its result may help to validate predictions from Computational Fluid Dynamics (CFD) models. There are many commercial CFD packages available but *Fluent* software has been used extensively in this area of research. Reference to the work of Stovin (University of Sheffield) has already been made in this regard, when discussing discrepancies between distorted laboratory model data and predicted flows in Lyby pond. In this case, the *Fluent* software showed a similar surface flow fields to those collected with PIV where a first and second vortex were generated at sections 1/3 and 2/3 of the pond. However, the discrepancies illustrated by the CFD experiments (see above) illustrate that, for further studies, there is a requirement for the grid to be far more smaller than that used previously and it should use the detailed scaling from the physical scale (distorted) model as well as the detailed survey from Lyby pond.

Lesson learn from current study shows that many natural ponds exhibit short-circuiting effects, which may be exacerbated mainly by vegetation and some by discharge and pond geometry.

7.2 Author further points of interest

Further PIV studies on the physical scale model should be conducted to focus on the vertical and horizontal flow within different layers and different cross sections, as these could show different flow profile and velocities from those measured at the surface. Such an approach would illuminate the following concerns:

1. Different pond depths will give different flow fields in different subsurface levels; this result is very important when seeking to understand and compare the behaviour of different discharge and vegetation conditions.
2. Not only subsurface variability of the horizontal flow fields needs to be investigated but also there is a need to investigate the vertical flow fields at different sections, since portions of the flow are undoubtedly three-dimensional. As indicated from previous studies on different ponds, shape, depth, vegetation and discharge may all contribute to the vertical penetration of vortex motions and trapping.
3. With the surface flow field alone, it is not possible to assess mixing process in the whole pond, so more information is needed (namely, from PIV studies on subsurface horizontal flow at different levels as well as vertical flow fields at different section of the pond). The fully 3D information on the pond flow field will than help to assess more completely the mixing processes in the pond, such that it may be possible to explain if there is surface jetting, secondary or tertiary circulation in the pond, vertical penetration of vortex motion and the existence of trapping or dead zones in the pond.

Further research should investigate on the new field pond, where the field pond design should be designed base on the detail data of distorted physical scale model in Warwick and then fully scaled up to 30:30:30 or 40:40:40 of X, Y and Z dimension.

8 References

Agunwamba, J., Field pond performance and design evaluation using physical Models. *Water Research*, **26** (10), 1992, pp. 1403-1407.

Agunwamba, J.C., Dispersion number determination in waste stabilization ponds, *Journal of Air, Water and Soil Pollution*, **9**, 3-4, 1992, pp. 241-247.

Agunwamba, J.C., Egbuniwe, N. and Ademiluyi, J.O., Prediction of the dispersion number in waste stabilization ponds. *Water Research* **26**, 1992, pp. 85–89.

Almasi, A. and Pescod, M., Wastewater treatment mechanisms in anoxic stabilization ponds. *Water Science and Technology*, **33**(7), 1996, pp. 125-132.

Arceivala, S. J., Hydraulic modeling for waste stabilization ponds (discussion), *Journal of Environmental. Engineering*. **109**, 1, 1981, pp. 265–268.

Beer, T., and Young, P.C., Longitudinal dispersion in natural streams. *Journal of Environmental Engineering*, **109**, 1983, pp.769-776.

Bojcevska, R., Hydraulic tracer study in a free-water surface flow constructed wetland /system treating sugar factory wastewater in Western Kenya, internal environmental report, 2005, pp. 1-6.

Brissaud, S., Lazarova, V., Ducoup, C., Joseph, C., Lewine, B. and Tournoud, M.G., Hydrodynamic behaviour and faecal coliforms removal in maturation Pond. *Journal of Water Science and Technology*, **42** (10), 2000, pp. 119-126.

British Standard Institution, BS 3680: Part 1, BS 3680 Part 4C, ISO 4373, Method of Measurement of Liquid in Open Channels, Weirs and Flumes. Method using Thin Plate Weirs, CPI/113, ISBN 0580122344, 1981, pp.34.

Chapple, L., *A Study of Bacterial Kinetics and Hydraulic Short-circuiting Master*

PhD Thesis; Department of Civil Engineering, University of Queensland; Brisbane, Australia.

Chapra, S., *Surface Water Quality Modelling*. The McGraw-Hill Companies, Inc., 1997.

CIRIA (Construction Industry Research and Information Association**),** *Sustainable Urban Drainage Systems - Design Manual for England and Wales,* ISBNC 532 0 860175235, 1999.

Charbeneau, R.J., *Groundwater Hydraulics and Pollutant Transport*, Prentice Hall, Upper Saddle River, New Jersey, 2000.

Chow, V., *Channel Hydraulics*. McGraw Hill, New York, USA, 1959.

Walker D. J., Modelling residence time in stormwater ponds. *Ecological Engineering* **10**, 1998, pp. 247-262.

Douglas, J., Gasiorek, J., and Swaffield, J., *Fluid Mechanics*, Longman Scientific and Technical, 1995.

Duncan,H.P., Urban stormwater treatment by storage: a statistical overview. CRC for Catchments Hydrology Report, Melbourne, Australia, 1997.

Ferrara, R.A., and Harleman, D.R.F., Hydraulic modelling for waste stabilization ponds, *Journal of Environmental Engineering*, **107-4**, 1981, pp. 817-831.

Finney, B.A., and Middlebrooks, E.J. Facultative waste stabilization pond design. *Journal of the Water Pollution Control Federation*. **52**, 1, 1980, pp 134-147.

Fischer, H.B., A note on the one-dimensional dispersion model. *International Journal on Air and Water Pollution*, **10**, 1967, pp. 443-452.

Frederick, G. and Lloyd, B., An evaluation of retention time and short-circuiting in waste stabilisation ponds using *Serratia marcescens* bacteriophage as a tracer. *Water Science and Technology*, **33-7**, 1996, pp.49-56.

Grue, J., Jensen, A., Rusås, P. O., and Sveen, J.K., Properties of large amplitude internal waves. *Journal of Fluid Mechanics*, **380**:, 1999, pp 257-278 .

Gurlek, C., and Sahin, B., Particle image velocimetry studies around a rectangular body close to a plane wall. Journal of *Flow Measurement and Instrumentation*, 21:, 2010, pp 322-329.

Hammer, M.J., *Water and Wastewater Technology*, Prentice Hall, Englewood Cliffs, New Jersey, 1986.

Hey, D.L., A.L. Kenimer, and K.R. Barrett., Water quality improvement by four experimental wetlands. *Ecologycal Engineering,* **3**, 1994, pp. 381–397.

Hoyt, J.W. and Sellin, R. H. J., A comparison for tracer and PIV results in visualizing water flow around a cylinder close to the free surface, *Experiments in Fluids*, **28**, 2000, pp. 261-265.

Ismail, A. and Ulrich, L., Large scale PIV-measurements on the water surface of turbulent open-channel flow, Laboratory of Environmental Hydraulics, Switzerland, 2007, pp. 1-6.

IWA., Constructed wetlands for pollution control: Processes, performance, design and operation. IWA Specialist Group on Use of Macrophytes in Water Pollution Control, IWA Publishing, London, UK, 2000.

Jansons K., German J. and Howes T., Evaluating hydraulic behaviour and pollutant removal in various storm water treatment pond configurations, 10th International Conference on Urban Drainage, Dopenhagen, Denmark, 2005, pp. 21-26.

Jensen, A., Sveen, J.K., Grue, J., Richon, J-B., and Gray, C., Accelerations in water waves by extended particle image velocimetry. *Experiments in Fluids*, **30**, 2001, pp. 500-510.

Johan, K., Wörman, A., Johansson, H., Lindahl A., Controlling factors for water residence time and flow patterns in Ekeby treatment wetland. *Advances in Water Resources*, **30**, 2007, pp. 838-850.

Kadlec, R.H. and Knight, R.L., *Treatment Wetlands*. CRC Press Inc., Boca Raton, Florida,1996.

Kadlec, R.H., Detention and mixing in free surface water wetlands. *Journal of Ecological Engineering*, **3**, 1994, pp. 345–380.

Kobus, H., (Editor), *Hydraulic Modelling*. Pitman Books; London, 1980.

Konyha, K.D., R.W.Skaggs, and Gilliam, J.W., Effects of drainage and water management practices on hydrology. *Journal of Irrigation Drainage Engineering,* **118**, 1992, pp. 807-819.

Levenspiel, O., *Chemical Reaction Engineering*. John Wiley and Sons; New York, USA, 1972.

Levenspiel O., Chemical Reaction Engineering; *An Introduction to the Design of Chemical Reactors*, John Wiley and Sons inc. 1966, pp. 242-256.

MacDonald, R. and Ernst, A., Disinfection efficiency and problems associated with maturation ponds. *Journal of Water Science and Technology*, 18-10, 1986, pp.569-577.

Mangelson, K.A. and Watters, G.Z., Treatment efficiency of waste stabilization Ponds. *Proc. Amer. Soc. Civil Engineers.* **98** , SA2, 1972, pp. 407–425.

Mara, D., Mills, S., Pearson, H. and Alabaster, G. Waste stabilization ponds: A viable alternative for small community treatment systems. *Journal of the IWEM*, **6**, 1992, pp. 72-79.

Marais, G.v.R., New factors in the design, operation and performance of waste stabilization ponds. *Bulletin of the World Health Organization*. **34**, 1966, pp.

737–763.

Marecos do Monte, M. and Mara, D., The hydraulic performance of waste stabilisation ponds in Portugal. *Journal Water Science and Technology*, **19-12**,1987, pp. 219-277.

Marecos do Monte., Hydraulic Dispersion in Waste Stabilization Ponds in Portugal. PhD Thesis, University of Leeds, Leeds, 1985.

Moreno, M., A tracer study of the hydraulics of facultative stabilization ponds, *Journal of Water Research*, **24-8**, 1990, pp. 1025-1030.

Nameche, T. and Vasel, J., Hydrodynamic studies and medelization for aerated lagoons and waste stabilization ponds. *Journal of Water Research*, **32-10**, 1998, pp. 3039-3045.

Patten, B.C., Introduction and overview. In: B.C. Patten (Editor), *Wetlands and Shallow Continental Water Bodies*. SPB Academic Publishing, The Hague, 1990, pp. 3-8.

Pedahzur, P., Nasser, A., Dor, I., Fattal, B. and Shuval, H., The effect of baffle installation on the performance of a single cell pond. Water Science and Technology, **27**, 1993, pp 45-52.

Persson J., The hydraulic performance of ponds of various layouts. *Urban Water* **213**, 2000,pp. 243-250.

Persson J., Wittgren, H.B., How hydrological and hydraulic conditions affect performance of ponds. *Journal of Ecological Engineering*, **21**, **4-5**,2004, pp. 259-269.

Polprasert, C., Bhattarai, K.K., Dispersion model for waste stabilization ponds. *Journal of Environmental Engineering*, **111-1**, 1985, pp. 45-59.

Raffel, M., Willert, C., Kompenhans, J., *Particle Image Velocimetry: A Practical*

Guide. Springer-Verlag. Berlin, 1998.

Reddy KR, Patrick WH Jr., Nitrogen transformations and loss in flooded soils and sediment interface in wetlands. *Limnology and Oceanography*, **34(6)**, 1984, pp. 1004-1013.

Richter, K.M., *Constructed Wetlands for the Treatment of Airport De-ice*. PhD thesis, University of Sheffield, UK, 2003.

Rostami, M., Ardeshir, A., Ahmadi, G. THOMAS, P.J., Development of a low cost and safe PIV for mean flow velocity and Reynolds stress measurements. *IJE Transactions* A, **20-2**, 2007, pp. 105-116.

Salter, H.E., Boyle, L., Ouki, S.K., Quarmby, J. and Williams, S.C., Tracer study and profiling of a tertiary lagoon in the United Kingdom: II, *Journal of Water Research*, **33-18**, 1999, pp. 3782-3788.

Schmid, B.H., Hengl, M.A. and Stephan, U., Density effects on salt tracer breakthrough curves from constructed wetland ponds, *Nordic Hydrology*, **35**, 2004, pp. 237-250.

Shelef, G. and Azov, Y., High-rate oxidation ponds; the Israeli experience. *Water Science and Technology*, **42(10-11)**, 2000, pp. 343-348.

Shelef, G. and Kanarek, A., Stabilization ponds with recirculation. *Journal of Water Science and Technology*, **32-12**, 1995, pp. 389-397.

Shilton A., *Pond Treatment Technologies*, IWA Publishing, 2005.

Shilton, A., Eilks, T., Smyth, J. and Bickers, P., Tracer studies on a New Zealand waste stabilisation pond and analysis of treatment efficiency. *Journal of Water Science and Technology*, **42-10**, 2000, pp. 343-348.

Shilton, A., *Studies into the Hydraulics of Water Stabilisation Ponds*, PhD thesis, Massey University, New Zealand, 2001.

Stockdale, A., Recent trends in urbanisation and rural population in Northern Ireland. *Irish Geography*, **24**, 1991, pp. 70–80.

Streeter V.L., Wyle E.B., Bedford K.W., *Fluid Mechanics*, 9th Edition, McGraw Hill, New York, 1998,

Struve, J., Falconer, R. A., Wu, Y., Influence of model mangrove trees on the hydrodynamics in a flume. *Estuarine, Coastal & Shelf Science*, **58**, 2003,163-171.

Sveen, J.K., and Cowen, E.A., Quantitative image techniques and their application to wavy flow. In Grue, J., Liu, P.L-F., and Pedersen, G.K., (Editors), *PIV and Water Waves*, World Scientific, 2004.

Tchobanoglous G., Schroeder D.A., *Characteristics, Modelling and Modification*, Prentice Hall, New York, 1985.

Thirumurthi, D. , Design criteria for waste stabilization ponds. *Journal of the Water Pollution Control Federation*. **46-9**, 1974, pp. 2094–2106.

Thirumurthi, D. and Nashashibi, O., A new approach for designing waste stabilization ponds. *Water and Sewage Works*, 114-R, 1967, pp. 208-218.

Thirumurthi, D., Biodegradation in waste stabilization ponds (facultative lagoons). *Biological Degradation of Wastes*, Elsevier, London, England, 1991, pp. 231-246.

Uhlmann, D., BOD removal rates of waste stabilization ponds as a function of loading, retention time, temperature and hydraulic flow pattern. *Journal of Water Research*, **12-3**, 1979, pp. 193-200.

Uhlmann, D., Recknagel, F., Sandring, G., Schwarz, S. and Eckelmann, G., A new design procedure for waste stabilization ponds. *Journal of the Water Pollution Control Federation*, **55-10**, 1983, pp. 1252-1255.

Uluatam, S. and Kurum, Z., Evaluation of the wastewater stabilization pond at the

METU treatment plant. *International Journal of Environmental Studies*, **41**, **1-2**, 1992, pp. 71-80.

USEPA, Emerging technology assessment: Preliminary status of airplane fluid recovery system, Report No. EPA/832-R-95-005, Office of Waste Management, 1995.

Vorkas, C.A. and Lloyd, B.J., The application of a diagnostic methodology for the identification of hydraulic design deficiencies affecting pathogen removal, *Journal of Water Sciences and Technology*, **42-10-11**, 2000, pp. 99-109.

Vymazal, J., Introduction. In: J. Vymazal, H. Brix, P.F. Cooper, M.B. Green and R. Haberl (Editors), *Constructed Wetlands for Wastewater Treatment in Europe,* Bakhyuys, Leiden, NL,1998, pp. 1-16.

Westterweel, J., *Digital Particle Image Velocity- Theory and Application*. PhD Thesis, Delft University of Technology, The Netherlands, 1993.

Wood, M., *Development of Computational Fluid Dynamic Models for the Design of Waste Stabilization Ponds*, PhD Thesis, University of Queensland, Australia, 1997.

Wood, T., Interpretation of laboratory-scale waste stabilization pond studies. *Water Science and Technology,* **19 (2)**, 1987, pp. 195-203.

Wörman, A., Kjellin, J., Johansson, H. and Lindahl, A., Controlling factors for water residence time and flow patterns in Ekeby treatment wetland, Sweden. *Journal of Advances in Water Resources*, **30**, 2007, pp. 838-850.

Wörman, A. and Kronnäs, V., Effect of pond shape and vegetation heterogeneity on flow and treatment performance of constructed wetlands. *Journal of Hydrology*, **301**, 2005, pp. 123-138.

Wu, Y., Falconer, R.A., Struve, J., Mathematical modeling of tidal currents in

mangrove forests, *Environmental Modelling & Software*, **16**, 2001, 19-29,.

Wu, J.S., Holman, R.E. and Dorney, J.R., Systematic evaluation of pollutant removal by urban wet detention ponds. *ASCE Journal of Environmental Engineering*. **122, 11**, 1996, pp. 983–988.

Yong, P.C., Data-based mechanistic modelling of environmental systems. International Federation on Automatic Control (IFAC) Workshop on Environment Systems, Tokyo, Japan, 2001.

Young, P.C., and Wallis, S.G., The aggregated dead zone (ADZ) model for dispersion in rivers, International Conference on *Water Quality Modelling in the Inland Natural Environment*. BHRA, Bedford, England, Bournemouth, England, 1986, pp. 421-433.

9 Appendix A: Summary of experiment set up at laboratory physical scale pond, instrument calibration & background deduction

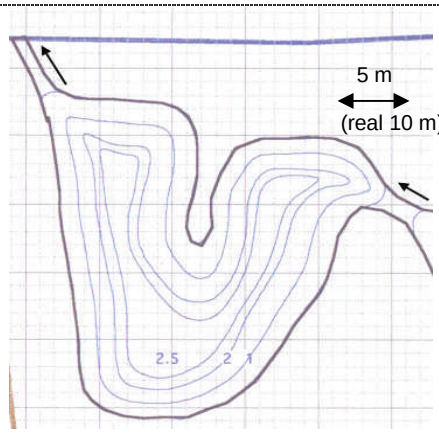
5 m
(real 10 m)
2.5
2
1


Lyby Pond

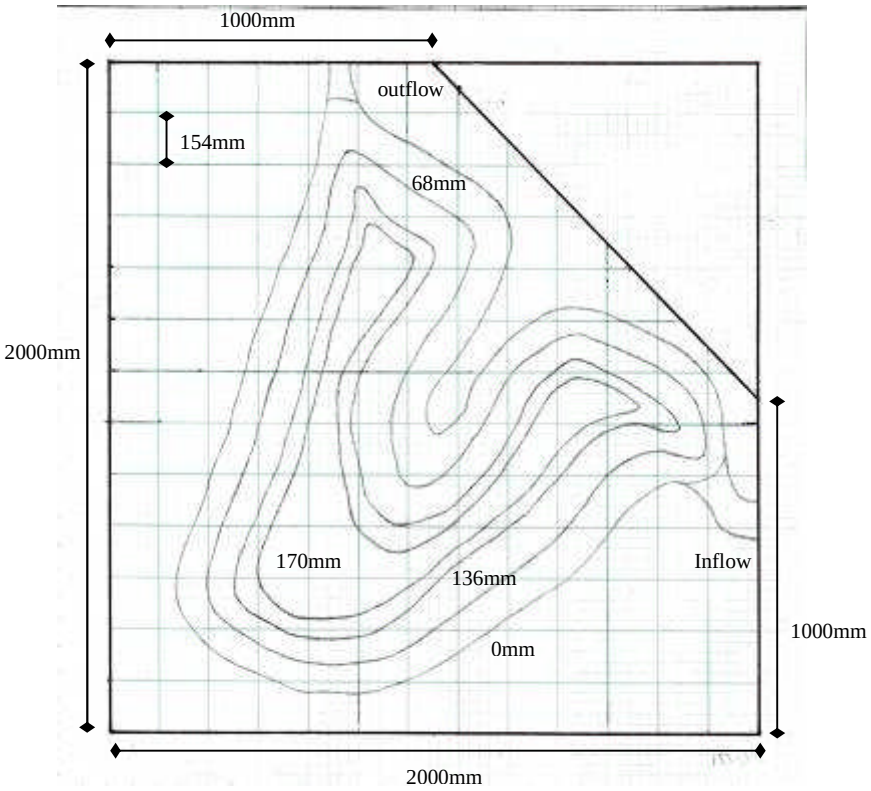
1000mm
outflow
154mm
68mm
2000mm
170mm
136mm
Inflow
0mm
1000mm
2000mm

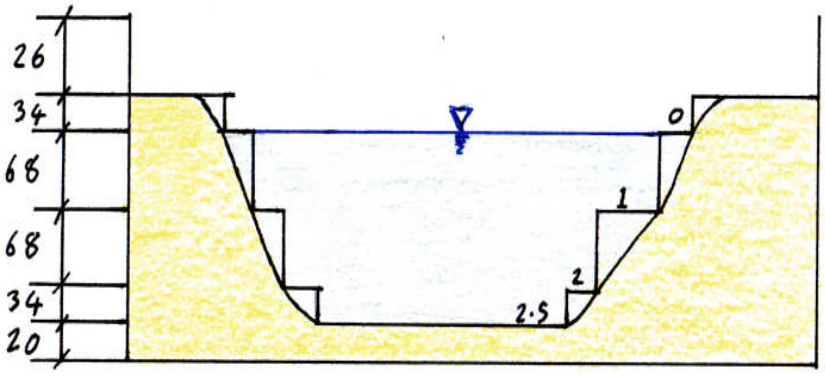
26
34
68
68
34
20
0
1
2
2.5

Figure 9-1. Pictures of design and build Physical Scale Model (3rd year student, Ian Chanler).

Figure 9-2. Pictures of Rhodamine dye test trace at Physical Scale Model Pond.

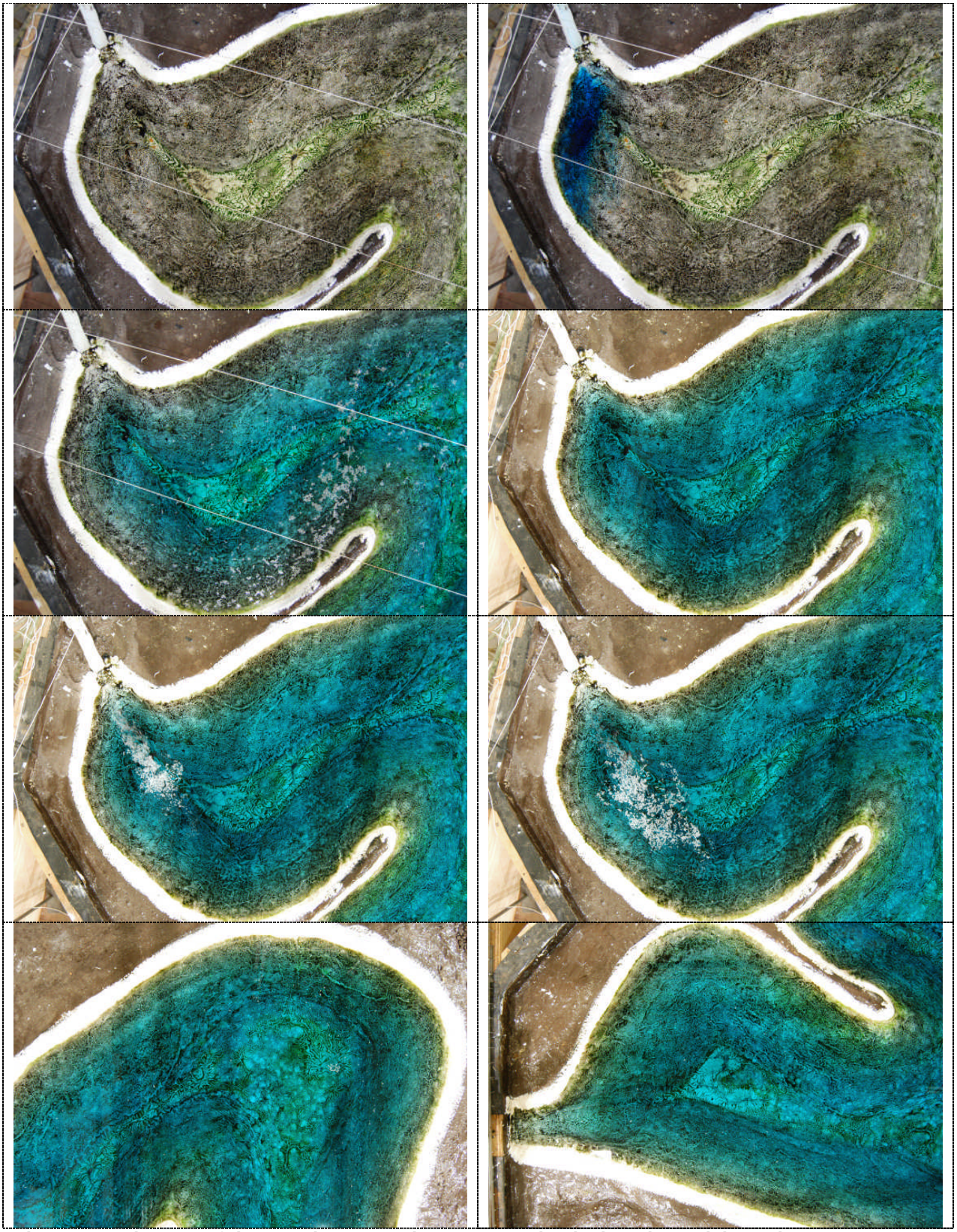

Figure 9-3. Pictures of dye pond water and PIV test at Physical Scale Model Pond.

Figure 9-4. Pictures of Rhodamine dye trace test and test of vegetation set up.

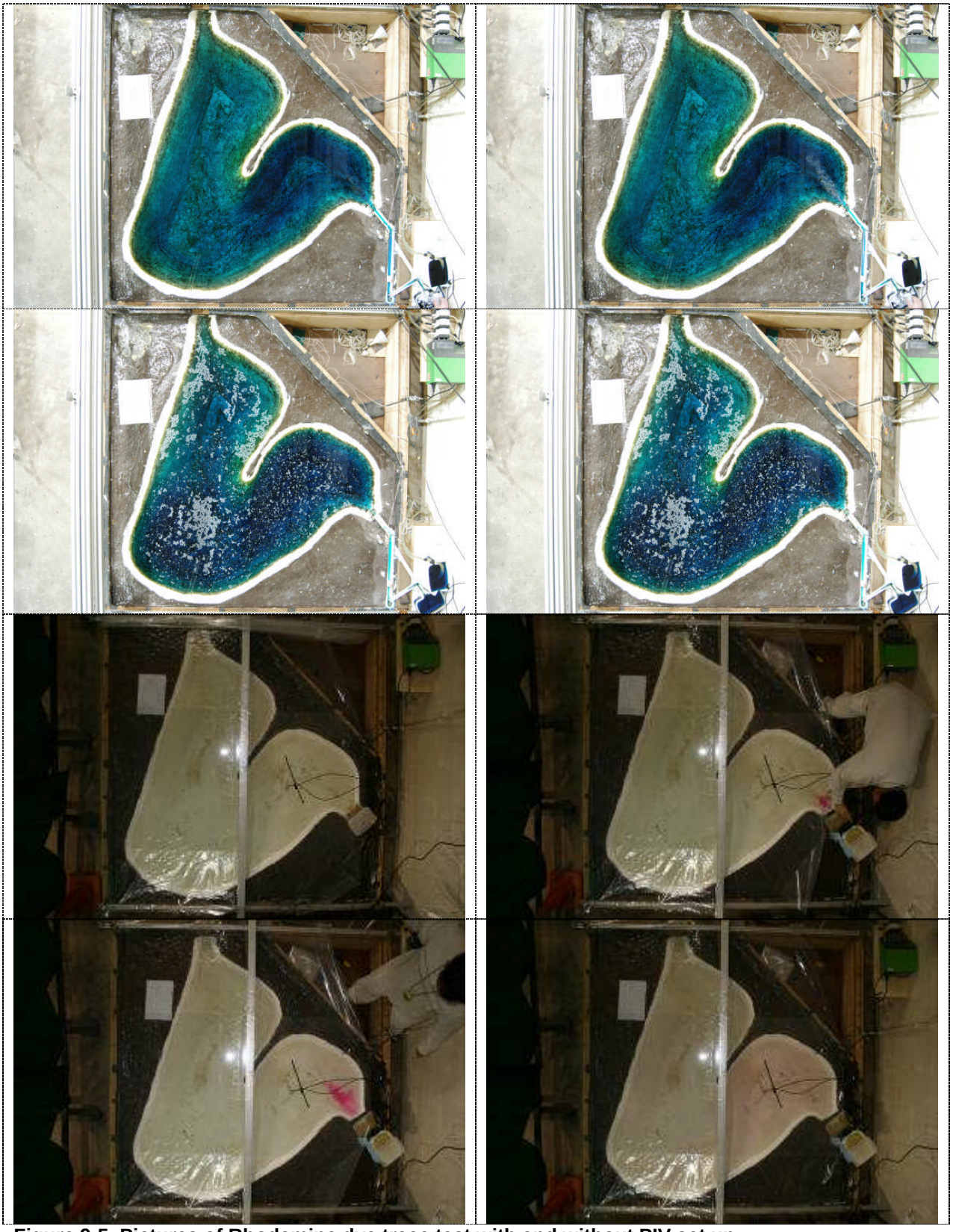

Figure 9-5. Pictures of Rhodamine dye trace test with and without PIV set up.

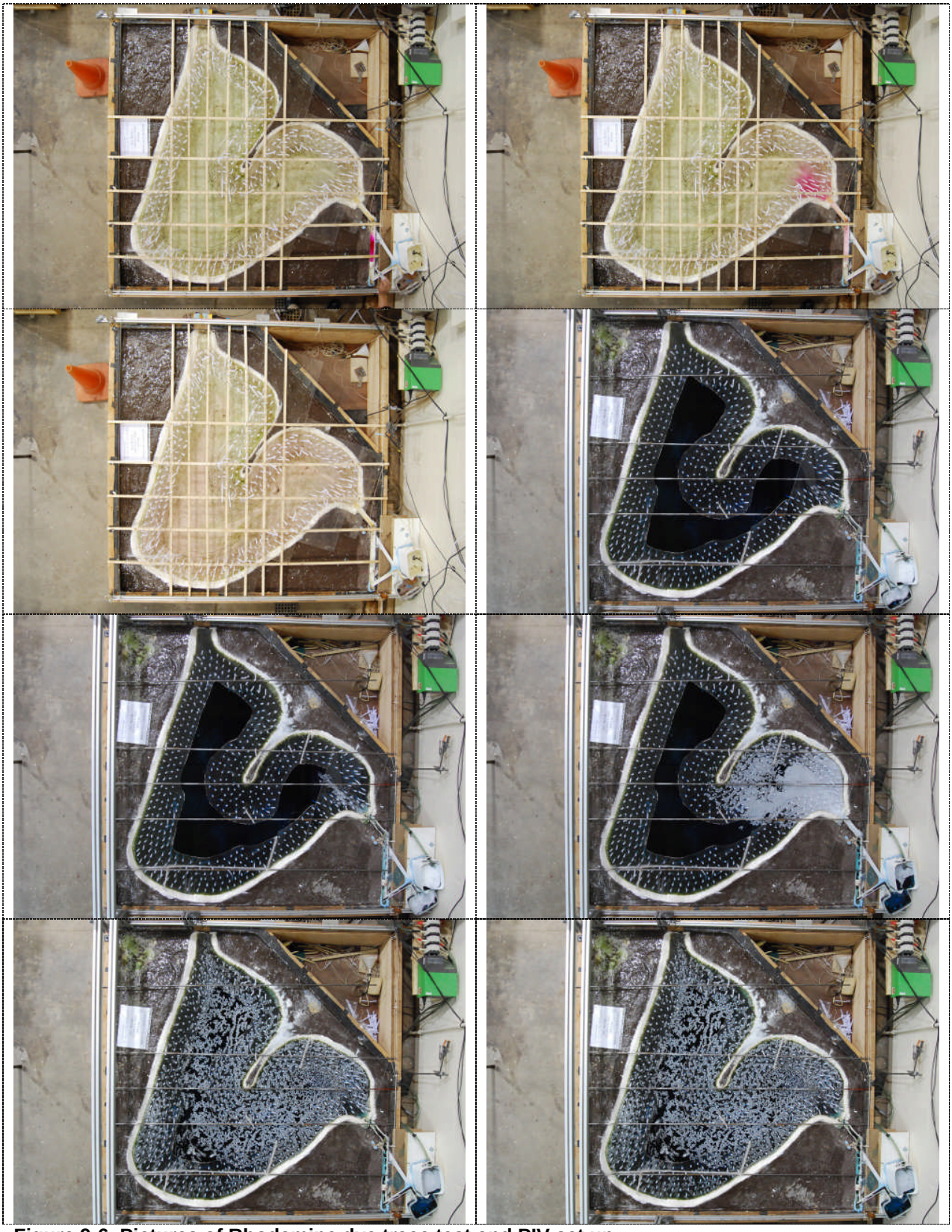

Figure 9-6. Pictures of Rhodamine dye trace test and PIV set up.

Figure 9-7. Pictures of Pond break down and Pond repair.

Figure 9-8. Pictures of Physical Scale Pond after completed all experiments.

Summary of experiment in laboratory physical scale pond with detail of instrument calibration and equation of background deduction of each experiment.

No	Run No	Discharge, Qin (ml/s)	Tracing Date (D:M:Y)	Time of intected Dye (hh:mm:ss)	10-AU Calibration Equation	BG deduction Equation (20 x 20 background points)	Veg. Condition
20	24.5	17.21	12-Feb-09	12:44:00	y = (253.16*x) - 5.0633	y = 1E-05x + 0.0383	0E
98	32.5	22.95	12-Feb-09	15:03:00	y =(253.16*x) - 5.0633	y = -5E-05x + 0.3421	0E
21	32.7	22.96	13-Feb-09	15:03:00	y = (253.16*x) - 5.0633	y = 5E-05x + 0.2166	0E
68	32.6	22.95	16-Feb-09	12:44:00	y = (253.16*x) - 5.0633	y = 3E-05x + 0.1086	0E
69	17.5	11.48	18-Feb-09	15:04:00	y =(253.16*x) - 5.0633	y = 0.0001x + 0.2485	0E
5	17.6	11.48	20-Feb-09	10:30:00	y = (253.16*x) - 5.0633	y = -6E-05x + 0.5181	0E
43	1.1	4.4	20-Feb-09	10:30:00	y = (253.16*x) - 5.0633	y = -3E-05x + 0.5665	0E
6	1.4	4.4	26-Feb-09	19:40:00	y =(253.16*x) - 5.0633	y = 4E-05x + 0.5658	0E
45	1.2	4.4	26-Feb-09	19:05:00	y = (253.16*x) - 5.0633	y = 8E-05x + 0.3304	0E
7	1.5	4.4	2-Mar-09	19:05:00	y =(253.16*x) - 5.0633	y = 8E-05x + 0.3484	0E
11	1.3	4.4	1-May-09	7:25:00	y = (253.16*x) - 5.0633	y = -2E-05x + 0.7242	0E
42	2	4.4	19-Mar-09	9:23:00	y = (253.16*x) - 5.0633	y = -7E-06x - 0.0357	11E
50	9.1	5.74	25-Mar-09	20:07:00	y =(253.16*x) - 5.0633	y = 7E-05x - 0.2225	11E
101	33	22.96	30-Mar-09	19:48:00	y = (253.16*x) - 5.0633	y = 0.0005x - 0.592	11E
64	18	11.48	2-Apr-09	17:10:00	y = 288.21x + 1.0809	y = -4E-06x + 4.9324	11E
73	25.1	17.21	1-Apr-09	13:28:00	y = 288.21x + 1.0809	y = 6E-05x + 4.8466	11E
38	3	4.4	6-Apr-09	18:52:00	y = 288.21x + 1.0809	y = 0.0002x + 4.9131	22E
48	10.1	5.74	22-Apr-09	19:06:00	y = 288.21x + 1.0809	y = 4E-05x + 4.8358	22E
70	19	11.48	27-Apr-09	17:58:00	y = 288.21x + 1.0809	y = -3E-05x + 4.8388	22E
78	26.1	17.21	29-Apr-09	13:30:00	y = 288.21x + 1.0809	y = -0.0002x + 5.1164	22E
100	34	22.96	30-Apr-09	12:06:00	y = 288.21x + 1.0809	y = -5E-05x + 5.3867	22E
93	35	22.96	1-May-09	12:07:00	y = 288.21x + 1.0809	y = -0.0001x + 5.5382	27E
74	27.1	17.21	2-May-09	13:20:00	y = 288.21x + 1.0809	y = -0.0001x + 5.5396	27E
66	20	11.48	4-May-09	13:37:00	y = 288.21x + 1.0809	y = 0.0001x + 5.1356	27E
46	11.4	5.74	6-May-09	12:45:00	y = 288.21x + 1.0809	y = -4E-05x + 5.54	27E
39	4	4.4	9-May-09	18:25:00	y = 288.21x + 1.0809	y = -0.0001x + 7.2574	27E
44	5	4.4	20-May-09	15:13:00	y = 288.21x + 1.0809	y = 3E-06x + 6.1162	27EL
51	14	5.74	25-May-09	14:53:00	y = 288.21x + 1.0809	y = -2E-05x + 6.442	27EL
71	21	11.48	29-May-09	19:58:00	y = 288.21x + 1.0809	y = -0.0011x + 9.1878	27EL
79	29	17.21	31-May-09	15:18:00	y = 288.21x + 1.0809	y = -0.0004x + 7.2612	27EL
92	36	22.96	1-Jun-09	17:45:00	y = 288.21x + 1.0809	y = -0.0005x + 8.1905	27EL
47	37	22.96	8-Jun-09	20:05:00	y = 288.21x + 1.0809	y = -0.0005x + 8.1958	27EM
94	30	17.21	2-Jun-09	19:05:00	y = 288.21x + 1.0809	y = 3E-05x + 6.7431	27EM
75	15	5.74	4-Jun-09	13:04:00	y = 521.55x - 9.5809	y = 0.0002x + 0.4271	27EM
67	22	11.48	6-Jun-09	14:43:00	y = 521.55x - 9.5809	y = -0.0002x + 1.1254	27EM
40	6	4.4	11-Jun-09	19:25:00	y = 521.55x - 9.5809	y = -8E-06x + 2.3339	27EM
41	7	4.4	18-Jun-09	10:59:00	y = 523.1x - 10.603	y = 0.0002x + 0.138	27EH
49	16	5.74	24-Jun-09	20:05:00	y = 524.31x - 11.407	y = -9E-05x + 2.5225	27EH
72	23.2	11.48	30-Jun-09	11:47:00	y = 638.33x - 16.489	y = 0.0009x - 2.6475	27EH
65	23.1	11.48	2-Jul-09	9:20:00	y = 638.33x - 16.489	y = -6E-06x - 0.1658	27EH
76	31.76	17.21	5-Jul-09	16:20:00	y = 684.92x - 17.693	y = 0.0003x - 1.0817	27EH
95	38.1	22.96	6-Jul-09	16:26:00	y = 684.79x - 17.689	y = 0.0014x - 2.024	27EH
96	38.2	22.96	7-Jul-09	9:35:00	y = 684.79x - 17.689	y = -0.0012x - 0.5718	27EH
97	38.3	22.96	8-Jul-09	12:21:00	y = 684.79x - 17.689	y = 0.0012x - 2.4901	27EH

Table 9-1. Summary of traces using different four calibration equations.

No	Run No	Discharge, Qin (ml/s)	Tracing Date (D:M:Y)	Time of injected Dye (hh:mm:ss)	10-AU Calibration Equation	BG deduction Equation (20 x 20 background points)	Veg. Condition
12	24.1	17.21	16-Feb-08	11:20:00	Y= (32.623*x) - 3.2349	y = -1E-07x - 0.8333	0E
13	24.2	17.21	18-Feb-08	17:27:00	Y= (32.623*x) - 3.2349	y = 1E-05x - 0.7151	0E
14	24.3	17.21	20-Feb-08	11:40:00	y= (32.623*x) - 3.2349	y = -3E-05x - 0.6652	0E
15	24.4	17.21	22-Feb-08	16:30:00	Y= (32.623*x) - 3.2349	y = 2E-05x - 0.7465	0E
1	17.1	11.48	24-Feb-08	15:06:00	Y= (32.623*x) - 3.2349	y = 6E-06x - 0.5773	0E
2	17.2	11.48	27-Feb-08	8:25:00	Y= (32.623*x) - 3.2349	y = 2E-05x - 0.5527	0E
3	17.3	11.48	29-Feb-08	10:40:30	Y= (32.623*x) - 3.2349	y = 7E-06x - 0.4787	0E
4	17.4	11.48	2-Mar-08	11:15:00	Y= (32.623*x) - 3.2349	y = 2E-05x - 0.4589	0E
8	8.1	5.74	24-Apr-08	18:39:00	Y= (32.623*x) - 3.2349	y = -1E-05x + 0.4397	0E
9	8.2	5.74	27-Apr-08	13:09:00	Y= (32.623*x) - 3.2349	y = 3E-05x + 0.4387	0E
10	8.3	5.74	29-Apr-08	20:19:00	Y= (32.623*x) - 3.2349	y = 7E-05x + 0.4106	0E
26	43.1	34.43	13-May-08	10:20:00	Y= (32.623*x) - 3.2349	y = 7E-06x + 0.3345	0E
27	43.2	34.43	13-May-08	18:57:00	Y= (32.623*x) - 3.2349	y = -9E-05x + 0.3103	0E
28	43.3	34.43	14-May-08	10:54:00	Y= (32.623*x) - 3.2349	y = 0.0003x + 0.2455	0E
29	43.4	34.43	14-May-08	18:04:00	Y= (32.623*x) - 3.2349	y = -0.0001x + 0.3442	0E
22	39.1	28.69	15-May-08	10:06:00	Y= (32.623*x) - 3.2349	Y= (32.623*x) - 3.234	0E
23	39.2	28.69	15-May-08	19:40:10	Y= (32.623*x) - 3.2349	y = 0.0001x + 0.3589	0E
24	39.3	28.69	16-May-08	18:36:30	Y= (32.623*x) - 3.2349	y = 0.0003x + 0.4758	0E
16	32.1	22.95	17-May-08	22:26:10	Y= (32.623*x) - 3.2349	y = 0.0001x + 1.0313	0E
25	39.4	28.69	17-May-08	12:45:00	Y= (32.623*x) - 3.2349	y = 0.0004x + 0.792	0E
17	32.2	22.95	18-May-08	14:28:00	Y= (32.623*x) - 3.2349	y = 0.0001x + 1.1232	0E
18	32.3	22.95	19-May-08	9:45:00	Y= (32.623*x) - 3.2349	y = 0.0002x + 1.3111	0E
19	32.4	22.95	19-May-08	22:15:00	Y= (32.623*x) - 3.2349	y = 0.0001x + 1.3994	0E
34	51.1	45.9	20-May-08	19:10:00	Y= (32.623*x) - 3.2349	y = -0.0001x + 1.6225	0E
35	51.2	45.9	21-May-08	9:30:00	Y= (32.623*x) - 3.2349	y = 0.0002x + 1.5448	0E
36	51.3	45.9	21-May-08	15:17:30	Y= (32.623*x) - 3.2349	y = 2E-05x + 1.5957	0E
30	48.1	40.15	22-May-08	18:55:00	Y = (32.623*x) - 3.2349	y = -3E-05x + 1.5179	0E
37	51.4	45.9	22-May-08	8:55:00	Y= (32.623*x) - 3.2349	y = -2E-05x + 1.5293	0E
31	48.2	40.15	23-May-08	11:46:05	Y= (32.623*x) - 3.2349	y = -0.0001x + 1.543	0E
32	48.3	40.15	23-May-08	19:07:50	Y= (32.623*x) - 3.2349	y = -8E-05x + 1.4835	0E
33	48.4	40.15	24-May-08	12:24:30	Y= (32.623*x) - 3.2349	y = -8E-05x + 1.4192	0E
77	8.4	5.74	6-Feb-09	17:45:00	Y= (32.623*x) - 3.2349	y = -1E-05x + 0.4363	0E
124	49.1	40.15	3-Jul-08	17:40:05	Y= (32.623*x) - 3.2349	y = -5E-05x + 1.1748	11E
125	49.2	40.15	4-Jul-08	9:45:00	Y= (32.623*x) - 3.2349	y = -7E-05x + 1.133	11E
126	49.3	40.15	4-Jul-08	17:20:05	Y= (32.623*x) - 3.2349	y = -4E-05x + 1.1078	11E
111	44.1	34.43	5-Jul-08	11:45:05	Y= (32.623*x) - 3.2349	y = 3E-05x + 1.0663	11E
112	44.2	34.43	5-Jul-08	21:18:10	Y= (32.623*x) - 3.2349	y = 3E-05x + 1.1003	11E
113	44.3	34.43	6-Jul-08	10:58:10	Y= (32.623*x) - 3.2349	y = 6E-05x + 1.1098	11E
105	40.1	28.69	7-Jul-08	10:18:10	Y= (32.623*x) - 3.2349	y = 5E-05x + 1.1177	11E
106	40.2	28.69	7-Jul-08	22:00:05	Y= (32.623*x) - 3.2349	y = 1E-05x + 1.1347	11E
83	25.2	17.21	9-Jul-08	22:02:10	Y= (32.623*x) - 3.2349	y = 3E-05x + 1.1346	11E
107	40.3	28.69	9-Jul-08	9:48:05	Y= (32.623*x) - 3.2349	y = 4E-05x + 1.119	11E
84	25.3	17.21	10-Jul-08	9:48:05	Y= (32.623*x) - 3.2349	y = 5E-05x + 1.1637	11E
85	25.4	17.21	11-Jul-08	10:27:20	Y= (32.623*x) - 3.2349	y = 2E-05x + 1.229	11E
58	9.2	5.74	12-Jul-08	12:55:30	Y= (32.623*x) - 3.2349	y = 5E-05x + 1.3345	11E
59	9.3	5.74	15-Jul-08	11:53:05	Y= (32.623*x) - 3.2349	y = 1E-04x + 1.5865	11E
60	9.4	5.74	18-Jul-08	14:38:05	Y= (32.623*x) - 3.2349	y = 1E-04x + 1.9989	11E
142	52.1	45.9	24-Jul-08	17:46:05	Y= (32.623*x) - 3.2349	y = -0.0001x + 2.5548	11E
143	52.2	45.9	25-Jul-08	17:46:05	Y= (32.623*x) - 3.2349	y = -0.0002x + 2.4014	11E
144	52.3	45.9	25-Jul-08	21:03:05	Y= (32.623*x) - 3.2349	y = 8E-05x + 2.3154	11E
145	52.4	45.9	26-Jul-08	11:49:05	Y= (32.623*x) - 3.2349	y = -2E-05x + 2.3835	11E
136	53.1	45.9	28-Jul-08	10:05:05	Y= (32.623*x) - 3.2349	y = 7E-06x + 2.3369	22E
137	53.2	45.9	28-Jul-08	17:18:05	Y= (32.623*x) - 3.2349	y = 5E-05x + 2.3285	22E
130	50.1	40.15	29-Jul-08	20:27:05	Y= (32.623*x) - 3.2349	y = 6E-05x + 2.3632	22E
138	53.3	45.9	29-Jul-08	11:08:30	Y= (32.623*x) - 3.2349	y = 3E-05x + 2.3931	22E
131	50.2	40.15	30-Jul-08	9:20:05	Y= (32.623*x) - 3.2349	y = -7E-05x + 2.422	22E
132	50.3	40.15	30-Jul-08	18:27:05	Y= (32.623*x) - 3.2349	y = 7E-05x + 2.3739	22E
117	45.1	34.43	31-Jul-08	10:20:20	Y= (32.623*x) - 3.2349	y = 4E-05x + 2.4025	22E
118	45.2	34.43	31-Jul-08	20:38:05	Y= (32.623*x) - 3.2349	y = 0.0002x + 2.3692	22E
102	41.1	28.69	1-Aug-08	19:32:10	Y= (32.623*x) - 3.2349	y = 5E-05x + 2.3905	22E
119	45.3	34.43	1-Aug-08	9:36:05	Y= (32.623*x) - 3.2349	y = -0.0001x + 2.4713	22E
103	41.2	28.69	2-Aug-08	19:32:10	Y= (32.623*x) - 3.2349	y = -5E-05x + 2.4335	22E
104	41.3	28.69	3-Aug-08	12:14:05	Y= (32.623*x) - 3.2349	y = -8E-05x + 2.3835	22E
80	26.2	17.21	4-Aug-08	11:14:05	Y= (32.623*x) - 3.2349	y = -8E-06x + 2.269	22E
81	26.3	17.21	5-Aug-08	10:41:10	Y= (32.623*x) - 3.2349	y = -3E-05x + 2.2499	22E

Table 9-2. Summary of traces using calibration equation Y= (32.623*x) - 3.2349.

No	Run No	Discharge, Qin (ml/s)	Tracing Date (D:M:Y)	Time of injected Dye (hh:mm:ss)	10-AU Calibration Equation	BG deduction Equation (20 x 20 background points)	Veg. Condition
82	26.4	17.21	6-Aug-08	15:45:05	Y= (32.623*x) - 3.2349	y = 1E-05x + 2.1685	22E
55	10.2	5.74	7-Aug-08	17:48:10	Y= (32.623*x) - 3.2349	y = 2E-05x + 2.174	22E
56	10.3	5.74	11-Aug-08	10:52:10	Y= (32.623*x) - 3.2349	y = -1E-07x + 2.2924	22E
57	10.4	5.74	14-Aug-08	14:38:05	Y= (32.623*x) - 3.2349	y = 9E-05x + 2.5741	22E
133	54.1	45.9	19-Aug-08	19:42:05	Y= (32.623*x) - 3.2349	y = -0.0002x + 2.2876	27E
134	54.2	45.9	20-Aug-08	20:10:05	Y= (32.623*x) - 3.2349	y = -2E-06x + 2.0297	27E
135	54.3	45.9	21-Aug-08	11:13:20	Y= (32.623*x) - 3.2349	y = 0.0003x + 2.0305	27E
61	11.1	5.74	22-Aug-08	11:17:00	Y= (32.623*x) - 3.2349	y = 0.0003x + 2.0427	27E
62	11.2	5.74	27-Aug-08	16:49:00	Y= (32.623*x) - 3.2349	y = 0.0001x + 5.6241	27E
63	11.3	5.74	1-Sep-08	13:52:00	Y= (32.623*x) - 3.2349	y = -1E-05x + 6.3925	27E
127	51.1	40.15	9-Sep-08	18:30:10	Y= (32.623*x) - 3.2349	y = -0.0003x + 5.9862	27E
128	51.2	40.15	10-Sep-08	11:27:10	Y= (32.623*x) - 3.2349	y = -0.0004x + 5.7574	27E
129	51.3	40.15	10-Sep-08	20:08:05	Y= (32.623*x) - 3.2349	y = -0.0001x + 5.4717	27E
86	27.2	17.21	11-Sep-08	11:17:05	Y= (32.623*x) - 3.2349	y = 6E-06x + 5.23	27E
87	27.3	17.21	12-Sep-08	13:14:05	Y= (32.623*x) - 3.2349	y = 7E-05x + 5.2199	27E
88	27.4	17.21	13-Sep-08	14:16:10	Y= (32.623*x) - 3.2349	y = -5E-05x + 5.2821	27E
108	42.1	28.69	15-Sep-08	10:43:10	Y= (32.623*x) - 3.2349	y = 0.0002x + 5.1967	27E
109	42.2	28.69	15-Sep-08	19:08:05	Y= (32.623*x) - 3.2349	y = -0.0001x + 5.305	27E
110	42.3	28.69	16-Sep-08	9:59:30	Y= (32.623*x) - 3.2349	y = -0.0001x + 5.207	27E
120	46.1	34.43	16-Sep-08	20:45:10	Y= (32.623*x) - 3.2349	y = -5E-05x + 5.1093	27E
121	46.2	34.43	17-Sep-08	9:32:10	Y= (32.623*x) - 3.2349	y = -0.0012x + 5.0575	27E
122	46.3	34.43	18-Sep-08	10:30:00	Y= (32.623*x) - 3.2349	y = -0.0004x + 3.3147	27E
123	46.4	34.43	19-Sep-08	9:27:00	Y= (32.623*x) - 3.2349	y = -0.0009x + 2.6328	27E
52	13.1	5.74	1-Oct-08	20:07:05	Y= (32.623*x) - 3.2349	y = 3E-05x - 1.0461	27ED
53	13.2	5.74	5-Oct-08	14:12:10	Y= (32.623*x) - 3.2349	y = 3E-05x - 0.8563	27ED
54	13.3	5.74	9-Oct-08	17:30:00	Y= (32.623*x) - 3.2349	y = 4E-05x - 0.6952	27ED
114	47.1	34.43	23-Sep-08	10:57:05	Y= (32.623*x) - 3.2349	y = 7E-05x - 0.7732	27ED
115	47.2	34.43	23-Sep-08	20:34:30	Y= (32.623*x) - 3.2349	y = 3E-05x - 0.7315	27ED
116	47.3	34.43	24-Sep-08	9:51:05	Y= (32.623*x) - 3.2349	y = 2E-05x - 0.7319	27ED
89	28.1	17.21	25-Sep-08	11:45:10	Y= (32.623*x) - 3.2349	y = 3E-05x - 0.7187	27ED
90	28.2	17.21	26-Sep-08	15:35:05	Y= (32.623*x) - 3.2349	y = 2E-05x - 0.6651	27ED
91	28.3	17.21	27-Sep-08	18:39:10	Y= (32.623*x) - 3.2349	y = 2E-05x - 0.6355	27ED
139	55.1	45.9	29-Sep-08	12:47:10	Y= (32.623*x) - 3.2349	y = 1E-05x - 0.8498	27ED
140	55.2	45.9	29-Sep-08	20:36:06	Y= (32.623*x) - 3.2349	y = -0.0001x - 0.8436	27ED
141	55.3	45.9	30-Sep-08	9:36:05	Y= (32.623*x) - 3.2349	y = -4E-05x - 0.9224	27ED

Table 9-3. Summary of traces using calibration equation Y= (32.623*x) - 3.2349 (Cont.).

10 Appendix B Flumes Manufacture and Calibration

Flume design and Calibration

Below shows the formula and restricted condition which applied on the V-notch weir based on BS 3680-4A:1981:

$$Q = C_e \frac{8}{15} \tan \frac{\alpha}{2} \sqrt{2g_n} h_e^{5/2} \quad (10.1)$$

in which

Q is the discharge;

C_e is the coefficient of discharge;

h_e is the head.

The coefficient of discharge C_e has been determined by experiment as a function of three variables (see Figure 7)

$$C_e = f\left(\frac{h}{p}, \frac{p}{B}, \alpha\right) \quad (10.2)$$

In which

p is the height of the vertex of the notch with respect to the floor of the approach channel;

B is the width of the approach channel;

h_e is defined by the equation

Practical limitations on *α* h_e */p*, *p/B*, h_e and *p*:

For reasons related to hazards of measurement-error and lack of experimental data, the following practical limits are applicable to the use of Kindsvater-Shen formula:

a) α shall be between π/9 and 5 π/9 radians (20^o and 100^o);
b) *h/p* shall be limited to the range shown on Figure 4.1 for α = π/2 radians (90^o);
c) *p/B* shall be limited to the range shown on Figure 4.1 for α = π/2 radians (90^o);
d) h_e shall be not less than 0.06 m;
e) *p* shall be not less than 0.09 m

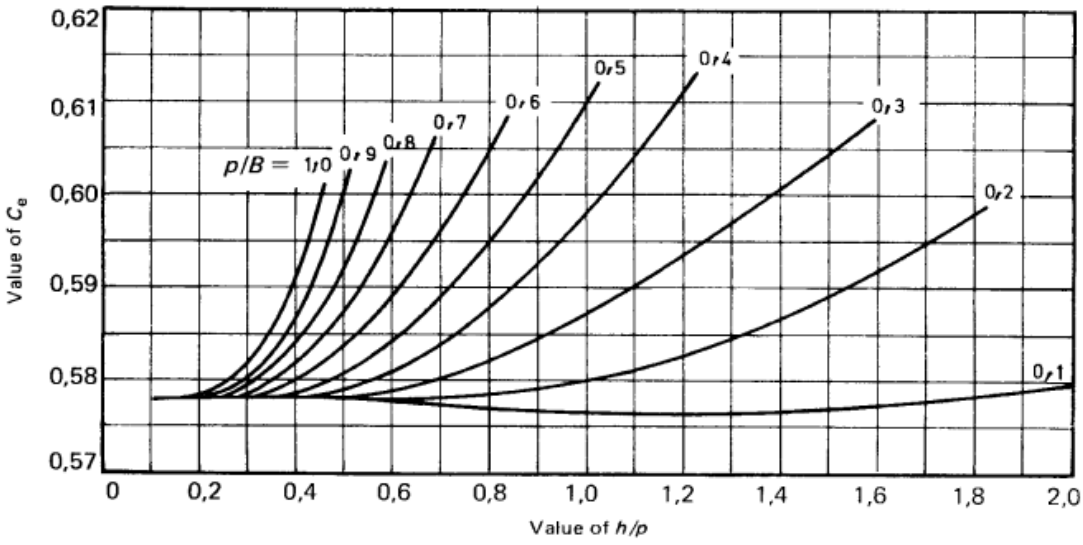

Figure 10-1. Coefficient of discharge Ce (= 90°) (Source BS3680-4A: 1981).

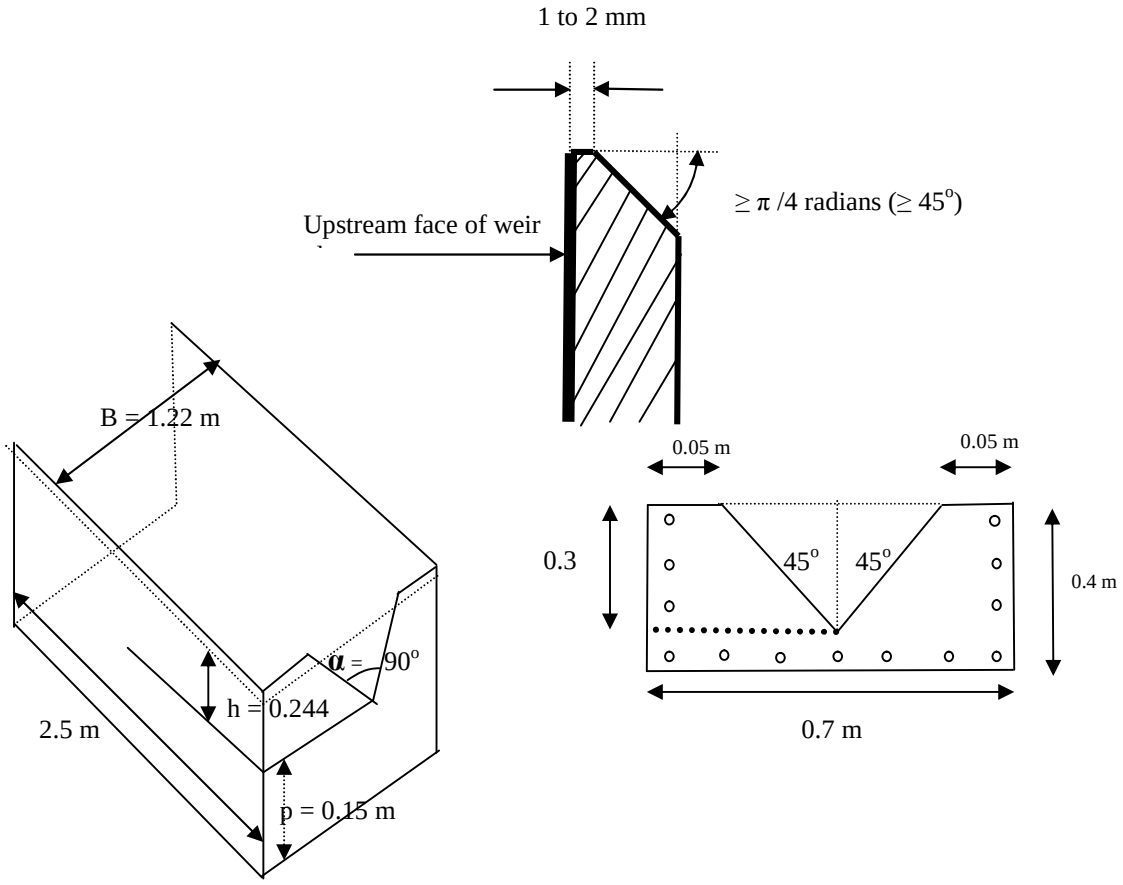

Figure 10-2. BS 3680-4A: 1981 Designed V-notch weir for Lyby Pond.

Note: for the third flume (Inlet Bottom Pond), one feature that is different from the previous one is that the length of the flume is only 2 m (due to the availability of space).

Figure 10-3. Volumetric (bucket) measurement.

Figure 10-4. Dye Tracing.

Figure 10-5. Constructed Flume at the outlet of third pond.

From 15 July 2007 and 28 March 2008 fluorescent tracing techniques were performed on the outlet channel (Outlet Bottom Pond, the total distance from injection point to measuring point was 6.75 m, from injection to constructed flume is 3.5 m) and Inlet Bottom Pond (the total distance from injection point to measuring point was 8.5 m, from injection to constructed flume is 4 m). Two to three injections of Rhodamine WT, for each discharge, were made: 1ml (2ml for high flow rate) of neat Rhodamine WT diluted with 2 litres was taken from the pond's outlet. The Turner design Cyclops and Scufa were installed to read the temporal concentration distribution passing through the installed instrument. Each discharge was controlled by diverting flow (by closing or opening) at the top in-flow channel to the pond systems. From March 2008, the area velocity meter was installed, about 1.2 m from V-notch weir, at the inlet bottom pond and outlet bottom pond with reading level every two minutes. Before starting each trace, volume and level measurement were taken. Levels were recorded at the head measurement section (1.2 m upstream of the installed v-notch weir) and the bucket collected the volume of water from the V-notch weir over a specific time.

The table below (Table 10.1) shows the calculated discharge from each tracing using the conservation of tracing mass against the discharge results from bucket measurement and compared with the standard discharge by BS 3680-4A: 1981. To obtain the tracing discharge results, the voltage (v) output from Cyclops had been converted to concentration (in ppb) by using the calibration data from 27 July 2007 (See Figure 10.1) but from March 2008 the Scufa output is in ppb so it was not necessary to convert from Voltage to ppb.

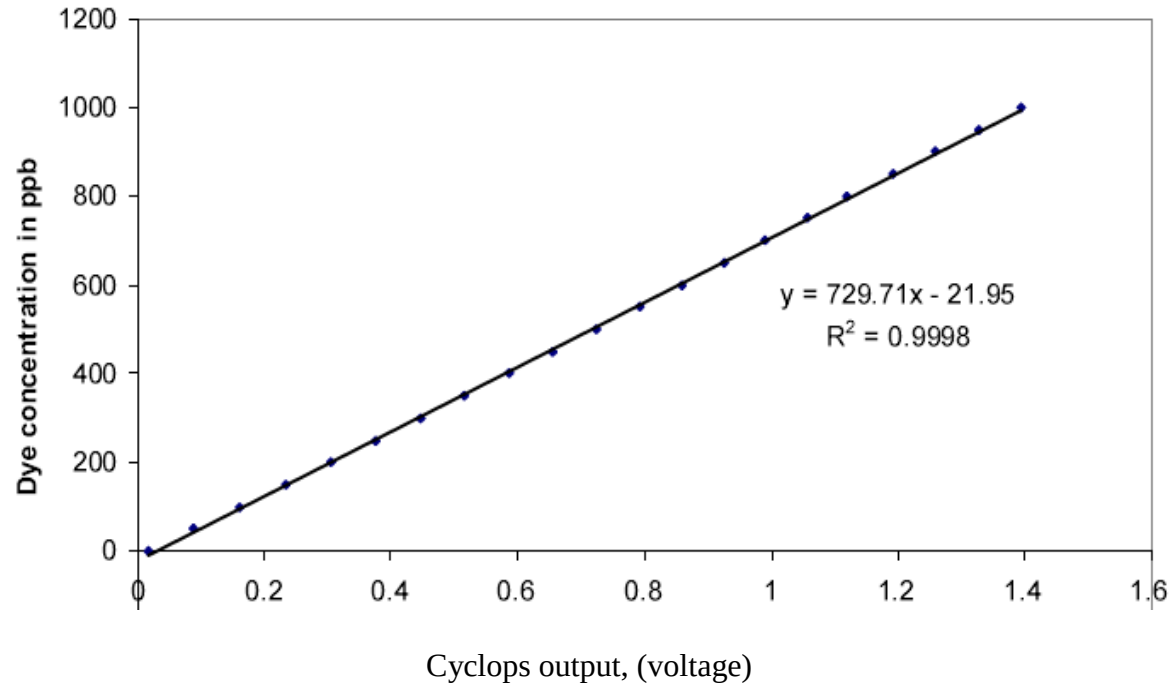

Figure 10-6. Cyclops calibration data on 27/July/2007.

Trace N^{o}	Date and Time*	Level or head: h in (mm)	Discharge, Qin (l/s)		
			Solute	Bucket	BSI
1	15/07/07, 16:58	126	8.22	5.35	7.83
2	15/07/07, 17:33	115	7.85	6.17	6.24
3	16/07/07, 09:42	203	28.65	20.65	25.65
4	16/07/07, 10:05	203	28.80	29.95	25.65
5	16/07/07, 10:25	203	30.56	26.37	25.65
6	16/07/07, 12:21	230	41.68	33.50	35.04
7	16/07/07, 12:37	231	43.59	37.85	35.42
8	16/07/07, 17:02	184	21.87	29.35	20.07
9	16/07/07, 17:15	184	22.74	29.35	20.07
10	17/07/07, 09:33	108	6.03	5.57	5.34
11	17/07/07, 10:06	108	5.45	6.38	5.34
12	17/07/07, 19:10	63	1.99	1.57	1.42
13	17/07/07, 20:13	63	2.02	1.57	1.41
14	18/07/07, 12:37	60	1.60	1.61	1.26
15	19/07/07, 09:13	56	1.70	0.97	N/A
16	19/07/07, 15:24	53	1.38	0.99	N/A
17	20/07/07, 10:09	107	6.36	5.03	5.22
18*	20/07/07, 14:41	105	5.01	4.27	4.98
19*	20/07/07, 15:50	105	4.52	3.90	4.98

Note: * mean trace at the Top Flume

Table 10-1. Summary results from Solute Tracing, Bucket and BSI.

As the V-Notch flume was constructed according to BS 3680-4A: 1981, the head (*h*) and discharge (*Q*) based on BSI should be considered; Figures 11.6, 11.7 and 11.8 show the final discharge formula obtained by plotting discharge (l/s) against head (m) above the Sweden V-notch weir, with this final curve being the consolidation of bucket calibrations, solute calibrations and combined bucket and

Solute Calibrations respectively. Below is shown the bucket discharges (Q_{b07}), (Q_{b08}), (Q_{b0708}), solute discharges (Q_{s07}), (Q_{s08}), (Q_{s0708}) and combined bucket and solute discharge (Q_{bs07}), (Q_{bs08}) and (Q_{bs0708}).

Note: *b* denotes bucket calibration, *s* is solute calibration and $b_{07/}$ S_{08} denotes mean bucket or solute measured in year 2007 / 2008;

$$Q_{b07} = 1.4139 * \mathrm{h}^{2.51} \quad (10.3)$$

$$Q_{b08} = 1.2528 * \mathrm{h}^{2.5119} \quad (10.4)$$

$$Q_{b0708} = 1.1823 * \mathrm{h}^{2.47} \quad (10.5)$$

$$Q_{s07} = 1.1381 * h^{2.32} \quad (10.6)$$

$$Q_{s08} = 0.4488 * h^{1.93} \quad (11.7)$$

$$Q_{s0708} = 0.8097 * h^{2.21} \quad (10.8)$$

$$Q_{sb07} = 1.3046 * h^{2.45} \quad (10.9)$$

$$Q_{sb08} = 1.182 * h^{2.467} \quad (10.10)$$

$$Q_{sb0708} = 1.1177 * h^{2.425} \quad (10.11)$$

Where:

Q_b is bucket discharge

Q_s is solute discharge

Q_{sb} is combined bucket and solute discharge

h is head above V-notch flume

The results from the combined Bucket and Solute Discharge formula were substituted from equation 10.5 into equation 5.1, to determine the value of the coefficient, C_e, shown in Figure 10.3. The general Sweden V-notch flume calibration obtained by plotting head (m) versus Q (l/s) is shown in Figure 10.4 and annex C shows the detailed coefficients and also the detail of discharges with different range of head above the V-notch weir.

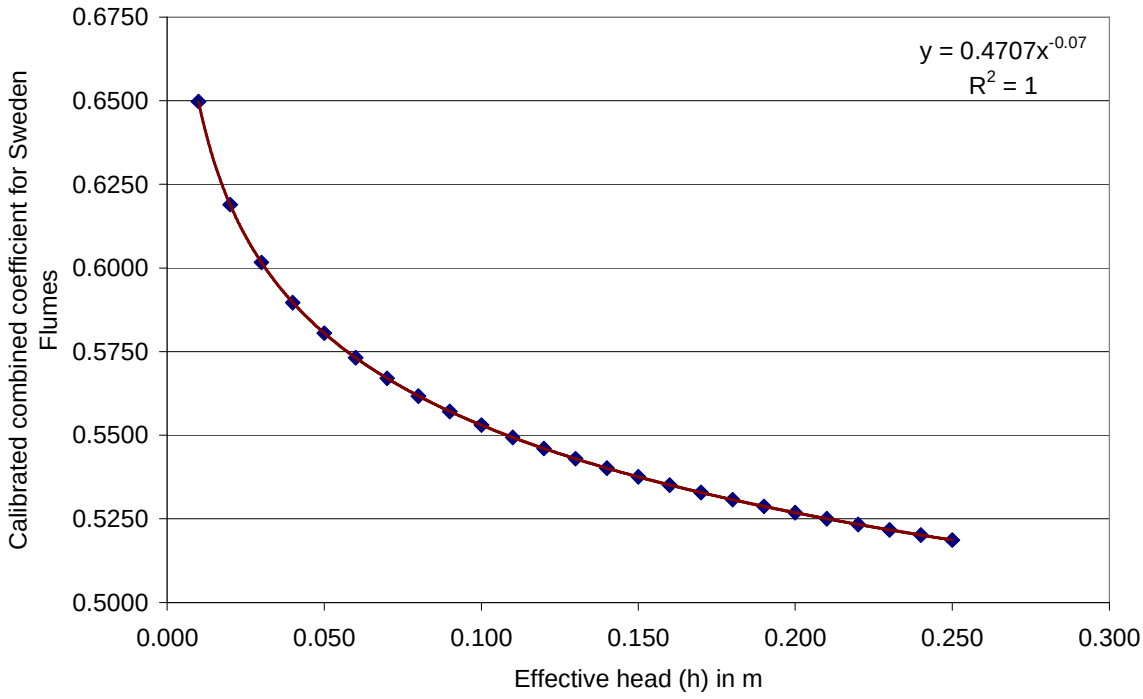

Figure 10-7. Coefficient for Sweden Flume from July 07 and March 08.

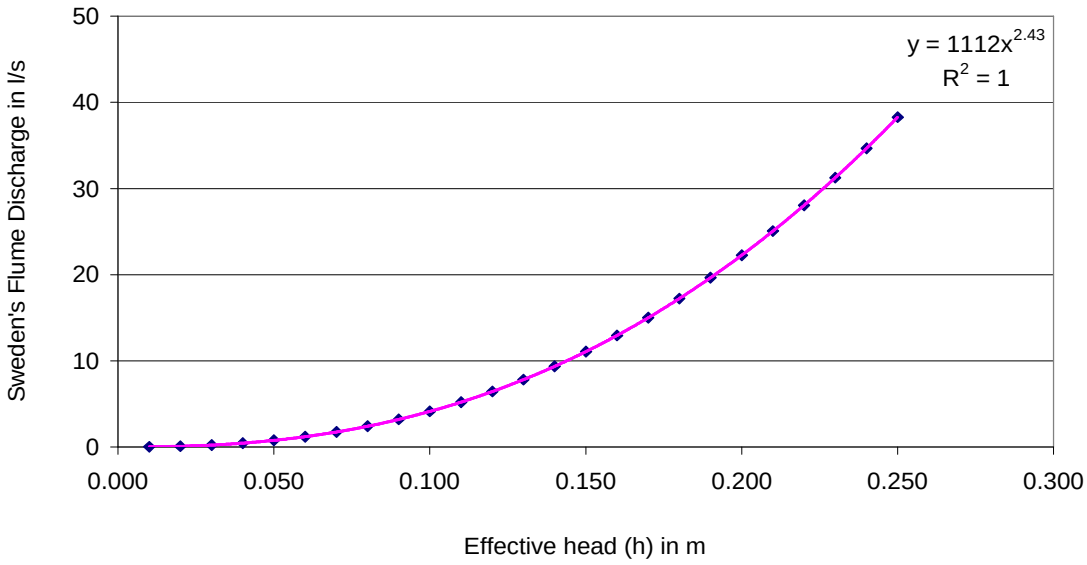

Figure 10-8. Sweden V-notch Flume Calibration.

The results from the combined Bucket and Solute Discharge formula clearly show that there were differ between BS 3680-4A: 1981 standard V-notch Weir and our Sweden V-notch Weir see Figure 10.9,; This difference may be caused from the accuracy of flume levelling or some other anticipated conditions. So the further study will use Sweden V-notch Weir as tool to measure inlet and outlet discharges from the lower pond.

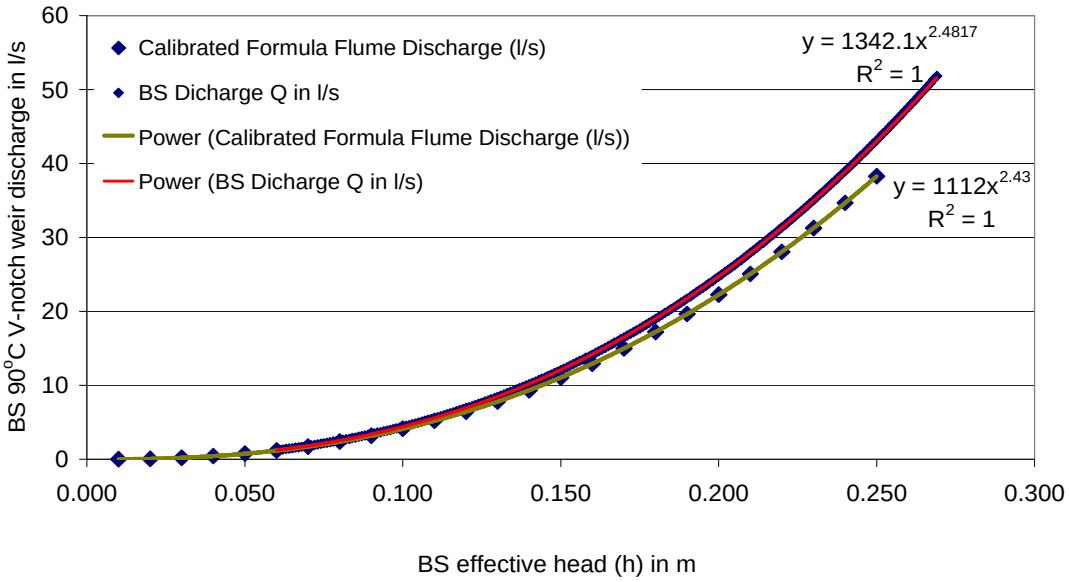

Figure 10-9. Sweden V-notch Flume Calibration and BS standard.

Figure 10-10. Pictures of preparation and construction of Lyby Field Flumes.

Figure 10-11. Pictures of design and build V-notch weir flumes for Lyby Field Pond.

Figure 10-12. Pictures of full trace at Lyby Pond during April and May.

Figure 10-13. Pictures of full trace at Lyby Pond during March-April.

Pictures of problems existing at Lyby Field Pond

Figure 10-14. Pictures of problems existed at Lyby Field Pond and pictures of family helping at Lyby field pond.

11 Appendix C - Experimental results from field pond

The last three full traces (in 2006, July 2007 and March 2008) showed unacceptable results. There were two reasons which were suspected on instruments which yielded unusable results: one was the instrument set up or calibration and the other was the pond ecosystem. The trip on Nov 2008 was to get a full useful trace on pond so there was a need to check all instruments. A series of calibrations and stability tests has been conducted on the instruments; stream and background outlet flume water test and the results are shown below:

11.1 Calibration and Stability Test

a. Calibrated instrument and stability test in the field

The calibration of all instruments has been conducted twice; the second time was acceptable (see Figure 11.1). When the first calibration was finished and set up for stability test it was found that there were two instruments, SN772 and SN664 showing an increasing reading the background from 1 to 64 ppb within 4 to 5 hours (See Figure 11.1) but all read 200 ppb smoothly. The reason may have been caused by the set up on temperature compensation, on “Other” not on “Rhodamine WT”, or from the power cable (one download cable and one small power cable was found not to function very well). The second calibration was conducted by setting the temperature compensated on “Rhodamine WT” as well as changing power cable; the stability test showed very smooth readings at both, low and high reading concentrations (see Figure 11.2).

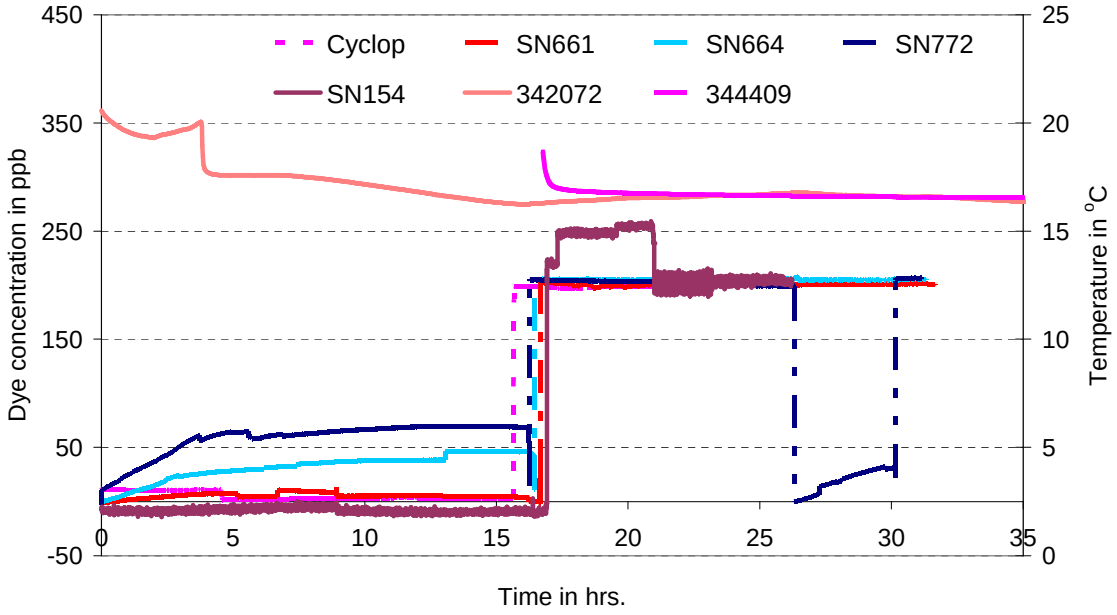

Figure 11-1. First instrument calibrated and stability tested.

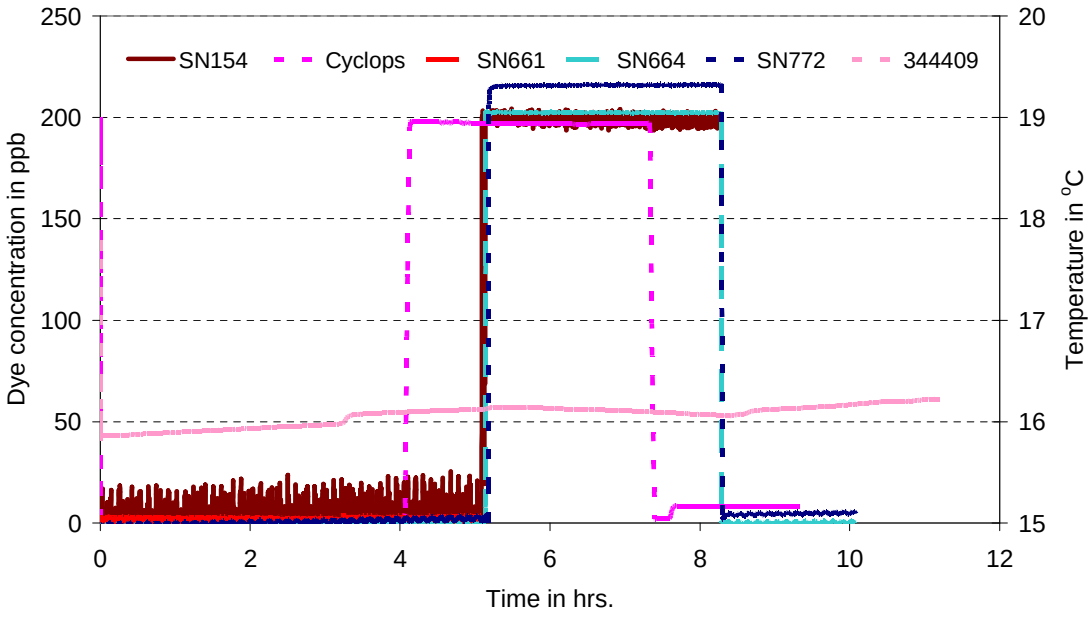

Figure 11-2.Second instrument calibrated and stability tested.

b. Stability tests of instruments on Small Stream and Outlet Flume

After the second calibration, all instruments read smoothly in both low and high Rhodamine WT concentration. The field tests on small stream and outlet flume have been conducted and the results from both stream and outlet flume tests showed smooth and accurate readings among all instruments (Scufa SN154, SN661, SN664, SN772 and Cyclops). This indicates that such instruments were working very well (see Figure 11.3, 11.4 and 11.5) except (see Figure 12.4 SN772) where the reading was observed to increase dramatically due to blocking of the sensor by some leaves. The methodology of the above tests are described as follows: all instruments were deployed parallel to each others to read low concentration (background) of the stream and the outlet flume; for high concentration readings, the small trace on stream was obtained by injecting dye (0.5 ml of neat dye) about 60 m from the installed instruments; all the instruments responded the same with low and high concentration reading as well (See Figure 11.3).

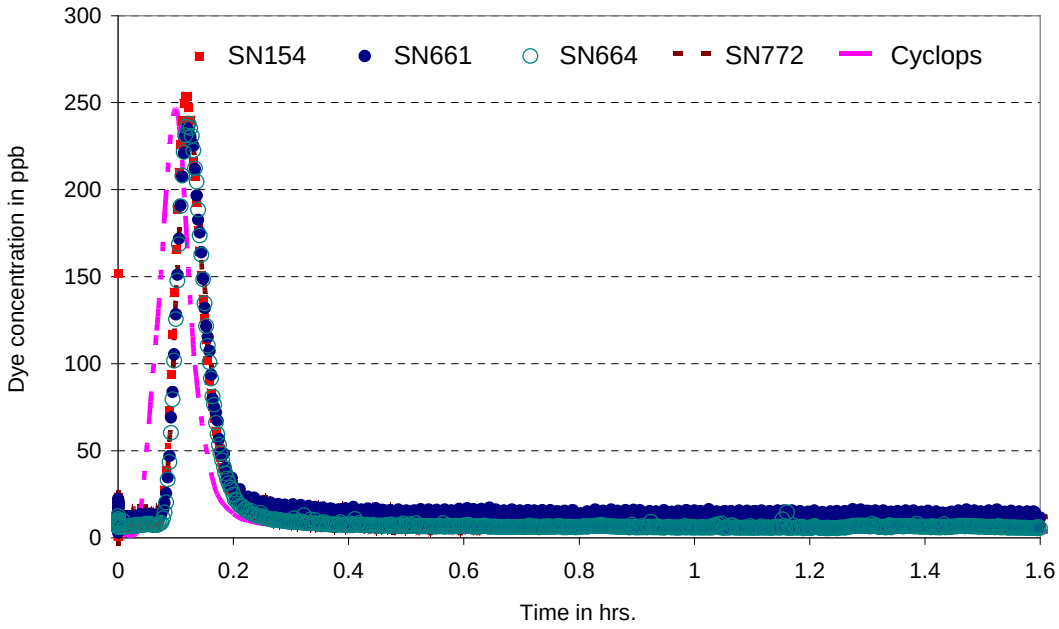

Figure 11-3. Stability tested on small stream.

Figure 11-4. The installation of instruments for stream stability tests.